

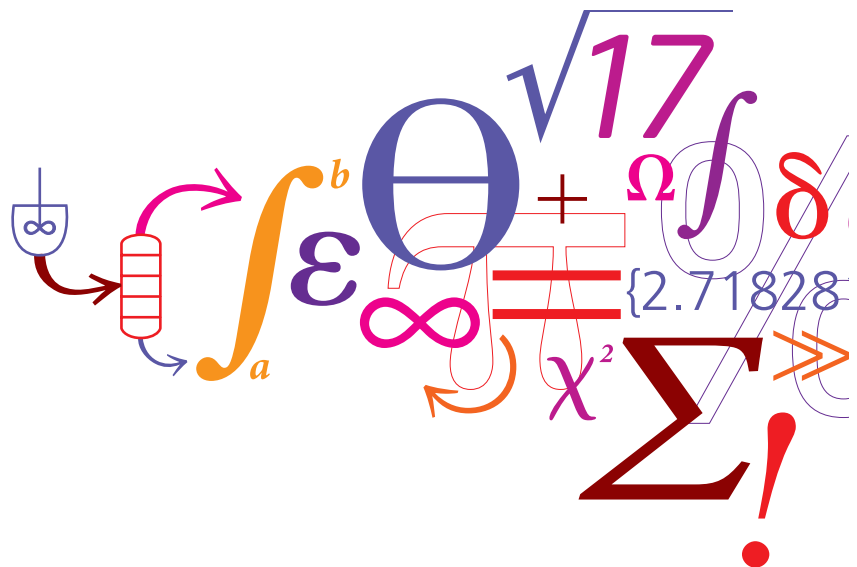
Graduate School Yearbook **2017**

Editors:

Professor, Head of Department, Kim Dam-Johansen

Industrial PhD student, Héctor Forero-Hernández

Associate Professor, Peter Szabo



PREFACE

Welcome to this year's Graduate School Yearbook.

In Denmark, the PhD study is a three-year fulltime programme after graduation with a MSc degree. At DTU Chemical Engineering we host about 100 PhD students. In this book, you can read about most of our current PhD projects. Some students have just initiated their work whereas others are close to writing their thesis.

The work of our PhD students is of utmost importance to fulfil the mission and vision of our department:

Mission

Being responsible for research, education and innovation, DTU Chemical Engineering will develop and utilize knowledge, methods, technologies and sustainable solutions within:

- Chemical and biochemical process engineering and production
- Design of chemical and biochemical products and processes
- Energy and environment

Vision

DTU Chemical Engineering:

- Is acknowledged as a world leading chemical engineering department
- Is an attractive partner for university departments and research-based industry
- Helps to retain, develop and attract knowledge-based national working places
- Supports development of sustainable solutions in the fields of chemistry, biotechnology, food, pharma and energy through research and research based consultancy
- Is attractive as a place to work for ambitious and technology-passionate staff members

We hope you will find the book interesting, and we invite all readers to contact us for further details.

Yours sincerely

Kim Dam-Johansen

Professor, Head of Department

Peter Szabo & Héctor Forero-Hernández

Editors

Contents

A

Sustainable process synthesis and design
Al, Resul 1

Anti-microbial polymers for catheter coatings
Andersen, Christian 3

Agglomeration in fluidized bed at high temperature
Aničić, Božidar 5

Syngas biomethanation by enriched anaerobic sludge in a trickle bed reactor
Asimakopoulos, Konstantinos 7

B

An in-situ measurement method for bubble size distributions in industrial pilot scale fermentation processes
Bach, Christian 9

Plant Wide Monitoring and Control of Bioprocesses
Böhner, Franz David 11

Enzyme Discovery for Tuber Processing Pulps by SDC
Barrett, Kristian 13

An empirical model for organic carbon recovery in a rotating belt filter
Behera, Chitta Ranjan 15

Enzyme production from agro-industrial residues for local application: a sustainable approach in Ghana
Bentil, Joseph Asankomah 17

Application of novel free-floating sensor device: flow characteristics in stirred vessels
Bisgaard, Jonas 19

C

Dynamics of physiological adaptation of yeast to main inhibitors found in lignocellulosic hydrolysate: a single cell analysis approach
Cabañero- Lopez, Pau 21

Alternative liquid fuels in burners optimized for low *NOx* emissions and high burn out
Cafaggi, Giovanni 23

Physicochemical properties of binary mixtures (*1-vinyl-3-acetamido imidazole bis(trifluoromethylsulfonyl) imide+acetonitrile*)
Cai, Yingjun 25

Phase behavior of inhomogeneous fluids: classical density functional theory approaches
Camacho-Vergara, Edgar Luis 27

Monitoring of bioprocesses: merging PAT, Kalman and uncertainty <i>Caroço, Ricardo Fernandes</i>	29
Methodology for modelling the freeze-drying of a fixed particle bed <i>Carvalho, Teresa Melo de</i>	31
Integrated solvent-membrane and process design method for hybrid separation schemes <i>Chen, Yuqiu</i>	33
Advanced wound care adhesives with excellent moisture handling properties <i>Chiaula, Valeria</i>	35
Selective catalytic reduction (SCR) of <i>NO_x</i> on ships <i>Christensen, Steen Müller</i>	37
D	
Catalytic hydrodeoxygenation of biomass pyrolysis vapor for green fuels <i>Dabros, Trine Marie Hartmann</i>	39
Oxygen supply to oxidative biocatalysis <i>Dias Gomes, Mafalda</i>	41
Surface properties correlate to the digestibility of steam-pretreated biomass <i>Djajadi, Demi Tristan</i>	43
E	
Deoxygenation of fast pyrolysis vapors using zeolites <i>Eschenbacher, Andreas</i>	45
F	
Optimization of the energy recovery in an industrial wastewater treatment plant <i>Feldman, Hannah</i>	47
Coatings for high pressure and high temperature <i>Ferrero, Gianni</i>	49
Validation and improvement of property and process modelling for oleochemicals <i>Forero-Hernández, Héctor</i>	51
Sustainable synthesis-design of carbon dioxide capture and utilization processes <i>Frauzem, Rebecca</i>	53
G	
Biomass gasification polygeneration <i>Gadsbøll, Rasmus Østergaard</i>	55
Sustainable and innovative chemical and biochemical solutions through an integrated and systematic framework <i>Garg, Nipun</i>	57

Feasibility study of Fixed Film Fixed Filter (FAD) reactor for anaerobic treatment of liquefied municipal solid wastes <i>Gonzalez-Londoño, Jorge Enrique</i>	61
Fermentation of synthesis gas by mixed microbial consortia for the production of liquid and gaseous biofuels <i>Grimalt Alemany, Antonio</i>	63
H	
Reversible and irreversible deactivation of <i>Cu-CHA NH₃-SCR</i> catalysts by <i>SO₂</i> and <i>SO₃</i> <i>Hammershoi, Peter Sams</i>	65
J	
Membrane-based in-situ product removal <i>Jaksland, Anders</i>	67
NO _x reduction in grate-firing waste-to-energy plants <i>Jepsen, Morten Søre</i>	69
A systematic methodology for property model-based chemical substitution <i>Jhamb, Spardha</i>	71
Design and optimization of oleochemical processes <i>Jones, Mark</i>	73
K	
Surface characterization of activated chalcopyrite particles <i>Karcz, Adam Paul</i>	75
Thermodynamics of petroleum fluids relevant to subsea processing <i>Kruger, Francois</i>	77
L	
Deposition properties of biomass fly ash <i>Laxminarayan, Yashasvi</i>	79
Mathematical modelling of sulfuric acid accumulation in lube oil in diesel engines <i>Lejre, Kasper Hartvig</i>	81
Application of improved computational fluid dynamic simulations for pulverized biomass combustion <i>Leth-Espensen, Anna</i>	83
Continuous biocatalytic processes <i>Lindeque, Rowan Malan</i>	85
Energy efficient hybrid gas separation with ionic liquid <i>Liu, Xinyan</i>	87

Kinetics of scale formation in oil and gas production <i>Lomsøy, Petter</i>	89
CFD Simulation of biomass combustion in fluidized beds <i>Luo, Hao</i>	91
M	
Modelling of thermal breakdown in dielectric elastomers <i>Madsen, Line Riis</i>	93
Morphology and grindability study of wood and combustion characterization at pulverized-fuel firing conditions <i>Masche, Marvin</i>	95
Biocatalytic Baeyer-Villiger oxidations <i>Meissner, Murray</i>	97
Efficient transformation of atmospheric CO ₂ to carbonates by DBU based ionic liquids under mild conditions <i>Meng, Xianglei</i>	99
Degradation and durability of acid resistant organic coatings <i>Møller, Victor Buhl</i>	103
Model library development for pharmaceutical process design and simulation <i>Montes, Frederico</i>	105
Enzymatic cleavage of lignin-carbohydrate complexes (LCCs) <i>Mosbech, Caroline</i>	107
Assessment of laccase catalyzed lignin modifications by Py-GC/MS analysis <i>Munk, Line</i>	109
N	
Physiological characterization of the impact of gradients on fermentation processes <i>Nadal-Rey, Gisela</i>	111
Multiphase flow and fuel conversion in cement calciner <i>Nakhaei, Mohammadhadi</i>	113
Anticorrosive coatings and pigment engineering <i>Nezhad, Sina Sedaghat</i>	115
Discovery and engineering of enzymatic biocatalysts for conversion of CO ₂ to industrially relevant C ₁ products <i>Nielsen, Christian Førgaard</i>	117
Measuring and modelling of chemical sulfur corrosion mechanisms in marine diesel engines <i>Nielsen, Henrik Lund</i>	119

O

Investigation of thermal degradation mechanisms of silicone elastomers
Ogliani, Elisa 121

Scale-up modeling and analysis of a pharmaceutical crystallization process
Öner, Merve 123

P

Control of Hydrogen Chloride (*HCl*) emission from cement plants
Pachtsas, Stylianos 125

Catalytic liquefaction of lignin to value-added chemicals
Parto, Soheila 127

Burners for Cement Kilns
Pedersen, Morten Nedergaard 129

Systematic computer aided methods and tools for lipids process technology
Perederic, Olivia Ana 131

Laccase structure-function relations for enzymatic lignin modification
Perna, Valentina 133

A biochemically structured model for *Methylococcus capsulatus*
Petersen, Leander Adrian Haaning 135

Systematic enzyme discovery, targeted to fungal and algal biomass
Pilgaard, Bo 137

Auto-sampling and monitoring of bioprocesses
Pontius, Katrin 139

R

Optimal model-based monitoring of tubular reactors
Ramirez-Castelán, Carlos Eduardo 141

Next generation methanol to formaldehyde selective oxidation catalyst
Raun, Kristian Viegaard 143

Tar conversion for gas cleaning in biomass gasification by using biochar
Ravenni, Giulia 145

Thermodynamic modelling and data evaluation for life sciences applications
Ruszczyński, Łukasz 147

S

Optimized waste recycling in an integrated melting furnace (IMF) for stone wool melt production
Schultz-Falk, Vickie 149

Sustainable production of higher alcohols from <i>CO</i> and <i>CO</i> ₂ <i>Schumann, Max</i>	151
Biomass particle ignition in mill equipment <i>Schwarzer, Lars</i>	153
Advanced mathematical data interpretation methods for the description of the processes inside microbioreactors and biosensors <i>Semenova, Daria</i>	155
Monolithic Thiol-ene materials with drastically different mechanical properties <i>Shen, Peng</i>	157
High performance immobilization of enzymes in inorganic membranes <i>Sigurðardóttir, Sigyn Björk</i>	159
The modification of PSf membranes with ionic liquids used for <i>CO</i> ₂ separation <i>Song, Ting</i>	161
Bioprocess risk assessment using a mechanistic modelling framework <i>Spann, Robert</i>	163
Hydrogen assisted catalytic biomass pyrolysis for green fuels <i>Stumann, Magnus Zingler</i>	165
Modeling Tetra-n-butyl ammonium halides aqueous solution with the Electrolyte CPA EoS <i>Sun, Li</i>	167
Cyclone reactors: experimental and modeling study <i>Svith, Casper Stryhn</i>	169
T	
Automating experimentation in miniaturized reactors <i>Tajsoleiman, Tannaz</i>	171
Thermodynamics, design, simulation and benchmarking of biofuel processes <i>Torli, Mauro</i>	173
U	
<i>NO</i> _x formation and reduction in fluidized bed combustion of biomass <i>Ulusoy, Burak</i>	175
V	
Insight into the dielectric breakdown of elastomers <i>Vaicekauskaite, Justina</i>	177
Application of advanced thermodynamic models to simultaneously describe phase equilibrium and critical properties of fluid mixtures <i>Vinhal, Andre</i>	179

W

K-capture by Al-Si based additives at suspension-fired conditions
Wang, Guoliang 181

Coating interlayer adhesion loss
Wang, Ting 183

Low friction anti-fouling coating for high fuel efficiency
Wang, Xueting 185

Extensional rheology and final morphology of polymeric fibers
Wingstrand, Sara Lindeblad 187

Y

A measurement-based cleaning-in-place recycle system
Yang, Jifeng 189

Z

Novel testing methods for intumescent coatings
Zeng, Ying 191

Catalytic oxidation of methane
Zhang, Yu 193

Ionic liquids as bifunctional cosolvents enhanced CO₂ conversion catalysed by NADH-dependent formate dehydrogenase
Zhang, Zhibo 195



Resul Al
Phone: +45 4525 2911
E-mail: resal@kt.dtu.dk

Supervisors: Gürkan Sin
Krist V. Gernaey
Alexandr Zubov

PhD Study
Started: May 2017
To be completed: April 2020

Sustainable process synthesis and design

Abstract

In the area of sustainable development, process design engineers are facing stringent constraints to meet the objectives imposed by today's business environment. Design of sustainable chemical and biochemical processes requires a holistic approach, combining economic, environmental, safety and health-related aspects, especially in early stage of process design, which also includes synthesis of the alternative processing routes. This project aims at the development of a stochastic computational framework to enable process designers to easily integrate various process design tools; such as life cycle analysis, global sensitivity analysis, and uncertainty analysis, into the early-stage of sustainable process design.

Introduction

Process systems engineering promotes the application of systematic computer-based methods to process design and synthesis, which encompasses a vast range of industries and requires integration of significant amount of knowledge from diverse scientific disciplines, practical industrial experience, and a number of tools and methods to carry out sustainable process design. One of the critical pain points for process design engineers is the lack of available tool regarding the comparative analysis and synthesis of alternative processing networks, which makes it not-so-easy for them to implement innovative processing configurations with newly arising process technologies. Given the lack of data regarding these new processes and the uncertainty in the available process data, there exists a need for new supporting methods and tools for both generating alternative processing flowsheets and the selection of the optimum flowsheet under uncertainty with sustainability aspects also incorporated into the early stage process design.

Specific Objectives

Among the two major approaches developed by process systems engineering community to the problem of how to find optimum flowsheet are hierarchical decomposition and superstructure optimization [1]. The first solves the problem sequentially by fixing some elements in the flowsheet, and then improving the flowsheet with the help of some heuristic rules. Although this approach has practically more use due to

its simpler to implement workflow, it often leads to suboptimal process designs. The latter, on the other hand, defines the problem as a mathematical programming problem based on a use-defined objective with the superstructure containing all the available process technologies being given to the program as the design space to search for. This approach performs simultaneous optimization of the configuration and the operating conditions. However, as most of the process models included in the superstructure are nonlinear, this approach results in an infamous type of optimization problems, mixed-integer nonlinear programs, which makes it practically very difficult to converge to a feasible solution. An alternative approach to optimization based superstructure way of solving process synthesis problem is Monte Carlo simulation. This approach explores the design space of the superstructure with millions of simulations based on sampled design parameters; however, this comes at a price of significantly increased computational cost. To address this problem, researcher have looked into the use of surrogate models in the case of complex process models to be used in process synthesis problems [2], which make the problem more feasible to solve.

This project aims at

- development of a surrogate-assisted Monte Carlo based computational framework for sustainable process synthesis and design

- Equipped with improved sustainability analysis methodology and robust design evaluation tools such as sensitivity and uncertainty analyses.

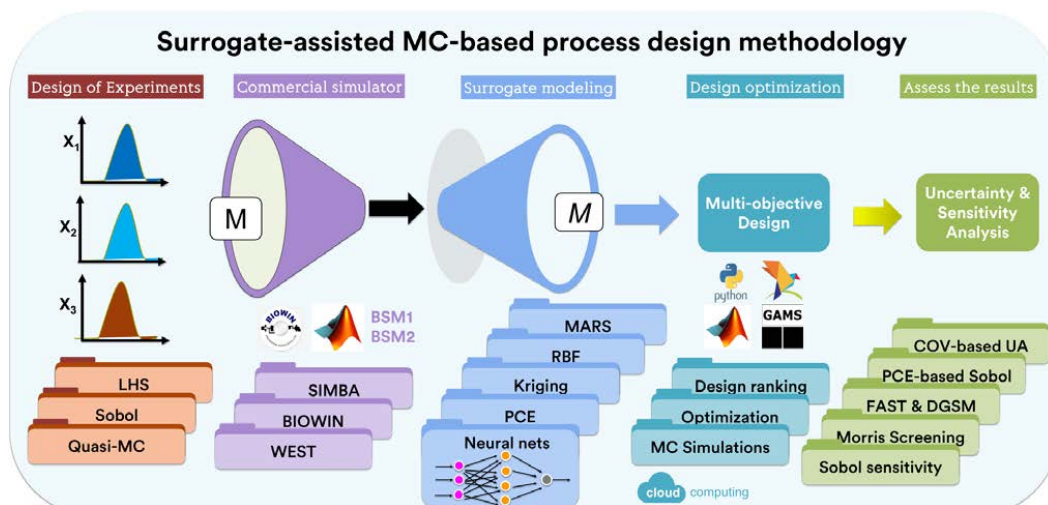


Figure 1: Surrogate-assisted Monte Carlo based process design methodology

Approach

The general methodology for surrogate-assisted Monte Carlo based process synthesis and design is illustrated in Figure 1. Design of experiments techniques are employed to cover the design space parameters. For each different set of design parameters, a rigorous model is run to create a dataset of inputs and outputs. This dataset is later used to create a mapping function, i.e. a metamodel or a surrogate model, using a class of advanced metamodeling techniques including artificial neural networks, polynomial chaos expansions, Gaussian process modeling (Kriging), radial basis functions, multi adaptive regression splines. This computationally cheaper model is then used to explore the design space of the superstructure with Monte Carlo simulations. Designs are ranked based on user-defined criteria, be it the most environmentally friendly design or the economically profitable design. Finally yet importantly, selected design are further evaluated for robustness under uncertainty and most sensitive parameters are identified with the help of global sensitivity analysis tools library.

Conclusions

A computational framework for sustainable process synthesis and design is currently being developed. The final framework is expected to provide novel methods and approaches for generation of process alternatives as well as for process analyses and evaluation. The final framework will also be validated at industrial partners of the ModLife project, namely Alfa Laval (Denmark) and Unilever (the UK).

Acknowledgements

This work has received funding from the European Union's Horizon 2020 research and innovation programme under the Marie Skłodowska-Curie grant agreement No. 675251.

References

1. Yeomans, H., & Grossmann, I. E. (1999). A systematic modeling framework of superstructure optimization in process synthesis. *Computers and Chemical Engineering*, 23(6), 709–731.
2. Henao, C. A., & Maravelias, C. T. (2011). Surrogate-based superstructure optimization framework. *AIChE Journal*, 57(5), 1216–1232.



Christian Andersen

Phone: +45 30 69 51 90
E-mail: chrand@kt.dtu.dk

Supervisors: Anders E. Daugaard
Niels J. Madsen, Coloplast A/S
Hanne Everland, Coloplast A/S

PhD Study
Started: January 2017
To be completed: January 2020

Anti-microbial polymers for catheter coatings

Abstract

Catheter users are generally experiencing an increased number of infections from daily or permanent use of catheters. This often requires treatments with antibiotics to knock down infections, which is a severe limitation in their everyday life. The main objective of this project is to develop a novel catheter coating that can prevent bacterial growth to reduce the number of infections. This is envisaged through synthesis of novel multifunctional polymers applied in hydrophilic catheter coatings.

Introduction

Catheter associated urinary tract infections (CAUTIs) is one of the most frequent types of infections related to medical devices. It is responsible for around 40% of all hospital acquired infections and prolongs the mean bed time for patients by up to 2.4 days[1][2]. The main cause for these infections are often that the bacteria is pushed into the bladder when inserted through the urethra, or for indwelling catheters, that the bacteria is able to adhere onto the surface of the catheter and form biofilm. Biofilm is a matrix consisting of proteins, lipids, polysaccharides and/or extracellular DNA and bacteria situated within biofilm is well protected from the outside environment. From here, they are able to avoid detection by the immune system and spread uncontrolled and unhindered. This leads to persistent infections that are difficult to exterminate even when using traditional antibiotics. Moreover, biofilm colonies often contains more than one strain/species of bacteria, making it necessary to use mixtures of antibiotics in order to give the most effective treatment. Biofilm further enables bacteria to develop resistance or tolerance towards antibiotics since it prohibits efficient diffusion of the drug[3]. This creates areas with non-lethal concentrations allowing for development of antibiotic resistant genes. Due to the close proximity of the cells, the genes are quickly spread to other bacteria. This is done through various mechanisms such as horizontal gene transfer, which is known to be important for bacterial evolution.

To reduce the number of infections, antimicrobial surfaces have been developed and applied on catheters, but only with limited effect[4]. Much effort have been

made in order to find new and better candidates and a wide range of compound classes have been studied for use in anti-microbial surfaces. A review of the current state-of-the-art literature within antibacterial polymers have been conducted, where many compounds with anti-microbial properties have been identified.

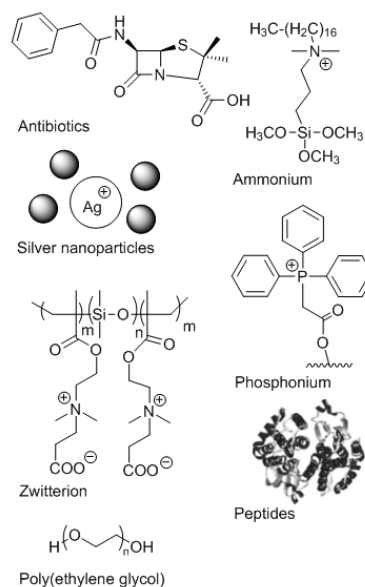


Figure 1: Structural illustration of anti-microbial agents.

Examples of such are shown in Figure 1. Even though they are structurally very different, the general mechanism by which these surfaces work to achieve antimicrobial activity, can be simplified into 3 categories:

1) repelling 2) leaching and 3) contact-killing surfaces[5]. For repelling surfaces, usually a hydrophilic polymer is used to establish a hydration layer, which is capable of protecting the surface against attachment of proteins and bacteria. Here, hydrogels, hydrophilic brushes and zwitterions are most commonly seen, due to their strong binding of water (See Fig. 2). Other factors such as entropic and osmotic repulsion from the polymer coils further helps in avoiding adhesion of pathogens[6]. Leaching surfaces have bactericidal agents incorporated into a given matrix and from here, the agent is able to steadily diffuse and kill surrounding bacteria. Silver and antibiotics are well-studied examples of such systems and have gained the most attention within this category (See Fig. 2). Silver has mainly been applied as nanoparticles that then degrades in order to release the encapsulated ions. Silver is non-toxic to mammalian cells and is able to coordinate to many types of proteins and enzymes in bacterial cells. The coupling blocks their biological function and destabilizes the cell wall and metabolism, causing cell lysis[7]. Antibiotics have been absorbed onto surfaces but also covalently attached with temporary labile bonds to create a steady release of the anti-bacterial agent. Finally, contact-killing systems kills bacteria only when in direct contact with the organism. The coupling of peptides and implementation of cationic phosphonium and ammonium groups have been used to create anti-microbial coatings (See Figure 2). The bactericidal effect originates from the strong electrostatic interaction with the cell membrane, which is able to disrupt and destabilize the membrane.

Current Challenges

The process of developing anti-microbial coatings is at present faced with a number of challenges such as having agents that works against a broad spectrum of organisms, fast acting, sufficient bacteriological testing and biocompatibility. Especially, anti-microbial activity are often based solely on *in vitro* testing, which is rarely sufficient to establish its potential in the final application.

When conducting such tests it is important to mimic the end system as close as possible. Here, *in vivo* experiments would give a more reliable and in depth analysis of the system but are on the other hand expensive and time consuming to conduct. Furthermore, having candidates that are both effective against many different organisms and fast acting are seldom biocompatible as well. Finding agents that are highly selective towards pathogens and have minimal impact on mammalian cells is important for use in relation to humans.

Specific Objectives

The aim of this project is to investigate the current state-of-the-art literature to identify possible candidates for antibacterial coatings and to develop new coatings that will prevent or reduce the number of CAUTIs.

References

1. H. Kiridis, Chalmers University of Technology (2011).
2. L. E. Fisher, A. L. Hook, W. Ashraf, A. Yousef, D. A. Barrett, D. J. Scurr, X. Chen, E. F. Smith, M. Fay, C. D. J. Parmenter, R. Parkinson, and R. Bayston, *J. Control. Release*, 202, (2015) 57–64.
3. A. E. Khoury, K. Lam, B. Ellis, and J. W. Costerton, *ASAIO J.*, 38 (1992) 174–178.
4. D. Campoccia, L. Montanaro, and C. R. Arciola, *Biomaterials*, 34 (34) (2013) 8533–8554.
5. R. Kaur and S. Liu, *Prog. Surf. Sci.*, 91 (3) (2016) 136–153.
6. J. Groll, Z. Ademovic, T. Ameringer, D. Klee, and M. Moeller, *Biomacromolecules*, 6 (2) (2005) 956–962.
7. E. M. Hetrick and M. H. Schoenfisch, *Chem. Soc. Rev.*, 35 (2006) 780–789.

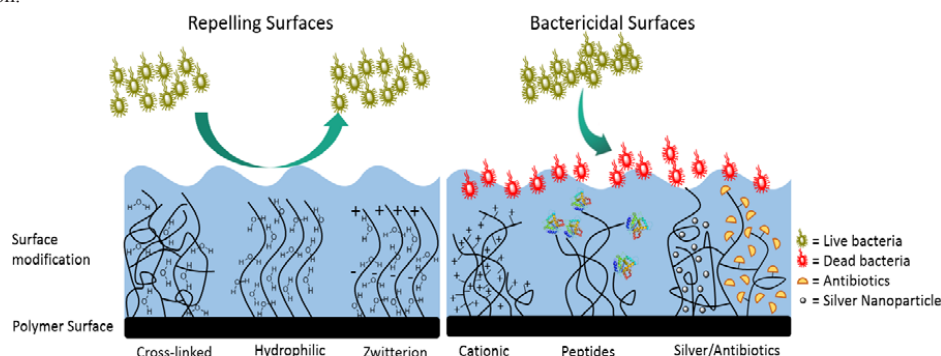


Figure 2: Schematic illustration of some of the working principles behind anti-microbial surfaces.



Božidar Aničić

Phone: +4525 2837
E-mail: boza@kt.dtu.dk

Supervisors: Kim Dam-Johansen
Weigang Lin
Hao Wu
Wei Wang, Chinese Academy of Sciences

PhD Study
Started: August 2015
To be completed: July 2018

Agglomeration in fluidized bed at high temperature

Abstract

The PhD project focuses on agglomeration in fluidized bed combustion of biomass. Bed agglomeration, as one of the main operational problems, is studied in order to understand the fundamental mechanisms, and to develop modelling tools and countermeasures that can be applied to minimize the problem.

Introduction

Fluidized bed combustion is a promising technology for efficient and flexible utilization of biomass to produce heat and power. However, bed agglomeration is one of the major operational problems that can influence bed hydrodynamics, change fluidization regime, and in severe cases cause defluidization [1]. It is primarily caused by interactions between bed material and biomass ash [2].

Objectives

The objectives of the PhD project:

- Understanding the fundamental bed agglomeration mechanism during biomass combustion at different operation conditions.
- Develop modeling tools to analyze agglomeration.
- Propose and evaluate the countermeasures to reduce bed agglomeration tendency.

Methodology

A small-scale fixed bed reactor and a thermogravimetric analyzer (TGA) are used to investigate the reactions between model potassium salts and model bed material (silica sand) under various conditions. Moreover, a lab-scale fluidized bed reactor is applied to study defluidization induced by model potassium compounds, and combustion of different types of biomass. The agglomerate samples are characterized by scanning electron microscopy coupled with energy-dispersive x-ray spectroscopy (SEM-EDX) and x-ray diffraction (XRD). In addition, CFD simulation of particle segregation in a fluidized bed is performed in order to evaluate the impact of continuous agglomerates formation on bed hydrodynamics.

Progress

Reaction between K_2CO_3 and silica sand

The interactions between sand particles and model potassium compounds (KCl , K_2CO_3 , K_2SO_4) have been studied in the fixed bed reactor. It was found that K_2CO_3 is able to react with silica sand forming agglomerates, and the other potassium species acts as physical glue to bind silica sand particles. Thus, the reaction between K_2CO_3 and silica sand was further investigated in the TGA. Figure 1 shows K_2CO_3 conversion rate under different conditions.

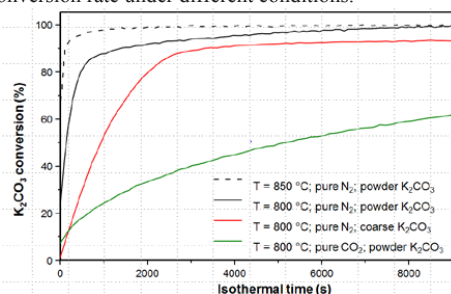


Figure 1: K_2CO_3 conversion under different operating conditions. K_2CO_3 :sand ratio = 0.03:1 wt.:wt.; premixing of reactants; 500 K/min heating rate.

The results show that the reaction rate increases with increasing temperature. With a large K_2CO_3 particle size the initial reaction rate was significantly reduced, and the final K_2CO_3 conversion degree reached 0.9. The presence of CO_2 strongly inhibited the reaction rate and reduced the final conversion degree. Based on the SEM-EDX results a plausible reaction mechanism is proposed. The reaction starts at the contact points between reactants and it is initially dominated by surface diffusion of the salt molecules into the silica

sand surface. This leads to the formation of a molten thin product layer that may cover complete sand surface. The reaction proceeds further by diffusion through the formed product layer.

Defluidization

Defluidization induced by different potassium species (KCl, K_2SO_4 , K_2CO_3 and $K_2Si_4O_9$) and their mixtures has been investigated in a lab-scale fluidized bed reactor. K-species were added to a sand bed and the reactor was heated up at a constant heating rate of 10 K/min, and with a constant gas flow until defluidization occurs (indicated by a sudden decrease of pressure drop over the bed). The temperature, at which defluidization occurs, is defined as defluidization temperature (DT). Figure 2 presents selected experimental results.

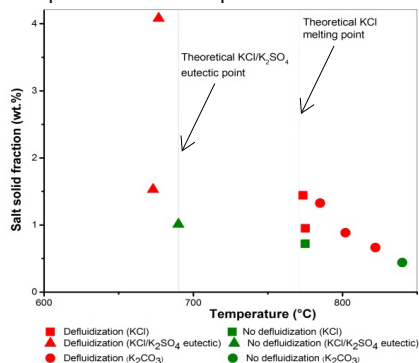


Figure 2: Defluidization temperature as a function of potassium content

A minimum weight ratio of salt to sand necessary for defluidization is 0.95 and 1.53 wt.% when adding KCl and KCl/ K_2SO_4 eutectic mixture up to 800°C, respectively. In these cases, DT corresponded to either KCl melting temperature (771 °C) or KCl/ K_2SO_4 eutectic point (690 °C). SEM-EDX analyses of the agglomerate samples reveal that the sand particles are covered by molten K-salts. However, addition of K_2CO_3 results in defluidization induced by reaction between K_2CO_3 and silica sand, as indicated by CO_2 release. The formation of potassium silicates is indicated by SEM-EDX analyses. The minimum salt content is 0.72 wt.% and the corresponding DT is 822 °C. As the salt content is increased to 1.5 wt.% DT decreases to 785 °C. When $K_2Si_4O_9$ is added, no defluidization is observed up to 850 °C for a high silicate content of 9.8 wt.%. The results of this work imply that defluidization can be induced by both, molten K-salts with low-viscosity and high-viscous K-silicates formed in reaction between potassium carbonate and sand.

CFD modeling of particle segregation

CFD simulation of particles segregation in a lab scale system has been carried out based on multi-fluid model. Experimental data from literature [3] are used for model validation. Different gas-solid drag, radial distribution and, solid pressure models are tested. It was found that

the fitting between experimental and simulation results is very poor when using standard gas-solid (Symalal O'Brien), and standard radial distribution and solid pressure models (Lun), as indicated at Figure 3. On the other hand, implementation of EMMS gas-solid drag force model [4], together with Ma-Ahmadi radial distribution and solid pressure models [5] improved simulation results and fitting to experimental data.

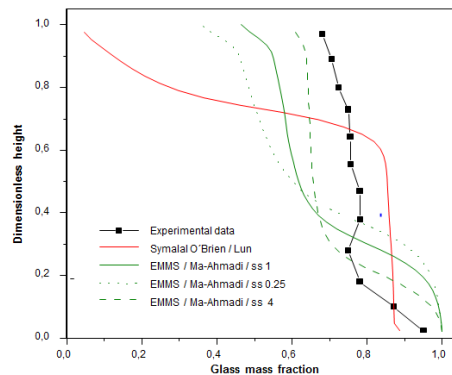


Figure 3: Comparison between simulation and experimental results

Furthermore, simulation results are very sensitive to solid-solid interaction, meaning that it is necessary to consider further modification or development of novel solid-solid interaction models in order to overcome general limitations of multi-phase approach and to improve the fitting between simulation and experimental results.

Future work

Biomass combustion experiments will be carried out in the lab-scale fluidized bed combustor. The impact of different types of biomass on bed agglomeration under well-defined operating conditions will be investigated. Countermeasures to reduce agglomeration will be evaluated.

Acknowledgment

This project is funded by Innovation Fund Denmark (DANCNGAS), Sino-Danish Center for Education and Research, and Technical University of Denmark.

References

1. M. Bartels, W. Lin, J. Nijenhuis, F. Kapteijn, and J. R. van Ommen, *Progress in Energy and Combustion Science*, vol. 34, no. 5, pp. 633–666, 2008.
2. B. Gattermig and J. Karl, *Energy & Fuels*, vol. 29, no. 2, pp. 931–941, 2016.
3. G. G. Joseph, J. Leboireiro, C. M. Hrenya, and A. R. Stevens, *AIChE J.*, vol. 53, no. 11, pp. 2804–2813, 2007.
4. W. Wang and J. Li, *Chem. Eng. Sci.*, vol. 62, no. 1–2, pp. 208–231, 2007.
5. G. Ahmadi and D. Ma, *Multiph. Flow*, vol. 16, no. 2, pp. 323–340, 1990.

**Konstantinos Asimakopoulos**

Phone: +45 5038 9784
E-mail: kona@kt.dtu.dk

Supervisors: Ioannis V. Skiadas
Hariklia N. Gavala

PhD Study
Started: February 2016
To be completed: January 2019

Syngas biomethanation by enriched anaerobic sludge in a trickle bed reactor

Abstract

Syngas has recently drawn attention as a gaseous feedstock for the biological production of chemicals and biofuels. Denmark is a country with an extended natural gas grid, so storage of energy deriving from unexploited biomass in the form of methane is highly important towards a sustainable development and a biobased economy. Our study focuses on the development and assessment of a bioprocess that will overcome the current bottlenecks of syngas bioconversion, that is the need to maintain sterile conditions and the mass transfer of sparingly soluble syngas compounds to the water-based media.

Introduction

In an industrial era that climate change is a real threat to the environment and as a result to the quality of our life, the transition towards a biobased economy is more urgent than ever; an economy in which the input from fossil fuels will be as little as possible, and fuels and chemicals will derive from renewable resources such as biomass.

Gasification of biomass results to the production of syngas with a very high (more than 90%) conversion efficiency. Syngas, consisting mainly of H_2 , CO and CO_2 , can be used as a substrate for carboxydrotrophic and hydrogenotrophic microorganisms towards the production of biofuels such as methane and alcohols. CH_4 is an important energy carrier and has the advantage to be easily introduced in the natural gas grid; therefore syngas biomethanation has the potential to contribute substantially to the storage of biomass-derived energy.

Existing syngas fermentation technologies face important challenges such as a) the need of maintaining sterile conditions due to the use of pure or well defined microbial cultures and b) the mass transfer of sparingly soluble syngas compounds (CO , H_2) to the water-based cultures.

Specific Objectives

The goal of this study is to propose and assess a methodology to remove the aforementioned bottlenecks. First, environments such as waste and wastewater treatment processes are a massive source for methanogenic microorganisms that come at no cost and

are already adapted in harsh conditions and secondly, trickle bed reactors (TBR) have been reported to provide higher mass transfer rates compared to conventional CSTR and bubble column bioreactors.

Design of the Bioreactor Setup

The designed TBR comprises of three main units, the gas cylinder, the trickle column and the liquid reservoir. The gas cylinder contains the gaseous substrate (H_2 , CO_2 , CO and CH_4), the trickle column contains packing material where biofilm is formed and the liquid reservoir acts as a sump that facilitates the recirculation of the liquid medium to the top of the column. A process flow diagram of the setup is presented in Figure 1. Syngas flows through the column where it is consumed by the microbes in the developed biofilm. The resulting gaseous mixture, after the bioconversion in the column, exits the reactor from a port positioned above the liquid level in the reservoir. The liquid is constantly recirculated from the reservoir to the column so that the bed is kept wet and the biofilm is provided with the necessary nutrients for its growth and maintenance.

After starting up, the bioreactor setup was subjected to specific adjustments aiming at keeping low and non-fluctuating concentration of liquid byproducts.

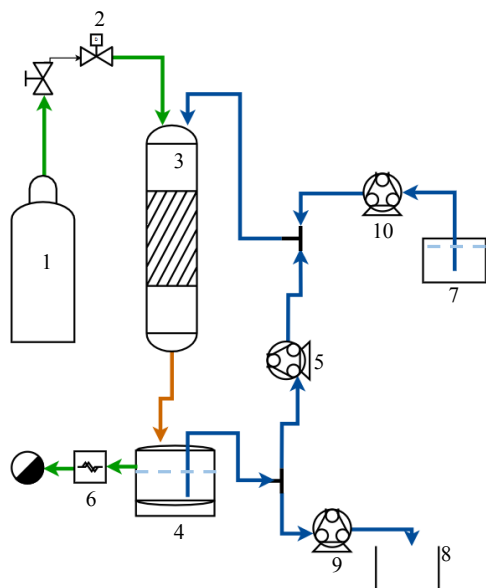


Figure 1: Process flow diagram of the bioreactor setup. 1: Syngas cylinder, 2: mass flow controller, 3: trickle bed column, 4: Liquid Reservoir, 5: Peristaltic Pump for liquid recirculation, 6: gas flowmeter. After the adjustment the following compartments were added 7: fresh medium container, 8: liquid effluent container, 9: Peristaltic pump for fresh medium inflow and 10: Peristaltic pump for liquid outflow. The green, blue and orange lines show the flow of the gas, liquid and combined gas-liquid, respectively

Inoculation of the bioreactor

The bioreactor was inoculated with enriched methanogenic mesophilic inoculum derived from anaerobic sludge. The enrichment process was necessary in order to segregate the microbes that can grow on syngas from the rest. This work was performed by a DTU project collaborator, PhD student Antonio Grimalt Alemany.

Results and Discussion

Primary results indicated that the liquid recirculation rate (LRR) is strictly connected to the fraction of the bed getting wetted and as a result higher LRR values led to a more uniform biofilm growth throughout the bed and higher CH_4 productivity rates. On the other hand, the hydraulic retention time (HRT) affected the concentrations of volatile fatty acids in the reactor due to carbon elongation phenomena from acetic acid which is the main byproduct. The maximum CH_4 productivity rate achieved so far was 2.1 mmol/l/h with a H_2 uptake rate of 7.1 mmol/l/h and a CO uptake rate of 3 mmol/l/h. The removal efficiency of CO and H_2 were at 86% and 91% respectively and the CH_4 yield reached 83% of its maximum theoretical value. These values are

comparable to the ones achieved in similar studies as presented in Table 1.

Table 1: Methane Productivity Rates comparison with literature on gaseous substrates based on CO , CO_2 and H_2

CH_4 Productivity Rate	Reactor Type	Reference
3.0 mmol/l/h	Trickle Bed	[1]
3.4 mmol/l/h	Trickle Bed	[2]
0.4 mmol/l/h	Membrane	[3]
2.1 mmol/l/h	Trickle Bed	This Study

Further experimentation is expected to lead to even higher values.

Conclusions

A trickle bed bioreactor was designed, assembled and operated with enriched mesophilic methanogenic anaerobic sludge under several different operational conditions. Preliminary results indicate that this is a promising technology for syngas biomethanation and with further optimization it is expected to surpass the highest productivity values reported so far in literature.

Acknowledgements

The research conducted is financially supported by DTU and Innovation Fund Denmark in the frame of SYNFERON project.

References

1. D.E. Kimmel, K.T. Klasson, E.C. Clausen, J.L. Gaddy, *Appl. Biochem. Biotechnol.* 28 (1991) 457–469.
2. K.T. Klasson, J.P. Cowger, C.W. Ko, J.L. Vega, E.C. Clausen, J.L. Gaddy, *Appl. Biochem. Biotechnol.* 24 (1990) 317–328.
3. S. Westman, K. Chandolia, M. Taherzadeh, *Fermentation*. 2 (2016)

**Christian Bach**

Phone: +45 4525 2949
E-mail: chrba@kt.dtu.dk

Supervisors: Krist V. Gernaey
Ulrich Krühne
Mads O. Albæk, Novozymes A/S

PhD Study
Started: March 2015
To be completed: April 2018

An in-situ measurement method for bubble size distributions in industrial pilot scale fermentation processes

Abstract

Mass transfer of oxygen from the gas phase to the liquid phase is the rate-limiting phenomenon in many industrial aerobic fermentation processes. This phenomenon is often described by the rate constant $k_L a$, which remains a key performance indicator for scale up and general operation of fermentation processes. The attributing variables to the rate constant, the mass transfer resistance k_L and interfacial surface area a , are however very rarely individually identifiable from standard experimental analysis. This co-dependency of the variables on the rate constant limits our understanding of how process conditions affect the mass transfer rate, and hence a tool for identifying them individually is required. An optical method for determining the interfacial surface area, based on bubble size identification has been developed using a high-speed camera and an endoscope. This *in situ* measurement illustrates the effect of process conditions on the size of the bubbles. The information of bubble sizes at different conditions is a valuable input to mechanistic models regarding gas-liquid mass transfer, for example computational fluid dynamics (CFD) models, in which the bubble size is a key input parameter.

Introduction

Aerobic fed-batch fermentations are generally rate limited by transfer of oxygen from the gas phase to the liquid. This is in particular the case for filamentous fungi fermentations due to the drastic increase in broth viscosity as the fermentation progresses [1]. A key parameter in these phenomena is the size of the gas bubbles in the broth, as this will determine the area available for mass transfer. A number of correlations exists which have been used in simple air-water systems, but they are not applicable for complex fermentation broth [2]. Alternatively, experimental methods for bubble size detection have been successfully developed for bubble column reactors using conductivity probes, or optical sensors [3]. These methods assume a certain flow direction of the gas bubbles, which is valid in a bubble column but not certain in stirred fermenters. Hence, there is a need for techniques that can determine the bubble size distribution in a turbulent flow inside industrial fermenters.

Specific Objectives

Develop a method that can measure the bubble size distribution of gas bubbles in industrial fermentation processes without relying on offline samples or modifications to existing fermenters. The developed

method relies on an endoscope and a high-speed video camera.

Method

The gas bubbles were detected using a 30 cm long and 10 mm wide Olympus surgical endoscope, which was used in combination with a Phantom Miro C110 high-speed camera from Vision research. The surgical endoscope is able to withstand sterilization, which is a crucial requirement when working with fermentation processes. The setup is able to capture 1200x1080 pixel images at 800 frames per second, which enables detection of bubbles even at high power inputs. The objects were illuminated by a 49 W LED matrix with a diameter of 9 mm, which delivers up to 6400 lm. A schematic drawing of the setup can be seen in Figure 1.

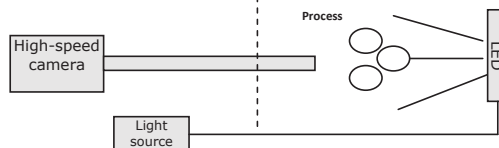


Figure 1 – Schematic illustration of the high-speed camera setup. The dashed line indicates the border between the process and the outside.

The collected images were analyzed in MATLAB to identify circular or elliptical shapes. The image detection algorithms were developed in collaboration with DTU-COMPUTE.

Results and Discussion

A 250 mL stirred vessel was fitted with the endoscope and the high-speed camera was used to test the technology in an aqueous medium containing 0.2 M $MgSO_4$. The test was carried out at different power inputs and aeration rates to test the sensitivity of the system. The images collected by the high-speed camera were analyzed and circular or elliptical shapes were identified. A common image is depicted in Figure 2, along with the image after object detection.

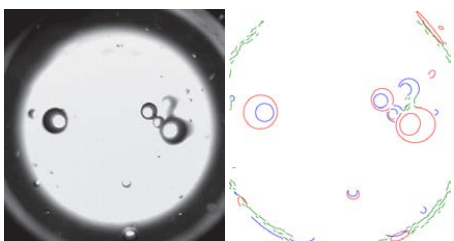


Figure 2: Captured image of bubbles during lab-scale test. The image on the left shows the raw image, and the figure on the right shows the image after image analysis.

Figure 2 shows a characteristic image from the setup, which emphasizes the capabilities of the optics. The image analysis algorithm identifies the objects in every frame, and various parameters are tuned in order to reject blurred or distorted objects. Data handling can be integrated automatically with MATLAB, but is currently carried out in batch mode.

The method was calibrated using well-defined glass beads with a fixed size of one millimeter. Using this calibration, it was possible to determine the bubble size distributions, which are depicted in Figure 3.

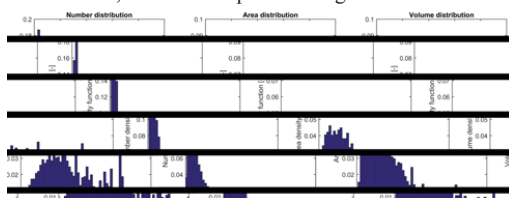


Figure 3: Number, area and volume distribution of bubble population in a 250 mL stirred vessel with a power input of 1.5 W/L. The Sauter mean diameter was determined to be 0.73 mm.

The size distribution shown in Figure 3 clearly indicates that it is important to distinguish between number, area and volume distribution when analyzing this data. The number distribution clearly indicates that the majority of

the bubbles are small, but larger bubbles account for the surface area available for mass transfer. For the conditions tested so far in this campaign the shape of the distributions were similar, but the mean and variance change.

Conclusion and Future Work

The developed method is able to capture bubble size distributions in a laboratory setting online and without altering the process. The method is fast enough to capture the motion of bubble at conditions similar to those observed at pilot scale. Being able to measure the bubble size distribution in situ and online enables novel process insights during the fermentation process.

The method will be tested in a pilot scale fermentation process at Novozymes A/S. This test will exemplify the applicability of the technology in an industrial setting, and will indicate the limitations of the technology. Bubble size distribution data is a key parameter in CFD simulations of aerobic fermentation processes and the gathered information can be applied directly and compared with previous findings [1].

Acknowledgements

The author would like to acknowledge the work of Mafalda Dias Gomes at PROSYS, who carried out the experiments in the laboratory. As well as Rayisa Moiseyenko from DTU-COMPUTE for her development of the image analysis algorithms.

The PhD project of Christian Bach has received funding from the Technical University of Denmark (DTU), Novozymes A/S and Innovation Fund Denmark in the frame of the Strategic Research Center BIOPRO2 (BIO-based PROduction: TOWards the next generation of optimized and sustainable processes).

References

1. C. Bach, J. Yang, H. Larsson, S. M. Stocks, K. V. Gernaey, M. O. Albaek, and U. Krühne, *Chem. Eng. Sci.*, vol. 171, pp. 19–26, 2017.
2. F. Garcia-Ochoa and E. Gomez, *Chem. Eng. Sci.*, vol. 59, no. 12, pp. 2489–2501, 2004.
3. P. M. Raimundo, A. Cartellier, D. Beneventi, A. Forret, and F. Augier, *Chem. Eng. Sci.*, vol. 155, pp. 504–523, 2016.



Franz David Böhner

E-mail: fdav@kt.dtu.dk

Supervisors: Jakob K. Huusom
Jens Abildskov

PhD Study
Started: February 2016
To be completed: October 2019

Plant Wide Monitoring and Control of Bioprocesses

Abstract

Plant wide control has been studied by chemical- and control engineers for more than three decades. By now the necessity of plant wide reasoning is widely accepted beyond academic circles. However, in contrast with the classical chemical industry, biochemical industries are more reluctant in changing their ways. This can be attributed to a variety of causes and goes as far as seeing production sites being run largely without the implementation of conclusive monitoring strategies or even feedback control. The ambition of the project is the derivation of a framework for the introduction of plant wide monitoring and control concepts into bioprocesses at industrial scale.

Introduction

Production processes that have been running for decades have seen changes for the better due to the involvement of capable engineers and operators. However, these heuristic findings, while robust in their applicability, are prone to be restricted to a local modus operandi. A first step toward gaining a deeper understanding as well as applying quantitative means to any process is the derivation of a reliable process model. Where this is not possible one should think about how to analyze a process qualitatively in a structured fashion.

A distinct feature of industrial bioprocesses in comparison to classical chemical plants is that the human supervisory control layer is much closer to the physical layer. I.e. this means that operators frequently change conditions on unit operation level, which can have drastic consequences on the surrounding up- and downstream line.

A large part of the process uncertainties can be attributed to short-lived product cycles and inconsistent feedstock (weather, region, pre-treatment, etc.) as well as the complications that arise when working with live organisms. The necessary adaptivity for dealing with these uncertain conditions is provided by keeping operators in the loop and would otherwise require sophisticated automation solutions.

Continuation of 1st Case Study: CP Kelco ApS

CP Kelco as one of the members of the BIOPRO[®] consortium was deemed an adequate choice as a first case study. Uncertainties in the processed biological

feedstock are the daily challenge in production, and the variability that is thereby induced into the process can only be handled by operators and engineers due to their extensive experience. A first step toward a minimization of uncertainties lies in the optimization of the process on unit operation level. To date, cake filtration is one of the workhorses of the biochemical industry when it comes to the separation of difficult slurries with a high concentration of suspended solids. However, the intermittent nature of dead-end filters alone already poses a challenge when they are deployed in a continuous downstream line (see Figure 1). Furthermore, most academic contributions in this field of expertise deal with constant pressure experiments conducted at laboratory or pilot scale – despite of the fact that cross-scale issues are well known for this type of process [1].

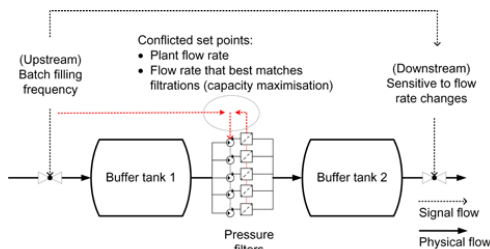


Figure 1: Set point hierarchy / conflicts: Flow rates that favor filtration performance may easily be in disagreement with the rest of the line for some time.

Therefore, an extensive analysis of full scale data was conducted using historical process data from the actual production site [2]. This revealed that the filters are not always run at conditions that maximize their capacities – which is undesirable due to this filtration step bottlenecking the plant frequently. A series of plant trials were conducted to investigate some of these properties in more detail. It should be noted that the uncertainty arising from the utilized biological feedstock requires the careful comparison of averaged values obtained in lengthy trials, if meaningful conclusions are to be drawn. Figure 2 elucidates this for a plant trial where the compressibility of filter cakes was assessed by imposing planned flow rate increases on a filter, while comparing to a stationary reference filter for a period of three weeks. Here the data clearly suggests that approximately 20 % of the filtration capacity is lost due to sudden cake compression, a conclusion that cannot be observed if just one or two filter cycles are compared (note the variability denoted by the height of the boxes). In everyday production, operators rely on flow rate in- and decrease to schedule the end times of the filters, unaware of the negative implications it has for the process as a whole. Scheduling of the filtration end times cannot be ignored, on the one hand due to the limited number of operators which are required to be idle in order to be able to reinitialize the filters, and on the other hand due to buffer tanks that could run full / dry, if too many filters ended concurrently.

This creates need for a predictive model to be deployed as a tool in production, allowing the operators to better schedule the filtrations, i.e. without having to rely on flow rate increases toward the end of a filtration. A model has been developed, largely based on classical filtration theory [3] with slight adjustments to better match the available measurements. The algorithm updates one parameter online at hand of the current cycle profile; the remaining parameters need to be identified at hand of historical data due to correlation issues. Two examples can be seen in Figure 3, notable the algorithm is able to capture a majority of the cycles, but some profiles and i.e. sudden changes cannot be described with high reliability. Ca. 250 predictions with the derived precision requirements are presented in Figure 4, and it can be seen that a majority of cycles can be predicted

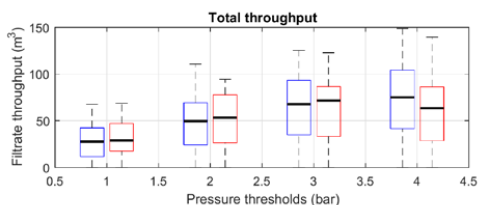


Figure 2: Plant trial: Evaluation of filtration capacity in the presence of flow increase at 3 bar (red) vs. a

reference filter operated at constant rates (blue). Evaluation period: Three weeks ~ 20 filter cycles each.

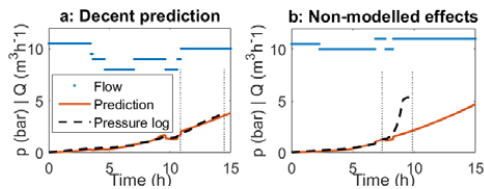


Figure 3: Prediction period between dotted lines. For some cycles the theory is descriptive, some outliers with extreme behavior cannot be captured. This is i.e. believed to depend on pre-coat inconsistencies and flow changes, thus there is a certain interdependence.

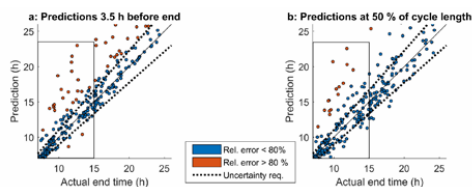


Figure 4: Parity plot showing ca. 250 cycles and their predicted end times at different points-in-time along the cycle profile.

with sufficient accuracy, however, a significant number of outliers remain, and a gradual implementation will have to show whether this is usable in the actual plant.

Conclusion and Outlook

The investigation of the pressure filtration area as part of the first case study has meritoriously elucidated the complications that arise from processing an uncertain feedstock. As a unit operation exposed to hybrid events in the context of a continuous downstream line, it is representative of many process steps encountered in the biochemical industry. Future work in the case study will encompass putting the unit operation into the plant wide context and plant wide analyses in general.

References

1. E. S. Tarleton and D. L. Hancock, "Using Mechatronics for the Interpretation and Modelling of the Pressure Filter Cycle," *Chem. Eng. Res. Des.*, vol. 75, no. 3, pp. 298–308, 1997.
2. "Analysis and Modelling of an Industrial Pressure Filtration using Process Data *," *IFAC-PapersOnLine*, vol. 50, no. 1, pp. 12137–12142, Jul. 2017.
3. C. Tien, "The conventional theory of cake filtration," in *Introduction to Cake Filtration*, 2006, pp. 13–16.



Kristian Barrett

Phone: +45 3057 3047
E-mail: kbaka@kt.dtu.dk

Supervisors: Lene Lange
Anne Meyer

PhD Study
Started: June 2016
To be completed: June 2019

Enzyme discovery for tuber processing pulps by SDC

Abstract

In China a massive extraction of starch from tuber crops are taking place, however the remaining processing pulp holds unexploited potential as e.g. animal feed, food ingredients, etc. To facilitate the farmers interest in using the pulp as animal feed it is necessary to upgrade the pulp. Due to too low nutritional content, the pulp as bulk product is not competitive as a source of animal feed. Increasing the protein content could make it more attractive as could converting the complex polysaccharides of the pulp into health promoting oligosaccharides by enzymatic hydrolysis of selected enzymes. The relevant enzymes are likely to be found produced by bacterial and fungal pathogens of the tuber crops in the field. However products derived from pathogenic microbes are not easily approved for industrial applications.

Introduction

Many genome assemblies are available in NCBI which have been more or less inspected for carbohydrate degrading enzymes. With development of new bioinformatics tools (such as Peptide Pattern Recognition [1]) and a continuously growing database of characterized enzymatic function and families [2] (Carbohydrate Active Enzymes database) more genes of previously unknown function can now be fully annotated and function-predicted.

Fungi are known to produce a lot of extracellular enzymes for degradation of all kind of plant materials but different species produce different enzymes which may be related to the substrate which the fungi prefer. To get an overview of which enzyme families and functions are present in different fungi, selected genome assemblies were screened *in silico* for enzymes with carbohydrate acting activities.

From this overview a subset of the enzyme functions relevant for tuber pulp conversion can be further investigated to identify the microbes with the broadest span of relevant enzymes for upgrade of industrial tuber processing pulp. In this way fungi known to decompose tubers may be found to share the same enzyme functions. Such candidates can be identified, cloned and expressed (Figure 1).

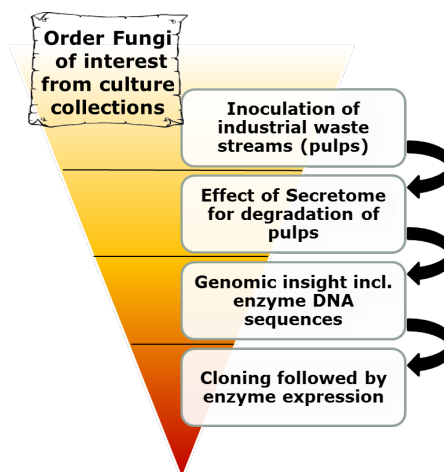


Figure 3 – A Pyramid Flowchart of the selection process of relevant fungal enzymes, believed to play an important role in the degradation of industrial processing pulps. The point of origin of the enzymes selected for expression is microbial strains obtained from culture.

The accumulation of processing pulp is growing proportional to the production of starch from tuber crops. This leads to increase in environmental pollution. If a large scale usage of the pulp could be developed the forthcoming environmental issues could be avoided and the underexploited biomass turned into nutritional animal feed possibly even with health promoting effect. The starch to pulp ratio depends on the processing techniques but a general example of a local (low efficient) processing unit takes 30 tons of sweet potato pr. day to generate about 25 tons of processing pulp and a starch yield of about 5 tons (Figure 2).

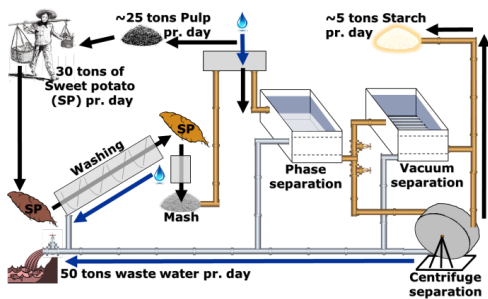


Figure 2 – Industrial extraction of starch from sweet potato. The farmer comes to the factory with the tuber crops which is converted into starch, waste water and processing pulp. The crops are washed and mashed before water is passed through, extracting the water soluble starch from the pulp. Next phase is to separate the starch from the water; done in a pool by phase separation. The starch is then pumped out from the bottom of the pool thus concentrated. Depending on the amount of tuber, either vacuum separation or centrifuge separation is used after the phase separation to be further concentrated.

External Collaborators



The processing pulp was obtained from the factory and selected fungi with large number of relevant secreted enzymes were incubated together in the lab-scale incubation. After 6 days of incubation the supernatant was separated from the non-soluble fraction (hereby separated from remaining processing pulp and fungal mycelium) and screened for relevant enzyme activities using AZCL assay at varying pH and temperature (Figure 3). The AZCL profile of various substrates correlated to the predicted enzyme functions (based on *in silico* analysis of genome assemblies).

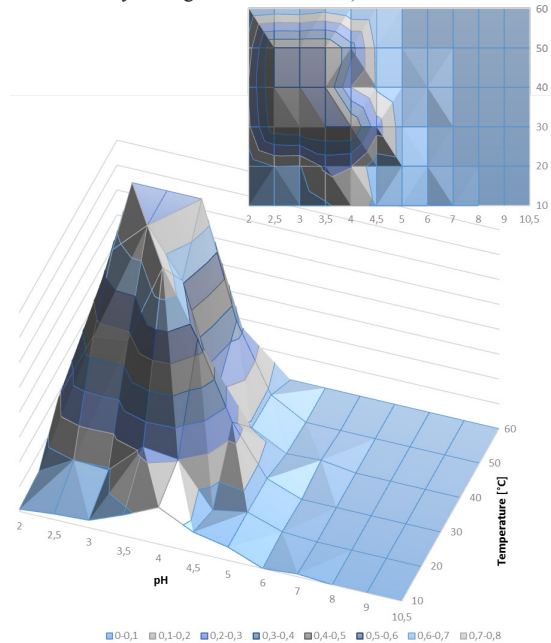


Figure 3 – Enzymatic hydrolysis of AZCL polysaccharide substrate after incubation of fungal supernatant for 18 hours with varying reaction temperatures (10, 20, 30, 40, 50 and 60 C) and pH (2.0, 2.5, 3.0, 3.5, 4.0, 4.5, 5.0, 6.0, 7.0, 8.0, 9.0 and 10.5). The height represents the absorbance created as a result of the hydrolysis of the dyed AZCL polysaccharide substrate. The surface plot is viewed twice; one from the side and another from the top down.

References

1. P.K. Busk, B. Pilgaard, M.J. Lezyk, A.S. Meyer and L. Lange, Homology to peptide pattern for annotation of carbohydrate-active enzymes and prediction of function. *BMC Bioinformatics* 18 (214) (2017) 1-9
2. V. Lombard, R.H. Golaconda, E. Dula, P.M. Coutinho B. Henrissat, The carbohydrate-active enzymes database (CAZY) in 2013. *Nucleic Acids Res.* 42 (D1) (2013) D490-D495



Chitta Ranjan Behera

Phone: +45 71435647
E-mail: cbeh@kt.dtu.dk

Supervisors: Gürkan Sin
Krist V. Gernaey

PhD Study
Started: August 2016
To be completed: August 2019

An empirical model for organic carbon recovery in a rotating belt filter

Abstract

The rotating belt filter (RBF) is an emerging and enabling technology for organic carbon recovery and also an alternative to the primary clarifier (PC), sludge thickening and dewatering. A recent study indicates that the RBF has the potential to reduce capital cost, footprint and improve energy and nutrient recovery in comparison to a conventional PC. Moreover, it is also believed that the RBF can fractionate carbon (enrichment of cellulose, namely toilet paper) based on particulate size, more efficiently than a PC. This study emphasizes the development of a simplified empirical model for describing carbon recovery in an RBF which requires a minimal number of experimental measurements to calibrate and can be used for plant-wide simulation.

Introduction

In recent years, resource recovery from wastewater treatment plants (WWTP) is gaining more attention and the organic carbon recovery in the form of toilet paper fibers is in focus in the present study. The wastewater (mainly in western countries) contains cellulose fibers that represent 30 - 50 % of the total suspended solids [1, 2]. These cellulose fibers originate from toilet paper. The use of the toilet paper per person is expected to reach a range of 10 - 14 kg per year [1] and it can further grow based on population growth and sanitary awareness. The dominant component in the toilet paper is fibrous cellulose which has a slower microbial hydrolysis rate. The cellulose can directly enter into the activated sludge (AS) process if it is not efficiently separated in the primary treatment stage.

The primary treatment in a wastewater treatment plant (WWTP) is crucial, and its role in fostering the performance of anaerobic digestion (AD) by diverting more carbon to the AD is gaining more and more attraction. In a traditional WWTP, the primary clarifier (PC) is one of the unit operations (for primary treatment) which works based on gravity separation to remove total suspended solids (TSS) and lower the biological oxygen demand. However, the footprint and capital cost associated with it are not competitive enough to meet the modern plant design philosophies (such as higher carbon recovery, compact size, etc.). A recent study [1] confirms that the cellulose fibers can be efficiently recovered by using a rotating belt filter

(also known as Salsnes filter) with a fine mesh size of 0.35 mm. It is (as shown in Figure 1) predominantly used as a mechanical treatment with special focus on achieving a higher suspended solids removal, and it works based on cake filtration and sieving. The sludge collected from the RBF is enriched in cellulose fibers (approximately 80 - 90 % of the recovered organic mass [1, 2]) and has significantly higher volatile solids content with excessive methane production potential compared to sludge collected from a traditional primary clarifier (PC) (cellulose fiber fraction is only 30 - 40% of recovered organic mass) [1]. The suspended solid removal depends on multiple operating conditions (such as sieving rate, water flow rate, fine mesh size, etc.) and inlet wastewater constituents (mainly TSS).

Literature review suggests that only a few studies are available related to developing a mathematical model for the rotating belt filter [3, 4]. The mechanistic model presented recently by De Groot et al. [3,4] is mainly used for design exploration and sizing of the RBF. However, its application for plant-wide analysis may not be suitable due to the computational limitations (considering plant-wide simulation). Moreover, calibration of the mechanistic model parameters may also need significantly more effort (as it requires measurement of specific cake mass, influent TSS, local removal efficiency, total flow resistance, etc.). Therefore, a simplified model such as an empirically based model with a lower number of model parameters will be more pragmatic to initiate

plant-wide assessment studies of RBF performance

Results and discussions

The purpose is to describe TSS removal performance in the RBF, which can then be used in the plant-wide assessment. Therefore a simple model is identified from the trends observed in experimental datasets reported in the literature [5]. The proposed RBF model (as mentioned in Equation 1) relates the TSS removal efficiency to influent TSS concentration. It has only two parameters (such as $K_1 - 1.14$ and $K_2 - 2.87$) which are determined by using a robust regression technique. Here each residual is weighted by using the Cauchy weight (w_i): putting a higher weight on small residuals and lower weight to large residuals. W_i is updated recursively in order to reduce the influence of outliers. The tuning parameters values such as $tune - 2.385$ and $h - 0$ are set by trial and error procedure in order to build higher accuracy model.

$$\eta_{TSS} = 100.(1 - k_1.e^{-k_2.TSS_{in}}) \dots\dots\dots(1)$$

The adjusted regression coefficient (R^2_{adj}) for the developed model is found to be 0.87, which indicates that the model is not overfitted and able to capture the pattern despite the wide variation in the dataset (as shown in Figure 1 b). Further, the model is also tested with two independent data sets (as reported in Figure 1 -

c, d). The model is clearly able to predict the removal efficiency with higher accuracy (within 95 % confidence interval).

Conclusion

In this study, an empirical model is proposed for prediction of organic carbon recovery in an RBF. The developed model is simplified and requires few number of measurements to calibrate. Therefore, it can use in various applications such as plant-wide evaluation.

References

1. C. Ruiken, G. Breuer, E. Klaversma, T. Santiago, M. Van Loosdrecht. Water research 47 (1) (2013) 43-48.
2. D. S. Ghasimi, Y. Tao, M. de Kreuk, B. Abbas, M. H. Zandvoort, J. B. van Lier, Water research 87 (2015) 483-493
3. DeGroot, C. T., Sheikholeslamzadeh, E., Santoro, D., Sarathy, S., Lyng, T. O., Wen, Y., ... & Rosso, D. (2016).Water Environment Federation, 2016(14), 1158-1168.
4. Franchi, A., Williams, K., Lyng, T. O., Lem, W., & Santoro, D. (2015). Proceedings of the Water Environment Federation, 2015(13), 1743-1749.
5. Franchi, A., & Santoro, D. (2015). Water Practice and Technology, 10(2), 319-327.

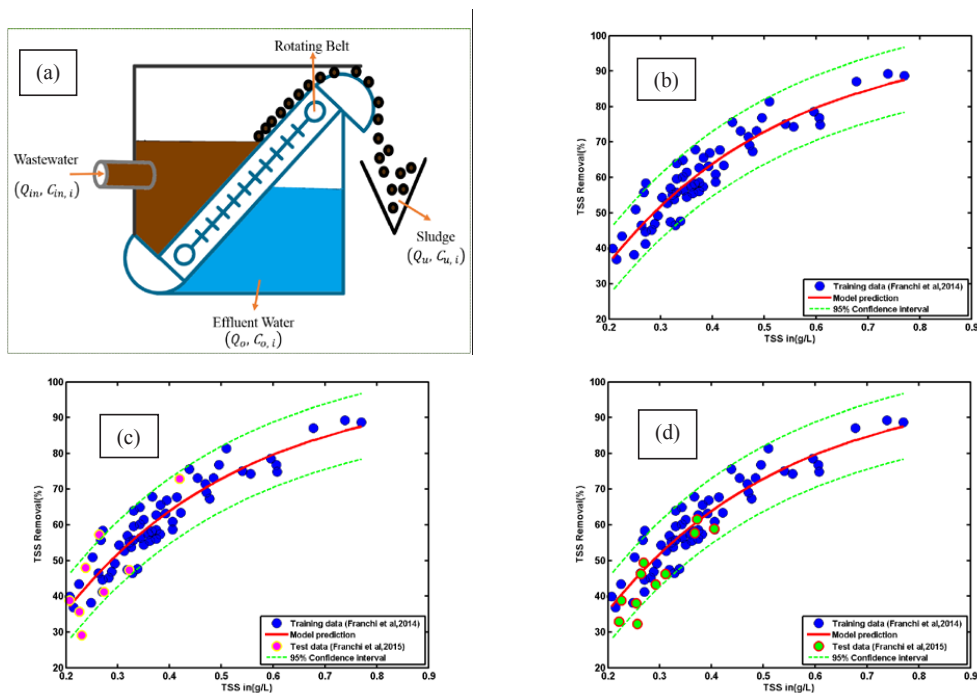


Figure 1: (a) Schematic diagram of the rotating belt filter, (b) development of organic carbon recovery model on training dataset (c, d) validation of the model on independent datasets



Joseph Asankomah Bentil

Phone: +45 5032 5190
 Email: joben@kt.dtu.dk

Supervisors: Anne S. Meyer
 Lene Lange
 Anders Thygesen
 Moses Mensa

PhD Study:
 Started: January 2015
 To be completed: December 2017

Enzyme production from agro-industrial residues for local application: a sustainable approach in Ghana

Abstract

Agro-industrial residues are produced in vast quantities from agricultural and industrial processes. However, they are posing environmental threat and generating greenhouse gases by disposal and burning due to their underutilization especially in developing countries like Ghana. This has raised research concern to seek alternative uses for these residues. The present study seeks to produce blend of enzymes from these residues that are mostly glycoside hydrolases fungal sources using simple technologies.

Introduction

Large quantities of agricultural residues are generated annually in Ghana from post-harvest activities (Table1). Agricultural residues are heterogeneous materials that are lignocellulosic in nature and mainly composed of cellulose, hemicellulose and lignin. This heterogeneity gives the plant its rigidity and defense against biological attack. The composition and proportions of these polysaccharides vary between plants. The polysaccharides are biodegraded by the production of enzymes during the growth of microbes on the plant residues [1,2]. Fungi are predominantly responsible for lignocellulosic degradation [3]. These organisms degrade the residues by using them as carbon and energy sources and usually depend on the composition of the residue. One group of fungi that are capable of efficiently degrading lignocellulosic residues is the white-rot fungi. White-rot fungi are wood-rotting species and constitute about 90%. They are capable of producing wide range of plant polysaccharide-degrading enzymes during the degradation of these residues [4]. The production of enzymes from these residues by white-rot fungi could be an alternative approach to add value to these residues regarded as “wastes”. Secondly, the enzymes could be used for local application for generation of sugars for ethanol production. This

strategy can help achieve a sustainable process by reducing the high dosage of commercial enzymes application. The present study focused on assessing the enzyme profile of some selected agro-industrial residues obtained from processing sites in Ghana.

Table 1: Production of different agricultural crops in Ghana for 2008 and estimated potential of residues

Crop	Crop Production (x1000 tonnes)	Type of residue produced	Residue to product ratio	Residue(wet) x1000 tonnes	Residue(dry) x1000 tonnes	Residues energy potential(PJ)
Maize	1,100	Stalk	1.5	1650	1403	25.76
Sorghum	350	Stalk	2.62	917	779	15.59
Cocoa	700	Pods, husk	1	700	595	10.84
Millet	160	Stalk	3	480	408	7.44
Oil palm fruits	1,900	EPB	0.25	475	190	7.37
Rice	242	Straw	1.5	363	309	5.65
Coffee	165	Husk	2.1	347	295	0.04
Coconut	316	Shell	0.6	190	171	2.01
Sugarcane	145	Baggasse	0.3	44	11	0.58
Total				5166	4161	75.28

Data taken from Quarthey and Chýlková,[5]

Results

Table 2: Chemical composition of some agricultural residues

Residue	Dry matter (%)	Ash (%)	Cellulose (%)	Xylose (%)	Klason Lignin (%)
Cocoa pod husk	87.4	11.6	26.6	6	30.3
Corn husk	92.4	11.2	41.4	29.2	5.2
Rice husk	91.3	20.2	30.8	10.6	21.6
Saw dust	89.8	1.7	29.5	7.3	28.9
Pretreated barley straw	95.8	7	66.3	3.5	26.6

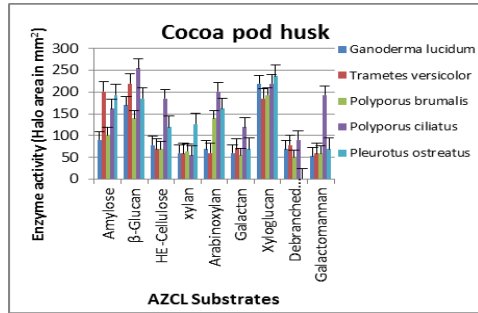


Fig. 1: Enzyme activities profile using cocoa pod husk as solid substrate for 15days

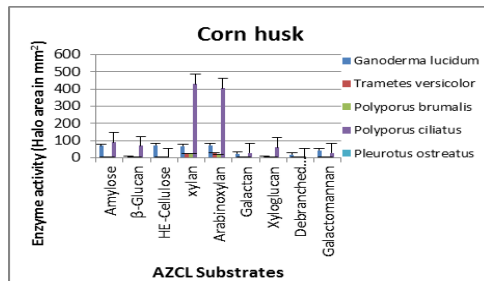


Fig. 2: Enzyme activities profile using corn husk as solid substrate for 15days

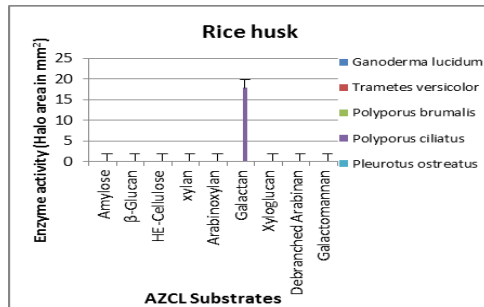


Fig. 3: Enzyme activities profile using rice husk as solid substrate for 15days

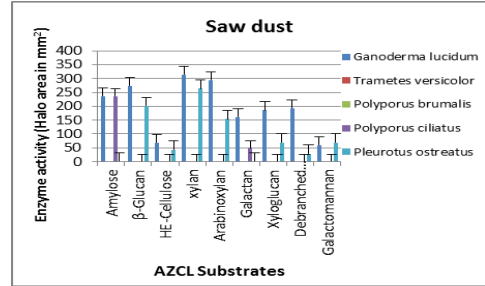


Fig. 4: Enzyme activities profile using saw dust as solid substrate for 15days

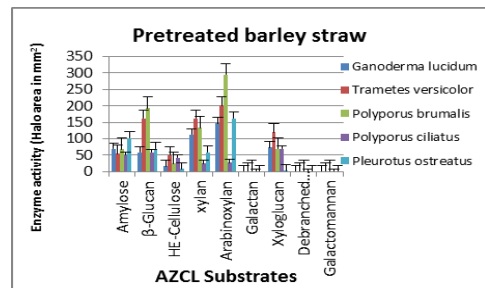


Fig. 5: Enzyme activities profile using pretreated barley straw as solid substrate for 15days

Conclusions

The profile of enzymes produced from residues largely depends on the nature and composition of the biomass residue used and their suitability to support growth

Acknowledgements

Sincere thanks to DANIDA Fellowship Centre for financial support

References

1. M. Choudhary, S. Dhanda, S. Kapoor, G. Soni, Chinese Mushroom, 43 (2009) 223–226.
2. A. Husaini, F. Fisol, J. Biochem. Technol. 3 (2011) 245–250.
3. C. Sánchez, Biotechnol. Adv. 27 (2009) 185–194. doi:10.1016/j.biotechadv.2008.11.001.
4. J. Rytioja, K. Hildén, J. Yuzon, A. Hatakka, R.P. de Vries, M.R. Mäkelä Microbiol. Mol. Biol. Rev. 78 (2014) 614–49. doi:10.1128/MMBR.00035-14.
5. E.B.O.T. Quartey, J. Chýlková, Adv. Environ. Biotechnol. Biomed. (2012) 235–239.



Jonas Bisgaard
Phone: +45 20837204
E-mail: jonbis@kt.dtu.dk

Supervisors: Krist V. Gernaey
Jakob K. Huusom
Ole Skyggebjerg, Freesense ApS

PhD Study
Started: September 2017
To be completed: August 2020

Application of novel free-floating sensor device: Flow characteristics in stirred vessels

Abstract

In this initial study, novel free-floating sensor particles developed by Freesense ApS have been tested in a pilot-scale stirred tank reactor ($V = 0.7 \text{ m}^3$) at different impeller speeds. Circulation times and spatial distributions were determined based on measurements of hydrostatic pressure by the sensor particles. The determined circulation times were proportional to experimentally determined mixing times, which has proven the sensor particle as a powerful tool for characterization of mixing during fermentation processes.

Introduction

As the sizes of bioreactors in an industrial process increases (i.e. scale-up), practical limitations concerning design and monitoring emerges. Despite the fact that CFD is considered a potentially useful tool to better understand the effects of scale on bioreactor performance, its practical usefulness is hampered by the lack of full-scale bioreactor data, providing a detailed picture of the real conditions in a tank, and not just at a single point. With technological advances it is now possible to fit multiple sensors into free-floating particles with reasonable sizes that can gather data on both gradients in process parameters and information about the flow characteristics throughout the bioreactors.

Two useful features about the flow can be determined by the sensor particles: Axial distributions and circulation times. Circulation time is proportional to the mixing time and is a useful measure of the degree of mixing in the bioreactor. The mixing time in a stirred reactor can be approximated by $t_m \approx 4t_c$ [1] or by $t_m \approx 5t_c$ [2].

Specific Objectives

Development of a simple method for determination of axial distributions of the sensor particle and determination of circulation times inside stirred bioreactors, and to show that the calculated circulation times are correlated with the corresponding mixing times, determined by tracer responses under the same conditions.

Results

Figure 1 shows the axial distributions of the sensor particles at impeller speeds: $N = 60 \text{ rpm}$, $N = 115 \text{ rpm}$, $N = 175 \text{ rpm}$ and $N = 230 \text{ rpm}$. Four sensor particles were used in each experiment. The y-axis is normalized to the liquid height (i.e. 0 = top and 1 = bottom) and the x-axis shows the percentage of the total time that the particles spent in each compartment. The average axial velocity can be read from the colorbar.

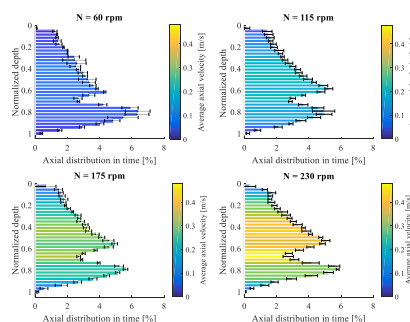


Figure 1: The axial distributions of the sensor particles in different compartments of equal size and at different speeds of impeller rotation. The y-axis is normalized to the liquid height (i.e. 0 = top and 1 = bottom) and the x-axis shows the percentage of the total time that the particles spent in each compartment. The average axial velocity can read from the colorbar.

The determined circulation time does not yield a single value, but rather a distribution. An example is shown in Figure 2. The distribution gives an overview of all the circulation times that the particles experience and how common they are. In this case, a circulation time of little less than 1 second is the most probable, while the mean circulation time is around 2 seconds.

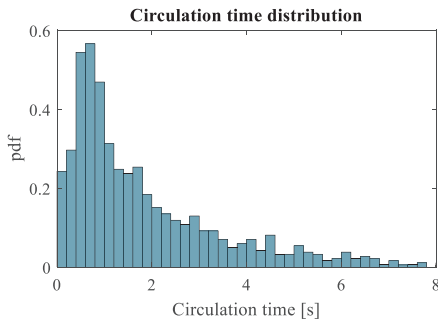


Figure 2: Example of a probability density function of the circulation times determined by the sensor particles. The distribution gives an overview of all the circulation times that the particles experience and how common they are.

A comparison between the mean circulation times determined by the sensor particles and experimentally and theoretically determined mixing times are shown in Figure 3. The circulation time were determined at four different values of Reynolds number in the turbulent region.

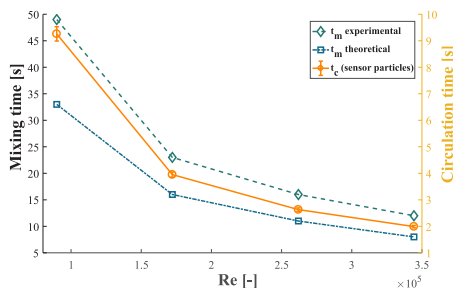


Figure 3: Determined mean circulation times (○) and a comparison with both experimentally [3] (◇) and theoretically (◻) determined mixing times under the same conditions. It is evident that the circulation times and mixing times are correlated.

Discussion

It is evident that the axial distributions of the particles are independent of the impeller speed, except at low degrees of agitation. It is likely that this is due to fact that the drag force and small a density deviation between the particle and the liquid has higher impact at low impeller speeds. It appears that the particles move in the same pattern, but with higher velocities (compartments are visited more often but at shorter time

intervals). This kind of data can be used to detect areas with deficient mixing inside large-scale bioreactors.

The circulation time seems to correlate very well with the experimental and theoretical mixing times. However, at low values of Re, the theoretical mixing deviates. The low standard deviation in the mean circulation times, together with the correlation with the experimental mixing times, suggests that the particles can be used as a reliable method to determine circulation times in stirred reactors.

Conclusions

- The axial distributions of the sensor particles are independent of impeller speed, N (more times through compartments, but at higher velocities).
- The circulation times determined by the sensor particles correlates with the experimental and theoretical mixing times: $t_c \approx (1/4) t_{m,theoretical}$ and $t_c \approx (1/6) t_{m,experimental}$.

References

1. Voncken, R. M. (1966). Circulatierstroming en menging in geroerde vaten. PhD thesis, University of Rotterdam.
2. Khang SJ and Levenspiel O (1976), New scale-up and design criteria for stirrer agitated batch mixing vessels, Chem Eng Sci 31,569-577.
3. Pickering, C. and Johnson, A (2015). DTU course report. 1C Agitation.



E-mail: **Pau Cabañeros López**
pacalo@kt.dtu.dk

Supervisors: Anna Eliasson Lantz
Krist V. Gernaey

PhD Study
Started: January 2017
To be completed: December 2019

Dynamics of physiological adaptation of yeast to main inhibitors found in lignocellulosic hydrolysate: a single cell analysis approach

Abstract

The production of 2G bioethanol is often limited by the inhibitors generated during the pretreatment. The tolerance of yeast to such compounds can be improved by exposing it to controlled concentrations of inhibitors in an adaptation step. In this project, flow cytometry was used to study how different physiological features of yeast change during the adaptation step. The cell membrane integrity, potential and cytosolic ROS concentration were monitored during 9 fermentations with different concentrations of inhibitors. The results showed how these features are affected due to the inhibitors and how they change as the culture adapts to the media. These experiments also gave valuable insights on how the individual and synergic effect of the inhibitors affect the cell culture.

Introduction

The inhibitors generated during the pretreatment of lignocellulosic biomass inhibit the growth of yeast, reduce their yields and productivities and limit the possibilities for the production of second-generation (2G) bioethanol. In order to improve these processes and to achieve robust and efficient fermentations, it has been suggested to enhance the tolerance of yeast by exposing them to controlled concentrations of inhibitors in a step prior to the fermentation, a propagation step [1]. In this step the cells get adapted to the hydrolysate and get ready for the main fermentation step.

Flow cytometry is a versatile tool that allows to target and analyze specific physiological properties of the cell culture at a single cell level. This results in the possibility to analyze thousands of cells within a few seconds, and to get detailed information about the different subpopulations in the cell culture. In this study 3 different physiological features were targeted: the membrane integrity (relates to cell viability) the membrane potential and the cytosolic ROS concentration (both relate to cellular stress). All features were monitored during the course of 9 fermentations containing different combinations of inhibitors.

Specific Objectives

The objective of this study was to elucidate the individual and combined effects that inhibitors typically found in hydrolysate have on the physiology of *Saccharomyces cerevisiae* during the course of a fermentation. 3 inhibitors (vanillin, furfural and acetic

acid) representing the main inhibitory groups found in 2G feedstocks (phenolic compounds, furan derivatives and weak acids respectively). A 2³ full factorial design with a central point and low and high concentrations of each inhibitor was used for the experimental design. Samples for HPLC, OD₆₀₀ and flow cytometry were taken every 1.5 hours during the course of the fermentations.

Results and Discussion.

The results showed the dynamics of adaptation and the changes on the targeted physiological features during the different fermentations. The results are classified in 1) single-factor effects, 2) two-factor effects and 3) three-factors effects (Figure 1). Whilst cells growing in the presence of only vanillin or furfural showed a slightly extended lag phases (of 2 to 3 hours), the cells growing in the presence of acetic acid showed a very extended lag phase of 10 hours (Figure 1, 1st row). During the lag phase the cell culture experienced a decrease in the membrane potential, and an increase in the concentration of cytosolic ROS, which indicates high metabolic stress in the cells. However, as the fermentation took place, detoxification and adaptation occurred, restoring the initial values for the membrane potential and cytosolic ROS, and resulting in the start of the cell growth. The viability of the cell culture (measured by the membrane integrity) remained close 100% during all the fermentations. When two inhibitors were used simultaneously, two different behaviors were observed.

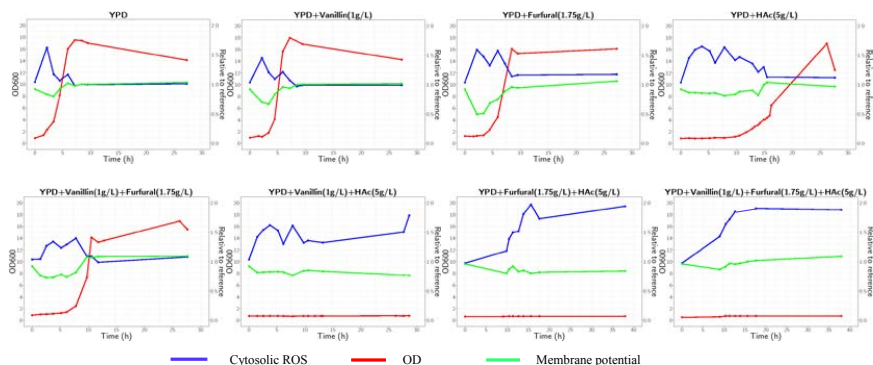


Figure 1: Membrane potential, cytosolic ROS concentration and optical density.

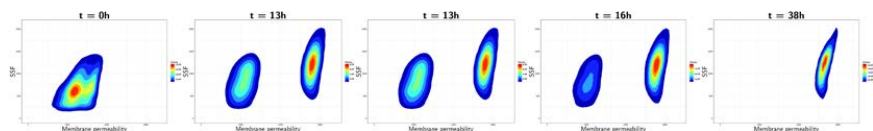


Figure 2: Cell viability in the experiment with three inhibitors. The population on the right represents alive cells whilst the population on the left represents dead cells.

In the combination vanillin-furfural, an extended lag phase of 5 hours was observed. This lag phase was larger than the one obtained when each inhibitor was used individually (the detoxification took longer time). As previously observed, the membrane potential and the cytosolic ROS were altered, indicating a state cellular stress. The combinations including acetic acid resulted in a complete inhibition of the cell growth and in persistent high levels of ROS and low membrane potential. Despite the high metabolic stress no loss of viability was detected in these experiments. The combined effect of the three inhibitors resulted in high metabolic stress and in an increasing loss of cell viability (Figure 2).

Phenolic compounds and furan derivatives inhibit the glycolysis at different steps, limiting the production of ATP and NADH+H. Without these compounds the cells cannot grow and struggle to survive (showing high cellular stress). However, if the concentration of inhibitors is not high enough, the cells are able to detoxify them and initiate a normal growth phase. Acetic acid has an inhibitory effect closely related to the pH of the media. When the pH outside the media is below the pKa of acetic acid, it moves the equilibria towards the protonated form. The protonated acetic acid can freely penetrate the cell membrane and enter the cell, where it finds a pH higher to its pKa. In consequence it gets deprotonated and the internal pH of the cells decreases, causing a situation of cellular stress [2]. In order to keep the internal pH stable, the cells actively pump out the protons using the ATP generated

in the glycolysis. When the glycolysis is completely inhibited (either due to high concentrations of one inhibitor or to a combination of two inhibitors) the availability of ATP becomes very limited, hindering the cell to maintain the internal pH and causing loss of viability (situation described in the Figure 2).

Conclusions

The dynamics of physiological change and adaptation of yeast to different inhibitors, and the mechanisms of inhibition have been studied in this project. The knowledge gained through this project will be used to optimize the propagation step in order to develop robust cell cultures able to increase the yield and productivity of 2G bioethanol processes.

Acknowledgments

Professor Nils Arneborg and the PhD candidate Chuen Tao Peng from the Food Science Department at the University of Copenhagen are both acknowledged in this project. The Technical University of Denmark, EUDP, MEC (Maabjerg Energy Center), the University of Copenhagen, Novozymes A/S and Vestforsyning are also acknowledged in this project.

References

1. Tomás-Pejó, E., & Olsson, L. 8(6)(2015) *Microbial Biotechnology*, 999–1005.
2. Freitas, C., Neves, E., Reis, A., Passarinho, P. C., & Da Silva, T. L. *Applied Biochemistry and Biotechnology* 168(6) (2012) 1501–1515.



Giovanni Cafaggi
Phone: +45 4525 2837
E-mail: gioc@kt.dtu.dk

Supervisors: Peter Arendt Jensen
Peter Glarborg
Kim Dam-Johansen

PhD Study
Started: January 2017
To be completed: December 2019

Alternative liquid fuels in burners optimized for low NO_x emissions and high burn out

Abstract

The marine industry is changing with new demands concerning high energy efficiency, fuel flexibility and lower emissions of NO_x and SO_x. A collaboration between the company Alfa Laval and Technical University of Denmark has been established to support the development of the next generation of marine burners. In this framework, the purpose of the present study is to support the development of a new generation of burners. To this end Computational Fluid Dynamic simulations and experimental methods will be used. A spray characterization setup has been built and used, as a first step to gather detailed knowledge about the influence of fuel spray conditions on marine utility boiler flames.

Introduction

On ships of large size, auxiliary boilers are used to meet the steam demand when the heat recovery system of the main engine is not sufficient. Currently, the marine sector is confronting new demands regarding these boilers. It is foreseen that in the next years legislators will demand decreased NO_x, SO_x and particulate emissions in coastal areas. Moreover, ship owners are increasingly interested in fuel flexibility: this would enable them to use the cheaper fuel on the local market instead of running solely on heavy oil fuels. The possibility to use renewable fuels on ships would also help in decreasing their net CO₂ emissions and fuel switching could be done according to the local legislation. An attractive application would be to use a relatively cheap renewable fuel, such as pyrolysis oil produced from wood. This fuel has some limitations as high water content, viscosity and acidity. Pyrolysis oil can be combusted in swirl stabilized burners, however only very limited work have been done to optimize burners using pyrolysis oil. The specific boiler object of this study uses a swirl stabilized liquid fuel burner, with a pressure swirl spill-return atomizer.

Specific Objectives

The goals of the project is to support the development of new marine burners that can cope with the above-mentioned demands, providing the partner companies with a technology that will help their future global competitiveness, while adding to the current knowledge

in the use of renewable energy and providing improved and verified CFD calculations on swirl stabilized flames. The first priority is to evaluate and test the combustion of multiple types of fuels, both liquid and gaseous, in the boiler and possibly improve its performances with a new burner geometry; the second is to minimize emissions of NO_x, particulates and unburnt hydrocarbons.

At this stage of the project, the current goal is to improve them to use the cheaper fuel on the local market instead of running solely on heavy oil fuels. The possibility to use renewable fuels on ships would also help in decreasing their net CO₂ emissions and fuel switching could be done according to the local legislation. An attractive application would be to use a relatively cheap renewable fuel, such as pyrolysis oil produced from wood. This fuel has some limitations as high water content, viscosity and acidity. Pyrolysis oil can be combusted in swirl stabilized burners, however only very limited work have been done to optimize burners using pyrolysis oil. The specific boiler object of this study uses a swirl stabilized liquid fuel burner, with a pressure swirl spill-return atomizer.

CFD Simulations

Experimental and computational methods have been used in the past for simulating both liquid fuel flames and the atomization processes [1] [2] [3]. Results obtained via Computational Fluid Dynamics (CFD) provide detailed information about the local temperatures, compositions and flow fields within the furnace chamber [4]. However, due to its stochastic [5] nature and to the very small length- and time-scales at which it takes place, to simulate the droplet formation process with reasonable accuracy, huge computational resources would be required. To overcome this issue, the spray has not been directly simulated, and the fuel is instead injected into the computational domain as already formed droplets. The commercial software ANSYS CFX has been used to do 3D CFD simulations of the boiler. During the simulation campaign, several models have been tested for turbulence, radiation and

reaction chemistry. For turbulence and radiation, the Shear Stress Transport model and the discrete radiation model have been used. Being the CO emissions of interest for the project, the combustion was simulated with a two-step global reaction (Reactions 1-2) [6] [7], while the NO_x formation can be calculated by post-processing of the results. Thanks to a sensitivity analysis, the size of the particles used to simulate the fuel spray was singled out as a crucial factor for flame stability and simulation accuracy. No documentation is given from the manufacturers regarding droplet size and velocity distribution, and the range of estimates obtained using correlations found in literature [8] proved to be too broad. Therefore, a spray characterization setup has been built to observe the atomization quality of the nozzle and gain a better understanding of the atomization process at different operating conditions and for different fluids.

Spray Setup

The spray characterization setup was built to work at the same operating condition of the actual burner. A preliminary measuring campaign has been conducted by using water as a fluid, but the setup should be able to handle also water-glycerol mixtures, thus reproducing the physical characteristics of fuels for spray analysis [9] [10]. The spray generated with the setup is then captured with an optical system and the pictures analyzed with a tailor made software to obtain information about droplet size and velocity distributions [11].

Current Results and Conclusion

To prepare the CFD simulations a number of different models, parameters and algorithms has been tested. While not universal and limited to the software used, the obtained combination can be considered as a starting point for future modelling. During the CFD study insights in the boiler operation has been obtained: fuel conversion, vortex shedding frequencies in different parts of the geometry and positions of the recirculation zones have been determined. In addition, a sensitivity analysis showed that under the same conditions, a

change from 10 to 25 μm of droplet mean diameter, leads to flame lift off. Using the spray setup, it was possible to measure droplet size and velocities in different regions of the spray (Fig.1). The data thus obtained has now been used to improve the accuracy of the CFD, bringing us one step closer to predict burner performances through computational methods.

Acknowledgements

The author would like to express his gratitude to the Blue INNOShip project and the Chemical Engineering Department of DTU for funding this PhD project.

References

1. P. Jenny, D. Roekaerts, N. Beishuizen, Prog Energ Combust 38 (2012) 846-887.
2. M. Linne, Prog Energ Combust 39 (2013) 403-440
3. Z. Ling, X. Zeng, T. Ren, H. Xu, Appl Therm Eng 79 (2015) 117-123.
4. I. Bonefačić, W. Igor, P. Blechich, Appl Therm Eng 110 (2017) 795-804
5. C. K. Westbrook, F. L. Dryer, Combust Sci Technol 27 (1981) 31-43.
6. B. Franzelli, E. Riber, M. Sanjosé, T. Poinso, Combust Flame 157 (7) (2010) 1364-1373.
7. A. H. Lefebvre, Atomization and Sprays, Hemisphere Publishing co., 1989, p. 214.
8. A. Sängler, T. Jakobs, N. Djordjevic, T. Kolb, ILASS Europe 2014, Bremen, Germany.
9. A. Davanlou, J. D. Lee, S. Basu, R. Kumar, Chem Eng Sci 131 (2015) 243-255.
10. F. Cernuschi, C. Rothleitner, S. Clausen, U. Neuschaefer-Rube, J. Illemann, L. Lorenzoni, C. Guardamagna, H. Engelbrecht Larsen, Powder Technol 318 (2017) 95-109.
11. J. K. Park, S. Park, M. Kim, C. Ryu, S. H. Baek, Y. J. Kim, H. H. Kim and H. Y. Park, Fuel (2015) 324-333.

List of Publications

1. G. Cafaggi, P.A. Jensen, P. Glarborg, S. Clausen, K. Dam-Johansen, Proceedings of Nordic Flame Days 2017, Stockholm, Sweden.

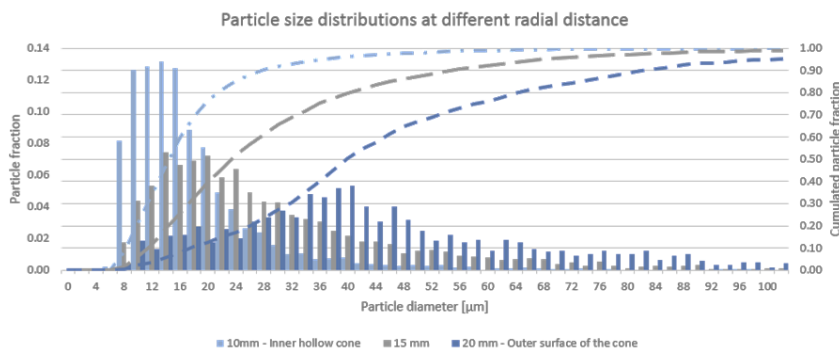


Figure 1: The plot shows the number based particle size distribution of a sample of 6628 droplets. The measurements have been taken 24 mm downstream of the nozzle orifice at 10, 15 and 20 mm from the axis of the hollow cone spray.



Yingjun Cai

Phone: +45 4525 2821
E-mail: ycai@kt.dtu.dk
Center: Center for Energy Resources Engineering

Supervisors: Kaj Thomsen
Nicolas von Solms
Suojiang Zhang

PhD Study

Started: February 2017
To be completed: February 2020

Physicochemical properties of binary mixtures (1-vinyl-3-acetamido imidazole bis(trifluoromethylsulfonyl) imide+acetonitrile)

Abstract

Pure ionic liquid 1-vinyl-3-acetamido imidazole bis(trifluoromethylsulfonyl)imide was synthesized. The physicochemical and electrochemical properties of the pure ionic liquid 1-vinyl-3-acetamido imidazole bis(trifluoromethylsulfonyl) imide ([VAIM][TFSI]) and its binary liquid mixtures with acetonitrile were measured at temperatures from (298.15 to 333.15) K and at pressure of 0.1 MPa over the whole composition range.

Introduction

High-voltage and fast-charging lithium-ion batteries (LIB) are being considered as attractive power sources for portable electric devices, electric vehicles and energy storage systems [1-3]. Electrolytes used as a medium for charge transfer in lithium batteries greatly influence the performance with respect to cycle life, charging/discharging rate, and safety. Current state-of-art electrolytes are highly flammable, volatile and have low conventional voltage limitation (~4.2V) based on organic carbonate. This feature prohibits the development of batteries with safe and wide operating temperature range.

Ionic liquids were intensively studied as one component of the electrolyte in LIB, owing to their perfect characteristics of having low melting-temperature, being non-volatile, having high specific conductivity and having a wide ranging electrochemical window. Development of ionic liquids as solvents of the LIB electrolyte was limited by: i) the high viscosity reduces the specific conductivity, ii) the incompatibility of ionic liquids and electrodes decreases the cyclic lifetime [4]. Fortunately, many experts are committed to develop new types of functionalized ionic liquids to enhance the performances of new LIB.

Acetonitrile has a convenient liquid range and a high dielectric constant of 38.8, which is often used as solvent in electric devices such as LIB and supercapacitors [5,6]. Acetonitrile can easily dissolve solutes exhibiting excellent ionic conductivity that may contribute to fast-charging lithium batteries.

In this research, a new type of functional ionic liquid 1-vinyl-3-imidazole bis(trifluoromethylsulfonyl) imide ([VAIM][TFSI]) was synthesized. The physicochemical

and electrochemical properties of pure ionic liquid and binary mixture of [VAIM][TFSI] and acetonitrile were measured at temperatures from 298.15 to 333.15 K and at pressure of 0.1 MPa.

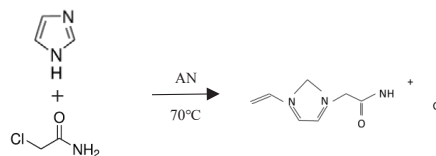
Objective

The objective of this study is to evaluate physicochemical and electrochemical properties of [VAIM][TFSI] and AN to check if they can be used in the lithium-ion batteries. The goal is to create one kind of electrolyte for fast-charging or high voltage lithium-ion batteries.

Results and discussion

The functional ionic liquid was synthesized in two-step procedures as follow:

(1)



(2)



The chemical shifts (DMSO, δ /ppm relative to TMS) appear as follows: ^1H NMR (600 MHz, DMSO) δ 9.41 (s, 1H), 8.19 (t, $J = 1.8$ Hz, 1H), 7.87 (s, 1H), 7.83 (t, $J = 1.6$ Hz, 1H), 7.59 (s, 1H), 7.37 (dd, $J = 15.6, 8.7$ Hz, 1H), 5.98 (dd, $J = 15.6, 2.5$ Hz, 1H), 4.99 (s, 2H). The chemical shift of the peaks corresponded to the structure of [VAIM][TFSI], and no impurity peaks were observed in the ^1H NMR spectrum.

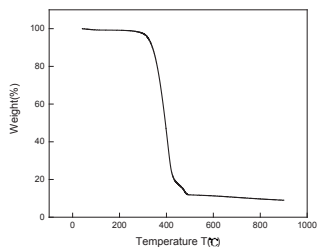


Figure 1: The TGA of [VAIM][TFSI]

The thermal stability of [VAIM][TFSI] was evaluated by Thermal Gravimetric Analyzer (TGA). Figure 1 shows the TGA curve of the IL [VAIM][TFSI], which exhibits outstanding thermal stability up to about 300 °C.

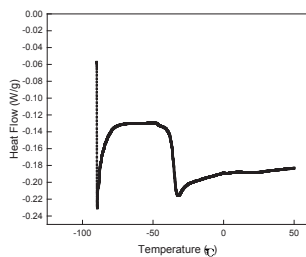


Figure 2: The DSC of [VAIM][TFSI]

The phase transition of [VAIM][TFSI] investigated by Differential Scanning Calorimetry (DSC) is shown in Fig.2. The melting point of [VAIM][TFSI] obtained from the DSC curve is -35.443 °C. The DSC in combination with TGA analysis shows that the ionic liquid has a large convenient liquid range which suggests a wide temperature adaptability in lithium-ion batteries.

Conductivity plays an important role for fast-charging lithium-ion batteries, and the higher the better. The conductivities of binary mixtures of [VAIM][TFSI] and AN were measured using a three-electrode flow cell by impedance analyzer (CHI 660E) at different temperatures from 298.15 to 333.15 K. From figure 3, it can be seen that the conductivities of the mixture increased with the increase of temperature. Meanwhile, the conductivities of the mixture increased at first with the adding of ionic liquid, and reached the maximum value at a mole fraction of about 0.07 at all temperatures.

Then, the conductivities decreased sharply as shown in figure 3. This phenomenon was detected in other mixed solvent [7]. The explanation is that the ionic liquid exists in the solvent as a “salt in solvent” at low concentration, the higher the concentration, the higher the conductivities. However, when the concentration of the ionic liquid reached a mole fraction 0.07, the viscosity of the mixture become higher and the ionic liquid gradually associated into huge clusters, which results in the decrease of the conductivity.

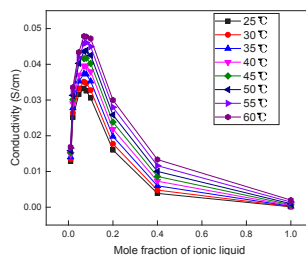


Figure 3: The conductivities of binary mixture of [VAIM][TFSI] and AN.

Conclusion and future works

A new type of functional ionic liquid [VAIM][TFSI] has been synthesized in a two-step method. The ionic liquid has high thermal stability and wide temperature adaptability. In combination with acetonitrile, the mixture display excellent conductivity.

In the future, more physicochemical and electrochemical properties will be evaluated, such as density, viscosity, diffusion of lithium-ion in the mixture, and the charge-discharge performance in lithium batteries.

Acknowledgements

The PhD project is supported by China Scholarship Council.

References

1. P. G. Bruce, S. A. Freunberger, L. J. Hardwick, J. -M. Tarascon, *Nature Materials* 11 (2012) 19–29.
2. M. Armand, J.-M. Tarascon, *Nature* 451 (2008) 652–657.
3. J. B. Goodenough, Y. Kim, *Chemistry of Materials* 22 (2010) 587–603.
4. M. Egashira, H. Todo, N. Yoshimoto, M. Morita, J. I. Yamaki, *Journal of Power Sources* 174 (2) 2007 560-564.
5. F. Mizuno, S. Nakanishi, A. Shirasawa, K. Takechi, T. Shiga, H. Nishikoori, H. Iba, *Electrochemistry* 79 (2011) 876–881.
6. Z. Peng, S. A. Freunberger, L. J. Hardwick, Y. Chen, V. Giordani, F. Bardé, P. Novák, D. Graham, J.-M. Tarascon, P. G. Bruce, *Angewandte Chemie International Edition* 123 (2011) 6475–6479.



Edgar Luis Camacho-Vergara

Phone: +45 7148 8080
E-mail: elcver@kt.dtu.dk
Center Center for Energy Resources Engineering

Supervisors: Georgios M. Kontogeorgis
Xiaodong Liang

PhD Study
Started: November 2016
To be completed: November 2019

Phase behavior of inhomogeneous fluids: classical density functional theory approaches

Abstract

The aim of this PhD project is the implementation of a classical Density Functional Theory (DFT) framework for the study of thermodynamic properties of inhomogeneous fluids, where the uniformity of the microscopic particle density, characteristic of bulk fluids, is broken due to the presence of interfaces or surfaces, i.e. vapor-liquid and liquid-liquid interfaces, solid-fluid surfaces. An appropriate inhomogeneous fluid model for the Helmholtz free energy based on a bulk equation of state within the framework of classical DFT is to be proposed, capable of predicting the phase equilibria, surface tension, adsorption, solvation force, among other surface thermodynamic properties.

Introduction

Bulk or uniform fluids are those in which the local particle density is constant and equal to the average density of the whole system. However, the homogeneity of bulk fluids is broken with the presence of interfaces or surfaces where the local density of the system varies along the interface or surface, producing inhomogeneities, e.g. confining walls or coexistence of different fluid phases. The study of non-uniform or inhomogeneous fluids is of great interest because they play an important role in different phenomena in chemical and petroleum engineering: interfacial tension on liquid-liquid and vapor-liquid interfaces, phenomena due to solid-fluid surfaces such as adsorption, wettability, capillarity, confining geometries, etc.

Statistical mechanics has become an important tool for the study of uniform and non-uniform thermodynamic systems because it provides a link between the microscopic probability distribution of particles and the macroscopic state properties of these systems. In this project, the thermodynamic properties of inhomogeneous fluids will be studied within the framework of the classical density functional theory (DFT) [1], [2]. Classical DFT offers the versatility of retaining the theoretical concepts of statistical mechanics and only requiring a modest amount of computation power in comparison to molecular simulations.

The key of the classical DFT is that it defines the Helmholtz free energy as a functional of the particle density distribution, which for uniform fluids reduces to the average bulk density, and for non-uniform fluids is variable along the presence of inhomogeneities caused by confining surfaces or an interface between coexisting phases. The Helmholtz free energy is therefore a unique functional of the particle density distribution, and in practice, most resulting functionals are designed specifically for the applications of interest. A good and reliable model of an inhomogeneous fluid would require that the Helmholtz free energy functional within the classical DFT framework could be used for different types of inhomogeneous systems, and that it should also reproduce the phase equilibria of bulk fluids. As the Helmholtz free energy functional has the versatility of being approximated in different ways, it is possible to directly integrate thermodynamic models for bulk fluids into the framework of DFT. With a consistent framework, the existing pure component parameters for the bulk fluids can be applied to study the thermodynamic properties of inhomogeneous fluids.

The developed DFT framework will also be compared to other methods used for the determination of surface properties. It will be applied to model the interfacial tensions of vapor-liquid interfaces, as well as liquid-liquid interfaces, and compared to the Density Gradient Theory (DGT). Secondly, it will be applied to model adsorption and compared to the Multicomponent

Potential Theory of Adsorption (MPTA). Thirdly, it will be applied to model the phase equilibrium and flow behavior of fluids in confined spaces, which are important for many processes, e.g. underground reservoir fluids and chemical reactions in catalysts, etc.

Specific Objectives

1. Develop of a unique Helmholtz free energy functional suitable for its application to various systems within the framework of classical DFT.
2. Use an advanced thermodynamic model together with classical DFT in a consistent framework, so the parameters from homogeneous fluids can be applied to study the thermodynamic properties of inhomogeneous fluids.
3. Compare the developed DFT framework with other versions of DFT, and different models such as DGT and MPTA.

DFT formalism

The classical DFT framework is defined for an open system with fixed volume V , temperature T and chemical potential μ . For a bulk system with these natural variables the most adequate thermodynamic potential is the grand potential $\Omega = -PV$, where P is the pressure. An inhomogeneous system is then created by the introduction of an external potential $v(\mathbf{r})$ with a local particle density $\rho(\mathbf{r})$ that varies along the geometry of the system. Therefore, the grand potential functional is defined as

$$\Omega[\rho] = \mathcal{F}[\rho] + \int \rho(\mathbf{r})(v(\mathbf{r}) - \mu) d\mathbf{r} \quad (1)$$

Where $\mathcal{F}[\rho]$ is the intrinsic Helmholtz free energy functional of the local particle density of the inhomogeneous fluid. This functional can for example be approximated similar to the SAFT model and its variants, e.g.

$$\mathcal{F}^{\text{res}}[\rho] = \mathcal{F}^{\text{id}}[\rho] + \mathcal{F}^{\text{hs}}[\rho] + \mathcal{F}^{\text{disp}}[\rho] + \mathcal{F}^{\text{chain}}[\rho] + \mathcal{F}^{\text{assoc}}[\rho] \quad (2)$$

Equation 2 implies that existing models derived for the study of uniform fluids may be used in the classical DFT framework to study their inhomogeneous counterpart which may allow the use of the current pure component parameters already fitted for the phase equilibria.

Results

Once the Helmholtz free energy functional is defined, the equilibrium particle density of an inhomogeneous fluid can be found with the minimization of Eq. 1. The grand potential functional is derived in such a way that when the particle density equals the equilibrium particle density it reduces to the bulk grand potential and then thermodynamic properties can be calculated. In the current state of the project the first two contributions to the intrinsic free energy functional have been implemented for the study of hard sphere systems close to walls and confined in slit-like pores and the phase behavior of Lenard-Jones fluids as a preliminary test for

the calculation of the properties of the vapor-liquid interface. Figure 1 shows the resulting equilibrium density profile of a hard sphere fluid obtained with classical DFT and the Carnahan-Starling equation of state for hard spheres treated with Fundamental Measure Theory. Figure 2 shows the results of using the implementation of the dispersive attraction between the hard spheres with the Lenard-Jones potential for the determination of the vapor-liquid envelope.

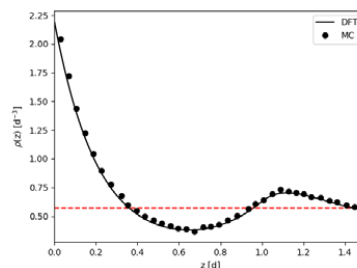


Figure 1: Equilibrium particle density (solid line) for a hard sphere close to a hard wall with $\rho^{\text{bulk}} = 0.57$ against Monte Carlo simulation (Snook and Henderson 1978).

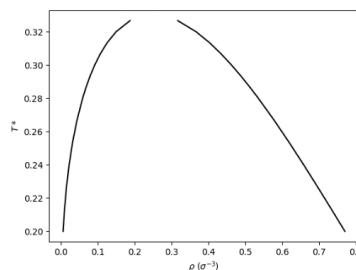


Figure 2: Phase envelope for a Lennard-Jones fluid using classical DFT with $T^* = k_B T / \epsilon$.

Conclusion and Future Work

A classical DFT framework has been successfully implemented for the study of simple inhomogeneous systems. In the following, implementation of Eq. 2 for the different interactions of the particles will allow the use of the classical DFT framework for the calculation of the surface tension and adsorption of real fluids.

Acknowledgements

To the Department of Chemical and Biochemical Engineering of the Technical University of Denmark for a full PhD-scholarship given to this project.

References

1. J. Wu, "Density functional theory for chemical engineering: From capillarity to soft materials," *AIChE J.* 52 (3) (2006) 1169–1193.
2. J.-P. Hansen and I. R. McDonald, *Theory of simple liquids*. Elsevier Academic Press, 2006.



Ricardo Fernandes Caroço
Phone: +45 5270 3333
E-mail: rcar@kt.dtu.dk

Supervisors: Jakob K. Huusom, DTU
Jens Abildskov, DTU
Paloma Santacoloma, CP Kelco

PhD Study
Started: September 2015
To be completed: August 2018

Monitoring of bioprocesses: merging PAT, Kalman and uncertainty

Abstract

The project focuses on assessing the challenges of implementing model-based monitoring strategies in industrial settings, exploring the development possibilities of a cross-(bio)industry workflow/guideline. A case-study focusing on the performance monitoring of a pectin batch extraction process is conducted in a way to take advantage of the first principle dynamic models, which describe the reactions and transport phenomena of the pectin extraction, that were developed for the considered critical quality attributes: pectin bulk concentration, degree of esterification (%DE) and intrinsic viscosity (IV). An wholesome procedure for a full-scale monitoring is envisioned, making use of state-of-the-art state estimation algorithms together with chemometric models, with the ultimate goal of providing the process operators with guidelines for process optimization and a decision making tool within a known uncertainty range.

Introduction

Monitoring and control strategies are crucial in several stages of a product/process life-cycle, from development to the optimization of an established process. These strategies are used to address a large number of objectives such as process understanding, troubleshooting, real-time control actions and continuous process optimization. Currently one of the major limitations in the biochemical industry is the multitude of disturbances that each process is subjected to, which can derive from processing biological feedstock. Nowadays the large segments of the industry operate in a heuristic recipe-driven way, dependent on rule-of-thumb experience which results too often in batch-to-batch discrepancies. These difficulties can be mitigated by an appropriate monitoring strategy and model building comes as an integral part of such a strategy. Models supply a representation of the underlying physical/chemical phenomena, allowing prediction and subsequent control decisions.[1]

Monitoring and control strategies applied in the biochemical industry have not reached the same level of maturity as the traditional bulk pharma & chemical industry, within the process analytical technology (PAT) initiative framework. Furthermore the use of mechanistic models and online optimization algorithms is still new. There is an opportunity to explore state feedback algorithms which combined with PAT allow for the development of robust feed-forward monitoring

and consequently a way to reduce process variations, improve product quality and lower the cost of operation.[2][3]

Workflow Formulation

The ultimate goal of the project is to develop a workflow/guideline that provides a knowledgeable and tailored approach to monitoring bio-process operations in plants using soft sensors.

Two types of soft sensors described in the literature: model-driven and data-driven: data-driven are based on chemometric models, informed by historical process data to predict other process variables on-line; and model-driven are mainly based on established models that describe mass and energy balances, known as the "First Principles", making use of Kalman filters or extended Kalman filters.

The work intends to provide a methodology for applying wholesome monitoring schemes within the PAT framework (including identification of critical quality attributes (CQAs) and critical process quality parameters (CPPs)), as well as to make use of Bayesian and Kalman techniques in order to monitor robustly the desired key performance indicators, and their uncertainty.

The focus will be set on the models, which have to be complex enough to be able to accurately predict the dynamics of the system, but still usable to day-to-day application of the strategies in the plants.

Some of the major questions raised by this effort are:
 1) Identifying what are currently the monitoring strategies employed in the industry. Is there currently any systematic logic behind the selection of a given approach?

2) Theory vs Industry reality. What is feasible to implement in a settled industry? What is needed from a current process to develop a monitoring strategy? What needs to be abdicated from a theoretical optimal strategy, to fit with the real process possibilities?

3) Relationship between type of process and monitoring strategy. Is there any correlation between the type of process and a type of strategy, or is it a “case-by-case” scenario? Is it possible to construct a decision making tool based on the type of process, monitoring objective, available information, etc. This effort will be done in an iterative way and taking into account the projected case studies. The final goal is set on the development of a methodology, critically re-visiting what was previously done in the case-studies and testing it on a variety of different scenario cases.

Raw Material as a source of uncertainty – Pectin Extraction

Production comprises four core steps: extraction from the plant material, purification of the liquid extract, precipitation of pectin from the solution, and further de-esterification and/or amidation of the high methylester pectin with acid or alkali. [4]

This process is subjected to wide quality fluctuations in the raw material which result in production performance issues and undesired deviation of the critical quality attributes (CQA) of the end product: degree of esterification (%DE) and intrinsic viscosity (IV). Peel fingerprinting and determination of mechanistic model parameters that are inherent to each peel is a way to include this variability in the model. Figure 1 represents a partial least squares regression of the DE_0 (initial DE in peel) obtained using NIR spectra of the peels and an analytical reference.

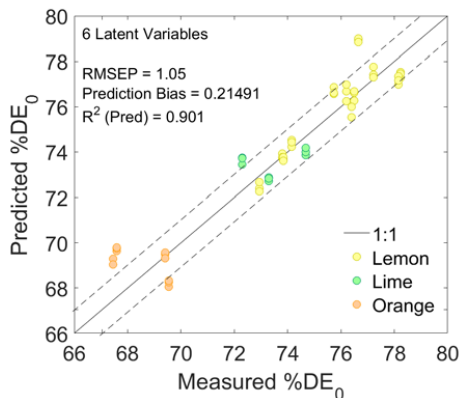


Figure 1: Externally validated PLS model for DE_0 . The different colors represent different citrus fruits

The development of this PAT application allows us to obtain predicted values, and their uncertainties, for key parameters of the mechanistic model.

This project is continues as well previous efforts to model this process, and will try to reach plant scale implementation of an adequate monitoring strategy. The mechanistic model should be as such that describes the dynamics of the extraction that are immeasurable or that are not possible to measure, in a timely manner.

Work towards model robustness is key as the parameters that describe the models were tuned based pilot plant data and have now to be verified to describe production process behavior and validated to for a variety of different raw material and conditions, to ensure the which shows that the model is able to cope with the discrepancies in the raw material, allowing the product quality to hold consistently at the required standards despite variations. To take this into account the monitoring strategy has to be thought as whole and every step of that leads to the process (type of raw material, conditioning, handling, etc.) should be considered, as well as possible hybrid approaches, utilizing data obtained data-driven soft-sensors.

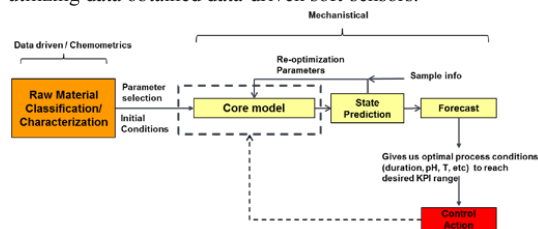


Figure 2: Representation of an integrated monitoring strategy approach.

The integrated monitoring strategy will involve a combination of first principle models with chemometric data-driven models, supplemented with online process measurements such as volume, temperature, pH as well as discrete sampling for NMR analysis at-line (Figure 2).

Acknowledgements

The project is part of the Danish cluster in biotech manufacturing - BIOPRO. The financial and logistical support from the industry participants is acknowledged.

References

1. D. Dochain (Ed.), Bioprocess Control, Control Systems, Robotics and Manufacturing Series, ISTE, London, UK., 2008, p. 11-16.
2. L. R. Formenti, A. Nørregaard, A. Bolic, D.Q. Hernandez, T. Hagemann, A.-L. Heins, L. Mears, M. Mauricio-Iglesias, U. Krühne, K. V. Gernaey. Challenges in industrial fermentation technology research. Biotechnology Journal, 9(6), 727–38.
3. J. K. Huusom. Challenges and opportunities in integration of design and control. Computers & Chemical Engineering, 81, 138–146.
4. CP Kelco. GENU® pectin Book. 2008.



Teresa Melo de Carvalho
Phone: +45 53 39 30 29
E-mail: antsca@kt.dtu.dk

Supervisors: Ulrich Krühne, DTU
Krist V. Germaey, DTU
Michelle Madsen, Chr. Hansen
Anders Clausen, Chr. Hansen

PhD Study
Started: August 2015
To be completed: July 2018

Methodology for modelling the freeze-drying of a fixed particle bed

Abstract

Freeze-drying is a process widely used in industry due to its capacity to give products good shelf stability. However, it is an expensive and time-consuming process where often the scale-up is based on empirical knowledge. Therefore, the aim of this project is the development of a model that will facilitate and optimize the scale-up of the freeze-drying process. The proposed methodology suggests the use of both experimental and model-based approaches to capture scale-up effects. Techniques for characterization of the product are proposed since it is essential for an improved understanding of the process. A CFD method is chosen to investigate the sublimation phenomena and to identify critical material attributes and process parameters.

Introduction

Freeze-drying is widely used in the pharmaceutical and food industry due to its capacity to preserve the original properties of the resulting dried products. This process increases stability, preserves the physical structure of the product and gives products that can easily be rehydrated upon the addition of water. However it is an expensive and time-consuming process, frequently not operated in a robust and efficient way [1]. Overly conservative freeze-drying cycles and scale-up based on empirical knowledge result in drawbacks not just from an economic standpoint but also from a product point of view. Thus, process development in this area has been focused on minimizing drying times while maintaining product quality [2],[3].

The development of mathematical models is increasingly important for process development and to accomplish the need for improved process understanding. Therefore, in freeze drying, robust theoretical models which can accurately predict product temperature, residual water, glass transition temperature, and primary drying time have been developed. Several different models are reported in the literature with differences regarding the geometry of the ice sublimation interface, initial and boundary conditions, and several other basic assumptions. However, this process is also very dependent on the physical form of the material to be dried and on the physical parameters and characteristics of the freeze dryer itself.

Specific Objectives & Theory

This project focuses on bulk freeze-dryers with open trays, mainly used in the food industry. In this kind of freeze-dryers particles have irregular shapes and follow a random distribution in the trays.

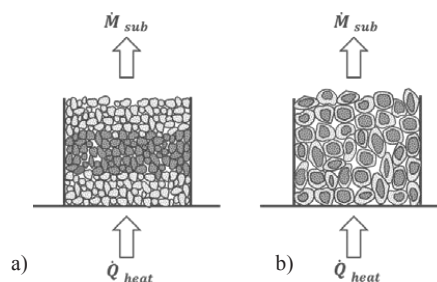


Figure 1: Schematic illustration of basic model assumptions for freeze-drying of particulate solids. Dark grey: frozen region, light grey: dried porous region. a) fixed particle bed with two planar drying fronts; b) fixed particle bed with drying fronts evolving within each particle. The particles are initially fully saturated with ice, while the inter-particle space (in white) is completely free of ice during the whole process.

As can be seen in Figure 1 frozen particulate matter is characterized by a bimodal pore size distribution based on the different pore sizes of the inter-particle void space. Pore size distribution of the particle bed is determined by the particle size and by the way that particles are packed ($\text{pac} = V_{\text{solid}}/(V_{\text{solid}}+V_{\text{void}})$), while pore size distribution inside the particles is dependent on the initial solid concentration and the freezing rate that will influence the size of the ice crystals. The ratio between the two pore size distributions plays an important role for the dynamics of the freeze-drying process.

Mass is transported in a porous medium by a variety of mechanisms: (i) by ordinary diffusion, described by the Maxwell-Stefan equations; (ii) by Knudsen diffusion; (iii) by viscous flow according to the Hagen-Poiseuille equation. The aim of this project is the development of a model that will facilitate and optimize the scale-up of a freeze-drying process. Therefore it is essential to obtain a fundamental understanding of water vapor flows during drying in a freeze-dryer for the construction of an accurate model [4].

The Knudsen number ($\text{Kn} = \lambda/D_{\text{pore}}$) is a dimensionless number defined as the ratio between the molecular free path length (λ) and the pore diameter (D_{pore}). This number defines which diffusion model best describes the fluid dynamics in a system. This discussion will focus on the two limiting situations within the pores of the solid matrix: (i) free-molecule flow of gases, in which the molecular diameters are short and mean free paths are long relative to the characteristic dimensions of the pores ($\text{Kn} \gg 1$); (ii) continuum flow of gases or liquids, in which both the diameters and the spacing of the intrapore molecules are short compared to the pore dimensions ($\text{Kn} \ll 1$).

Methodology

One particle

The first step will be to determine the effect of pore diameter and porosity on the mass flux of water in freeze-dried samples. There are several techniques to study the morphology of dried solids; 3D μ -CT was the method chosen in this project to characterize the porous structure of the samples.

A software for multi-scale 3D image processing and visualization is used in order to characterize the material properties: characteristic length, pore diameter, porosity, effective diffusivity and tortuosity.

The Knudsen number is calculated and the correct diffusion model is applied.

Particles packed tray

Once the effects of the material characteristics are known, it is possible to model a tray of packed particles assuming that the inner pores (defined as the pores created from the drying process in each particle) have the same characteristics as the particles studied above. A Computational Fluid Dynamic (CFD) method was chosen as the computational tool to investigate the

sublimation phenomena during freeze-drying. By defining a porous material when setting up the problem in CFD it is possible to take into account the porosity described by the outer pores - empty space between the particles that define the tray ($\epsilon = 1-\text{pac}$). Once the simulation is defined with the correct material properties and initial and boundary conditions, the overall mass flux in the packed bed as well as the impact of inner pore to outer pore ratio can be analyzed. The established model represents a good starting basis to determine the effect of different operating conditions during the freeze-drying of pellets in open trays. The simulation of different freeze-drying and product settings, like shelf temperature, total chamber pressure, slab thickness and pellet size and distribution, significantly enhances the understanding of heat and mass transfer during drying which is of great importance for process development and the scale-up of freeze-drying cycles.

Conclusion

Within the Marie Skłodowska-Curie Innovative Training Network “BioRapid” and considering the current state of freeze-drying modeling this project suggests the development of a mechanistic model to facilitate and optimize the scale up of a freeze-drying process. Starting from a model system, a mathematical model will be developed using a model system that attempts to describe the fluid motion during freeze-drying of pellets contained on trays. The methodology suggests the use of both experimental and model-based approaches.

Acknowledgement

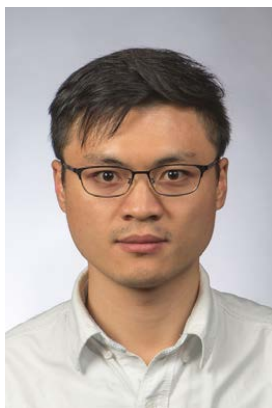
This project has received funding from the European Union’s Horizon 2020 research and innovation programme under the Marie Skłodowska-Curie grant agreement No 643056.

Web-link: <http://www.bio-rapid.com/>



References

1. G.-W. Oetjen and P. Haseley, *Freeze-Drying*, Wiley-VCH Verlag GmbH & Co. KGaA, Weinheim, Germany, 2003.
2. A. A. Pisano, Roberto; Fissore, Davide; Velardi, Salvatore A.; Barresi, J. *Pharm. Sci.*, 99 (11) (2010) 4691–4709.
3. H. Sadikoglu, A. I. Liapis, and O. K. Crosser, *Dry. Technol.* 16 (3–5) (1998) 399–43.
4. R. Byron Bird, W. E. Stewart, and E. N. Lightfoot, *Transport Phenomena*, John Wiley & Sons, USA, 2002.



Yuqiu Chen
Phone: +45 4525 8046
E-mail: yuqch@kt.dtu.dk

Supervisors: John M. Woodley
Georgios Kontogeorgis
Rafiqul Gani

PhD Study
Started: November 2017
To be completed: November 2020

Integrated solvent-membrane and process design method for hybrid separation schemes

Abstract

In bio-processes, downstream separations are usually very difficult. Meanwhile, in petrochemical and chemical processes, most separations of mixtures with low relative volatilities are energy intensive. Thus, the ability to select an appropriate separation method for such energy intensive processes or dilute system in a timely and systematic manner is of key importance. Ionic liquids (ILs) based separation and membrane based separation are two emerging and potential technologies in separation processes, however, both separation methods are limited to their own characteristics for efficient operation. Therefore, combinations of processing units operating at their highest efficiencies are promising options.

Introduction

The pressing issues in energy has forced industry to reorganize current process designs and develop new process designs. Consequently, integrated new technologies into process designs, especially in dilute system and energy intensive processes is of growing importance to industry.

Most biological reactions are carried out in dilute aqueous medium leading to an ineffective feed to the downstream process, which means that product concentration steps following the upstream process operations are operating energy intensive and capital costs [1,2]. Therefore, it can be advantageous to invest in a recovery technology that allows the efficient separation of the product from water.

Among many emerging technologies of separation, ILs used as solvents are being paid more attention in energy intensive processes recently. Unlike volatile organic compounds (VOCs) that easily escape into the atmosphere because of their high volatility, ILs pose attractive features such as almost negligible vapor pressure, low-melting point, and high thermal and chemical stability. Moreover, ILs also have been found to provide good selectivity, which is important for separation processes. Therefore, they provide promising alternatives for the replacement of volatile organic solvents in separation processes. For example, ILs-based extractions have been proposed for common azeotropes, some of them are encountered in many

downstream separations following the synthesis step of pharmaceutical and/or biochemical processes [3].

Membrane based technology has been established recently as one of the most promising separation methods to the well-established mass transfer processes, since it offers many advantages over traditional separation processes, such as high selectivity, low energy consumption, compact and modular design [4]. For example, pervaporation was regarded as one potential means of overcoming some limitations of traditional separation methods in a wide range of applications from the separation of azeotropic mixtures to the recovery of bioproducts from water. However, in many cases membrane based separation alone may not supply products suitable for further processing or waste disposal in accordance with environmental standards. On the other hand, the recovery of bioproducts from water and the separation of mixtures with low relative volatilities by solvent-based separation alone requires a lot of energy. Thus, hybrid processing schemes that combine processing units operating at their highest efficiencies to perform one or more process tasks are increasingly being considered as promising innovative and sustainable processing options.

Hybrid schemes are superior to the single separation processes due to the potential in saving capital costs and energy consumption, especially for the processes of requiring high product purities, such as in the pharmaceutical industry there is a requirement to meet

high product specifications of very high purity for making safe and effective medicines [1].

Most of studied distillation/membrane hybrid schemes focused on processes that include an existing solvent-based distillation unit and a vapor permeation or pervaporation module to separate azeotropic mixtures. However, in some cases of hybrid schemes the existing distillation operation itself is not an optimal operation, such as in the part of distillation column the employed entrainers or azeotropic agents are not optimal solvents. Consideration of solvent has the significant impact on the overall performance and economics of separation processes, optimal hybrid schemes including solvent (ILs) molecular design are introduced and discussed in this work. One of the simple flowsheets of the proposed hybrid schemes shown as in Figure 1.

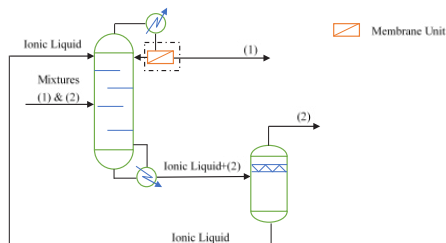


Figure 1: Proposed hybrid schemes of combining ionic liquid-based separation and membrane

In such hybrid processing schemes, the membrane generally performs part of the 'separation work' of the column, which allows one to reduce the number of equilibrium trays or the energy input in a membrane-augmented column.

Framework

The framework of developing hybrid schemes for dilute system or energy intensive separation processes was illustrated in Figure 2.

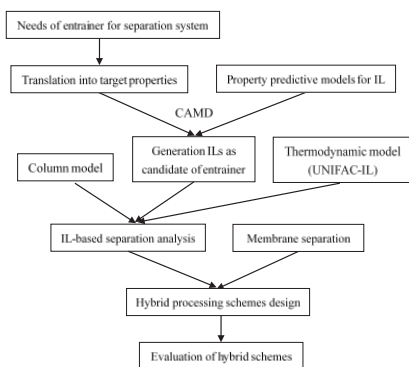


Figure 2. Structure outline of the hybrid processing schemes design methodology

As we all known, the physical properties of solvent impact separation processes directly or indirectly. To achieve an optimal separation process using ILs as solvent, trade-offs between different properties of ILs,

such as viscosity, heat of capacity and enthalpy of vaporization should be addressed based on their effects on the overall separation process performance. To predict the properties and functionalities of designed ILs, suitable prediction models should be identified.

Solvent was always selected based on experience, heuristic rules, or a few exploratory experiments. To overcome some limitations of above methods, computer-aided molecular design (CAMD), a novel and systematic approach in selecting processing solvent, has been developed and successfully applied to design solvent molecular. Because of the molecular structure of ILs, they are also regarded as "designer" solvents, similar rules of CAMD for traditional organic solvent have also been proposed for ILs.

To predict the molecular interactions between ILs and the components to be separated, the UNIFAC-IL thermodynamic model will be employed in my work due to its high prediction accuracy [5]. For the UNIFAC based model, the most important work is how to determinate the group binary interaction parameters by fitting the experimental activity coefficients at infinite dilution and the liquid-liquid equilibria (LLE) data at finite concentration.

For membrane separation unit, the effect of several operating parameters such as membrane area, membrane cut and membrane feed compositions will be investigated. Furthermore, the evaluation of proposed hybrid processing schemes is another import part of this work.

Conclusion

A framework of integrated design method for energy efficient hybrid processing schemes regarding dilute system or energy intensive separation processes has been proposed, wherein two emerging and potential separation technologies, ILs-based extraction and membrane separation unit are combined. Meanwhile, the UNIFAC-IL model and computer-aided molecular design (CAMD) are employed as thermodynamic model and ILs screening method, respectively.

References

1. J.M. Woodley, M. Bisschops, A.J. Straathof, M. Ottens, *Journal of Chemical Technology and Biotechnology*, 83 (2008) 121-123.
2. J.M. Woodley, *Computers and Chemical Engineering*, 105 (2017) 297-307
3. B.C. Roughtona, B. Christianb, J. White, K.V. Camarda, R. Gani, *Computers & Chemical Engineering*, 42 (2012) 248-262.
4. E. Drioli, A.I. Stankiewicz, F. Macedonio, *Journal of Membrane Science*, 380 (2011) 1-8.
5. Z.G. Lei, C.N. Dai, J.Q. Zhu, B.H. Chen, *AIChE Journal*, 60 (2014) 3312-3329.



Valeria Chiaula
Phone: +45 4525 6813
E-mail: valchi@kt.dtu.dk

Supervisors: Anne Ladegaard Skov
Piotr Mazurek
Anders Christian Nielsen, Coloplast A/S
Jens Tornøe, Coloplast A/S

PhD Study
Started: August 2017
To be completed: August 2020

Advanced wound care adhesives with excellent moisture handling properties

Abstract

Wound healing is a dynamic process characterized by three overlapping cellular phases: inflammation, new tissue formation, and remodeling. Chronic wounds, which are often manifested in elderly and diabetic patients, result from anomalies in the cellular and molecular wound repair mechanism. Such wounds can lead to significant disability, amputation and increased mortality. Here, we propose a novel, skin-friendly, industrially relevant glycerol-silicone hybrid adhesive with improved moisture handling due to the incorporation of emulsified glycerol. Various parameters will be taken into account in order to develop a relevant adhesive, in particular glycerol content, glycerol domain size and adhesive thickness to allow for a controlled moisture absorption.

Introduction

Broadly, for wounds to heal, a moist, clean and warm environment is required. A moist wound bed easily promotes growth factors and many cell types including epithelial cells to migrate, facilitating wound edge contraction. Thus, appropriate dressings play a significant role to create and maintain such environment [1]. Ideally, an optimal dressing must:

- Create a moist, clean and warm environment;
- Provide hydration if wounds prove to be dry;
- Absorb excessive wound exudates;
- Allow for gaseous exchange;
- Protect periwound area;
- Form an effective bacterial barrier;
- Minimize pain and trauma during application and removal.

Silicone adhesives are silicone elastomers which are not fully crosslinked but remain close to the gelation threshold (i.e. with a low crosslinking degree) [2, 3].

Within the field of advanced wound care, silicone adhesives are currently the preferred, state-of-the-art adhesive system due to its gentle skin adhesion properties. However, due to their hydrophobic nature, current silicone adhesives for wound care are challenged when it comes to moisture handling. As fluid handling and transportation in silicones are normally limited and since silicone adhesives attach poorly to moist surfaces, basic perspiration from the user's skin can cause the dressing to lose adhesive properties and eventually fall off. Furthermore, absorption through a

silicone contact layer is usually low compared to "classic" adhesives, such as alginates or hydrofibers, which renders silicone incompatible with highly exuding wounds.

To minimize such effects, silicone adhesives with improved fluid handling would help transmitting fluid away from the interface between either skin and adhesive, or the wound and the adhesive. The consequence of fluid build-up in either type of interface can be failure of adhesion or local maceration. To overcome such scenarios, holes in the silicone layers are normally introduced in the products, which not only is extra complication in the manufacturing process, but generally renders less flexibility in the product design. Furthermore, the nature of the adhesives itself cause the adhesives to partially flow throughout the holes, therefore making those smaller.

Specific Objectives

The main objective of this project is to develop a novel, industrially relevant, skin-friendly glycerol-silicone hybrid adhesive with several new properties, including:

- Improved moisture handling due to the incorporation of emulsified glycerol;
- Beneficial skin care effects due to the incorporated glycerol.

Silicone elastomers do not provide any significant liquid transport through them, but they are permeable to water vapor, e.g. sweat. Contrarily to the hydrophobic silicone elastomer, glycerol droplets cause water to be absorbed in significant amounts. This allows for the glycerol

content as a tunable parameter that directly affects the moisture handling capabilities of the hybrid adhesives since it determines the amount of water absorbed.

Experimental

In order to create the hybrid adhesives silicone and glycerol are speedmixed together and the resulting emulsion is cured. Desired amounts of silicone and glycerol were mixed at 3500 revolutions per minute (rpm) for 5 min using a dual asymmetric centrifuge SpeedMixer DAC 150 FVZ-K. The obtained glycerol in silicone emulsions were coated with various commercial knives to obtain adhesives with thicknesses of around 0.2, 0.3 or 0.4 mm, respectively. The samples were subsequently cured at 80 °C for 1 h. The study of droplet size was performed by taking images through optical microscope at $t = 0$ min and $t = 60$ min respectively. The images were analyzed by particles analyzer software in order to obtain the size distributions relative to glycerol domains. Samples name are formed using the pattern GX_MG7-9900, where G stands for 'glycerol' and X denotes glycerol content as phr (glycerol weight amount per hundred weight parts of silicone rubber) added to the silicone prepolymer. MG7-9900 is the applied silicone elastomer system (Dow Corning).

Results and Discussion

Four different glycerol in silicone emulsions were prepared by applying high shear forces for a minimum mixing time, which provides sufficient shear forces for obtaining reasonably mono-dispersed emulsions for a broad range of glycerol incorporated into silicone [4]. High shear forces caused the glycerol to form discrete droplets distributed evenly within the silicone matrix. The morphology of the resulting emulsions was analyzed using optical microscopy. Figure 1 shows that the higher glycerol loading the more tightly packed the domains were and the thinner the space between them became. Subsequently, the emulsions were investigated with respect to the stability during 60 min. Complete curing is known to occur after this time at room temperature and the system can be assumed to be immobilized with no further changes expected. Specifically, we studied changes in the size of the glycerol domains, which might occur due to agglomeration, coalescence or disproportion. The results presented in Figure 2 highlighted a slight increase of glycerol domain size over this time period. This indicates a partial instability in all four systems. The stability of the emulsions is a crucial parameter to control, because it directly affects the properties of the final adhesives. Since the glycerol content is a tunable parameter that influences the moisture handling properties, the droplet size may affect the moisture handling capabilities as well.

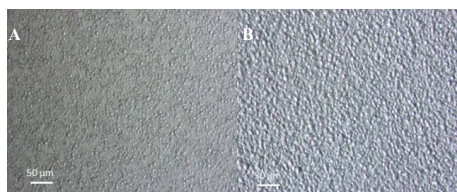


Figure 1: Optical microscopy images of 10 phr (A) and 20 phr (B) glycerol in silicone emulsion, respectively. Scale bars correspond to 50 µm.

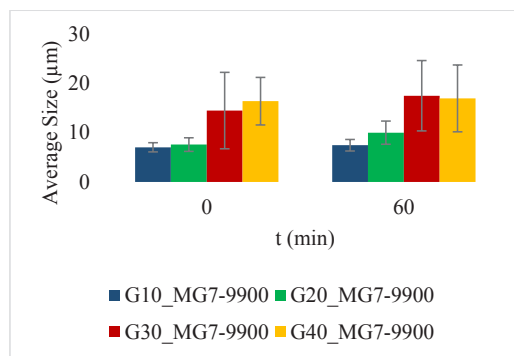


Figure 2: Average glycerol domain size in four different compositions at $t = 0$ min and $t = 60$ min, respectively.

Several strategies will be applied in order to improve the stability of our systems and thus improve ease of processing. Furthermore, the influence of droplet size and concentration of glycerol will be investigated with respect to fluid handling properties. The droplet size is directly tunable by the addition of elastomer-stabilizing fillers or surfactants.

References

1. A. Sood, M. S. Granick, N. L. Tomaselli, *Adv Wound Care (New Rochelle)* 3 (2014), 511-529
2. S. M. G. Frankær, M.K. Jensen, A. G. Bejenariu, A. L. Skov, *Rheologica Acta* 51 (2012), 559-567
3. M. K. Jensen, A. Bach, O. Hassager, A. L. Skov, *Int. J. Adhesion and Adhesives* 29 (2009) 687-693
4. P. Mazurek, S. Hvilsted, A. L. Skov, *Polymer* 87 (2016), 1-7



Steen Müller Christensen

Phone: +45 2666 1700
E-mail: stmuch@kt.dtu.dk

Supervisors: Anker D. Jensen
Brian B. Hansen
Keld Johansen, Haldor Topsøe A/S

PhD Study
Started: September 2015
To be completed: September 2018

Selective catalytic reduction (SCR) of NO_x on ships

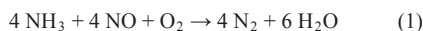
Abstract

The introduction of MARPOL Annex VI Tier III (1st January 2016) requires a high degree of NO_x reduction for shipping within NECA (NO_x emission control areas) in addition to a global SO_x reduction. The SCR technology, for NO_x control holds a great potential for application on-board ships, but the performance is not yet optimized with respect to marine equipment and operating conditions. Important considerations include performance at elevated pressures, minimal N₂O by-product formation and potential SO₂ oxidation and subsequent ammonium bisulfate/sulfate formation and fouling of the catalysts and ship boilers surfaces. With respect to pressurized (up to 4.5 bar) SO₂ oxidation, the performed monolith tests showed minimal oxidation and a first order SO₂ dependence.

Introduction

Denmark is one of the world's foremost shipping nations, leading in cargo transport, tanker shipping, refrigerated cargo, and offshore. Maritime transport and shipping benefits from low CO₂ emissions and low noise levels but emissions of SO_x, NO_x, and particles are generated. The issues related to NO_x/SO_x emissions are being targeted by the introduction of NO_x emission control areas (NECAs) for new ships and global SO_x regulations, both of which are introduced through the MARPOL 73/78 Annex VI[1] which generates a need for new technologies and engineering solutions.

Selective Catalytic Reduction (SCR) of NO_x using ammonia (NH₃) as reductant is a well-established abatement technology and was first used to control NO_x from stationary sources in the late 1970s in Japan[2] and nowadays introduced on multiple places such as power plants, waste incinerators and in the cement industry, the main SCR reaction can be described as:



The SCR technology has later been introduced for mobile applications *i.e.* vehicles and ships for which urea is used as the reductant. Urea is sprayed into the hot exhaust gas and decomposes into 2 moles of ammonia and 1 moles of CO₂ [3].

The highly unwanted oxidation of SO₂ into SO₃ is also to a minor extent catalyzed by the typical vanadia (V₂O₅) based SCR catalyst. Subsequent reaction of SO₃

with water forms sulfuric acid aerosol, which can further react with NH₃ and produce solid products such as ammonium sulfate (AS) and ammonium bisulfate (ABS). The presence of AS and ABS poses an operational problem since they may condense and block the catalyst pores or stick on heat recovery systems surfaces, reducing the heat transfer, overall efficiency and operation time between cleaning of such systems.

The highest activity of a vanadium SCR catalyst is achieved around 300-400 °C[4], such high temperatures are only achievable before the turbocharger at a 2-stroke marine diesel engine. Placing the SCR reactor before the turbocharger would both increase the temperature, but also the pressure within the reactor to around 5 bars. The influence of pressure on both the SCR reactions (including NH₃ oxidation and the formation of additional pollutants such as N₂O) and the SO₂ oxidation is poorly known and hence before introducing the SCR technology within this part of the maritime sector a thorough investigation must, therefore, be conducted to ensure stable, efficient, and competitive SCR technology.

Specific Objectives

The overall goal of this project is to provide the tools, mathematical models, and knowledge needed for the industry to supply optimal and competitive SCR technology solutions for fuel oil based ships. The optimal SCR system should have a high efficiency and

avoid/address the problem of formation of byproducts such as AS or ABS.

Investigation of Pressurized SO₂ Oxidation.

Pressurized oxidation of SO₂ into SO₃ across two commercial vanadium based SCR catalyst was measured at Haldor Topsoe A/S. The general conditions used to measure the SO₂ oxidation was 8% O₂, 5 % H₂O, 1000 ppm SO₂ and balance N₂. The SO₂ oxidation was measured across both a low and a high vanadia content honeycomb marine catalyst, and similar results were found for both. Therefore, only the results obtained across the low vanadium catalyst will be shown here. SO₂, SO₃, and H₂SO₄ were measured using controlled condensation of SO₂/SO₃ and subsequent titration with BaCl₂O₈ and thorin as an indicator as described by Nielsen et al.[5].

The total flow rate was increased proportionally to the pressure in the setup, to keep the actual residence time in the catalyst more or less constant. The total flow rate in the setup is shown in Table 1, and was calculated based on the measured amount of SO_x and the added amount of SO₂.

Table 1: The total flow rate and pressure used for measurements of SO₂ oxidation.

Pressure Bar	Total Flow Nm ³ /h	Linear Velocity m/s @ P, 0 °C
1.04	4.3	0.79
2.98	13.8	0.88
4.49	18.8	0.89

The linear velocity, as shown in Table 1, indicates that a constant residence time was present at 3 and 4.5 bar and that a higher residence time was present at 1 bar.

The kinetic behavior of the pressurized SO₂ oxidation was investigated by assuming plug flow through the catalyst channels and then fitting of the rate expression shown in Equation 2.

$$F_{SO_2} \cdot \frac{dX}{dW} = k(T) \cdot p_{SO_2}^\alpha \cdot p_{SO_3}^\beta \quad (2)$$

Results and Discussion

The measured SO₂ oxidation across the low V-SCR catalyst is shown in Figure 1. Figure 1, shows that the measured oxidation of SO₂ is minimal, which is also as expected for a kinetically limited reaction and similar results can be found in the literature at atmospheric pressure. Based on the measured oxidation, as shown in Figure 1, the rate was found to be of fractional order, close to 1 with respect to SO₂ and of fractional order close to 0 for SO₃. Therefore, for practical purposes a reaction order of 1 in SO₂ and a reaction order of zero for SO₃ can be used, also at the increased pressure of up to 4.5 bar.

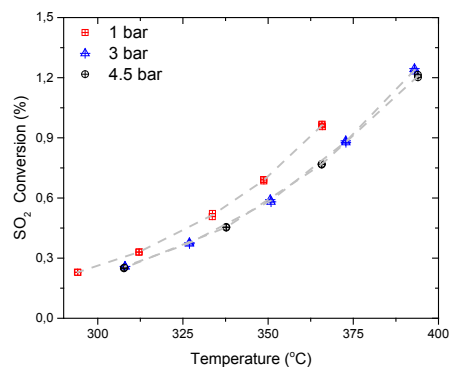


Figure 1: The measured SO₂ oxidation as a function of temperature at three pressures using the flow rates as shown in Table 1.

Conclusion

The pressurized oxidation of SO₂ was measured across two commercial vanadium based SCR catalyst. The reaction order with respect to SO₂ is found close to one also at increased pressure (4.5 bar), the reaction order of SO₃ is found close to zero. Therefore, for practical purposes, a first-order dependency with respect to SO₂ and a zero order dependency with respect to SO₃ can be used also at an increased pressure of 4.5 bar, which is interesting for a marine SCR reactor placed upstream of the turbocharger.

Acknowledgements

This project is part of the private-public society partnership named Blue INNOship. The project is a collaboration between the CHEC research center at DTU Chemical and Biochemical Engineering, Haldor Topsoe A/S, Alfa Laval Aalborg and Maersk Maritime Technology.

References

1. "Marpol 73/78 Annex VI." [Online]. Available: http://www.dnv.com/binaries/marpol_brochure_tcm4-383718.pdf.
2. P. Forzatti and L. Lietti, *Heterog. Chem. Rev.* 3 (1) (1996) 33–51.
3. M. Koebel, M. Elsener, and M. Kleemann, *Catal. Today* 59 (3–4) (2000) 335–345.
4. S. Amanatidis, L. Ntziachristos, B. Giechaskiel, A. Bergmann, and Z. Samaras, *Environ. Sci. & Technol.* 48 (19) (2014) 11527–11534.
5. "On the relative importance of SO₂ oxidation to high dust SCR DeNO_x units" [Online]. Available http://www.topsoe.com/sites/default/files/topsoe_importance_of_so2_oxidation_to_high_dust_scr_april_08.ashx_.pdf



Trine Marie Hartmann Dabros
Phone: +45 4525 2809
E-mail: trina@kt.dtu.dk

Supervisors: Anker Degn Jensen
Martin Høj
Jan-Dierk Grunwaldt, KIT
Jostein Gabrielsen, Haldor Topsøe A/S

PhD Study
Started: April 2014
To be completed: November 2017

Catalytic hydrodeoxygenation of biomass pyrolysis vapor for green fuels

Abstract

Catalytic hydropyrolysis combines fast pyrolysis with catalytic upgrading by hydrodeoxygenation (HDO) in a single step for the production of fuel oil from woody biomass. This project comprises a combined catalytic activity, characterization, and theoretical study of catalytic HDO of biomass pyrolysis vapor model compounds over MoS₂ based catalysts. The work is focused on understanding reaction and deactivation mechanisms with emphasis on the influence of H₂O, H₂S, and different model compound functionalities. The PhD study is part of the project “H₂CAP - Hydrogen Assisted Catalytic Biomass Pyrolysis for Green Fuels”.

Introduction

Conventional pyrolysis of biomass produces a high yield of condensable bio-oil at moderate temperature and low pressure [1]. However, the higher heating value of this oil (16-19 MJ/kg) is less than half of that of crude oil (44 MJ/kg) [2]. This is due to a high content of oxygen which is present as water (15-30 wt%), carboxylic acids, aldehydes, ketones, alcohols, furans, phenols and more [1-3]. Apart from the low energy content, the oxygenates present in pyrolysis oil are also responsible for a range of other poor fuel properties, e.g. a poor stability upon storage and heating, immiscibility with hydrocarbon fuels and a high acidity [1,2]. Therefore, the oil must be upgraded by decreasing the oxygen content (to <1 wt%) to achieve a fuel grade oil.

Pyrolysis oil oxygenates can be converted into fuel grade hydrocarbons and water by HDO in the presence of hydrogen over a suitable catalyst. In catalytic hydropyrolysis, HDO is performed in-situ directly in the pyrolysis reactor so that reactive oxygenates are upgraded and stabilized immediately when formed; either through catalytic hydropyrolysis or by downstream HDO on the pyrolysis vapors prior to condensation (see also Magnus Zingler Stummann, pg. 165 - 166).

Catalytic HDO is currently challenged by rapid catalyst deactivation caused by coke deposition on the catalyst surface and by poisoning from e.g. water and sulfur present in pyrolysis oil. It is crucial to develop catalysts and optimize operating conditions that enable an appreciable activity, selectivity and stability.

Specific objectives:

- ❖ Preparation of HDO catalysts in the laboratory.
- ❖ Test of prepared catalysts in a high pressure experimental setup along with investigation of process conditions.
- ❖ Detailed catalyst characterization (fresh and spent).
- ❖ Selection of catalysts for hydropyrolysis and downstream deep HDO. Investigation of catalyst stability, reaction mechanisms and deactivation mechanisms.

MoS₂ based catalysts (supported Co-MoS₂ and Ni-MoS₂) are promising HDO catalysts due to their sulfur tolerance and known activity in the analogous hydrodesulfurization (HDS) reactions [2].

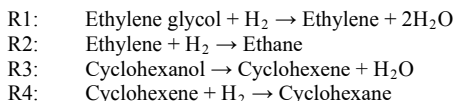
Results and discussion

Experimental HDO was carried out in a Pyrolysis Oil Converter (POC) setup; a fixed bed catalytic reactor with a typical bed volume < 10 cm³. The setup is capable of operation up to 120 bar and 550 °C. The reactor effluent was separated into gas (analyzed online by GC-TCD) and liquid (analyzed offline by GC-MS/FID). With the composition of pyrolysis oil and vapors being very complex [3], model compounds were used (individually and in mixtures) to investigate reaction mechanisms of individual compounds and interactions such as competitive adsorption. Ethylene glycol (EG), acetic acid, cyclohexanol (Cyc), and

phenol (Phe) were used as representative model compounds.

HDO of model compounds over MoS₂ catalysts

(Co/Ni)-MoS₂/MgAl₂O₄ catalysts with 3.3 wt% Mo and Co/(Ni):Mo molar ratio = 0.3 have been prepared by incipient wetness impregnation and sulfidation with 10-12% H₂S/H₂ at 360-400 °C. Catalytic HDO activity tests were conducted at 380-450 °C, 27 bar H₂ and 550-2200 ppm H₂S ($m_{\text{cat}} = 0.5\text{-}4.0$ g, $\text{feed}_{\text{model comp.}} = 0.14\text{-}0.16$ mL/min, weight hourly space velocity ($\text{WHSV}_{\text{model comp.}} = 2.3\text{-}21$ h⁻¹ (g_{model comp./g_{cat}/h), 40 barg, balance N₂). The catalysts were active and moderately selective for ethylene glycol and cyclohexanol HDO. 100 % ethylene glycol conversion was obtained for 50 h on stream at 400 °C with 550 ppm H₂S and $\text{WHSV}_{\text{EG}} = 2.3$ h⁻¹. At these conditions, a moderate HDO product yield (ethane and ethylene) of 40-45 % was observed together with an undesired cracking (C₁: CO, CO₂, CH₄) yield of 30-35 %. 100 % cyclohexanol conversion was obtained for 102 h at 390-450 °C with 550 ppm H₂S and $\text{WHSV}_{\text{Cyc}} = 18$ h⁻¹ with no observed cracking, and high yields of cyclohexene (60-80 %) and cyclohexane (14-30 %). The HDO of ethylene glycol and cyclohexanol followed consecutive dehydration and hydrogenation reactions:}



As Table 1 shows, ethylene glycol HDO was not notably affected by the presence of phenol or cyclohexanol. The rate of hydrogenation (R2) was > 20 times faster than that of the initial dehydration/hydrogenation step (R1). Cyclohexanol HDO, however, was inhibited by the presence of ethylene glycol. The dehydration of cyclohexanol (R3) is catalyzed by the MgAl₂O₄ support. Ethylene glycol HDO was correlated with significant carbon deposition, which was primarily believed to occur on acid sites of the support, but also on the active phase. Coke deposition from ethylene glycol could thus inhibit cyclohexanol HDO without markedly affecting ethylene glycol HDO over the active MoS₂ particles.

Table 1: Kinetic parameters for the HDO of ethylene glycol over Ni-MoS₂/MgAl₂O₄. Lumped rate constants for R1-R2 at 390 °C, and apparent activation energy, $E_{A,1}$, based on data from 380-415 °C. $E_{A,2}$ was ≤ 22 kJ/mol.

Feed	k_1 [L/min/g]·10 ³	k_2	$E_{A,1}$ [kJ/mol]
Pure EG	12	264	93
21 wt% Phe in EG	11	235	96
22 wt% Cyc in EG	13	331	85

Deactivation and Regeneration

Carbon deposition occurred with a linear dependence on operating time and was the main reason for catalyst deactivation. Transmission electron microscopy (TEM, see Figure 1) revealed how deposited carbon could cover MoS₂ particles thus limiting the accessibility to reactants. This carbon could be removed by oxidation in 7.6 % O₂ at 460 °C followed by resulfidation.

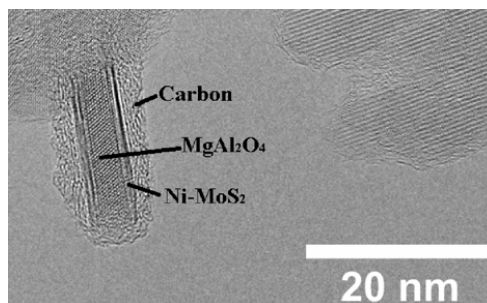


Figure 1: TEM image of spent Ni-MoS₂ from the conversion of ethylene glycol at 380-450 °C, $\text{WHSV}_{\text{EG}} = 19$ h⁻¹, 27 bar H₂, 550 ppm H₂S, 3-3.5 mol% EG in the feed, and 40 barg total (balance N₂).

Conclusions

Promoted MoS₂/MgAl₂O₄ catalysts are active in the HDO of ethylene glycol and cyclohexanol. A moderate selectivity towards HDO products was obtained for ethylene glycol, while cyclohexanol was readily converted into cyclohexene and cyclohexane in the absence of ethylene glycol. Carbon deposition deactivated the catalysts, but reactivation was possible by oxidation and resulfidation.

Acknowledgements

This work is part of the Combustion and Harmful Emission Control (CHEC) research center at The Department of Chemical and Biochemical Engineering at DTU. The project is funded by The Danish Council for Strategic Research (Innovation Fund Denmark, project 1377-00025A), The Programme Commission on Sustainable Energy and Environment. DFT calculations have been performed by collaboration partners at Stanford University. XAS studies have been performed together with collaboration partners from Karlsruhe Institute of Technology, KIT. Other catalyst analysis techniques have been performed in collaboration with KIT and Haldor Topsøe A/S.

References

- A.V. Bridgwater, Biomass and Bioenergy 38 (2012) 68-94.
- P.M. Mortensen, J.-D. Grunwaldt, P.A. Jensen, K.G. Knudsen, A.D. Jensen, Applied Catalysis A: General 407 (2011) 1-19.
- A.M. Azeez, D. Meier, J. Odermatt, T. Willner, Energy Fuels 24 (2010) 2078-2085.



Mafalda Dias Gomes

Phone: +45 4525 2886
E-mail: macoad@kt.dtu.dk

Supervisors: John M Woodley
Mathias Nordblad

PhD Study
Started: September 2015
To be completed: September 2018

Oxygen supply to oxidative biocatalysis

Abstract

Oxygen-dependent enzymes are becoming increasingly relevant in the synthesis of fine chemicals, flavours and fragrances as well as pharmaceutical intermediates. Oxidases can use molecular oxygen as an electron acceptor, the most inexpensive and innocuous oxidant available. Traditionally, oxygen is supplied by sparging air to a reactor however, the enzymatic reaction rate is commonly limited by the amount of oxygen that can be transferred from the gas to the liquid phase. Another drawback when using isolated enzymes in oxidation reactions, is their insufficient stability under relevant reaction conditions at industrial scale. In particular, oxygen-dependent enzymes may deactivate at gas-liquid interfaces due to interactions with the interface of air/oxygen bubbles. This PhD project is focused on the characterisation of biooxidation reactions and process technologies for oxygen supply in order to guide process design and development for this type of reactions.

Introduction

Oxidases are a notable subclass of oxidizing enzymes, which use molecular oxygen either as oxidant or as electron acceptor. This property makes them highly attractive for the production of chemicals since it avoids the use of harmful metal oxidants. Alcohol oxidases (AOX) convert alcohols to aldehydes or ketones. During this reaction, molecular oxygen is reduced to hydrogen peroxide (H_2O_2). In order to avoid enzyme deactivation, H_2O_2 is scavenged by addition of a catalase that converts it to H_2O and O_2 (Figure 1).

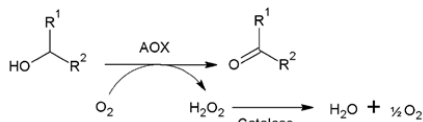


Figure 1 – Oxidation of an alcohol to an aldehyde or ketone catalysed by an alcohol oxidase (AOX). Hydrogen peroxide is scavenged using a catalase.

Flavin-dependent oxidases are enzymes where flavin adenine dinucleotide (FAD) or flavin mononucleotide (FMN) function as primary hydride acceptor. The outstanding property of flavin is the chemical versatility that enables flavoenzymes to catalyse a large variety of reactions with no need of adding a cofactor [1], [2]. This property is very attractive for implementing biooxidations in industry since the cofactor requirement of an enzyme has a significant impact in increasing the

costs of the process. With these reaction features that AOXs can provide, the main challenge to implement them in industry emerges from the requirement of molecular oxygen. Indeed, this particularity is a great benefit for biooxidations but supplying oxygen with the desired transfer rates is still a major challenge when high reaction productivities need to be achieved to develop an economic feasible process.

Common bioreactors supply oxygen by sparging air into the reaction medium but the mass transfer of oxygen from the gas to the liquid phase has proved to be a limiting factor due to high oxygen demand to achieve high enzymatic reaction productivities. Furthermore, enzyme stability might become an issue since oxidases may deactivate at a gas-liquid interface [3].

There are different alternative process technologies to sparging air for supplying oxygen to bioreactors such as sparging pure oxygen, pressurize the system or bubble-free oxygenation methods. The latter can be done by using membranes, enzymes, organic solvents or oxygen vectors [4]–[6]. All of these different options can be considered when there is a need to increase the oxygen solubility in the aqueous reaction medium or to avoid gas-liquid interfaces when dealing with unstable enzymes. However, the high oxygen transfer rates desired are still very hard to achieve.

Specific Objectives

With this in mind, there is a necessity to quantify the oxygen that an oxidase needs to catalyse a target

reaction, explore the enzyme stability and quantify how much oxygen can be provided by different process technologies. This understanding of the target enzyme and reaction can be achieved by a characterisation of the enzyme and reaction kinetics, enzyme stability and characterisation of different process technologies for oxygen supply. This PhD is focused on these three aspects in order to provide inputs and guidance to process design and development using oxidases.

Results and Discussion

This contribution presents reaction and enzyme kinetics results for a glucose oxidase (GOX) to exemplify the importance of enzyme and reaction kinetics for the design and development of a biooxidation process.

GOX catalyses the oxidation of glucose to gluconolactone, that immediately forms gluconic acid, with the production of hydrogen peroxide (H_2O_2), using molecular oxygen. In order to characterise the GOX, the enzyme kinetics as function of substrate concentration was studied. The enzyme kinetic parameters (k_{cat} , K_{MS} and K_{MO}) were found by two different methods:

1. Spectrophotometric Activity Assay (under atmospheric conditions):

The quantification of glucose oxidase activity was measured by following a secondary reaction with hydrogen peroxide (H_2O_2). Horseradish peroxidase (HRP) catalyses the reaction between 4-aminoantipyrine (AAP), sodium 3,5-dichloro-2-hydroxybenzenesulfonate (DCHBS) and H_2O_2 , that forms a pink product. The formation of this product was measured by an increase in absorbance at 515 nm in a spectrophotometer. The apparent kinetic parameters were estimated using Michaelis-Menten kinetic.

2. Automated Tube-in-Tube Reactor (TiTR) [7]:

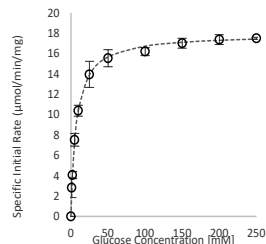
The experiments were performed in a tubular flow reactor where the initial rates were found for different glucose concentrations and different oxygen concentrations. TiTR was pressurized up to 2 bar to achieve oxygen concentrations above atmospheric pressure. Gluconic acid was measured by UV-Vis detection, as carried out in HPLC. The kinetic parameters were found by fitting all the data points in a two substrates kinetic equation ($r = (k_{cat}C_{O_2}C_S) / (C_{O_2}C_S + K_{MS}C_{O_2} + K_{MO}C_S)$).

The apparent K_{MS} , estimated based on lower oxygen concentrations in the spectrophotometric assay, was found to be 7.21 mM and the k_{cat} 17.9 U/mg. In the TiTR, the K_{MS} was found to be 29.8mM, K_{MO} 0.842mM and the k_{cat} 50.9U/mg.

First of all, it can be seen that the kinetic parameters are strongly dependent on the oxygen concentration. The enzyme is more active (higher k_{cat}) when it is not limited by oxygen concentration. According to the K_{MO} found in the TiTR, which is higher than the solubility of oxygen in water when using air at atmospheric pressure and 25 °C (0.265 mM), the enzyme kinetics is oxygen limited. Therefore, the kinetic constants estimated with the spectrophotometric assay results are limited by the oxygen concentration possible to achieve in the method. These results show the extreme significance of the

oxygen concentration in the enzyme kinetics. To work at higher efficiency of these enzymes, reactions must be carried out at concentrations above the K_{MO} and K_{MS} for the reaction rate be only depended on the enzyme concentration. These parameters are key inputs for developing a process with these enzymes, together with the reaction kinetics, which will define the oxygen transfer rate needed to supply to not limit the reaction.

A



B

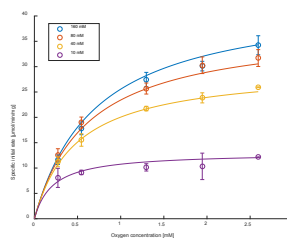


Figure 2 - Enzyme activity as a function of glucose concentration for GOX, obtained by the spectrophotometric assay (A). The assay was performed at room temperature and under atmospheric pressure in 1 mL cuvettes with phosphate buffer at pH 7.5. The reaction for each substrate concentration was performed in triplicate; error bars reflect standard deviation. The Michaelis-Menten kinetic estimation is represented by the dotted line. Enzyme activity as a function of oxygen concentration for GOX, obtained in the TiTR (B). The experiments were carried at 25 °C and up to 2 bar.

Acknowledgements

The research for this work has received funding from the European Union (EU) project ROBOX (grant agreement n° 635734) under EU's Horizon 2020 Programme Research and Innovation actions H2020-LEIT BIO-2014-1.

References

1. A. Mattevi, Trends Biochem. Sci., vol. 31, no. 5, pp. 276–283, 2006.
2. N. J. Turner, Enzym. Catal. Org. Synth. Third Ed., vol. 3, pp. 1535–1552, 2012.
3. A. S. Bommarius and A. Karau, Biotechnol. Prog., vol. 21, no. 6, pp. 1663–1672, 2005.
4. G. Quijano, J. Rocha-Rios, M. Hernández, S. Villaverde, S. Revah, R. Muñoz, and F. Thalasso, J. Hazard. Mater., vol. 175, no. 1–3, pp. 1085–1089, 2010.
5. L. M. K. Dassama, T. H. Yosca, D. a Conner, M. H. Lee, B. Blanc, B. R. Streit, M. T. Green, J. L. DuBois, C. Krebs, and J. M. Bollinger, Biochemistry, vol. 51, no. 8, pp. 1607–16, 2012.
6. P. Côté, J. Bersillon, A. Huyard, and G. Faup, Water Pollut. Control Fed., vol. 60, no. 11, pp. 1986–1992, 1988.



Demi Tristan Djajadi

Phone: +45 4525 2979
E-mail: dtdj@kt.dtu.dk

Supervisors: Anne S. Meyer, DTU
Manuel Pinelo, DTU
Henning Jørgensen, KU

PhD Study
Started: February 2015
To be completed: April 2018

Surface properties correlate to the digestibility of steam-pretreated biomass

Abstract

Steam pretreatment has been utilized to reduce the recalcitrance of lignocellulosic biomass. However, the factors underlying recalcitrance across biomass feedstocks have not been fully understood. In this work, several key grasses, corn stover (CS), *Miscanthus × giganteus* stalks (MS) and wheat straw (WS) were steam-pretreated at different severity levels to infer possibly correlated factors. Composition analysis revealed that the extent of hemicellulose removal among the biomass which has been correlated to digestibility was similar. However, MS was less enzymatically digestible compared to the other biomass. Surface properties, namely wettability and relative surface abundance of lignocellulosic components correlated better to biomass digestibility.

Introduction

Steam pretreatment has been applied to overcome the recalcitrance of lignocellulosic biomass for production of renewable chemicals, fuels and materials. In the process, biomass is treated with water typically at 180-200°C for 10-20 min without catalyst [1]. During the process, biomass undergoes several structural and chemical changes. Hemicellulose was solubilized and lignin was redistributed (depending on severity factor, which is a function of temperature and residence time of the pretreatment), while cellulose remained stable [2,3].

After steam pretreatment, the biomass fiber fraction is processed with enzymes to convert mainly cellulose into glucose. The subsequent digestibility of cellulose has been correlated to the extent of hemicellulose removal where linear correlation with severity was usually found [4]. However the underlying cause of recalcitrance across biomass is still not fully understood.

Specific Objectives

The objective (as published in Djajadi et al. 2017) is to find factors that correlate with the digestibility of lignocellulosic Poaceae biomass feedstocks that were steam-pretreated at different severity factors.

Experimental

Corn stover (CS), *Miscanthus × giganteus* stalks (MS) and wheat straw (WS) were steam-pretreated at three different severity factors ($\log R_0$): 3.65 (190°C, 10 min), 3.83 (190°C, 15 min) and 3.97 (195°C, 15 min). The fiber fraction of the biomass were analyzed for bulk

composition, enzymatically hydrolyzed to test the digestibility and analyzed for surface properties using contact angle measurement and ATR-FTIR.

Results and Discussion

Composition of the fiber fraction of pretreated biomass revealed that major fractions of hemicellulose (mainly arabinoxylan which is abundant in grasses) have been solubilized during steam pretreatment (Fig. 1). The extent of hemicellulose removal increased according to the elevated severity factor. Since the extents of removal were similar in all biomass, it can be expected that they correlate to the corresponding digestibility.

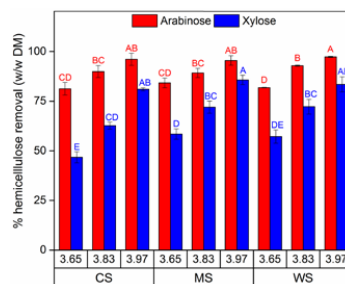


Figure 1: Removal of arabinose (red) and xylose (blue) relative to the amount in untreated (raw) biomass for CS, MS and WS at different severity factors ($\log R_0$) = 3.65; 3.83; 3.97. Different letters indicate significant statistical difference based on ANNOVA ($p \leq 0.05$).

The digestibility however differed among the biomass. After enzymatic hydrolysis with Cellic[®] CTec3 for 72 h, MS was found to have ~24-67% lower glucose release across severity and enzyme dosage (Fig. 2). Even though digestibility increased with severity, this indicated that other factors governed recalcitrance seen across biomass in response to steam pretreatment.

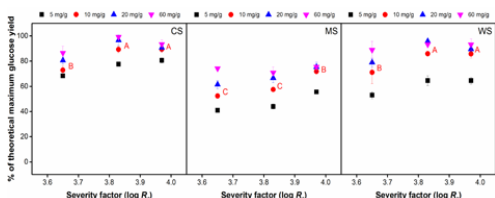


Figure 2: Glucose release after hydrolysis of steam-pretreated CS, MS and WS at different severity factors ($\log R_0$) and enzyme dosages (mg protein/g DM biomass). Different letters indicate significant difference based on ANNOVA ($p \leq 0.05$).

Since bulk composition of the biomass did not reflect the corresponding digestibility, it was hypothesized that surface properties will correlate better. Surface wettability was assessed by contact angle measurement. Higher contact angle value indicates lower wettability of the material. The results revealed that wettability increased in response to pretreatment and increasing severity, although MS responded less than others (Fig. 4 A). There was a strong negative correlation between contact angle and digestibility of biomass (Fig. 4 B).

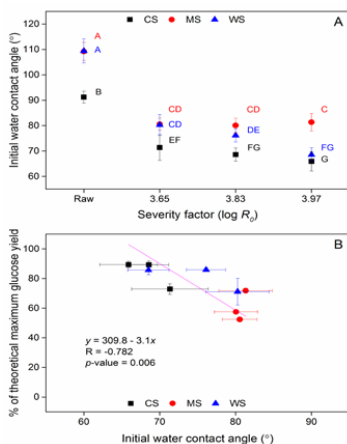


Figure 3: Initial water contact angle (A) of raw and steam-pretreated biomass. Different letters indicate significant difference based on ANNOVA ($p \leq 0.05$). Correlation of water contact angle and glucose release (B) of the steam-pretreated biomass after 72 h hydrolysis at 10 mg/g dosage. The strength of linear relationship is indicated by Pearson's correlation coefficient (R) and *t*-test of slope (significant if $p < 0.05$).

The wettability test, which correlated to digestibility, indicated that the correlating factor can be present in the surface of the biomass material. Attenuated total reflectance Fourier-transform infrared (ATR-FTIR) spectroscopy was performed to assess the relative surface abundance of lignocellulosic components. The results (Fig. 4) revealed that there was higher abundance of hemicellulose and lignin in MS which can confer its higher recalcitrance relative to the other biomass.

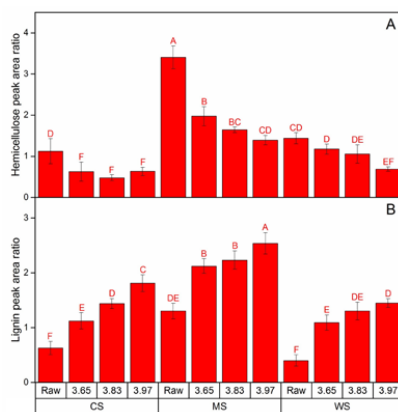


Figure 4: Relative surface abundance of hemicellulose (A) and lignin (B) compared to cellulose based on ATR-FTIR peak ratios. Different letters indicate significant difference based on ANNOVA ($p \leq 0.05$).

Conclusions

To a large extent, surface properties correlate better to the digestibility of steam-pretreated biomass compared to bulk composition.

Acknowledgements

This was funded by the BioValue SPIR, Strategic Platform for Innovation and Research on value added products from biomass, which is co-funded by The Innovation Fund Denmark, case no.: 0603-00522B.

References

1. J. Larsen, M. Ø. Haven, L. Thirup, Biomass Bioenerg. 46 (2012) 36-45.
2. J. B. Kristensen, L. G. Thygesen, C. Felby, H. Jørgensen, T. Elder, Biotechnol. Biofuels 1:5 (2008).
3. H. A. Ruiz, R. M. Rodríguez-Jasso, B. D. Fernandes, A. A. Vicente, J. A. Teixeira, Renew. Sust. Energ. Rev. 21 (2013) 35-51.
4. C. K. Nitsos, K. A. Matis, K. S. Triantafyllidis, ChemSusChem. 6 (2013) 110-122.

List of Publications

1. D. T. Djajadi, A. R. Hansen, A. Jensen, L. G. Thygesen, M. Pinelo, A. S. Meyer, H. Jørgensen, Biotechnol. Biofuels 10:49 (2017).



Andreas Eschenbacher

Phone: +49 151 17868639

E-mail: aesc@kt.dtu.dk

Supervisors: Anker Degn Jensen,
Peter Arendt Jensen, Ulrik Birk Henriksen,
Jesper Ahrenfeldt

PhD Study

Started: February 2017

To be completed: January 2020

Deoxygenation of fast pyrolysis vapors using zeolites

Abstract

Process optimization of a bench scale fast pyrolysis set-up has been performed in order to screen the performance and stability of modified MFI zeolites in the ex-situ upgrading of straw and wood derived pyrolysis vapors. Repeated regeneration of the parent zeolites was demonstrated at the bench scale unit. Harsh regeneration conditions led to temperature peaks and permanent loss in the zeolite's acidity. A certain extent of mesopores is introduced to the parent zeolites by post-synthesis desilication to increase the zeolite's active time on stream.

Introduction

Fast pyrolysis of biomass produces a high yield of bio-oil at optimized process conditions [1]. Reducing the oxygen content of the obtained bio-oils increases its stability and heating value [2], which can render the upgraded bio-crude suitable for further processing in oil refineries. Downstream catalytic upgrading of the pyrolysis vapors over solid acid catalysts in a close-coupled process can offer processing and economic advantages over high pressure hydrotreating [3].

To date, the medium pore size ZSM-5 zeolite yields a high aromatic yield and the least amount of coke [4] in upgrading of pyrolysis vapors. However, the reactive pyrolysis vapors still lead to rapid coking of the zeolite, which must be regenerated by oxidative burnoff. At the high operating temperatures, the water introduced by the biomass moisture and from the pyrolysis process itself can lead to permanent deactivation of the zeolite structure via steaming. By modifications of the zeolite, this study aims to improve both the active time on stream and the long-term stability throughout multiple regeneration cycles. The Si/Al ratio and the operating temperature are main parameters for the catalyst's performance. Also combinations of several types of catalysts have been demonstrated for physically mixing microporous with mesoporous catalysts [5] and dual beds comprised of solid acid and basic catalysts [6]. Furthermore, the yield of aromatics can be improved by metal incorporation [7].

Despite promising laboratory results, long term experiments of pilot plants showing stable catalyst operation with multiple regeneration steps are needed to prove the economic attractiveness of bio-oil plants.

Specific Objectives

It is investigated how the operation and interaction of the pyrolysis unit, hot gas filtration and catalyst fixed bed (Fig. 1) influences the product distribution. While mostly nitrogen is used as sweeping gas, the recycling of non-condensable pyrolysis gases may have a positive effect on the oil yield [8] and is currently being investigated.

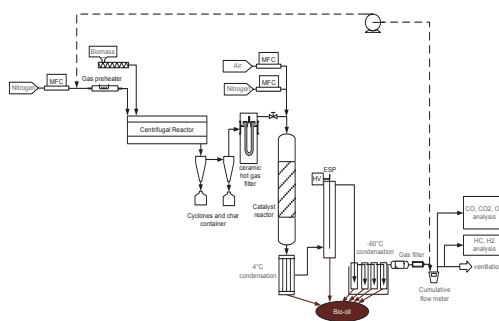


Figure 1: Process scheme of fast pyrolysis set-up with ex-situ vapor upgrading, downstream oil collection, gas analysis and recycle option (dashed)

Results and Discussion

The performance of the ZSM-5 type zeolite for pyrolysis vapor upgrading is influenced by the operating temperature and the zeolite's acidity and pore structure. Mesopores have been introduced into the microporous

bulk structure via NaOH leaching in order to reduce diffusion limitations and prolong the catalyst's active operation by reduced coking. The characterization of the modified zeolites via nitrogen and argon physisorption, NH₃-TPD, XRD, XRF and TEM analysis confirmed the successful introduction of mesopores (Fig. 2) and the accompanied reduction in acid sites (Fig. 3) due to the removal of Al containing framework. Thus, it is desirable to obtain a considerable amount of mesopores without losing too much of the micropore bulk volume containing the majority of active sites.

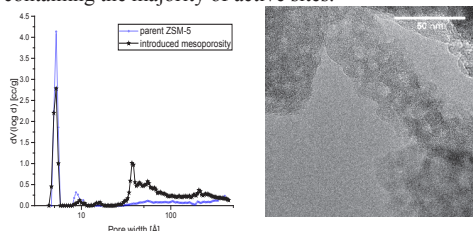


Figure 2: Argon physisorption and TEM confirm the introduction of mesopores.

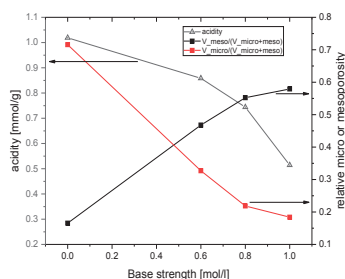


Figure 3: Change in acidity and relative micro/mesopore volume of modified MFI zeolite.

The yield of organic liquid obtained from wood derived pyrolysis vapors decreases considerably once the vapors are passed over the zeolite (see Fig. 4). This is mainly due to the enhanced CO/CO₂ production and formation of water during the vapor cracking reactions. Table 1 lists a comparison of the oxygen content and heating values (HHV) of the wood feedstock and the derived oils from pure pyrolysis and from ZSM-5 vapor upgrading. The energy content of the upgraded oil is increased.

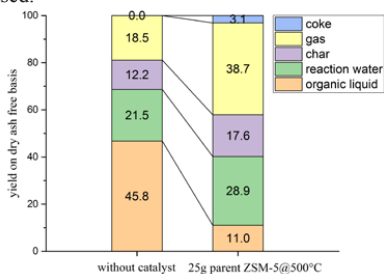


Figure 4: Change in product distribution for pure wood pyrolysis and upgraded vapors over ZSM-5

Table 1: Comparison of feedstock and bio-oil oxygen content and higher heating values

source	oxygen [wt-%] _{daf}	HHV _{ab} [MJ/kg]
wood feedstock	40.8	22.0
heavy fraction of pyrolysis oil obtained without recycling gases	30.8	25.4
heavy fraction of catalytically upgraded pyrolysis oil (parent ZSM-5)	22.6	29.9

For the upgrading of straw derived fast pyrolysis vapors a repeated intermittent oxidative regeneration step was conducted. The injection of 5% oxygen allowed regeneration to occur in a similar time frame compared to the catalyst's time on stream; however, it also led to permanent loss of the zeolite's acidity (Table 2).

Table 2: Comparison of acidity of parent and frequently regenerated zeolite determined via NH₃-TPD

catalyst	acidity [mmol/g]
fresh zeolite	1.02
used zeolite, removed from beginning of bed	0.75
used zeolite, removed from end of bed	0.56

Conclusion

The parent zeolite deactivates rapidly due to coking, thus, it requires modifications. The pore structure of the ZSM-5 type zeolite with an acidity range relevant for the upgrading of biomass derived fast pyrolysis vapors can be tuned by introduction of a certain extent of mesopores. Too harsh leaching conditions lead to significant loss of pore volume and acid sites.

Future work

A selection of the most promising modified zeolites in terms of acidity and mesoporosity will be tested for their catalytic performance. This way it is aimed to obtain further insights how the interplay between pore structure and distribution of acid sites affects catalyst activity.

Improvements of the zeolite's hydrothermal stability are needed in order to speed up regeneration cycles and limit the extent of dealumination via steaming. The current reactor dimensions will be increased to allow collection of larger amounts of upgraded bio-oil for more thorough characterization.

References

- Akhtar, J. & Saidina Amin, N., *Renew. Sustain. Energy Rev.* 16, 5101–5109 (2012).
- Bridgwater, A. V., *J. Anal. Appl. Pyrolysis* 51, 3–22 (1999).
- Bridgwater, A. V., *Catal. Today* 29, 285–295 (1996)
- Jae, J. et al., *J. Catal.* 279, 257–268 (2011).
- Rezaei, P. S., PhD thesis, Faculty of Engineering, University of Malaya (2016).
- Wang, J. et al., *Energy Convers. Manag.* 139, 222–231 (2017).
- Schultz, E. L., Mullen, C. A. & Boateng, A. A., *Energy Technol.* 5, 196–204 (2017).
- Mante, O. D., Agblevor, F. A., Oyama, S. T. & McClung, R., *Bioresour. Technol.* 111, 482–490 (2012).



Hannah Feldman

Phone: +45 4525 2811
E-mail: hafe@kt.dtu.dk

Supervisors: Krist V. Gernaey
Xavier Flores-Alsina
Gürkan Sin
Ulf Jeppsson (Lund University)
Kasper Kjellberg (Novozymes A/S)

PhD Study
Started: April 2015
To be completed: March 2018

Optimization of the energy recovery in an industrial wastewater treatment plant

Abstract

The focus of this study is to research different methods to increase the energy recovery in an industrial wastewater treatment plant. The strategies applied in this study were: 1) Model-based optimization of the operational conditions. In order to maintain economic viability, the chemicals needed for pH dosing were also taken into account. It was found that the chemicals have a significant effect on the reactor performance index (RPI), and reducing the pH to 6.8 increases the RPI by 45%. 2) The effect of multiple mineral precipitation on the granular structure of the sludge in the anaerobic digester. Simulations have shown that on the long-term, biomass is lost and the energy recovery efficiency decreases due to precipitates out-competing the biomass for space. 3) Alternative nitrogen removal through the anammox process, which can result in the redirection of organic material to biogas production (energy recovery). This work is ongoing.

Introduction

In recent years a shift has occurred in wastewater treatment plants, where the water is not just seen as a waste that has to be treated, but also as a resource of nutrients and energy. The focus of this study is on the recovery of energy in an industrial wastewater treatment plant operated by Novozymes A/S in Kalundborg, Denmark. Energy is produced in an anaerobic digester in the form of methane, which can be converted to heat and electricity. While this process removes organics (chemical oxygen demand; COD) from the wastewater, it does not remove nitrogen. The conventional nitrogen removal process takes place in activated sludge reactors, where ammonium is converted to nitrite, nitrate and subsequently nitrogen gas by nitrification and denitrification (Figure 1). COD is needed for this process, which means the COD loading rate to the anaerobic digester is limited by nitrogen removal. Another way to remove nitrogen is through the anammox (anaerobic ammonium oxidation) process, which uses nitrite as electron acceptor to convert ammonium directly to nitrogen gas. The anammox bacteria responsible for this reaction are anaerobic and autotrophic, so do not need oxygen or COD.

Specific objectives

The objective of this study is the optimization of the energy recovery in an industrial wastewater treatment

plant. This is done through three case studies, which each look at a different area of optimization:

- 1) Model-based optimization of the operational conditions of the anaerobic digester.
- 2) Effect of the granular structure in the anaerobic digester.
- 3) Autotrophic nitrogen removal to redirect the organics to biogas formation (ongoing).

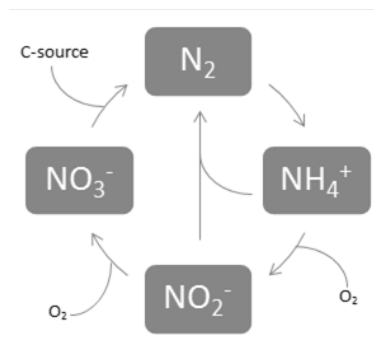


Figure 1. Schematic overview of the nitrogen cycle, where the reaction from NH_4^+ to NO_2^- represents nitrification, the reaction from NO_2^- to NO_3^- represents nitratation and the reaction from NO_3^- to N_2 represents denitrification. The anammox reaction is represented by the two interconnecting arrows from NH_4^+ and NO_2^- to N_2 .

Results

Case 1

The IWA Anaerobic Digestion Model no. 1 (ADM1) [1] was modified to fit the reactor hydraulics and conditions. The output of the simulations is the reactor performance index (RPI), which takes into account the profit from energy recovery minus the cost of NaOH dosing for pH control.

Simulation of the operational conditions revealed the largest effect can be obtained by decreasing the pH (+ 45 %; Figure 2). This is due to a decrease in NaOH dosing needed for pH control. The pH should not be lowered below 6.8, as lower values can destabilize the process. Removing the sulfate and sulfide in the influent increases the RPI with 25 %. This is partly due to the removal of the inhibitory effect of sulfide on methanogens. Another contribution is the removal of acidity, which decreases the NaOH dosing. However, the cost of removing sulfur compounds in the influent exceeds the gain. This strategy is therefore not attractive under the current loadings.

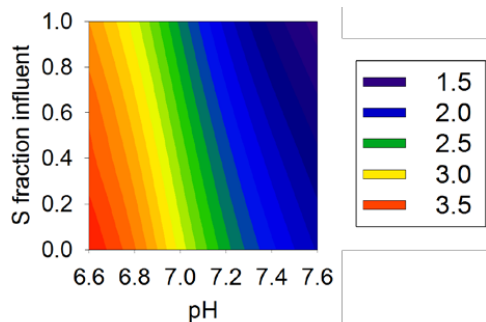


Figure 2. Response surface plot of the influence of pH vs S in the influent on the industrial anaerobic digester. The results are given as the reactor performance index (RPI) in MC/year. Default operational conditions are at pH 7.2 and an S fraction of 1.0.

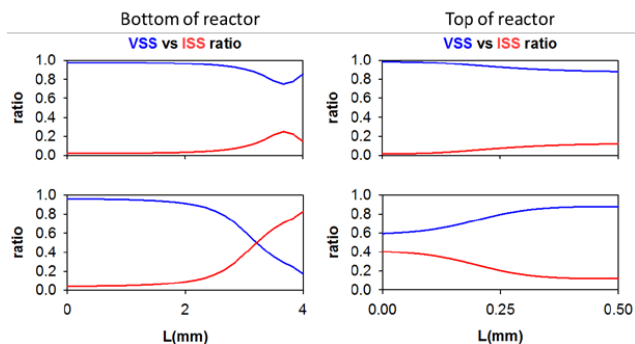


Figure 3. Predicted volatile suspended solids (VSS) versus inert suspended solids (ISS) content within the granule at different reactor heights and simulation times (top: $t = 0$ days, bottom: $t = 100$ days).

Case 2

Simulating the granules inside the reactor with a biofilm model [2] revealed a competition for space between biomass and precipitates such as CaCO_3 , in the case of a high mineral content in the influent. On long-term operation, the precipitates will out-compete the biomass for space, resulting in a loss of biological activity, and thus energy recovery. This is mainly apparent in the bottom of the reactor, as larger granules are heavier and will sink to the bottom. Figure 3 shows the evolution of the VSS (biomass) and ISS (inerts, including particulates) concentrations in the bottom and top of the reactor over time.

Conclusions

The goal of this project is to increase the energy recovery from an industrial full-scale granular sludge reactor. The study is comprised of three different strategies to reach this goal. The reactor itself has been modelled through a hydraulic model in order to optimize the reactor conditions, as well with a biofilm model, to study the biomass inside the reactor. Furthermore, the potential application of an autotrophic nitrogen removal reactor is currently researched, which can further increase the sustainability of the wastewater treatment plant.

Acknowledgements

The author would like to thank the Technical University of Denmark and Novozymes A/S for the financing of this PhD study.

References

1. Batstone DJ, Keller J, Angelidaki I, Kalyuzhnyi SV, Pavlostathis SG, Rozzi A, Sanders WTM, Siegrist H, Vavilin VA. 2002a. The IWA Anaerobic Digestion Model No 1. *Water Sci. Technol.* **45**:65–73.
2. Feldman H, Flores-Alsina X, Ramin P, Kjellberg K, Jeppsson U, Batstone DJ, Gernaey KV. 2017. Modelling an industrial anaerobic granular reactor using a multi-scale approach. *Water Res.* **126**: 488-500.



Gianni Ferrero

E-mail: giferr@dtu.dk

Supervisors: Søren Kiil
Claus Erik Weinell
Kim Dam-Johansen
Lars Thorslund Pedersen, Hempel A/S

PhD Study
Started: August 2017
To be completed: August 2020

Coatings for high pressure and high temperature

Abstract

This project is focused on the investigation and understanding of coating degradation mechanisms at high pressure and high temperature conditions. Epoxy coatings perform typically well in harsh environments. However quick failures can be observed in the presence of specific chemicals which can significantly hinder the performance of the coatings. Preliminary tests showed that p-xylene, and possibly low-weight aromatics, can enhance the degradation of the coatings. Further experiments will be performed to comprehend this degradation mechanism and verify if other parameters such as temperature, pressure and presence of different gases contribute to the failure of the coating.

Introduction

Although the world community is trying to switch to more sustainable forms of energy, the oil and gas industry has still a major role in the production of energy and the demand is steadily growing every year. [1] For these reasons, the industry is constantly trying to find alternative reservoirs and this lead to the exploit, among other sources, of deeper oil and gas wells, commonly known as high pressure and high temperature (HPHT) wells (205 °C and 138 MPa). [2] Extraction of natural resources from this type of wells can be challenging due to the fast deterioration of the equipment in such conditions. Corrosion of the pipelines is one of the most common problems in this field. In general, the presence of saline water, oxygen and other aggressive gasses such as hydrogen sulphide (H₂S) are the main causes of corrosion in oil and gas pipelines. [1,3] Protective coatings have been successfully developed to protect the pipelines from the harsh environment in which they operate. Epoxy coatings are extensively used due to their excellent stability, impermeability towards water and gasses and reactive inertia against aggressive agents. [3] However, HPHT wells pose new challenges due to the high temperature and high pressure in which the pipes operate. The degrading effect of water, hydrocarbons and gas mixtures in such conditions is enhanced and most of the coatings suffer from severe failures in a short time, leading to high maintenance costs and risk of leaks with possibility of vast environmental pollution [1]. Thus, it is of utmost importance to find new coatings able to

withstand such extreme working conditions. In order to be able to formulate new improved coatings it is necessary to understand the causes of the coating degradation. High temperature and pressure might accelerate the degradation by affecting directly the coating or by making the liquids and gasses present in the pipeline more aggressive towards the latter.

Specific Objectives

HPHT conditions are believed to affect the degradation of the epoxy coatings in a severe way. A meticulous testing and characterization of the coatings need to be performed in presence of different liquids and gasses to assess degradation mechanisms and coating lifetime. The main steps on the project are described below:

1. Assessment of the effect of high temperature and high temperature in presence or absence of different liquids, gasses and exposure times in the pilot plant batch reactor
2. Determination of the degradation effects in presence of a single component in the batch reactor (e.g. water, saline water, hydrocarbons, CO₂, O₂, H₂S, high temperature, high pressure etc.)
3. Determination of the degradation effects in presence of multiple components combined in the batch reactor

4. Characterization of the degradation mechanisms through microscopy, spectroscopic methods and mechanical testing
5. Estimation of the coatings lifetime by assessing the degradation rates in different conditions
6. Development of new coatings specifically designed to withstand extreme working conditions and development of new characterization techniques

Results and Discussion

The first part of the project is focused on gaining a deep understanding on the properties and possible effects that each compound might have on the coating. This includes solubilities, diffusion and possible synergies of the species present in the HPHT reactor. The second part of the project will deal with the characterization and quantification of the coatings' degradation mechanism(s). Development of improved coatings that can impede or at least delay the degradation of the latter will be considered in the last period of the project. Various tests at HPHT conditions (180 °C and 150 bar in presence of nitrogen gas) have been already performed during previous MSc projects and showed that degradation and blistering only occurs on the coating surface in contact with the seawater. In addition, the presence of p-xylene is needed for the blistering to form. [4]

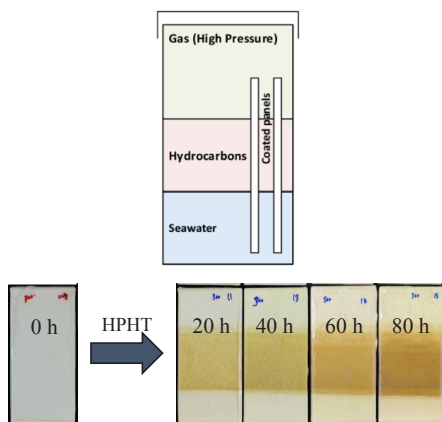


Figure 1: Above, schematic showing coated panels in the HPHT set up. Different areas are in contact with different phases. Below, coating degradation at 180 °C and 150 bar in nitrogen atmosphere after 0, 20, 40, 60 and 80 hours of exposure. [4]

N-paraffin did not induce degradation. Further experiments must be conducted in order to understand if the coatings are sensible specifically to p-xylene or to a broader range of low-weight aromatics. However, it is also important to understand how the p-xylene is inducing blisters not to the coating area directly in contact with the aromatic but only to the area in contact with the underlying aqueous phase. The fact that p-xylene is poorly soluble in water even at high

temperature and pressures, makes this phenomenon even more interesting. [5]

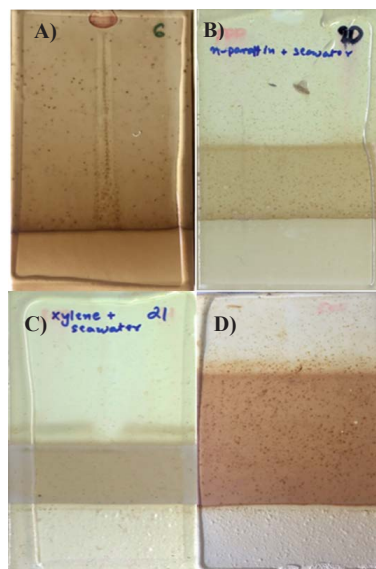


Figure 2: coated panels after being exposed to different chemicals at HPHT conditions (180 °C and 150 bar in nitrogen atmosphere). (A) seawater only, (B) n-paraffin and seawater, (C) p-xylene and seawater, (D) p-xylene + n-paraffin and seawater. It is clearly visible that blistering only occurs in the water phase when p-xylene is present. [4]

Future work

Further investigations on the cause of blistering is needed. The same experiments will be repeated in the presence of different gasses and chemicals to comprehend the nature and causes of the degradation. Possible degradation mechanisms and pathways will be proposed and measures to prevent coating failure developed and tested.

References

1. Popoola, L., Grema, A., Latinwo, G., Gutti, B. & Balogun, A. Corrosion problems during oil and gas production and its mitigation. *Int. J. Ind. Chem.* 4, 35 (2013).
2. DeBruijn, G. High-pressure, high-temperature technologies. *Oilf. Rev.* 20, (2008).
3. Sørensen, P. A., Kiil, S., Dam-Johansen, K. & Weinell, C. E. Anticorrosive coatings: a review. *J. Coatings Technol. Res.* 6, 135–176 (2009).
4. Srinath S. Venkateswaran, Anticorrosive coatings at high temperatures and high pressure, DTU master thesis, 2017
5. Kevin G. Knauss and Sally A. Copenhavert, The solubility of p-xylene in water as a function of temperature and pressure and calculated thermodynamic quantities *Geochimica et Cosmochimica Acta*, Vol. 59. No. 12, pp. 2443-2448, 1995



Héctor Forero-Hernández

Phone: +45 4525 2910
E-mail: hafh@kt.dtu.dk
hector.hernandez@alfalaval.com

Supervisors: Bent Sarup, Alfa Laval Copenhagen A/S
Gürkan Sin
Jens Abildskov
Anker Degn Jensen

PhD Study

Started: June 2016
To be completed: June 2019

Validation and improvement of property and process modelling for oleochemicals

Abstract

While oleochemicals, with an estimated output of 100 million metric tons per year, are small compared to primary petrochemicals, they are an important component in today's market place. To a large extent, this is due to the high technological standard of this mature industry. A most important factor, however, is that natural oils and fats are biodegradable. It furthermore has become possible to better respond to consumer needs by modifying the carbon chain and distribution of the oleoproducts and by understanding their behavior and properties. Nevertheless, reviewing the technical development of the oleochemicals manufacture one finds that some basic facts related the thermodynamic and kinetics have only been partly recognized because of the rather harsh physical conditions at what oleochemicals are exposed during their processing. The purpose of the project is the provision of a systematic methodology and framework to design and optimize selected oleochemical processes, in particular the fat-oil splitting process.

Introduction

This project is part of the Marie Skłodowska-Curie Innovative Training Network "ModLife: Advancing Modelling for Process-Product Innovation, Optimization, Monitoring and Control in Life Science Industries" in the Horizon 2020 Program of the European Commission (H2020-MSCA-ITN-2015 call, Project No.675251). It aims to collect, validate and improve properties and models of selected oleochemical processes (including recovery of high value added products) so as to optimize them.

Purpose and objectives

The study will first determine what the gaps in the property models are and the needs for data for further improvement and validation. Then, the study will generate and collect new pure component as well as mixture data relevant for oleochemicals (Vapor Liquid Equilibria, Liquid Liquid Equilibria and chemical kinetics). Further, the obtained properties and models will be used to improve the overall design of selected oleochemical processes including fat-oil splitting and fatty acids distillation.

This study seeks to fulfill the following objectives:

- Study, validation and improvement of kinetic and thermodynamic models.
- Process development ontology.

- Methodologies for process development, process design framework and optimization.

Methodology

The methodology contains the development of experiments, different ways to assess properties, and an approach to examine and validate the properties and models. The major challenge to apply this methodology, though, involves the fact that feasible solutions are very reliant on the nature of the components being addressed. There will be carried out an efficient analysis of an extensive variety of thermodynamic properties of the components to be generated and separated, description of appropriate processing methods (which takes advantages of the dissimilarities in the properties inherent in every component) and identification of methods to solve these tasks (solution of the problem using different techniques). The employment of the interactions between thermodynamic properties and process engineering principles, the physical viability restrictions for specific processes will be analysed and then it will be possible to determine optimal process flowsheets [1,2].

Experimental set-up

Batch autoclaving of vegetable oils was employed to generate fatty acids. Commercial vegetable oils and water were introduced in a batch autoclave and heated

to about 180C-250C under autogenous pressure of about 20-45 bar. In the non-catalyzed hydrolysis the oil is almost completely miscible in water. The mixture of liberated fatty acids, washed free of glycerin by the water, was separated by mechanical means. Due to its heterogeneous nature, the hydrolysis reaction is affected not only by the chemical kinetics but also by the rate of mass transfer between the oil and water as well as their specific contact area [3]. Considering these properties, a model was developed and evaluated by comparing the results with the obtained experimental data. Figure 1 shows the proposed experimental set-up:

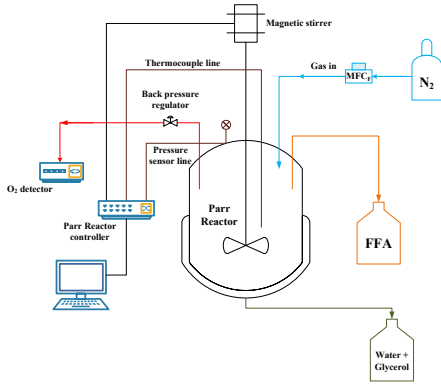


Figure 1: Batch autoclaving of vegetable oils

Mathematic model

Due to an excess of water, the conversion of triglycerides to fatty acids follows pseudo-homogeneous second order reaction kinetics that can be represented as:

$$-r_A = \frac{dC_A}{dt} = k_1 C_A^2 \quad (1)$$

In Equation (1) k_1 is the irreversible reaction rate constant for the pseudo homogeneous regime and CA is the concentration of triglyceride. Equation (1) can also be expressed in terms of conversion:

$$-\frac{dx_A}{dt} = k_1 C_{A0} (1 - x_A)^2 \quad (2)$$

When the hydrolysis is reaching the chemical equilibrium, the forward and reverse reaction rates follow second order reaction kinetics as described by:

$$-r_A = -\frac{dC_A}{dt} = k_2 C_A C_B - k_3 C_D C_F \quad (3)$$

In Equation (3) k_2 and k_3 represent the forward and reverse reaction rate constants, C_B , C_C and C_D are concentrations of water, fatty acids and glycerol in the reacting mixture. The initial concentration of water C_{B0} , fatty acids $C_{D0} = 0$ and glycerol $C_{F0} = 0$. Since

$$C_B = C_{A0} (M - 3x_A), C_D = 3C_{A0}x_A, C_F = C_{A0}x_A$$

Equation (5) can be modified as:

$$\frac{dx_A}{dt} = k_2 C_{A0} (1 - x_A)(M - 3x_A) - 3k_3 C_{A0} x_A^2 \quad (4)$$

In Equations (2) and (4) the parameters k_1 , k_2 and k_3 are kinetic constants to be calculated.

Estimation of kinetic parameters

Experimental information is used in order to estimate the kinetic parameters of the hydrolysis reaction of vegetable oils and to analyze the uncertainty of the parameters as well as the model prediction by means of the bootstrap method. These parameters are presented in Table 1:

Table 1. Confidence intervals for the estimated parameters

	Lower 97.5% Confidence	Mean	Upper 97.5% Confidence
k_1	0.227	0.271	0.315
k_2	0.00388	0.0044	0.005
k_3	0.0062	0.008	0.01

In this work a bootstrap based uncertainty analysis was performed to rank the accuracy of estimated parameters and model output. Thereafter, uncertainty and sensitivity analysis were performed to rank the accuracy of estimated parameters and model output. Both the data and the model were studied showing a practical significance of the methods proposed in this work [4]. The kinetic results obtained were used in predicting the mass transfer coefficient as a function of observable variables e.g. agitation speed, temperature, pressure, density and viscosity.

Conclusions and future work

The results proved that the estimated parameters enhanced the fitting to the experimental data with a narrow confidence interval, confirming the validity of the proposed model. Since the lack of experimental data is a crucial issue in the hydrolysis of vegetable oils, this model-based analysis of data is of substantial value to provide necessary information for detailed modeling and characterization of the process.

References

1. Aniya, V. K., Muktham, R. K., Alka, K., & Satyavathi, B. (2015), *Fuel*, 161, 137-145.
2. Vicente, G., Martínez, M., Aracil, J., & Esteban, A. (2005), *Industrial & Engineering Chemistry Research*, 44(15), 5447-5454.
3. Patil, T. A., Butala, D. N., Raghunathan, T. S., & Shankar, H. S. (1988), *Industrial & engineering chemistry research*, 27(5), 727-735.
4. Sin, G., & Gernaey, K. (2016), *Data Handling and Parameter Estimation*. In *Experimental Methods in Wastewater Treatment*. IWA Publishing Company.

**Rebecca Frauzem**

Phone: +45 4525 6173
E-mail: rebfra@kt.dtu.dk

Supervisors: Rafiqul Gani, DTU
John M. Woodley, DTU

PhD Study
Started: October 2014
To be completed: December 2017

Sustainable synthesis-design of carbon dioxide capture and utilization processes

Abstract

Increased need for sustainable practices has resulted in a push for research and development in emission reduction. This is particularly prevalent for carbon dioxide emissions. Carbon dioxide capture and utilization is a promising method of reducing emissions due to the ability to offset (economically) the cost of carbon capture. To achieve this, a 3-stage framework for the sustainable synthesis-design of carbon dioxide capture and utilization has been developed. This framework integrates a number of computer-aided tools, including a database, superstructure optimization interface (Super-O), analyses and simulation software. This framework has been applied to the design and analysis of carbon dioxide capture and utilization processes to produce various value-added chemical products, including methanol, dimethyl carbonate, dimethyl ether, succinic acid and acetic acid, via conversion.

Introduction

Carbon dioxide (CO₂) is the most prevalent greenhouse gas constituting over 80% of greenhouse gas emissions. Methods to reduce the concentration of carbon dioxide in the atmosphere, including carbon dioxide capture, utilization and storage, are needed. Carbon dioxide capture and utilization is a promising method, in addition to carbon capture and storage, which removes the carbon dioxide from emission streams and reuses it or transforms it to commercial products. Superstructure optimization has been performed in other works to optimize the types of capture and determine supply chain for carbon capture and utilization. However, these contain fixed utilization scenarios or only consider sequestration; superstructure optimization has not been applied to determining the optimal utilization path considering chemical conversion.

Therefore, a framework has been developed following a 3-Stage approach: (1) synthesis, (2) design, and (3) innovation for the sustainable design of carbon dioxide capture and utilization processes. This framework decomposes the problem into the stages, first using superstructure optimization to determine the optimal processing route, then performing rigorous simulation and analyses to determine areas for improvement, and finally implementing process intensification methods [1] to find innovative and more sustainable solutions. The production of numerous value-added products (methanol, dimethyl ether, etc.) have been designed and

analysed to show that conversion processes can be economically competitive and environmentally beneficially.

3-Stage Framework

An overview of the developed 3-Stage framework is shown in Figure 1. In this method, the problem is decomposed to enable the solution of complex and large problems. In each stage, the model complexity increases as the number of alternatives decreases. In Stage 1, the processing route is selected from a network of alternatives. This stage incorporates reaction path synthesis to find different reaction opportunities (currently over 100 reactions have been generated producing commercial chemical products), a database to store the information, and an interface, Super-O, to facilitate the synthesis. In this way, unique opportunities and products are explored. In Stage 2, the selected processing route is designed and analysed by using simulation software and sustainability (economic, environmental and LCA) analysis tools. From this stage, hot spots and areas for improvement are also generated. In Stage 3, the targets for improvement are used to develop novel and more sustainable design alternatives, including the use of process intensification. The framework can be started at any stage provided the input information. The framework also incorporates computer-aided methods and tools within the steps.

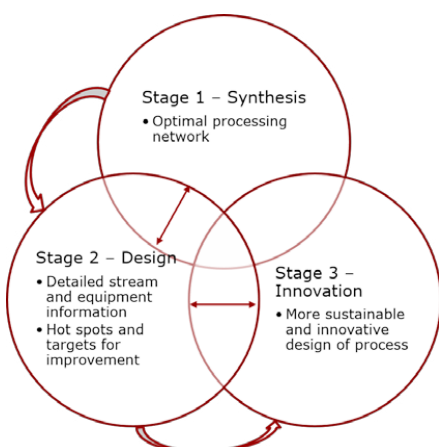


Figure 1. The 3-Stage framework for the synthesis-design are carbon dioxide capture and utilization processes.

Results and Discussion

The developed framework has been applied to an illustrative case study. The objective is to highlight the application of the framework including the necessary methods and tools. In addition, this case study shows the sustainability and innovative possibilities for carbon dioxide capture and utilisation.

In the first stage, a superstructure of the different process routes taking CO₂ to the value-added products is developed and optimized. First, a network of reactions is developed targeting smaller carbon, hydrogen and oxygen containing compounds. Using the reaction path synthesis tool, a network of over 100 reactions is generated. Then, data is required. For this, an ontology-based database has been developed. The necessary data is then retrieved so that the network is defined by a mathematical model. Using superstructure optimization, this can be optimised. This network is optimized considering various scenarios in order to determine the influence of prices, locations, and demand have on the optimal processes and the potential that CCU has in mitigating climate change. In the various scenarios, dimethyl carbonate via ethylene carbonate synthesis and dimethyl ether are considered optimal.

These resulting processes, are then considered in detailed design and analysis (Stage 2) and for innovation (Stage 3). In Stage 2, the processes are rigorously simulated and analysed using sustainability metrics, economic assessment and life-cycle assessment. These show that these processed can be designed sustainably (reducing carbon dioxide by up to -0.22 kg CO₂/kg product). Finally, the downstream separation of methanol and DMC is targeted for improvement by the introduction of hybrid technology (distillation and membrane) and process intensification [2]. By using reactive distillation for DMC synthesis and the hybrid methanol separation, the overall process can be improved, reducing the costs and increasing the sustainability.

Conclusion

A framework for the sustainable synthesis-design of carbon dioxide capture and utilization processes has been developed. This framework adopts a 3-stage approach, comprising of: (1) synthesis, (2) design, and (3) innovation, which also incorporates computer-aided methods and tools. This framework has been applied to the design of conversion processes to value-added chemicals, including methanol, dimethyl ether and dimethyl carbonate. With improvements to technology and increasing research in carbon dioxide capture and utilisation, such processes can help reduce over 10% of all carbon dioxide emission and with changing demands even more.

References

1. Babi, D.K., Holtbruegge, J., Lutze, P., Gorak, A., Woodley, J.M., Gani, R. Sustainable process synthesis-intensification, *Comput. Chem. Eng.* 81 (2015) 218–244.
2. Kongpanna, P., Babi, D.K., Pavarajarn, V., Assabumrungrat, S., Gani, R. Systematic methods and tools for design of sustainable chemical processes for CO₂ utilization, *Comput. Chem. Eng.* 87 (2016) 125–144.

List of Publications

1. Frauzem, R., Woodley, J.M., Gani, R. Application of a computer-aided framework for the design of CO₂ capture and utilization processes. *Comput. Aided Chem. Eng.* 40 (2017) 2653-2658.
2. Bertran, M.-O., Frauzem, R., Sanchez-Arcilla, A.-S., Zhang, L., Woodley, J.M., Gani, R. A generic methodology for processing route synthesis and design based on superstructure optimization. *Comput. Chem. Eng.* 106 (2017) 892-910.
3. Roh, K., Frauzem, R., Gani, R., Lee, J.H. Process systems engineering issues and applications towards reducing carbon dioxide emissions through conversion technologies: Review. *Chem. Eng. Res. Des.* 116 (2016) 27-47.
4. Bertran, M.-O., Frauzem, R., Zhang, L., Gani, R. A generic methodology for superstructure optimization of different processing networks. *Comput. Aided Chem. Eng.* 38 (2016) 685-690.
5. Roh, K., Frauzem, R., Nguyen, T.B.H., Gani, R., Lee, J.H. A methodology for the sustainable design and implementation strategy of CO₂ utilization processes. *Comput. Chem. Eng.* 91 (2016) 407-421.
6. Frauzem, R., Kongpanna, P., Roh, K., Lee, J.H., Pavarajarn, V., Assabumrungrat, S., Gani, R. Sustainable process design: Sustainable Process Networks for Carbon Dioxide Conversion, in: You, F. (Ed.), *Sustainability of Products, Processes and Supply Chains*. Elsevier Ltd, (2015) 175–195.



Rasmus Østergaard Gadsbøll

Phone: +45 6066 8815
E-mail: rgad@kt.dtu.dk

Supervisors: Ulrik Birk Henriksen, CHEC, DTU
Jesper Ahrenfeldt, CHEC, DTU
Lasse Røngaard Clausen, MEK, DTU
Jens Dall Bentzen, Dall Energy

PhD Study
Started: December 2014
To be completed: June 2018

Biomass gasification polygeneration

Abstract

The project is centered around a polygeneration system that consists of biomass gasification and solid oxide cells, which can operated as either fuel cells or electrolysis cells dependent on the immediate power prices. The project seeks to clarify the potential of this joint technology platform by carrying out several experiments with the TwoStage Viking gasifier coupled with a solid oxide fuel cell stack and oxygen utilization instead of air. In addition, the project seeks to develop the TwoStage gasification concept by designing and evaluating large-scale 100MW_{th} configurations of the system.

Introduction

This project is a part of the Biomass Gasification Polygeneration (BGP) project under ForskVE. The projects aim is to design and optimize a flexible and integrated biomass gasification-solid oxide cell platform. The system consists of a biomass gasifier and solid oxide cell, which can be operated as either a fuel cell (SOFC) by converting the product gas from the gasifier into power, or as an electrolysis cell (SOEC) that can convert electricity and steam into oxygen and hydrogen that the gasifier can process along with biomass into Bio-SNG (synthetic natural gas). The operating mode depends on the immediate power prices, meaning that the polygeneration system will produce power at high prices and consume it at low ones. Hence the system offers both grid balancing and storage of power. Figure 1 displays the overall conceptual plant.

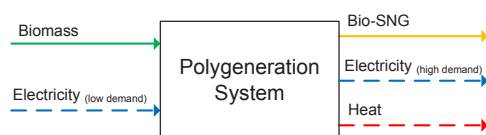


Figure 1: Flexible biomass gasification polygeneration concept.

This project is centered around the TwoStage Viking

gasifier that has been developed for many years at DTU and is commercialized. The gasifier processes wood chips into high quality product gas at high temperatures that can be utilized in a variety of applications including engines and chemical synthesis. The gasifier is shown in Figure 2 in its engine configuration. The gasifier is mainly characterized by its high cold gas efficiency of 87%_{dry,LHV} and very high gas quality with <0.1mg/Nm³ tar [1].

With the polygeneration concept and TwoStage gasifier as the research focus, this project will:

- Investigate the potential of coupling of the TwoStage gasifier with SOFC technology for power generation via experimental tests
- Modify and operate the gasifier with oxygen instead of air in order to minimize the N₂ content of the product gas and enable effective fuel synthesis
- Research and develop upscaled designs of the gasification concept to 10-100MW_{th} and investigate the use of alternative biomasses.

SOFC and engine operation on product gas

In relation to the polygeneration concept, the power production mode is investigated as a solid oxide fuel

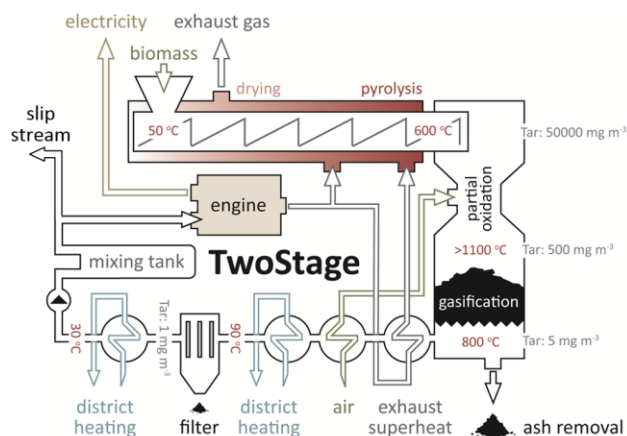


Figure 2: Flow diagram of the TwoStage Viking biomass gasifier at DTU

cell is operated with product gas. The use of these gases with SOFCs is still relatively unknown and thus there is a lack of test campaigns with fuel cell stacks and live product gas. This project will investigate the use of TwoStage product gas with such a fuel cell and operate a state-of-the-art 2kW_{th} Topsøe Fuel Cell stack. This will enable analysis of performance with regards to gas composition fluctuations, impurities, part-load operation and so on. The results have been promising, estimating 40% biomass-to-electricity with potential above 60% [2].

Oxygen-blown operation of the TwoStage gasifier

In the power consuming mode of the polygeneration concept, the project will investigate the practical aspects of an oxygen-blown plant. The 80kW_{th} TwoStage ‘Viking’ gasifier at DTU will be used for the experimental work. The project includes both installation and testing of new equipment, operation of the gasifier and gas analysis.

It is unknown to what extent the oxygen-injection will affect the tar, soot and particle content of the produced gas and therefore measurements of the product gas will be made. The gas impurity levels are very important when utilizing the gas in e.g. engines, fuel cells, chemical synthesis and advanced chemical analysis are needed to clarify the mechanisms and contents. The chemical analysis will be carried out during an external stay at the Danish Gas Technology Centre (DGC). Experimental efforts will be made to map the gas composition under different operational conditions. The product gas from the biomass gasifier will also be tested on the solid oxide fuel cell (SOFC) stack during operation, in order to assess the performance of the fuel.

Design and modeling of upscaled TwoStage gasifiers

The project includes theoretical projections of upscaled versions of the TwoStage gasifier in order to assess the plants technical feasibility, scaling potential and fuel flexibility. Several reactor designs (e.g. fluid beds, fixed beds etc.), tar conversion mechanisms and reactor configurations will be investigated and analysed in order to design large-scale TwoStage gasifier system with very high efficiency and very low tar content. The Viking gasifier is currently exclusively operated with wood chips, but it is desired to increase the fuel flexibility and use alternative fuels such as low-grade and/or high-ash fuels (e.g. straw, sludge, waste). Several design considerations are however needed to utilize the fuels, as they feature relatively high concentrations of corrosive inorganics (e.g. chlorine). System designs will be modeled mathematically using the DNA software and evaluated on energy and exergy basis. The process has resulted in a submitted patent application of gasification system and very promising results.

Acknowledgements

This project is co-funded by ForskVE (project no. 12205) and is carried out in collaboration with DTU MEK, Dall Energy and Dansk Gasteknisk Center (DGC).

References

- Ahrenfeldt J, Henriksen UB, Jensen TK, Gøbel B, Wiese L, Kather A, et al. Validation of a continuous combined heat and power (CHP) operation of a Two-Stage biomass gasifier. *Energy & Fuels* 2006;20:2672–80.
- Gadsbøll RØ, Thomsen J, Bang-Møller C, Ahrenfeldt J, Henriksen UB. Solid oxide fuel cells powered by biomass gasification for high efficiency power generation. *Energy* 2017;131.



Nipun Garg
Phone: +45 4525 6180
E-mail: nipgar@kt.dtu.dk

Supervisors: John M. Woodley
Georgios M. Kontogeorgis
Rafiqul Gani

PhD Study
Started: October 2016
To be completed: October 2019

Sustainable and innovative chemical and biochemical solutions through an integrated and systematic framework

Abstract

In this volatile and globalized world, ensuring sustainability has become an ever-growing challenge for the chemical and related industries [1]. Thus, an extension of current process synthesis and design methods is required not only to achieve economical improvements but also of sustainability/LCA factors. An approach to achieve this is by performing process synthesis and process intensification together in the early stages of process design where the current search space of unit operations is extended by generating new unit operations (or a new combination of operational tasks and associated phenomena). A systematic synthesis, design and phenomena [2] based intensification methodology to generate intensified alternatives for a given process has been developed by Babi et al. 2015 [3]. A major benefit of this approach is that truly innovative solutions can be found. Thus, the major focus of this project is to find integrated solutions, expansion of the PI database, enhancement of the existing methodology to make it more generic in terms of chemical and biochemical processes resulting in the creation of a computer-aided framework to automatize the steps involved for the intensification.

Introduction

Process Intensification (PI) can be defined as an improvement of a process at unit operational, functional and/or phenomena level that can be obtained by either integration of unit operations, integration of functions and phenomena's or targeted enhancement of the phenomena for a given operation. During the last decade, PI has become a major potential method by which an overall improvement of a process can be achieved sustainably while improving its overall efficiency (e.g. resource and energy efficiency, waste reduction etc.). Initially, existed PI methodologies operates at the unit operations (Unit-Ops) level [4] and functional (task) level [5] which has further been developed to a process level [3]. Generation of novel and more sustainable designs i.e. going beyond the existing intensified unit operations for example reactive distillation, divided wall column etc.; one must operate at lower level of aggregation, namely the phenomenon level and investigate the underlying driving forces associated with the unit operations [4].

In this methodology, the process flowsheets options are synthesized or evaluated that corresponds to acceptable values for a set of targeted performance criteria. This defined set of performance parameters is then referred to as the base case for intensification. Then at the phenomena level, the phenomena involved in

performing a specific task are identified and restructured using a systematic and generic approach to find intensified unit operations generating more flowsheet options that improves the base case design and corresponds to even better values of performance parameters. Thus, this methodology generates more innovative, sustainable and non-trade off intensified solutions.

In this work, the phenomena based synthesis approach is extended and applied to bio processes. It includes the expansion of library and algorithms to identify the phenomena building blocks (PBB's), generation of basic structures that translates to unit operations. In its application, new synthesis tasks has also been introduced which is a novel approach for the selection of different cell strains for fermentation that are formulated in a form of superstructure (figure 3) to identify the best along with the downstream separation process.

Specific objectives

The research conducted in this field is primarily within the field of process systems engineering (PSE). The main objective of this work is to extend the current methodology, making the framework more generic and develop its corresponding computer-aided framework to systematically solve process synthesis, design and

intensification problems. The generic framework should be able to

- Generate all feasible intensified flowsheet alternatives for a given problem such that it can identify more sustainable and novel/innovative solutions.
- Rapidly, efficiently and reliably screen and evaluate the generated intensified alternatives using shortcut models.
- Includes process operability and control as a performance analysis parameter to ensure safe and operable process alternatives.

Integrated framework for Process Synthesis, Design and Intensification

An integrated and systematic framework for Process Synthesis, Design and Intensification is shown in figure 1. This computer aided framework is based upon a generic 3 stage approach to sustainable process design, which has been presented by Babí et al., 2015 [3].

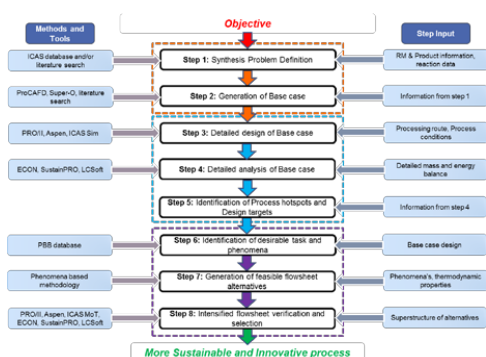


Figure 1: Integrated and Systematic framework for Process Synthesis, Design and Intensification [4, 6]

The first stage of the framework is Synthesis (step 1 and step 2) where the optimal process flowsheet is identified among numerous alternatives. In step 1 the synthesis problem is defined while in step 2, the base case flowsheet is identified. This can be done by either using computer aided flowsheet design method (ProCAFD) [7], performing the superstructure optimization using Super-O [6] or by doing literature search. In stage 2 detailed design to extract mass and energy balance data (step 3) and process analysis (step 4) in terms of sustainability, life cycle assessment and economics is performed to identify the process hotspots and set the design targets (step 5) to be achieved in stage 3. In stage 3, a phenomenon based process synthesis intensification method [4] is applied to generate flowsheet alternatives that matches the specified set of design targets and therefore determines more sustainable alternatives compared to the base case. In this approach the tasks performed by the unit operations involved in the optimal route are identified and from which the associated phenomena are identified (step 6). These phenomena are combined using combination rules to generate new

and/or innovative, intensified and more sustainable flowsheet alternatives (step 7). The final designs are then verified and compared with the base case (step 8) through a set of pre-defined performance criteria.

Case Study

The application of methodology is highlighted through a case study involving production of bio succinic acid. The main objective of the case study is to identify more sustainable, intensified and non-trade off alternatives along with testing of the current methods, tools and identify limitations and improvements for production of bio succinic acid.

Stage 1: Synthesis

Step 1: General problem definition

The synthesis problem is defined here as to find the optimal processing route for production of succinic acid with at least a purity of 99%. The starting raw materials considered are Glucose, Glycerol, Maltose and Sucrose along with CO₂. Using these raw materials different reaction path using different bacterial and yeast strains are identified along with required reaction data.



Figure 2: General reaction for bio succinic acid (Bioamber)

Step 2: Generation of base case flowsheet

The base case process flowsheet is generated by using superstructure optimization approach where a novel superstructure is generated that includes new synthesis tasks such as different cell strains to produce succinic acid. Overall, the superstructure consists of multiple processing routes including 10 different fermentation models followed by 7 recovery and purification processing steps, where data was collected through available information on reaction as well as succinic acid production related technologies reported in literature. Using this information, generic superstructure is created describing a network of configurations for different processing routes. The superstructure consists of 8 processing steps and 33 intervals excluding raw material and product steps from which potentially 2604 alternatives can be generated. Then the superstructure based optimization problem is set up in Super-O [6], where the MILP problem is solved to determine the optimal processing route. The optimal process flowsheet alternative obtained is a novel processing route (green color) while other existing processing routes (other colors except green) reported in literature [8] are also identified in the superstructure as shown in figure 3.

The optimal process synthesis flowsheet (figure 4) consists of a fermenter followed by centrifuge for broth clarification, distillation for concentrating the broth and removal of unwanted organic acids and alcohols, followed by activated carbon treatment for removal of

soluble solids causing color and then finally low pH crystallization and drying to get pure crystals of succinic acid.

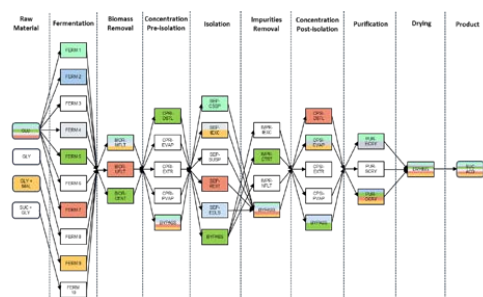


Figure 3: Superstructure (PSIN) of alternatives for succinic acid case study

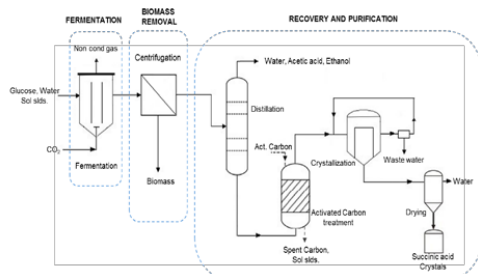


Figure 4: Optimal Process flowsheet (Base case flowsheet)

Stage 2: Detailed design and analysis

Step 3: Generation of base case design

Once we have the optimal process flowsheet, the detailed steady state simulation is performed using PRO/II to get the base case design. Then from the base case design detailed mass and energy balance data is extracted for further process analysis.

Step 4: Process analysis

Using detailed mass and energy balance data, process analysis is performed in terms of sustainability, life cycle analysis and economics. This is performed using in-house tools SustainPro [9] LCSof [10] and ECON. Based on LCSof and ECON analysis, reboiler of distillation column for broth concentration is found out to be consuming most energy with highest carbon footprint. By performing sustainability analysis, two open paths have been identified where raw material, product and energy is being lost.

Step 5: Identify process hotspots and design targets

Based on process analysis, major process hotspots (inefficient operations) were identified. The examples of identified process hotspots are high energy consumption and demand for succinic acid recovery and loss of product in open path. These hotspots are then translated to design targets such as reduction of energy demand, increase in product recovery, reduction in number of

unit operations and improvement in sustainability and LCA factors.

Stage 3: Phenomena based intensification

Step 6: Identify desirable task and phenomena

The base case flowsheet here is represented in terms of tasks and then in terms of phenomena resulting in 15 phenomena building blocks (PBB's). Here, the tool library to identify the PBB's has been extended to incorporate wide range of unit operations. Here ICAS [11] software is used to get the pure component and mixture properties of the system. By analyzing these properties, an azeotrope between water and ethanol is identified. As in this case study our main objective is to get pure succinic acid, the azeotrope between water and ethanol has not been considered in further steps. Thus, using thermodynamic insights and process hotspots, additional list of PBB's is identified and added to the existing list leading to an increase of search space. The new list consists of 20 PBB's: R, M (assuming four types i.e. ideal, flow, rectangular and vapor), 2phM, PC(VL), PT(VL), PT(VV), PS(VL), PS(VV), PC(LL), PS(LL), PC(LS), PT(LS), PS(LS), D, H, C. Here R is reaction, M is mixing, 2phM is two phase mixing, PC is phase contact, PT is phase transition, PS is phase separation while with in bracket are phases: Vapor (V), liquid (L) and solid (S) respectively.

Step 7: Generation of feasible flowsheet alternatives

The list of PBB's are combined to form simultaneous building blocks (SPB's) using combination rules. These SPB's are then further combined to form basic structures that performs a task that are further translated to unit operations. Once these desirable tasks are identified, the basic structures are selected for each of the task and thus are further translated to unit operations to generate intensified alternatives.

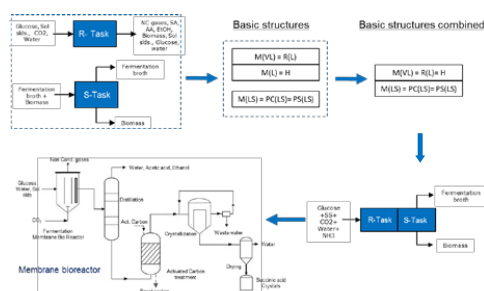


Figure 5: Alternative 1 (Combination of basic structures)

In alternative 1, starting with the first task of reaction, the second task, cell removal or clarification of the fermentation broth could be combined to obtain a new basic structure of phenomena's that translates into a membrane bioreactor (figure 5). In this unit operation, the fermentation broth is clarified i.e. the reaction product is removed continuously and the cell culture remains in the membrane bioreactor leading to increase

in cell concentration. There are many literature studies [12] available where it has been shown experimentally that with increase of cell density and continuous removal of broth, the problem of product inhibition can be encountered yielding high productivity and high concentration of product in some cases while reducing the formation of side products.

Using the concepts presented above for flowsheet generation, 2 other intensified flowsheets are generated out of which alternative 2 is based on combination of basic structures for last separation tasks which translates to membrane crystallizer. Further, alternative 3 is a combination of alternative 1 and alternative 2.

Step 8: Verification and selection

Selection of the best alternative is dependent on economic factors, sustainability metrics and LCA factors that are defined in the performance criteria. Figure 6 shows all the intensified alternatives along with the base case. For each alternative the required purity of product has been achieved, no solvents have been used and the number of unit operations have been reduced from 6 (the base case) to 4 (alternative 3).

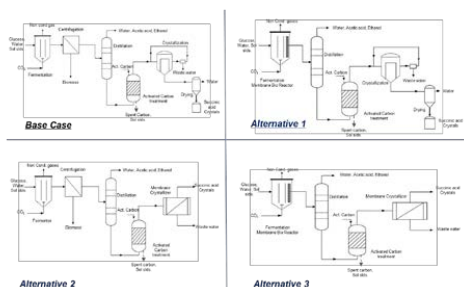


Figure 6: Flowsheets for base case and intensified alternatives

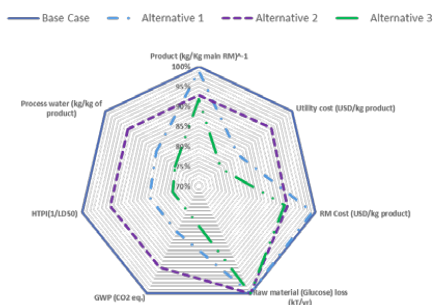


Figure 7: Base case vs intensified alternatives

The concept of generation of more sustainable process designs by matching a set of targeted performance criteria is illustrated via radar plot in figure 7, where, the ratios of different performance criteria with respect to the base-case multiplied by 100 have been plotted (for profit, the inverse has been taken). It can be seen that the base-case design is at the boundary while the more sustainable alternatives are all within the boundary,

indicating that these intensified alternatives are non-trade off i.e. more sustainable and economic than the base-case. Out of the intensified alternatives generated, alternative 3 give the best results.

Conclusion

In conclusion an overview of systematic framework for process synthesis-design and intensification has been presented and is extended to be applied to generate sustainable and innovative process alternatives for the production of bio succinic acid utilizing CO₂. It has also been shown that based on superstructure optimization, numerous processing alternatives can be generated and screened to identify a novel optimal processing route followed by the application of a phenomenon based synthesis-intensification to generate more sustainable and intensified solutions for the next generation chemical and biochemical processes.

Current and Future Work

The future work of this PhD project will be to make the methodology more generic to have wide range of applications, expansion the PI database and list of phenomena by its application to further case studies coupled with the development of computer-aided framework for the automation of the steps involved in the methodology.

References

1. "Chemical Industry Can Be A Driver of Sustainable Change", The Dow Chemical Company, accessed on September 3, 2017, <http://www.dow.com/en-us/science-and-sustainability/chemical-industry-can-be-a-driver-of-sustainable-change>
2. P. Lutze, R. Gani, J.M. Woodley, *Comp. & Chem. Eng.* 36 (1) (2012), 189-207.
3. D. K. Babi, J. Holtbruegge, P. Lutze, A. Gorak, J.M. Woodley & R. Gani, *Comp. & Chem. Eng.*, 81(2015), 218-244.
4. C.A. Jaksland, R. Gani, K.M. Lien, 1995, *Chemical Engineering Science*, 50, 511-530.
5. J. J. Siirola, *Comp. & Chem. Eng.*, 20(1996), S1637-S1643.
6. Bertran, M.O., Frauzem, R., Arcilla A. S., Zhang L., Woodley J. M., Gani, R., 2017, *Comp. & Chem. Eng.*, 106, 892-910.
7. A. K. Tula, M. R. Eden & R. Gani, *Comp. & Chem. Eng.*, 81(2015), 245-259.
8. Schroder, H., Haefner, S., Abendroth, G., Hollmann, R., Raddatz, A., Ernst, H., Gurski, H., U.S. Patent 8,673,598 B2.
9. A. Carvalho, H. A. Matos, R. Gani, *Comp. & Chem. Eng.*, 50 (2013): 8-27.
10. S. Kalakul, P. Malakul, K. Siemanond, R. Gani, *Journal of Cleaner Production*, 71 (2014): 98-109.
11. R. Gani, G. Hytoft, C. Jaksland, A. K. Jensen, 1997, *Comp. & Chem. Eng.*, 21, 1135-1146.
12. C. Wang, W. Ming, D. Yan, C. Zhang, M. Yang, Y. Liu, Y. Zhang, B. Guo, Y. Wan, J. Xing, *Bioresource technology*, 156(2014), 6-13.



Jorge Enrique Gonzalez Londoño

Phone: +45 99556750
E-mail: joregol@kt.dtu.dk

Supervisors: Anne S. Meyer
Bjarne Uller, Ørsted
Anders Peter Jensen, Ørsted

PhD Study
Started: February 2015
To be completed: February 2019

Feasibility study of Fixed Film Fixed Filter (FAD) reactor for anaerobic treatment of liquefied municipal solid wastes

Abstract

The focus of this work is to investigate the feasibility of novel Fixed Film Fixed Filter Anaerobic Digestion (4FAD) for the treatment of pre-hydrolysed Organic Fraction of Municipal Solid Waste (OFMSW) containing high concentration of suspended solids. The strategy consists of a controlled start-up to enhance biofilm formation through continuous operation of a 3 series of plug flow reactors containing fixed oriented matrix for the adhesion of the microorganisms. In this phase, the organic load was progressively increased by monitoring the concentration of Volatile Fatty Acids (VFA) and maintaining the threshold below 2 g/L. The start-up was successfully carried out in 60 days, where it was possible to operate at Hydraulic Retention Time (HRT) of 10 days. After the biofilm adhesion was confirmed, the continuous feeding of the reactor was carried out for a total of 210 days, with ulterior decrease of HRT until achieving 4,5 days and VS reduction higher than 60% in the first reactors of the series. Anaerobic digestion; Municipal Solid Waste; high Suspended Solids, fixed biofilm.

Introduction

Waste management has become of great interest due to the refuse to continue landfill and incineration practices that for decades have led to uncontrolled contamination of air and soil. Anaerobic digestion has proved to be a viable option to treat the disposed MSW, as it is possible to utilize the energy content to produce a valuable energy source in the form of methane [1]. Conventional CSTRs are widely used for anaerobic digestion of MSW in wet processes, however these can be prone to high VFA inhibition due to high organic content of the substrate. Furthermore, the loading rates in these type of reactors is often limited due to microbial flushout in operation at low HRTs that renders process instability.

An alternative to “free-floating” AD reactors are high-rate systems based on self-immobilization such as upflow anaerobic sludge blanket (UASB), expanded granular sludge blanket (EGSB) and internal Circulation (IC) reactors [2]. These types of reactors are able to withstand elevated organic loads while maintaining high conversion efficiencies, but are disposed to clogging or other mechanical issues when treating substrates containing substantial suspended particulate solids.

In the present study is investigated the start-up phase and continuous operation of fixed film reactor with fixed orientation of the filters. The disposition of the 3

series plug flow reactor aims to provide improved contact of the liquid phase to the immobilization filters where the biofilm develops. Special attention has been given to the start-up phase of the process since it has been shown to be a crucial for the later performance of the process [2]. The methane production of each reactor of the series has been evaluated to estimate the overall performance of the system regarding productivity and yields.

Lab Scale Reactors and Set-up

Reactor Description: The lab scale FAD consists of a series of three stainless steel reactors purchased to Bioprocess Control AB, Sweden. The volume of each reactor is 10L of which 7.5L is liquid and 2.5L occupied by extruded polyethylene fixed filters, Bio-Blok® (Expo-net Denmark A/S) type 100. The plug flow is accomplished by agitation in top and bottom the vertical oriented cylindrical filters and through active recirculation within each reactor of the series.

The pre-hydrolysed OFMSW was supplied by Renescience A/S, and the initial seed used in this investigation came from Foulum Biogas, a plant in Denmark treating OFMSW and secondary sludge. The feed-in was supplied hourly from a 25L agitated storage tank. As the substrate was pumped from the feed tank,

the volume displacement in the first digester pushes the flow of liquid to the next digesters in series until it leaves the system into the effluent tank. The process was held at the thermophilic range, 51°C.

The start-up commenced at an HRT of 100 days and increased daily by approx. 2% V/V when the expected gas production is perceived, while maintaining a threshold of VFA below 2 g/L. This phase was finalized when the system achieved HRT 10 days, which is considered a point where flush-out should commence. After completion of the start-up, the flow rate was stopped and recommenced after 3 days at the most recent flow rate in order to verify the biofilm formation. Then the organic load was increased in order to access the yields and productivity of this reactor at lower HRT's treating pre-treated OFMSW.

Results and Discussion

The analysis of the pre-hydrolysed Organic Fraction of Municipal Solid Waste (OFMSW) used in this study had 134,3 gr-COD/l and 73,1 g-VS/L. In the batch test, there was found a yield of 0,51 l-CH₄/gr-VS which corresponds to 80% of the maximum theoretical methane yield calculated from the COD balance. The analysis has also revealed concentration of 100,1-TS/l of substrate, 23% of which resulted to be in form of suspended solids.

Start-up phase: The start-up phase was accomplished successfully in approximately 60. In this period, the organic loading was increased by a rate of 0,107 gr-VS/l/d. During this period, it was possible to increase the feed-in almost every day as intended in the experimental strategy. Only in few circumstances the VFA concentrations were measured to be above the threshold. To verify a proper microbial immobilization, the feed rate was paused and restored at the nominal feed-rate. The 4FAD reactors could re-establish the production soon after this point, few hours later the gas production had achieved the previous level. The total gas production of the 4FAD and the HRT of the entire experiment is plotted in Figure 1.

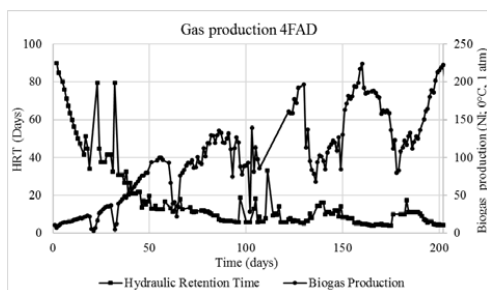


Figure 1: Gas Production and Hydraulic Retention Time.

The immobilization strategy has permitted to increase the feed rate under 10 days obtaining an important separation between the hydraulic and organic loads among the reactors of the series. The 1st reactor which is that to receive the entire load at each feed cycle was able to express more than 90 % of the gas potential in the start-up phase. The contribution of the successive reactors (2nd and 3rd) is always lower than in the first reactor. It is possible to elucidate that at the lowest retention times, these produce approximately 40% of the entire yield, while the precedent can cope with the rest of the organic conversion.

Conclusions

It was possible to maintain a production up to 206NL of biogas gas (62%CH₄) from 4 liters of pre-treated OFMSW in different occasions. The specific methane production equivalent at this rate was 0,44 l-CH₄/g-VS with a COD conversion higher than 80%. At this feed-rate, the HRT of the overall system was 5,6 days (1,88 days for each individual digester of the cascade). In this experience, it was possible to achieve up to 5l-OFMSW/day, corresponding to significant organic load of 16,2g-VS/l/day. Visual inspection of the fixed filters after the experience didn't show sign of clogging that could have arisen due to the high particulate in the feed. No evidence of channeling inside the filters was perceived. The average gas composition throughout the entire experiment was 61±2.

Acknowledgments

This project is funded by Ørsted entitled "Study of Fixed Film Fixed Filter AD (4FAD) Biogas System Performance at High Suspended Solids and COD loads".

References

1. Cresson. R et al. Control of start-up and operation of anaerobic biofilm reactors: An overview of 15 years of research. *Water Research* 2011, 1-10.
2. H. Hartmann, B. Ahring et al. Strategies for the anaerobic digestion of the organic fraction of municipal solid waste: An overview. *Water Science and Technology*, 2006, 7-22.

**Antonio Grimalt Alemany**

Phone: +45 50344426
E-mail: angral@kt.dtu.dk

Supervisors: Hariklia N. Gavala
Ioannis V. Skiadas

PhD Study

Started: March 2016
To be completed: March 2019

Fermentation of synthesis gas by mixed microbial consortia for the production of liquid and gaseous biofuels

Abstract

Mixed culture biotechnology is an emerging scientific field currently expanding towards the development of new technological platforms for the production of valuable chemicals and fuels. Syngas fermentation is one of such technological platforms in which mixed microbial cultures (or consortia) have the potential to deliver further advances by reducing the operational costs. Thus, this study focuses on the development of suitable microbial consortia for the production of ethanol and methane from syngas. The main results obtained so far are outlined here along with a description of the work that will follow in the future.

Introduction

Over the last decades, the production of biofuels has been fostered by policymakers in response to the rising concerns of the civil society about climate change and the increasing energy demands in the transportation sector. One of the most promising approaches within second generation biofuel technologies is the syngas fermentation process as it combines the benefits of thermochemical and biochemical processes. This process consists of the gasification of the biomass into syngas, a gaseous mixture of H_2 , CO and CO_2 , followed by its further biological conversion into either gaseous or liquid fuels. The thermochemical conversion of the biomass constitutes one of the main advantages as potentially any organic material can be gasified regardless of recalcitrance or toxicity [1]. Moreover, the biological conversion of syngas could potentially allow for reducing significantly the operating costs when compared to chemical catalytic processes.

The fermentation of synthesis gas has been typically studied using pure cultures. However, several acetogenic species have been reported to be partially inhibited by the impurities of raw syngas, which increases the syngas cleaning requirements prior to entering the reactor [2]. A suitable alternative for circumventing additional cleaning steps is using open mixed microbial consortia (MMC) as their inherent microbial diversity endows them with a higher resilience towards toxic compounds, thus reducing inhibition of microbial growth [3], [4]. Additionally, MMC-based bioprocesses do not require sterile

operation, which contributes to reducing further the utility consumption. On the other hand, the microbial interactions prevailing within MMC are often poorly understood, ultimately leading to a lower performance in terms of product yield and selectivity. Thus, gaining a better control on the activity of microbial consortia is essential for the further development of MMC-based bioprocesses.

Objectives

The aim of this PhD-study is to evaluate the behavior of mixed microbial consortia under different operating conditions, with the ultimate objective of developing suitable mixed microbial consortia for the conversion of syngas into both ethanol and methane. Thus, ongoing research focuses on the following topics:

- Design of microbial enrichment strategies based on ecological selection principles for boosting specific activities previously latent in microbial consortia.
- Study of the microbial interactions based on syntrophic association and kinetic competition within the consortia through their kinetic characterization.
- Study of the effects of operating parameters and influencing factors on the performance of MMC for the optimization of the yield and productivity in continuous fermentation processes.

Results

The microbial enrichment studies allowed developing enriched consortia with a high potential for the production of ethanol and methane. The results of the ethanogenic enrichments showed that decreasing the pH had a significant effect on the distribution of fermentation products. The maximum ethanol yield obtained in these enrichments corresponded to 17.7%, 33.3% and 59.8% of the theoretical maximum when operating in batch mode at an initial pH of 6, 5.5 and 5, respectively. In the case of methanogenic enrichments, the results showed that the enrichment at different temperatures led to the development of enriched consortia with different methane yields and productivities. A maximum methane yield of 92.6% of the theoretical maximum was obtained when operating at thermophilic conditions (60°C), while the methane yield at mesophilic conditions (37°C) corresponded to 81.4%.

Further studying the behavior of the methanogenic enriched consortia revealed significant differences in the patterns of activity of the mesophilic and thermophilic enriched consortia. While syngas was converted through acetic acid as the only intermediate product by the mesophilic consortium, the conversion by the thermophilic consortium took place strictly through H₂. Consequently, the mesophilic consortium presented a more intricate metabolic network involving the syntrophic interaction of four microbial groups. On the other hand, the thermophilic consortium consisted of only two microbial groups, which allowed obtaining higher conversion efficiency and methane productivity.

Future perspectives

The microbial enrichments resulted in the development of suitable microbial consortia for the production of ethanol and methane. Further studies in continuous mode will provide more insights on the effects of the operational parameters on product yields and productivities. Additionally, the development of kinetic models capable of describing the behavior of the enriched consortia will allow optimizing the process in terms of product yield and conversion efficiency.

Acknowledgements

This PhD study has been financed by DTU and Innovation Foundation in the frame of SYNFERON project.

References

1. A. Kumar, D. D. Jones, and M. a. Hanna, "Thermochemical Biomass Gasification: A Review of the Current Status of the Technology" *Energies*, 2, 556–581 (2009).
2. D. Xu, D. R. Tree, and R. S. Lewis, "The effects of syngas impurities on syngas fermentation to liquid fuels" *Biomass and Bioenergy*, 35, 2690–2696 (2011).
3. S. Redl, M. Diender, T. Ølshøj, D. Z. Sousa, and A. Toftgaard, "Exploiting the potential of gas fermentation" *Ind. Crop. Prod.*, 106, 21–30 (2017).
4. A. Grimalt-Alemany, I. V. Skiadas, and H. N. Gavala, "Syngas biomethanation : state-of-the- art review and perspectives" *Biofuels, Bioprod. Bioref.* 1–20 (2017). <http://dx.doi.org/10.1002/bbb.1826>



Peter Sams Hammershøj

Phone: +45 61926644
E-mail: pkrha@kt.dtu.dk

Supervisors: Prof. Anker D. Jensen
Ton V.W. Janssens, Haldor Topsøe A/S

PhD Study
Started: May 2015
To be completed: October 2018

Reversible and irreversible deactivation of Cu-CHA NH₃-SCR catalysts by SO₂ and SO₃

Abstract

The deactivation of a Cu-CHA catalyst for selective catalytic reduction (SCR) of nitrogen oxides with NH₃, by SO₂ and SO₃ (SO_x) was investigated. The catalytic performance was evaluated after exposure to SO₂ in presence and absence of SO₃ and H₂O, at 200 °C or 550 °C. The deactivation is partially reversible at 550 °C, and the irreversible part shows a 1:1 correlation with the S/Cu ratio, consistent with deactivation by formation of Cu-sulfates, whereas the reversible deactivation is much larger than the S/Cu ratios. The irreversible deactivation is enhanced at 200 °C or in presence of H₂O, and the deactivation is significantly increased in presence of SO₃ at 200 °C, but not at 550 °C.

Introduction

Combustion of diesel in automotive engines produces polluting compounds, which are removed to a certain extent in the diesel exhaust system. NO and NO₂ (NO_x) are removed by NH₃-SCR over a catalyst. State-of-the-art SCR catalysts are Cu-exchanged zeolites with the CHA topology [1]. The Cu-CHA materials are susceptible to poisoning by sulfur oxides [2,3], which are inevitably present in diesel exhaust. Therefore, SCR catalysts have to be regenerated or engineered to tolerate the amounts of SO_x in the exhaust, which is improved by a better understanding of the impact of the different operating conditions on the catalyst deactivation.

Specific objectives

The deactivation mechanism should be elucidated by comparison of the deactivation with the S-content after SO_x exposure and regeneration. The impact of H₂O and SO₃ on the deactivation, at 200 °C and 550 °C, was investigated by evaluating the SCR performance of a Cu-CHA catalyst in the SCR reaction before and after SO_x exposure, and after regeneration at 550 °C.

Experimental

The Cu-CHA catalyst had a Si/Al ratio of 16.6 and a Cu-loading of 2.5 wt% and was washed on a 300 cpsi cordierite monolith. SCR activity measurements were carried out on cylindrical samples of 20×27 mm (D×L) in a quartz flow reactor in the temperature range 130-250 °C, where steady state NO_x conversions are measured. The rate constant is used as measure of the

activity, and is calculated assuming first order kinetics in NO. The inlet SCR gas composition was 500 ppmv NO, 530 ppmv NH₃, 10 % O₂, 5 % H₂O in N₂-balance at 8 NL/min. The outlet gas was measured with an MKS MultiGas 2030 FTIR. The SO_x exposure conditions were at 8 NL/min with 100 ppmv SO₂ or a mixture of 70 ppmv SO₂ and 30 ppmv SO₃, and with 5 % H₂O or no H₂O at either 200 °C or 550 °C for 3 h. Regeneration was carried out for 4 h at 550 °C with the same gas and flow conditions as for SCR activity measurements. The S-content was estimated by measuring SO₂ desorption during regeneration and while heating to 900 °C in a pure N₂ flow after the last SCR activity measurement.

Results and Discussion

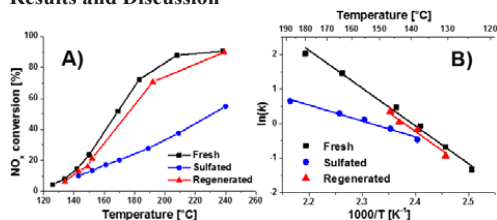


Figure 1: A) NO_x conversions as functions of temperature, and B) Arrhenius plot, of the fresh, sulfated and regenerated states of the catalyst. SO_x exposure conditions: 100 ppm SO₂ and 5 % H₂O at 200 °C.

The low-temperature NO_x conversion of the sulfated state of the catalyst shown in Figure 1A, is significantly lower than that of the fresh. After regeneration the NO_x

conversion is almost restored to the same level as the fresh, but not entirely. Thus, there are, at least, two different forms of deactivation. The deactivation restored by regeneration is *reversible*, and is the difference between the sulfated and regenerated states of the catalyst, and the deactivation left after regeneration is *irreversible*, and is measured directly on the regenerated state of the catalyst. The relation is shown in Eq.(1).

$$\text{Total deactivation} = \text{Reversible} + \text{Irreversible} \quad (1)$$

In Figure 1B, the slopes of the different states of the catalyst in the Arrhenius plot shows that the activation energy of the SCR reaction over the sulfated state is different to those of the fresh and regenerated states of the catalyst. This can be due to a different SCR mechanism over the sulfated state of the catalyst. The similar activation energy of the fresh and regenerated states is consistent with a deactivation that is due to a loss of sites. The trends observed in Figure 1A and B are similar for all the different SO_x exposure conditions. Formation of Cu-sulfates is a possible reason for the deactivation [2,3]. In that case, a 1:1 correlation between the deactivation and S/Cu ratio would be expected. In order to investigate this, the amount of S-species on the catalyst were measured, which can be done from SO₂ desorption [3]. Therefore, SO₂ desorption was measured during regeneration, and used to quantify the amounts of S-species related to the reversible deactivation. Also, the S-species related to the irreversible deactivation were quantified by measuring SO₂ desorption during heating to 900 °C in pure N₂ flow, after the final activity measurements on the regenerated state of the catalysts. The reversible and irreversible deactivations and S/Cu ratios are compared in Figure 2 for each SO_x treatment. The reversible deactivations are surprisingly larger than expected from their S/Cu ratios, whereas the irreversible deactivation has a close to 1:1 correlation with the S/Cu ratio. Again this is consistent with the irreversible deactivation being due to loss of sites, whereas the reversible deactivation must be caused by something else.

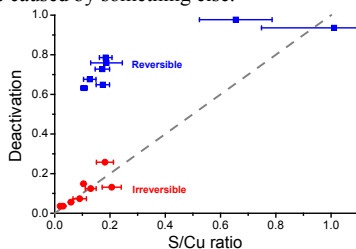


Figure 2: Reversible and irreversible deactivation for each SO_x exposure condition plotted as function of the molar S/Cu ratio. The grey dashed line shows the 1:1 correlation between deactivation and S/Cu ratio.

Due to the wide operating conditions of an SCR catalyst, it is important to know how the different conditions affect the deactivation. Therefore, the reversible and irreversible deactivations resulting from

the 8 different SO_x exposure conditions are compared in Figure 3.

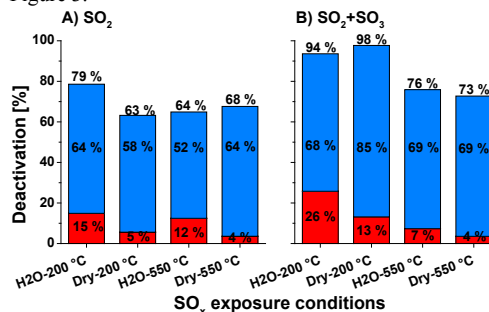


Figure 3: Reversible (blue bars) and irreversible (red bars) deactivation for each SO_x exposure condition. The percentages listed in each column are from the bottom: irreversible deactivation, reversible deactivation and the sum of the two being the total deactivation.

The irreversible deactivation is always larger when the SO_x exposure has been carried out at 200 °C, compared to at 550 °C, while there is no consistent trend for the reversible deactivation. Also in the presence of H₂O, the irreversible deactivation is always higher than at dry conditions. The presence of SO₃ has a large impact at 200 °C, where the deactivation is significantly enhanced by its presence, while at 550 °C the deactivations by SO₂ only and the mixture of SO₂ and SO₃ are similar.

Conclusions

By exposure to SO_x, a significant deactivation of a Cu-CHA NH₃-SCR catalyst is observed, which is partially reversible at 550 °C. The irreversible deactivation is directly proportional to the S/Cu ratio, consistent with formation of Cu-sulfates, while low S/Cu ratios infer disproportionately large reversible deactivations. The irreversible deactivation is slightly enhanced at 200 °C or in H₂O presence, while the presence of SO₃ greatly increases the deactivation at 200 °C, but has no apparent effect at 550 °C.

Acknowledgements

This project is a collaboration between Haldor Topsøe A/S and the CHEC group at DTU Chemical and Biochemical Engineering. It is sponsored by Innovation Fund Denmark who is gratefully acknowledged.

References

1. C. Paolucci, I. Khurana, A.A. Parekh, S. Li, A.J. Shih, H. Li, J.R. Di Iorio, J.D. Albarracín-Caballero, A. Yezerets, J.T. Miller, W.N. Delgass, F.H. Ribeiro, W.F. Schneider, R. Gounder, *Science* 357 (2017) 898-903
2. Y. Cheng, C. Lambert, D.H. Kim, J.H. Kwak, S.J. Cho, C.H.F. Peden, *Catal. Today* 151 (2010) 266-270.
3. W. Su, Z. Li, Y. Zhang, C. Meng, J. Li, *Catal. Sci. Technol.* 7 (2017) 1523-1528



Anders Jaksland
Phone: +45 4010 1875
E-mail: andjaks@kt.dtu.dk

Supervisors: John M. Woodley
Manuel Pinelo
Yinhua Wan, UCAS

PhD Study
Started: September 2017
To be completed: September 2020

Membrane-based in-situ product removal

Abstract

In-situ product removal is a promising technology in the pursuit of making biorefineries competitive with traditional refinery technology. Especially membrane based methods have proven successful. In-situ product removal works by selectively removing product from the bioreaction increasing both productivity and product concentration. In this project in-situ product removal will be applied to value-added chemicals for a future bioeconomy, but also the lack of targets for the research field will be addressed.

Introduction

To overcome the problem of global warming the chemical industry has to move away from fossil feedstocks and instead utilize sustainable feedstocks such as biomass in biorefineries. In the future all platform and bulk chemicals will have to be produced in this way, however for many processes either the yield, productivity or product concentration is insufficient for commercialization. A solution to this problem is in-situ product removal (ISPR) where especially membrane technology shows promising results. In-situ product removal via membrane technology overcomes several problems in current fermentation technology by 1) continuously removing the product eliminating product inhibition on the cell, 2) increasing the product concentration of the broth before the downstream processing, and 3) removing the product without removing the cells from the fermentation and thus potentially improving the yield.

Membrane-based ISPR technology

ISPR is defined as fast selective removal of products from the vicinity of the cells. [1] It thus works by selectively removing the products from the fermentation or biocatalysis process and keeping the product concentration at or below the toxicity limit to increase the product productivity. At the same time the product is removed selectively to the downstream process at an increased titer, thus reducing the cost of downstream separation. The ISPR membrane module can be configured internally and externally. If configured internally the selective removal happens inside the bioreactor straining the cells as little as possible, but is

more predisposed to clogging and fouling. An illustration of internal configuration can be seen in figure 1.

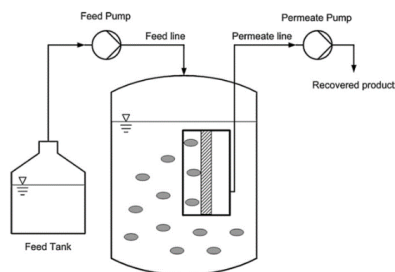


Figure 1: ISPR with internal configuration with the membrane module submerged into the bioreactor.[2]

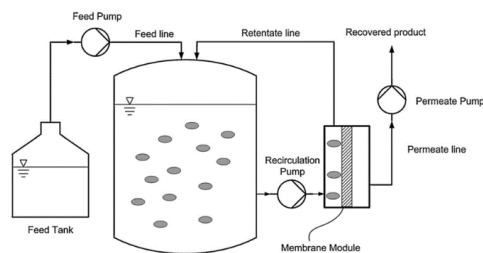


Figure 2: ISPR with external configuration with the membrane module connected in an external loop.[2]

If configured externally the selective removal happens in a recycle connected to the bioreactor. By circulating

the broth past the membrane module externally the flow is parallel to the membrane thus straining the cells more, but also reducing the potential for clogging and fouling. An illustration of external configuration can be seen in figure 2.

ISPR historically and state-of-the-art

Applications of ISPR with membrane technology exist as far back as 1984 by Groot et al.[3] Back then ISPR was introduced to a butanol/isopropanol system to overcome product inhibition. The fermentation was done with a clostridium bacteria and the ISPR with pervaporation through a silicon tubing. The experiment proved the concept with batch fermentation improving the glucose consumption from 20 g/L to 30 g/L while the productivity improved from 1.0 g/L/hr to 1.7 g/L/hr. In 1991 Qureshi et al.[4] applied ISPR to a system of immobilized cells producing acetone/butanol/ethanol (ABE). The system showed productivity of 3.5 g/L/hr and 97.9% lactose utilization in continuous fermentation. In 2011 Liu et al.[5] used an asymmetric membrane of PDMS with composite support. This increased the flux of the solvents hundred fold compared to the earlier studies significantly reducing the required membrane area. Neither yield, productivity nor product concentration were reported. In 2014 Liu et al.[6] again reported ISPR with the same membrane this time reporting the productivity. The use of ISPR increased it from 0.2 g/l/hr ABE to 0.42 g/L/hr, a doubling in productivity by removing the inhibiting product continuously. Most recently other membranes than the thoroughly studied PDMS membrane has been investigated. In 2015 Shin et al.[7] reported use of a block copolymer achieving a productivity of 0.94 g/l/hr ABE with a flux through the membrane of 1634 g/m²/hr, 2-4 times higher than the best reports of the PDMS membrane. In 2017 Van Hecke et al.[8] used a poly(octyl methyl siloxane) based pervaporation membrane reporting a productivity of 0.43 g/L/hr, yield of 0.33 and with concentrations in the permeate of over 200 g/L total ABE solvents. All the mentioned ISPR applications use pervaporation, but also perstraction has been reported with worse results and most recently vapor permeation with similar results to pervaporation by Sun et al.[9] in 2017 on an ethanol system.

Guiding the research through a review

The first goal of this PhD project is to guide all the research conducted in membrane-based ISPR with a review article. The article has several goals aside from reviewing the current state of the art.

Terminology used in ISPR applications

In the literature, there is no common terminology for talking about in-situ product removal. The last word removal is often interchanged with recovery, while in-situ product recovery is also used for the removal of product without any concentration of the product, e.g. through ultrafiltration, where the goal is simply to avoid removing the cells with the product stream. Another

cause of confusion is whether externally configured product removal via a recycle loop is still called in-situ removal or should be classified as ex-situ. The goal is thus to clarify that the use of in-situ product removal is reserved for applications with fast selective removal of the products from the vicinity of the producing cells no matter the method, where improvement is observed for productivity and product concentration.

Setting targets for development

Another problem with the current research is that no targets for the development has been set. The yield, productivity and final product concentration is being increased without any published consensus on at what point the development is sufficient and without any priority between the three. A techno-economic analysis of the three with accompanying sensitivity analysis could help setting the targets and priority for future development.

Future experimental work

With targets set for the development of ISPR experimental work on applying membrane-based ISPR to products in the price-range of 2\$/kg to 10\$/kg will be carried out. The experimental work will be done in several phases. The first phase is deciding on the product and establish the fermentation. The second phase is finding and investigating the removal of the product with membrane technology. The third phase is implementing the membrane and fermentation together in fermentation with ISPR. The last phase is modelling and economic analysis of the developed process. The ultimate goal of the experimental work is to show how ISPR can be used for non-fuel value added chemicals, but also to develop a generic method for implementing and testing ISPR to evaluate the performance on any fermentation or biocatalytic process.

References

1. A. Freeman, J.M. Woodley, M. D. Lilly, *Nat Biotechnol.* 11 (1993) 1007-1012
2. F Carstensen, A. Apel, M. Wessling, *J. Membr. Sci.* 421 (2012) 39-50
3. W. J. Groot, G. H. Schoutens, P. N. Van Beelen, C. E. Van Den Oever, N. W. F Kossen, *Biotech. Let.* 6 (1984) 789-792
4. N. Qureshi, A. Friedl, I. S. Maddox, *Biotechnol. Bioeng* 38 (1991) 518-527
5. G. Liu, W. Wei, H. Wu, X. Dong, M. Jiang, W. J. J. *Membr. Sci.* 373 (2011) 121-129
6. G. Liu, L. Gin, S. Liu, H. Zhou, W. Wei, W. Jin, *Chem. Eng. Process.* 86 (2014) 162-172
7. C. Shin, Z. C. Baer, X. C. Chen, A. E. Ozcam, D. S. Clark, N. P. Balsara, *J. Membr. Sci.* 484 (2015) 57-63
8. W. Van Hecke, H. De Wever, *J. Membr. Sci.* 540 (2017) 321-332

**Morten S e Jepsen**

Phone: +45 30924876
E-mail: mosje@kt.dtu.dk
Disciple: CHEC Research Center

Supervisors: Peter Glarborg
Peter Arendt Jensen
Thomas Norman, B&W V lund

Industrial PhD Study

Started: December 2014
To be completed: December 2017

NO_x reduction in grate-firing waste-to-energy plants

Abstract

Combustion of solid fuels in grate-firing waste-to-energy plants is one of the most competitive methods for conversion of solid fuels to electrical energy and heat. The emission of nitrogen oxides (NO_x) from waste-to-energy plants is a major environmental concern and the use of computational fluid dynamics (CFD) models to reduce the emission is of great interest. In this PhD project, a CFD model of NO_x formation and reduction in a municipal solid waste (MSW) waste-to-energy plant will be developed.

Introduction

Managing the large amounts of municipal solid waste (MSW) that is produced daily has become a significant challenge. Traditionally, the MSW has been disposed at landfills due to the low cost. In many regions this is no longer possible as an increase in municipal solid waste generation is experienced. Furthermore, according to the European Landfill Directive, the use of landfills has to be avoided whenever possible [1]. This has generated a shift in municipal solid waste handling, from disposal at landfills to extraction of energy through combustion. One of the main combustion technologies for solid waste is grate firing [2]. This technology is widely regarded as one of the most competitive, as it enables the use of a wide range of fuels, both biomass and solid waste, with varying moisture content, and the fuel preparation and handling requirements are limited [3]. Combustion of solid waste emits nitrogen oxides (NO_x). The emission of NO_x continues to be a major environmental concern [4] as it is an acid rain precursor and participates in formation of photochemical smog, which is problematic in urban areas [4,5]. Nitrogen oxides are formed either from oxidation of the N₂ in the combustion air (thermal NO_x formation), from reaction between hydrocarbon radicals and nitrogen from the combustion air [4] (prompt NO_x formation), or from oxidation of organically bound nitrogen in the fuel (fuel-NO_x formation) [4]. For solid fuels such as waste, which has a significant content of organic nitrogen, the fuel-NO_x mechanism is the dominating source of NO_x [4]. In grate combustion of waste, most of the nitrogen bound in the fuel is released during devolatilisation of the fuel in the fuel bed, mostly as ammonia (NH₃),

hydrogen cyanide (HCN) and aromatic N-compounds [3]. The reactive nitrogen species released from the fuel bed are subsequently oxidized to either NO or N₂ in the freeboard. The selectivity for forming NO, rather than N₂, depends strongly on the process in the freeboard, mainly temperature and stoichiometry [4], consequently the formation of NO can be limited by optimization of the combustion process.

Optimization of the combustion process can only limit the NO formation to a certain degree. Further reduction of the NO can be achieved by Selective Non-Catalytic Reduction (SNCR), among other methods. The SNCR process is a widely used and effective method for NO_x reduction by injection of amines or cyanides containing selective reducing agents such as NH₃, urea and cyanuric acid into the hot flue gases[6].

Specific Objectives

The project aims to develop suitable CFD models describing the formation and reduction of NO_x in grate-firing waste-to-energy plants, which can be used commercially by B&W V lund.

The main objectives of the project are:

- Determine appropriate inlet boundary conditions for the CFD model through full-scale measurements.
- Develop a chemical model for formation and a model the reduction of NO_x.
- Evaluate the CFD model through full-scale waste-to-energy plant measurements.

A new model for the reduction of NO_x in a SNCR system

CO has been shown to shift the temperature window towards lower temperatures as this replenish the radical pool [7]. The enhanced radical levels causes a higher degree of oxidation of NH₃ to NO competing more effectively with the NO removal reactions and thereby narrowing the temperature window for the SNCR system[7]. Through full scale measurements it has been shown that the flue gas in the SNCR zone can contain CO concentrations above 2000ppm.

The widely used global model by Brouwer and Heap [8] has been shown not to capture the effect of CO effectively. For this reason a new SNCR model was developed through reduction of the detailed chemical kinetic model by Glarborg et al. [7] using the SEM-CM reduction algorithm by Nagy and Turányi [9].

The effect of the higher radical levels caused by CO in the flue gas has been shown in figure 1. The full model by Glarborg et al. [9], the skeletal model developed in this study and the global model by Brouwer and Heap[8] have been compared with experimental data from Alzueta et al.[10].

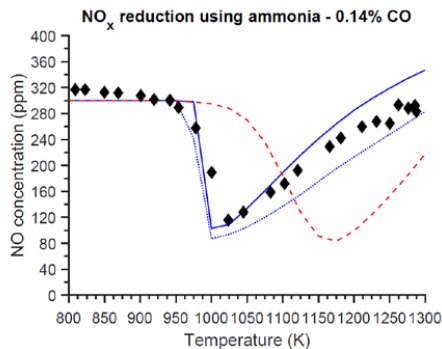


Figure 1 - Comparison of experimental data [10] and modelling predictions for the reduction of NO with NH₃; effect of CO. The symbols; experimental data, the full line: full mechanism [7], the dotted line: developed skeletal model and the striped line; using the global model by Brouwer and Heap [8] Inlet concentrations: NO=300ppm, NH₃=300ppm, O₂=4%, H₂O=4.5%, N₂=balance. τ = 150ms at 1200K (constant molar rate)

Both the full model and the skeletal model accurately predict the onset temperature and the optimal reduction temperature for the SNCR process for CO concentrations in the flue gas at 1400ppm. The global model by Brouwer and Heap breaks down when CO is introduced in the flue gas, overpredicting the onset temperature by more than 100K at 1400ppm CO.

For advanced control of the SNCR system it is important to take into account the shift in optimal reduction temperature; see figure 2.

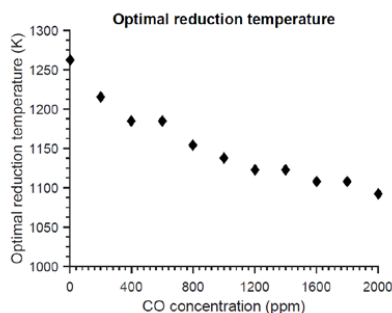


Figure 2 - The temperature at which the largest reduction of NO_x by NH₃ is achieved as a function of the CO concentration in the flue gas. The results are obtained by PFR simulations in CHEMKIN using the DCKM by Glarborg et al. [7]. Inlet concentration: NO=300ppm, NH₃=300ppm, O₂=6%, H₂O=25%, CO=varied, N₂=balance. τ =0.1s

Increasing the CO concentration from 0 to 2000ppm shifts the optimal reduction temperature by more than 150K. Consequently insufficient control of the CO concentration and temperature in the SNCR zone may decrease the performance of the SNCR system.

Acknowledgements

This project is a collaboration between B&W Vølund and the CHEC group at DTU Chemical and Biochemical Engineering. The project is funded by Innovation Fund Denmark and B&W Vølund.

References

1. Diverting waste from landfill, EEA Report No 7/2009
2. E. Ranzi, S. Pier. Pierucci, P.C. Aliprandi, S. Stringa, *Energy Fuels* 25 (2011) 4195–4205.
3. C. Yin, L. A. Rosendahl, S. K. Kær, *Grate-firing of biomass for heat and power production*, *Powder Technol.* 193 (2009) 266–273.
4. P. Glarborg, A. D. Jensen and J. E. Johnsson, *Prog. Energy Combust. Sci.* 29 (2003) 89–113.
5. Frank and M. J. Castaldi, *Waste Management Res* (2014).
6. S. W. Bae, S. A. Roh, and S. D. Kim. *Chemosphere* 65 (2006) 170–175
7. P. Glarborg, J.A. Miller, B. Ruscic, S.J. Klippenstein, *Prog. Energy Combust. Sci.*, submitted (2017).
8. J. Brouwer, M. P. Heap, D. W. Pehring, and P. J. Smith, *Twenty-Sixth Symposium (International) on Combustion*, (1996) 2117–2124
9. T. Nagy and T. Turányi, *Combustion and Flame*, 156(2):417–428, 2009.
10. M. U. Alzueta, H. Røjel, P. G. Kristensen, P. Glarborg and K. Dam-Johansen, *Energ. Fuel* 11 (1997) 716-723



Spardha Jhamb
Phone: +45 3062 8046
E-mail: spajha@kt.dtu.dk

Supervisors: Rafiqul Gani
Georgios M. Kontogeorgis
Xiaodong Liang
Kim Dam-Johansen

PhD Study
Started: October 2016
To be completed: September 2019

A systematic methodology for property model-based chemical substitution

Abstract

A general and systematic methodology for chemical substitution, which caters to different problem definitions depending on the reason for substitution, has been developed. The associated property models and modeling tools are also described. A set of new group contribution-based models for a number of useful properties of amino acids that have been developed [1]. Several practical examples on substitution of chemicals from chemical-based products in various sectors, like cosmetics and personal care with amino acids along with other well-known substitution problems from sectors like coatings and solvents, automobiles etc., together with the role of property models in chemical substitution, are highlighted.

Introduction

Chemical-based products, which could be structured product formulations or single molecule products have brought substantial benefits for us human beings and have been a significant part of our economies. Our life and the changes around us cannot be imagined without the presence or involvement of chemical-based products. But like every coin has two sides, some chemicals constituting these products can be detrimental to us and our surroundings. This is primarily due to the hazardous environment-related properties that some of these chemicals possess. Besides, there are many more chemicals which have not been evaluated due to lack of resources for rigorous, experimental-based estimation methods [2]. Hence, there is an urgent necessity to identify chemicals that may be dangerous to the environment, toxic to human health and harmful for our fragile eco-system. The concerns about the environment and human well-being has given rise to the REACH regulation implemented by the European Chemical Agency (EChA) and the Design for the Environment (DfE) alternatives assessments framework by the US-Environmental Protection Agency (EPA), which compels the industry to stop the use of hazardous substances and replace them with environmentally benign and safer chemicals. Therefore, there is a need to develop a systematic, model-based methodology that can help to find substitutes to existing chemicals in order to improve the environmental impact, while still delivering the same or improved product functionality.

Specific Objectives

The objective of the chemical substitution methodology is to quickly and reliably identify the promising candidates through model-based techniques and only then go on to conduct experiments in order to verify and evaluate their performance and applicability. In this way, the experimental resources are used for verification rather than for an inefficient, trial-and-error search. Besides, while seeking for alternative substitutes for the undesirable chemicals, the trial and error based approach will have a very large search space. This could be avoided by a reverse design approach [3], which makes use of predictive property models. Here, alternative chemicals are found by matching the target (desired) properties of the original product and avoiding the undesired properties of the chemical being substituted. The goal therefore is to investigate comprehensively the functions and properties of the chemicals of concern; develop a systematic framework to identify, compare and select safer and environmentally compatible alternatives to these; and finally design safe chemical product formulations with the same or better product performance.

Methodology

A seven task methodology has been developed for model-based chemical substitution (Figure 1). Three components of the methodology development namely: the 'Environment, Health and Safety (EH&S) property criteria to select the reason for substitution', 'Property model library' and 'Experimental property database' are

developed comprehensively in order to solve a wide range of chemical substitution problems.

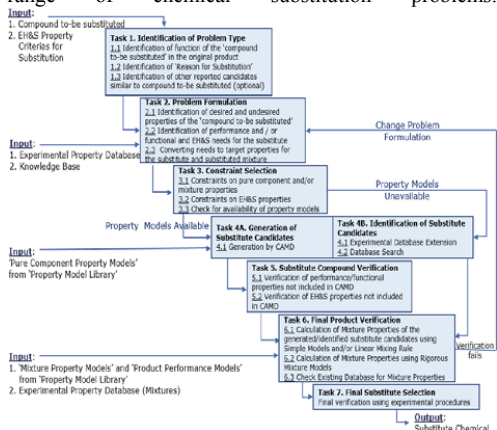


Figure 1: Methodology for Chemical Substitution

Results and Discussion

The developed substitution methodology has been discussed below with the help of two examples.

Example 1: Substitution of Ethylene Glycol from an Automobile Engine Coolant

Ethylene glycol is used as a freezing point depressant in an engine coolant (Prestone Extended Life 50-50 Ready to Use). However, it appears on EPA's Hazardous Groundwater Pollutant list due to its toxicity to mammals. In order to find a substitute, the needs were identified and converted to target pure component and mixture properties as shown in Table 1.

Table 1: Needs and Target Properties for Example 1

Need	Target Property
Heat Removal without much rise in its own temperature	Heat Capacity (C_p)
Good Heat Transfer Medium	Thermal Conductivity (k)
Not freeze in Cold Climates	Freezing point depression (ΔT), Heat of fusion (ΔH_{fus})
Liquid Phase	Normal Melting Point (NMP), Normal Boiling point (NBP)
Miscibility with the original mixture	Gibbs energy of mixing (ΔG^{mix}), Solubility Parameter (δ)
Non-toxic to mammals	Lethal Dose (LD_{50})

Since models for the prediction of the pure component properties were available, Computer-aided Molecular Design (CAMD) could be used to generate substitute candidates (with the tool, ProCAMD in ICAS), which were then evaluated for their mixture properties in order to check if these candidates fit in the original mixture. 1,2-propylene glycol was identified to be a viable substitute with maximum freezing point depression and lowest toxicity to mammals.

Example 2: Substitution of Cetrimeronium Bromide from a Hair Conditioner

Cetrimeronium Bromide is used as a surfactant in a hair conditioner (Rejuvenol Keratin After Treatment Conditioner). However, it is persistent in the

environment and toxic to freshwater fish. In order to find a substitute, the needs were identified and converted to target properties as shown in Table 2.

Table 2: Needs and Target Properties for Example 2

Need	Target Property
Ability to lower surface tension	Surface Tension (σ)
Ability to form micelle /Solubilize dirt and oil	Critical Micelle Concentration (CMC)
Soluble in Water	Water solubility ($\log W_s$)
Non-toxic to aquatic environment	Immobilization Concentration (IC_{50})
Biodegradable	Biodegradation Rate

Two amino acid based surfactants were found to be viable substitutes with a biodegradation rate of greater than 60% and low toxicity to the aquatic environment. However, due to lack of models for EH&S properties and the surface active properties for amino acids and their derivatives, the substitute candidate identification was carried out by means of a 'database search'[4].

Conclusion and Future Work

Hence, a systematic model-based methodology for chemical substitution has been developed and has been used to substitute environmentally hazardous and/or unsafe chemicals in liquid phase homogeneous formulations from various industrial sectors. The challenges and opportunities for chemical substitution in devices, solid state products, polymers and plastics etc. still need to be evaluated. While some of the missing property models are being developed and validated, for instance the group contribution models for predicting normal melting point, water solubility and octanol water partition coefficient of amino acids [1], the development of many others could be explored.

Acknowledgements

I would like to thank Hempel A/S for funding this project.

References

- S. Jhamb, X. Liang, R. Gani, A.S. Hukkerikar, Estimation of Physical Properties of Amino Acids by Group-Contribution Method. Chemical Engineering Science 175 (2018) 148-161
- A.S. Hukkerikar, S. Kalakul, B. Sarup, D.M. Young, G. Sin, R. Gani, Estimation of Environment-Related Properties of Chemicals for Design of Sustainable Processes: Development of Group-Contribution+ (GC+) Property Models and Uncertainty Analysis. Journal of Chemical Information and Modeling 52(11) (2012) 2823-2839
- R. Gani, Chemical Product Design: Challenges and Opportunities. Computers and Chemical Engineering 28(12) (2004) 2441-2457.
- L. Pérez, M.T. García, I. Ribosa, M.P. Vinardell, A. Manresa, M.R. Infante, Biological Properties of Arginine-based Gemini Cationic Surfactants. Environmental Toxicology and Chemistry 21(6) (2002) 1279-1285.



Mark Jones
 Phone: +45 4525 2910
 E-mail: Mark.Jones@alfalaval.com

Supervisors: Bent Sarup, Alfa Laval Copenhagen A/S
 Assoc. Prof. Gürkan Sin, ProSys, DTU

PhD Study
 Started: April 2016
 To be completed: April 2019

Design and optimization of oleochemical processes

Abstract

Oleochemical processes have been studied and applied thoroughly by the chemical industry for more than a century. Consequently, the global oleochemical industry has now grown to a worldwide market and is expected to reach 30 billion US Dollars by 2024 which the Southeast Asian (Asian-Pacific) region holds the biggest market share and fatty acids made up 55 per cent of the total demand in the year of 2015 [1]. Thus, a focus in this work is put on the recovery and processing of fatty acids which can be produced from vegetable oils and fats through hydrolysis. We successfully implemented a finite volume model for a counter-current spray column in Fortran 90 and embedded it in the Pro/II process simulator while still being able to perform sensitivity analysis and surrogate modelling (e.g. polynomial chaos expansion and Gaussian process regression) with the high-level programming language Python and the packages f90wrap, SALib, Chaospy and scikit-learn.

Introduction

We identified three process steps which the focus is put on in this project, namely the hydrolysis of vegetable oils (mixtures of triglycerides), purification of glycerol and the separation of fatty acids through distillation and solvent crystallization. The hydrolysis step is realized with a counter-current spray column which runs at temperatures between 240 to 260 degrees Celsius and high pressure (30-40 bar) to give fatty acids and glycerol.

This hydrolysis reaction is also termed as fat/oil splitting in industry and the counter-current spray column has been widely adapted as the most efficient unit operation for this process step in comparison to a CSTR or co-current reactor. [2]

SAFEPROPS: Property Prediction with Uncertainty Analysis

A software prototype for the prediction of properties has been developed based on the work by Frutiger et al. [3] The tool provides predictions based on group contribution methods with uncertainty analysis and can be accessed through a web-interface and an API to use SAFEPROPS directly in MATLAB or Python scripts. Properties which are predicted for the counter-current spray column model are liquid density and liquid viscosity.

Counter-Current Spray Column Model

We developed a finite volume model (FVM) as seen in Figure 1 and validated the results with the analytical solution from literature which we presented in the KT Yearbook 2016. The FVM is currently being extended to incorporate backmixing and allows the user to perform parameter estimation of e.g. mass transfer coefficients and equilibrium constants. This helps the employees at Alfa Laval to either design a new spray column unit or consult costumers with an existing spray column in operation.

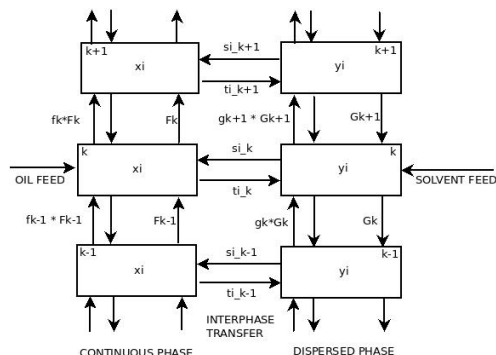


Figure 1: Schematic diagram of FVM for a counter-current spray column

Monte Carlo Simulation & Surrogate Based Optimization

The application of sensitivity analysis or surrogate modelling is subject to the variation of the input parameters of the model. Different experimental designs exist to cover the domain of variation such as Monte-Carlo samples obtained with random generators, Latin Hypercube samples or Quasi-random sequences (e.g. Sobol sequence). The model is then evaluated for each sample and the results are stored for the sensitivity analysis and surrogate modelling step.

Figure 2 depicts the optimization steps which are applied in this work.

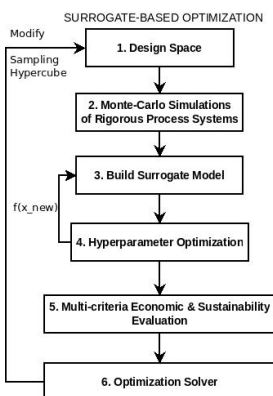


Figure 2: Surrogate-based optimization methodology

Sensitivity Analysis

We analyzed the important parameters (overall mass transfer coefficient, liquid-liquid distribution ratio, reaction coefficient and liquid density) for the spray column over the height of the column. Being the indirect measure of conversion, the glycerol weight fraction at the bottom of the column was used as the model output to obtain the first order and total effect indices with variance-based sensitivity analysis (also known as Sobol sensitivity analysis) as seen in Figure 3.

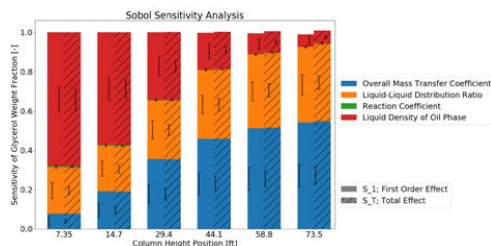


Figure 3: Variance-based sensitivity analysis of the finite volume spray column model

Surrogate Modelling

The rigorous model is treated as a black box for

applying surrogate modelling techniques such as multivariate regression splines, polynomial chaos expansion or Gaussian process regression. The coefficient of determination (R^2) values obtained for these methods are shown in Table 1.

Method	R^2
Multivariate Regression Splines	0.95
Polynomial Chaos Expansion	0.95
Gaussian Process Regression	0.99

Table 1: Coefficient of determination (R^2) for surrogate modelling methods applied to the finite volume spray column model

Conclusions & Future Work

As presented in the previous sections we aim for establishing a multi-scale design and optimization framework ranging from property prediction to process design and optimization. The framework is also described in Jones et al. [4]

The framework allows to analyze the effects of individual parameters of different property prediction methods on process design variables and economic benchmarks. Tasks currently worked on are the tuning of individual interaction parameters of the thermodynamic model (UNIFAC, Wilson) as described by Urlic et al. [5] and multivariate sensitivity analysis and optimization on a fat/oil splitting and glycerol purification process flowsheet with polynomial chaos expansion and Gaussian process regression.

A master thesis project under our supervision deals with the generation of hybrid distillation and solvent crystallization schemes subject to product specifications and raw material composition.

Feel free to contact us for more detailed information on the individual topics or for establishing a collaboration.

Acknowledgements

This work has received funding from the European Union's Horizon 2020 research and innovation programme under the Marie Skłodowska-Curie grant agreement no. 675251.

References

- Grand View Research, Market Research Report, Oleochemicals Market Analysis By Product (Fatty Acid, Fatty Alcohol, Glycerol) And Segment Forecasts to 2024, Report ID: 978-1-68038-282-2
- Namdev, Patil, Raghunathan; Ind. Eng. Chem. Res. 1988, 27, 739-743
- Frutiger, Andreasen, Liu, Spliethoff, Haglind, Abildskov, Sin; Energy, 2016, 109, 987-997
- Jones, Forero-Hernandez, Sarup, Sin; Computer Aided Chemical Engineering, 2017, 40, 1885-1890
- Urlic, Bottini, Brignole, Romagnoli; Computers & Chemical Engineering; 1991, 15, 7, 471-479



Adam Paul Karcz

Phone: +45 4525 2830
E-mail: adkr@kt.dtu.dk

Supervisors: Kim Dam-Johansen
Jytte Boll Illerup
Anne Juul Damø
Sally S. Rocks, FLSmidth

PhD Study
Started: May 2016
To be completed: April 2019

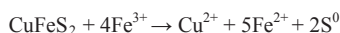
Surface characterization of activated chalcopyrite particles

Abstract

The world's most abundant copper mineral, chalcopyrite (CuFeS_2), is difficult to extract in atmospheric leaching using traditional ferric sulfate lixiviants, because of its unique physical properties. FLSmidth[®] has devised a novel approach, which utilizes a mechanochemical Rapid Oxidative Leach (ROL) assisted by a Stirred Media Reactor (SMRt). Due to the reduction of surface passivation problems associated with atmospheric leaching, this process is able to achieve copper recoveries >97% in under 3 hours. An important contribution to this is a preconditioning step, which uses a few percent or less of copper (II) ions to dope the mineral and thereby "activate" chalcopyrite. Because this activation plays a major role in accelerating the leach kinetics, it is critical to understand the associated phenomena and their part in the ROL. The project aims at using characterization techniques to study the mechanisms of the activation process. Design and conduction of relevant activation/leaching experiments will be supported by density functional theory (DFT) modelling of physical changes in the mineral. Through a better understanding of the mechanisms at play during the activation and subsequent leaching, methods to improve the process will be developed that maximize the efficiency of atmospheric leaching.

Introduction

Due to the near-term transitioning of a large number of mine sites from heap leaching and smelting of high-grade copper oxide ore to abundant, low-grade copper sulfide (i.e. chalcopyrite) ore processing, there is high interest in finding a cost-effective copper extraction method that is compatible with current industrial infrastructures [1]. However, the atmospheric leaching of chalcopyrite has proven to be arduous [2]. Most copper sulfide minerals require the application of both an acidic environment and an oxidizing agent to leach copper as Cu^{2+} . These conditions are achieved using oxidizers such as ferric (Fe^{3+}) ions, as either a sulfate or chloride:



However, atmospheric leaching of chalcopyrite concentrates using such leaching aids is well known to suffer from slow kinetics and poor copper recoveries, due to (a) the semiconducting properties of chalcopyrite and (b) the formation of a passivation layer (i.e. sulfur species) on the surface of the particles. Furthermore, the nature of this passivation layer is not well understood (partly due to the variety of species, which form around the chalcopyrite particles) [1].

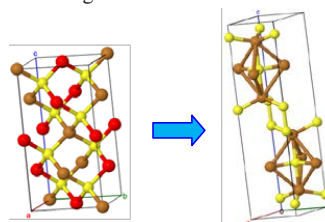


Figure 1: Chalcopyrite particles are partially converted (< 5 mol%) during activation to a copper-rich sulfide, e.g., covellite (Cu_6S_6), which causes copper and sulfur to rearrange bonds and coordination numbers, while iron atoms are removed.

To account for the slow kinetics, FLSmidth has developed the ROL process, which is compatible with existing extraction processes and is cost-effective. The ROL approach is two-stage process, which consists of the following:

1. Reductive activation through Cu^{2+} doping of chalcopyrite to form an intermediary copper sulfide (Cu_xS_y) surface for enhanced reactivity (see Fig. 1). A possible product is covellite (CuS):



- Oxidative leaching of copper in a batch or continuous leach circuit comprised of a continuous stirred tank reactor (CSTR) assisted by SMRt at 80°C and atmospheric pressure conditions. The CSTR provides the oxidative ferric sulfate leaching conditions, and the SMRt mitigates the passivation of the particles by collapsing the passivating layer.

The main advantage of the ROL process is that it can complete leaching within 3 hours (older technology required >10 hours) and it requires lower energy consumption compared to competition (<100 kWh/t for ROL process vs. >1,000 kWh/t for competitors [3]).

Specific Objectives

The main challenges of the PhD project are to elucidate the mechanisms involved in the surface reactions of activated and leached chalcopyrite particles. Important endeavors in this regard include the bulk (chalcopyrite particle) structural changes that occur after activation, the role of pH and redox potential during the activation reaction, and an understanding of activation's relation to leaching kinetics using fundamental principles, substantiated with atomistic modeling, i.e., density functional theory (DFT).

In particular: (1) the structural details, such as lattice parameters and crystal structure, and (2) chemical/electronic property identification/determination of the activated and leached chalcopyrite particles will be investigated; therefore, the application of advanced (nano-scale) characterization is needed. The project will aim at using surface and bulk materials characterization techniques, i.e. transmission electron microscopy (TEM), secondary ion mass spectrometry (SIMS), and x-ray adsorption spectroscopy (XAS), to explore – and to better understand – the structural details of activated and leached chalcopyrite particles. These results will be supported with appropriate quantum mechanical and reaction engineering models.

Results and Discussion

Activation of chalcopyrite particles was performed at FLSmidth Minerals in Salt Lake City, UT, U.S.A., to achieve 5% conversion to copper-rich sulfide. Characterization was then performed at DTU using electron microscopes (SEM and TEM) and powder x-ray diffraction (XRD)[4]. Because the SEM and XRD techniques have poor spatial and atomic resolutions, respectively, they were not able to capture the small changes due to the low amount of conversion, which nonetheless significantly affect the particles and their leach kinetics. Therefore, cross-sections of the particles were prepared using a focused ion beam (FIB) monitored with SEM (Fig. 2a). Afterwards, this section was transferred to a TEM where diffraction patterns (Fig. 2b) revealed planes of atoms in the crystal lattice that had interplanar spacings indicative of CuFeS₂ as well as CuS, but also many that did not match reference patterns for typical variations of Cu_xS_y or Cu_xFe_yS_z

(e.g., CuS, Cu₂S, Cu₅FeS₄, etc.). Such results indicate the presence of internal stresses, which create deformed lattice spacings, and they suggest that an intermediary product exists in the activated particles.

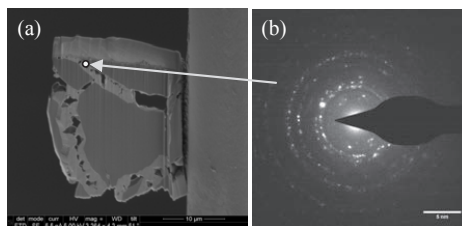


Figure 2: (a) FIB-SEM was used to produce a thin cross-section of an activated chalcopyrite particle (scale bar: 10 µm), and (b) diffraction patterns were generated at different areas of the particle, representing the crystallographic planes (scale bar: 5 nm⁻¹).

Future Work

Surface spectroscopy techniques, i.e., X-ray photoelectron spectroscopy (XPS), are currently being employed to provide information about chemical changes resulting from activation. The goal is to correlate these results with atomistic simulations in DFT (such as the calculated band structure in Fig. 3) that will be able to identify the structure and composition of the new phase formed during activation. Spectroscopic techniques provide information about the energies of important physical processes, which DFT can calculate from quantum mechanical models.

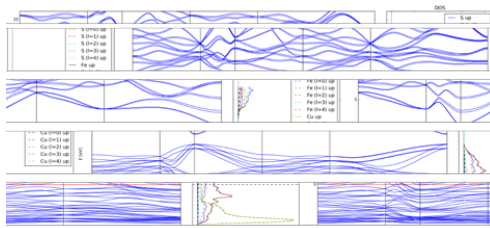


Figure 3: Calculated electronic band structure (left) and density of states (right) of chalcopyrite, CuFeS₂.

References

- C. Eyzaguirre, S.S. Rocks, R. Klepper, F.A. Baczek, D. Chaiko, in: *Hydroprocess*, Antofagasta, Chile, 2015, pp. 1–11.
- K. Osseo-Asare, *Hydrometallurgy* 29 (1992) 61–90.
- J.R. Cobble, C.E. Jordan, D.A. Rice, *Hydrometallurgical Production of Copper From Flotation Concentrates*. USBM RI 9472, USBM RI 9472, 1993.
- A.P. Karcz, A.J. Damø, J.B. Illerup, S. Rocks, K. Dam-Johansen, D. Chaiko, *J. Mater. Sci.* (2017).



Francois Kruger
Phone: +45 4525 2983
E-mail: fkru@kt.dtu.dk
Centre: Centre for Energy Resources Engineering

Supervisors: Nicolas von Solms
Georgios Kontogeorgis

PhD Study
Started: April 2016
To be completed: March 2019

Thermodynamics of petroleum fluids relevant to subsea processing

Abstract

Subsea processing (separation, boosting and compression) offers the opportunity for on-spec gas export direct from the seabed with improved recovery and extended reservoir lifetimes. The aim of this project is to generate new phase equilibrium data and improve existing thermodynamic models, in order to facilitate process designs relevant to subsea gas processing installations.

Introduction

The need for improved efficiency and recovery in offshore oil & gas production are driving the development of subsea processing facilities, which include [1]:

- Separation systems
- Boosting
- Injection

The main reasons for the development and installation of subsea processing (as opposed to topside processing) are given as:

- Increased hydrocarbon recovery
- Improved energy efficiency
- Decreased capital and operating expenditure
- Longer operational lifetimes
- A wider range of fields are economically viable
- Improved flow assurance

With the separation, boosting and injection already qualified technologies, the next step is to develop a subsea dehydration or dew point control unit. This technology was recently proposed by Statoil as the Gas-2-Pipe™ (G2P) [2] process, where gas-dominated well streams can be treated directly, allowing for export into the Norwegian transport system. Two glycols are being considered for the dehydration step: mono- and triethylene glycol (MEG and TEG).

Robust design and operation of these subsea developments requires new experimental equilibrium data (VLE/VLLE/LLE) and improved thermodynamic modelling to formulate a detailed understanding of the properties of reservoir fluids over a broad range of temperatures and pressures.

Objectives

As part of a research collaboration between the Centre for Energy Resources Engineering (CERE) at DTU and Statoil, a new equilibrium cell [3] was constructed and the first VLLE measurements for $\text{CH}_4 - n\text{-C}_6\text{H}_{14} - \text{CH}_3\text{OH} - \text{H}_2\text{O}$ have been reported in 2014.

The PhD here is proposed as a continuation of the collaboration between CERE and Statoil and will consist of three sections, each with specific objectives:

Measurements for clean systems

The purpose of this section of the project is to re-establish the high pressure VLE/VLLE measurement equipment and to extend the measurements to systems for which few/not data are available.

The following systems are of interest:

- Equilibrium data for $\text{CH}_4 - \text{H}_2\text{O} - \text{MEG}$
- $273 \text{ K} < T < 323 \text{ K}$ and $50 < P < 150 \text{ bara}$
- Specific interest: the vapour phase H_2O content

This work will be completed in the CERE laboratories at DTU.

Measurements for real world systems

This work will form a natural extension of the measurements of clean systems, by measuring equilibrium data for:

- Natural gas – H₂O – MEG
- The experimental apparatus is described by Folas *et al.* [4]

This work was completed during 6-month external research stay at the Statoil's R&D department in Trondheim, Norway. The data is currently being prepared for publication, with manuscript submission planned for the early 2018.

Thermodynamic modelling and process design

The experimental data will be modelled using the revised Cubic-Plus-Association (CPA) equation of state (EoS) of Kontogeorgis *et al.* [5]. While traditional cubic EoS provide very good description for gas – hydrocarbon mixtures, CPA extends the accuracy to mixtures also containing water, alcohols and glycols.

As a contribution to model development for glycols, three new association schemes (see Figure 1) have been developed and tested against literature data.

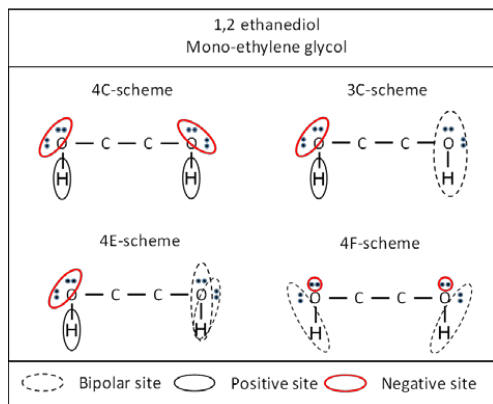


Figure 1: Representation of three new association schemes (3C, 4E & 4F) for MEG compared to the literature 4C site-scheme.

In the development of these new schemes, a statistical uncertainty procedure (bootstrapping) was used to determine the parameters for the new schemes. The bootstrapping technique was first applied for CPA parameterization by a former DTU-CERE PhD, Martin Bjørner [6]. The advantage of using this technique is that parameter confidence intervals are calculated, which will be utilized in later process design applications. The new association schemes and uncertainty analysis has been submitted for publication and were presented at the 2017 ESAT Conference [7].

The final element of this work will involve the combination of the experimental data and the CPA model into Aspen simulations of the G2P process. These simulations will be used to determine process feasibility and process design elements for specific subsea installations.

Acknowledgements

The authors wish to thank Statoil A/S for their financial support of this research, which is part of the CHIGP (Chemical in Gas Processing) project.

Abbreviations

CPA	Cubic-Plus-Association
G2P	Gas-2-Pipe
MEG	Mono-ethylene glycol
LLE	Liquid-liquid equilibrium
TEG	Tri-ethylene glycol
VLE	Vapour-liquid equilibrium
VLLE	Vapour-liquid-liquid equilibrium

References

1. Davies S., Bakke W., Ramberg R.M., Jensen R.O., Experience to date and future opportunities for subsea processing in StatoilHydro. Houston: Offshore Technology Conference, 2010.
2. Fredheim A.O., Johnsen C.G., Johannessen E., Kojen G.P., Gas-2-Pipe™, A Concept for Treating Gas to Rich Gas Quality in a Subsea or Unmanned Facility. Houston: Offshore Technology Conference, 2016.
3. Frost M., von Solms N., Richon D., Kontogeorgis G.M., Measurement of vapor–liquid–liquid phase equilibrium—Equipment and results. *Fluid Phase Equilibria* 405 (2015) 88–95.
4. Folas G.K., Berg O.J., Solbraa E., Fredheim A.O., Kontogeorgis G.M., Michelsen M.L., Stenby E.H., High-pressure vapor–liquid equilibria of systems containing ethylene glycol, water and methane: Experimental measurements and modeling. *Fluid Phase Equilibria* 251 (2007) 52–58.
5. Kontogeorgis G.M., Yakoumis, I.V., Meijer, H., Hendriks, E., Moorwood T., Multicomponent phase equilibria calculations for water-methanol-alkane mixtures. *Fluid Phase Equilibria* 201 (1999) 158-160.
6. Bjørner M.G., Sin G., Kontogeorgis G.M., Uncertainty analysis of the CPA and a quadrupolar CPA equation of state – With emphasis on CO₂. *Fluid Phase Equilibria* 414 (2016) 29-47.
7. Kruger, F.J., A new association scheme and CPA parameterization for mono-ethylene glycol. 29th European Symposium on Applied Thermodynamics (2017), Bucharest, Romania.



Yashasvi Laxminarayan

Phone: +45 4525 2853
E-mail: ylax@kt.dtu.dk

Supervisors: Peter Arendt Jensen
Peter Glarborg
Flemming Frandsen
Bo Sander, DONG Energy

PhD Study
Started: October 2014
To be completed: October 2017

Deposition properties of biomass fly ash

Abstract

Fly ash deposition on boiler surfaces is a major operational problem encountered in biomass-fired boilers. Reducing deposit formation is essential for maximizing boiler efficiency and availability. This study investigated deposit formation of biomass fly ash on steel tubes, in a lab-scale Entrained Flow Reactor. Model biomass fly ash particles were mixed with air and injected into the reactor, to form deposits on an air-cooled deposit probe, simulating deposit formation on superheater tubes in boilers.

Introduction

One of the major operational problems encountered in biomass-fired boilers is the formation of ash deposits on boiler surfaces. Ash deposits hinder heat transfer to steam cycle, cause corrosion of boiler surfaces, and may completely block flue gas channels in severe cases, causing boiler shut-downs. Therefore, reducing deposit formation is essential for maximizing boiler efficiency and availability.

The inorganic content in the flue gas may exist as vapor species, submicron aerosol particles, and larger ($>10\ \mu\text{m}$) fly ash particles. The vapor species may undergo diffusion and heterogeneous condensation on heat transfer surfaces. Deposition of submicron aerosol particles may occur via thermophoresis, while deposition of larger fly ash particles primarily occurs via inertial impaction.

Objectives

The present study quantified ash deposition on steel tubes in an Entrained Flow Reactor, at conditions simulating full-scale biomass-fired boilers. Experiments were conducted using model biomass fly ash, prepared from mixtures of $\text{K}_2\text{Si}_4\text{O}_9$, KCl , K_2SO_4 , CaO , SiO_2 and KOH , as well as three different boiler fly ashes: a wood fly ash, a straw fly ash, and a straw + wood cofired fly ash. The fly ashes were injected into the reactor, to form deposits on an air-cooled deposit probe. The influence of flue gas temperature, probe surface temperature, flue gas velocity, fly ash composition, fly ash flux, fly ash particle size and probe residence time was investigated. Furthermore, selected deposit samples were analyzed using a Scanning Electron Microscope.

Experimental Approach

The model fly ash was mixed with air, and injected into a 2 m long electrically heated furnace, as shown in Figure 1. Deposits were formed on a steel tube, mounted on an air-cooled deposit probe at the outlet of the furnace.

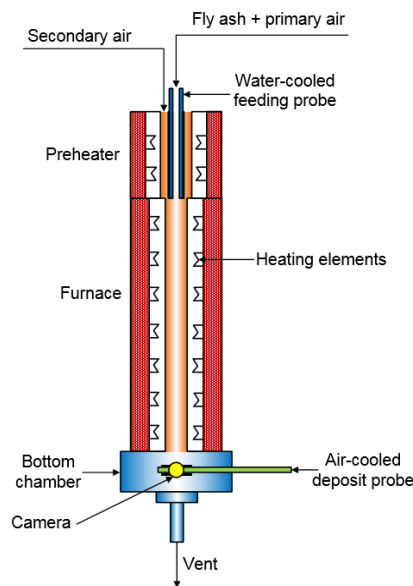


Figure 1: Schematic representation of the Entrained Flow Reactor.

Selected Results and Discussion

The effect of flue gas and probe surface temperature on the deposit formation rate of $K_2Si_4O_9$ is shown in Figure 2. It was observed that the deposit formation rate increased with increasing flue gas temperature at the investigated conditions. Visual observations of the formed deposits (see Figure 2) revealed that deposits were formed only on the upstream side of the steel tube, suggesting that $K_2Si_4O_9$ deposition occurred primarily via inertial impactation. Furthermore, increasing the probe surface temperature from 300 °C to 450 °C increased the deposit formation rate at the investigated conditions. However, further increasing the probe surface temperature up to 550 °C did not influence the deposit formation rate significantly. Increasing probe surface temperatures led to increased temperatures at the surface of the deposit, thereby decreasing the corresponding viscosity. This resulted in an increased sticking probability of the deposit surface, causing increased deposit formation.

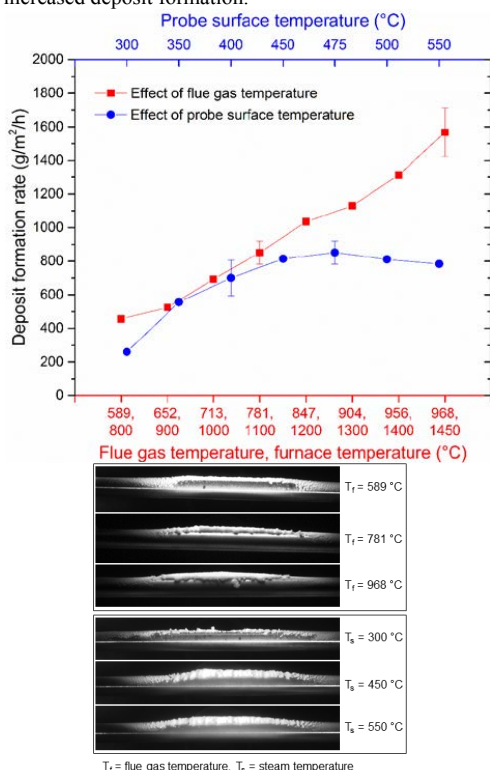


Figure 2: Effect of flue gas temperature and probe surface temperature on the deposit formation rate. Experiments performed with $K_2Si_4O_9$, with a flue gas temperature of 781 °C, probe surface temperature of 475 °C, flue gas velocity of 1 m/s, fly ash flux of 20412 $g/m^2/h$ for 15 min. Images captured at the end of the experiments.

Figure 3 shows the effect of flue gas velocity on the deposit formation rate for flue gas temperatures of 781

and 968 °C. It was observed that increasing the flue gas velocity decreased the deposit formation rate. Increasing the flue gas velocity, and thereby the particle velocity, increases the kinetic energy of the impacting particles. If the particle velocity exceeds the critical velocity of impactation, the particle is unable to dissipate its kinetic energy, and rebounds from the deposit after impactation.

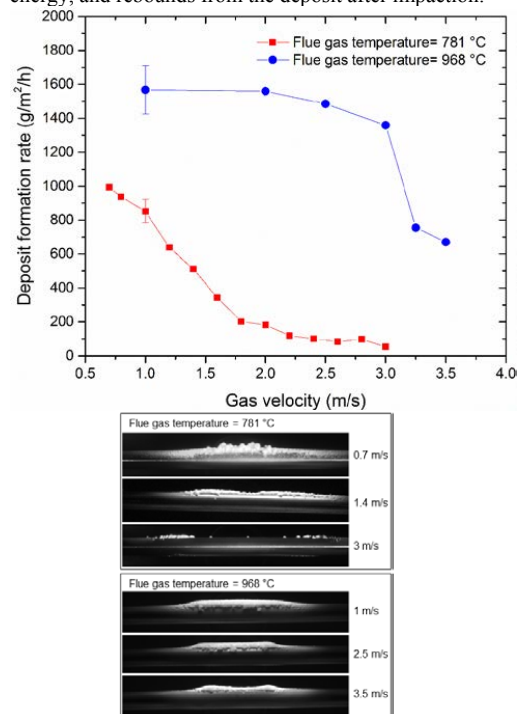


Figure 3: Effect of flue gas velocity on the deposit formation rate.

Conclusions

This study investigated deposit formation of biomass fly ash on a steel tube in a laboratory-scale Entrained Flow Reactor. It was observed that the deposit formation rate increased with increasing flue gas temperature, probe surface temperature, probe residence time, fly ash flux, and particle size. However, the deposit formation rate decreased with increasing gas velocity. Furthermore, it was observed that inertial impactation of fly ash particles was the major mechanism of deposit formation on the upstream side of the tube, especially when solid or semi-solid particles were injected into the reactor. However, deposition on the downstream side of the tube, via condensation and thermophoresis, was also observed, when vapors or submicron aerosol particles were present in the gas.

Acknowledgements

This work is part of the project, 'Flexible use of Biomass on PF fired power plants', funded by Energinet.dk through the ForskEL program, Ørsted Bioenergy & Thermal Power A/S and DTU.

**Kasper Hartvig Lejre**

Phone: +45 4525 2957
E-mail: kasphal@kt.dtu.dk

Supervisors: Søren Kiil
Peter Glarborg
Philip Fosbøl
Henrik Christensen, MAN Diesel & Turbo

PhD Study
Started: October 2015
To be completed: October 2018

Mathematical modelling of sulfuric acid accumulation in lube oil in diesel engines

Abstract

Slow-steaming operation and an increased pressure in the combustion chamber have contributed to increased sulfuric acid (H_2SO_4) condensation on the cylinder liners in large two-stroke marine diesel engines, thus causing increased corrosion wear. The scope of this project is to investigate how H_2SO_4 is formed, transported, and neutralized in the lube oil film on the cylinder walls. The conditions inside the cylinders will be reproduced in laboratory experimental setups, where the different subprocesses are studied separately.

Introduction

Slow-steaming became popular during the recession in the last part of the 2000s. This meant that the large two-stroke marine diesel engines were now operated at a lower engine load in order to save fuel. To ensure optimal specific fuel oil consumption the engines were further optimized in this new part load range. This resulted in increased cylinder pressures and colder cylinder liners at part load among others. The lower liner surface temperature, in combination with an increased operating pressure, has led to increased water and acid condensation in the cylinder lube oil film on the cast iron liner surfaces, which promotes “cold corrosion” [1]. The phenomenon is a mixture of chemical corrosion from acid and mechanical wear. It is generally thought that the cold corrosion phenomenon originates mostly from corrosion by condensed sulfuric acid (H_2SO_4), due to the sulfur-rich fuel used in marine diesel engines [2, 3]. Expensive lube oil with limestone ($CaCO_3$) is continuously added to the cylinder liners to neutralize the H_2SO_4 formed, but the efficiency of this procedure is not always optimal [4]. A small degree of corrosion is, however, beneficial on the cylinder liners, making the liner surface a little rough. This means that the cylinder liner surface can better maintain a protective oil film. However, uncontrolled cold corrosion destroys the liners and piston rings [5].

Specific Objectives

This PhD project is a part of a large research project (SULCOR) in corporation with MAN Diesel & Turbo SE, DTU Chemical Engineering (KT), and DTU

Mechanical Engineering (MEK), where the combined output from the different projects should lead to new engine designs and/or new operational engine procedures, which will improve the existing lubrication strategy. The main core of this PhD project is to develop a mathematical model that can predict conditions prevailing at the oil-cylinder liner interface, where corrosion takes place. The cast iron tribo-corrosion process is handled in another PhD project at KT, where this PhD project provides the boundary condition data required. Other PhD/postdoc projects at DTU-MEK will provide valuable information on e.g. oil flow pattern, gas phase composition, and the actual formation and condensation of H_2SO_4 on an oil film under laboratory conditions (lube oil test rig). The project objectives cover the following:

- A literature study on diesel engines, lube oils, and the chemistry of a selected running engine.
- Collection and analysis of spent lube oil from selected full-scale diesel engines.
- Development of the analysis technique.
- Design and construction of reactor setups for H_2SO_4/SO_2 -lube oil experiments.
- Mapping and quantification of acid generation, transport, and neutralization mechanisms in a running diesel engine.
- Mathematical modelling of sulfuric acid accumulation in lube oil in diesel engines.
- Recommendations for practical use of the results from the different subprojects.

Results and Discussion

A mixed flow reactor (MFR) setup has been constructed in order to investigate the neutralization mechanism between limestone (CaCO_3), present in lube oil, and H_2SO_4 , forming CaSO_4 , CO_2 , and water as products [2]. H_2SO_4 and lube oil are fed continuously to the reactor, thus it is possible to investigate the reaction between CaCO_3 and H_2SO_4 at different conditions, such as stirrer speed, H_2SO_4 concentration, residence time, and Ca/S molar ratio. The outlet from the reactor is analyzed by obtaining infrared spectra by an FTIR-ATR spectrometer. The experimental analysis procedure is as follows: immediately after sampling, the oil sample is analyzed by FTIR (denoted 'fast analysis'). After additional reaction time and stirring, to ensure complete conversion of remaining H_2SO_4 , if any, the same sample is analyzed again (denoted 'complete conversion analysis'). By comparison, it is possible to assess if complete conversion of H_2SO_4 was achieved in the MFR. A selected result is shown in Figure 1, showing the effect of varying Ca/S ratio on the H_2SO_4 conversion. At low Ca/S ratio, incomplete conversion of H_2SO_4 in the MFR is observed (red curve).

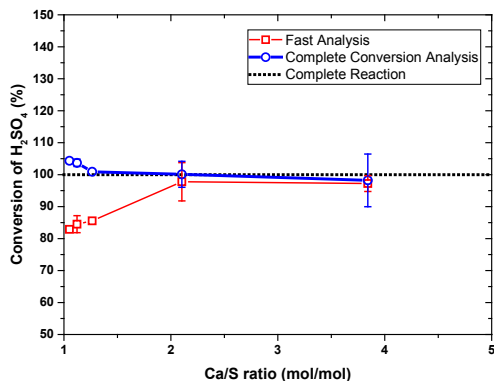


Figure 1: Effect of varying Ca/S molar ratio on the H_2SO_4 conversion. Operational conditions: stirrer speed = 1200 rpm, residence time = 2.5 min, and concentrated H_2SO_4 in inlet.

This indicates that the H_2SO_4 - CaCO_3 total reaction rate slows down, when reaching a critically low Ca/S. The explanation for such an observation could be that the neutralization reaction is controlled by the rate of micelle adsorption (or desorption) onto the acid droplets. According to Gibbs adsorption equation [6], a decrease in surfactant (in this work a CaCO_3 micelle) concentration results in a decrease in adsorption. At decreasing Ca/S molar ratio, the concentration of CaCO_3 micelles decreases significantly compared to the H_2SO_4 droplets. The reduction in conversion of H_2SO_4 droplets at lower Ca/S ratios can therefore be explained by a decrease in adsorption rate of the CaCO_3 micelles on the H_2SO_4 droplet, thereby reducing the total reaction rate of CaCO_3 micelles. The observation that the H_2SO_4 -consumption is diminished when the excess

of CaCO_3 is reduced (corresponds to a lower Ca/S molar ratio) could also indicate that the reaction is mixing limited. Even though maximum stirrer speed is applied, it may be impossible to achieve perfect mixing. Therefore, when most of the H_2SO_4 droplets are converted, insufficient contact between H_2SO_4 droplets and CaCO_3 micelles may arise, having some local depletion regions with excess of H_2SO_4 droplets in the lube oil compared to CaCO_3 , resulting in incomplete reaction of the added H_2SO_4 . Both explanations describe that the limiting factor is a reduced contact between CaCO_3 micelles and H_2SO_4 droplets at lower Ca/S ratio. It is also of interest to investigate, if SO_2 has a role on the consumption of CaCO_3 in the lube oil. This may happen either by direct reaction between SO_2 and CaCO_3 or by absorption of SO_2 by the lube oil followed by reaction to H_2SO_4 [7].

Conclusion

The cold corrosion phenomenon is a significant problem in the marine industry, where the cylinder liners and piston rings corrode; if not a proper lubrication strategy is used. Since the procedure is not always optimal and very expensive, it is desirable to understand the underlying processes in the lube oil-acid system inside the engines with the purpose of improving the existing lubrication strategy. This project is contributing to an increased knowledge about the neutralization mechanisms in the lube oil among others.

Acknowledgements

This work is part of the Combustion and Harmful Emission Control (CHEC) research center at the Department of Chemical and Biochemical Engineering at Technical University of Denmark. The project is funded by the Innovation Fund Denmark and co-sponsored by MAN Diesel & Turbo A/S and Technical University of Denmark through the SULCOR project.

References

1. MAN Diesel & Turbo, "Service Letter SL2014-587/JAP", 2014.
2. C. Amblard, J. Japan Inst. Mar. Eng. 50 (6) (2015) 54–62.
3. D. W. Golothan, Trans. Inst. Mar. Eng. 90 (Ser A) (1978) 137–163.
4. A. K. van Helden, M. C. Valentijn, H. M. J. van Doorn, Tribol. Int. 22 (3) (1989) 189–193.
5. D. Atkinson, 11th Int. Conf. Cond. Monit. Mach. Fail. Prev. Technol. C. 5 (2) (2014) 17–22.
6. G. M. Kontogeorgis, S. Kiil, Introduction to Applied Colloid and Surface Chemistry, John Wiley & Sons, Ltd., 2016, p. 82.
7. H. Nagaki, K. Korematsu, JSME Int. J. Ser. B. 38 (3) (1995) 465–474.

List of Publications

K. H. Lejre, S. Kiil, P. Glarborg, H. Christensen, S. Mayer, ASME ICEF, Seattle, 2017, paper ICEF2017-3580.



Anna Leth-Espensen

E-mail: annlete@kt.dtu.dk

Supervisors: Peter Glarborg
Peter Arendt Jensen
Kim Dam-Johansen

PhD Study
Started: May 2016
To be completed: April 2019

Application of improved computational fluid dynamic simulations for pulverized biomass combustion

Abstract

The need for an environmentally justifiable energy production has increased the interest in combustion of pulverized biomass particles in suspension firing boilers. The aim of this project is to provide computational fluid dynamics (CFD) simulations, which can aid in the process of understanding the physical processes taking place in swirl stabilized biomass flames. The project includes a char yield model used as input for the CFD flame simulations and a single particle biomass combustion model under development for future implementation into CFD. The combustion model is a shell model, which can account for drying, devolatilization, and char combustion concurrently.

Introduction

The Danish power and district-heating network is largely supplied by combined heat and power plants (CHPs). Due to environmental reasons, the industry is currently changing from coal-based energy production to pulverized biomass combustion. The implementation of biomass particles as the primary fuel entails challenges with regard to the design and operation of the combustion facilities. Typically, the large scale CHPs in Denmark utilize suspension firing. The process of biomass suspension firing is not yet fully understood, which courses challenges with regard to ensuring flame stability, full conversion of the particles, and minimizing emittance of harmful substances. Biomass particles differ from coal, because they have larger diameters, a wider size distribution, and a higher volatile content, which causes a different conversion and flow pattern for the particles.

Biomass particles used for suspension firing cannot, as opposed to coal particles, be treated as thermally thin. Because the biomass particles are generally larger, an isothermal approach has failed to generate reasonable modeling results. For particles with Biot number > 0.1 [1] a more complicated method with temperature gradients in the particle must be applied. This is the aim of this work.

Another topic of interest for this project is how the combusting biomass particles influence the stability and geometry of the flames in suspension fired boilers. The flames are generally turbulent swirling jet flames with

complicated geometries and their properties are dependent on the operation parameters, the burner geometry and the fuel properties. Computational fluid dynamic simulations are used in this project with the intention of studying the flame stability, energy release profile, and fuel burn out.

Specific Objectives

The aim of this PhD project is to make a model for combustion of biomass particles at suspension firing conditions and implement it in CFD simulations of a suspension firing unit. The project is divided into three subparts, a char yield model, a combustion model, and the implementation into CFD.

The char yield model should be able to determine the char yield after pyrolysis for biomass particles subjected to suspension firing conditions. These conditions include high heating rates (> 1000 K/s), high ambient temperatures (> 1000 K), and particle sizes in the range of 20-2000 μm . The char yield is an important parameter in most suspension firing CFD models and also necessary in combustion models. The char yield can be estimated from the amount of fixed carbon or TGA experiments, but both yield too high values. Conducting experiments at high heating rates to determine the char yield under the relevant conditions is time consuming and a simple model providing reasonably accurate estimates is hence favorable. The model presented as part of this project is a black box model building on the principles of partial least squares

(PLS) regression method. The model is based on data obtained by Trubetskaya[2] and evaluated against additional experimental data.

The biomass combustion model is developed in collaboration with the Department of Energy and Process Technology at NTNU and builds on work by Thunman et al.[3]. The model divides the particle into four shells. The innermost layer is the moist layer, then a dry layer, a char layer and the outermost layer is the ash layer. By considering the energy equations applicable to each individual layer and assuming that all reaction and/or phase change happens at the boundaries between the layers it is possible to formulate a sharp interface model (SIM). The four phases can exist concurrently, which is necessary to account for the phenomena taking place in thermally thick particles ($Bi > 0.1$). The model is produced as a standalone model in order to compare it to experimental data before it is implemented into CFD. To ensure reasonable computational time and smooth operation in the CFD simulations, there is a limit to the complexity of the model.

The CFD simulations conducted as part of this PhD are on a suspension firing unit located at Amagerværket. The aim is first to test the char yield model and the combustion model and establish whether they enhance the accuracy of already existing simulations. A large part of this evaluation of the simulations is the comparison to previously obtained measurements made by Johansen et al. [4]. The final objective is to determine which operation parameters are important for control of the combustion process, and see if design improvements can be made in order to establish a stable flame at different loads levels.

Results and Discussion

The char yield model is made using PLS regression and is limited by the amount of available experimental data for fully pyrolyzed particles devolatilized under suspension firing conditions. Currently the model is made for woody biomass for particles with the following parameters: Diameter $0.125 \cdot 10^{-3}$ - $0.925 \cdot 10^{-3}$ m, final temperature 873 – 1673 K, heating rate 100-10000 K/s. The model is thus only valid within these intervals, and more experimental data is necessary in order to expand the model to the full range of possible parameters for suspension fired particles. The model is evaluated against additional experimental data. The evaluation show that the model on average predicts the char yield to ± 1 percentage points of the char measured in weight percentage on a dry ash free basis (wt% daf). This is just above the uncertainty level of the experiments, which is the lower value of accuracy that can be obtained. The analysis of the parameters included in the model work additionally shows that the size of the particles is neglectable when calculating the final char yield for fully pyrolyzed particles. This is possibly because the size also influences the heating rate parameter and there is no need to account for the size effects twice and possibly because for particle sizes

relevant to suspension firing conditions a given finite fraction of the particle is pyrolyzable regardless of size given enough time to fully pyrolyze. Furthermore, the analysis shows that the most important parameters for the char yield are the potassium content and the heating rate, whereas the final temperature is of minor importance. The model shows that a high potassium content gives a higher char yield, whereas a high heating rate and/or high final temperature gives a lower char yield. For a woody biomass particle with parameters in the intervals mentioned above the char yield in wt% daf can be estimated using equation (1).

$$\text{Yield} = 39.6690 - 8.0043 \cdot \log(\text{FT}) - 3.2392 \cdot \log(\text{HR}) + 14.0761 \cdot K \quad (1)$$

Where FT is the final temperature in Kelvin, HR is the heating rate in Kelvin/second, and K is the potassium content in wt% daf.

The biomass combustion model is currently under development, but so far shows promising results when compared to experimental data.

Acknowledgements

This PhD project is part of the research conducted at the Combustion and Harmful Emission Control (CHEC) Research Centre at the Department of Chemical and Biochemical Engineering at the Technical University of Denmark. The project is conducted in collaboration with Ørsted (previously Dong Energy A/S) and Burmeister and Wain Scandinavian Contractor A/S (BWSC).

This PhD is a Nordic PhD project, taking place at the Technical University of Denmark as the main research location. A Nordic PhD includes a research stay at another university in the Nordic Five Tech (N5T) Collaboration, and a research stay at Norges teknisk-naturvitenskapelige universitet (NTNU) in Trondheim, Norway was conducted in the fall semester 2017. The Nordic Five Tech collaboration was founded to strengthen the research and academic environment within the Nordic countries.

References

1. H. Ström, H. Thunman, *Combustion and Flame*, 160 (2013) 417-431
2. A. Trubetskaya, *Fast Pyrolysis of Biomass at High Temperatures*, Ph.D. Thesis, Technical University of Denmark, 2015
3. H.Thunman, B. Leckner, F. Niklasson, F. Johnsson, *Combustion and Flame* 129 (2002) 30-46
4. J.M. Johansen, *Power Plant Burners for Bio-Dust Combustion*, Ph.D. Thesis, Technical University of Denmark, 2015



Rowan Malan Lindeque

Phone: +45 6166 3141
E-mail: rmalin@kt.dtu.dk

Supervisors: John M. Woodley
Ulrich Krühne
Kim Dam-Johansen
Tommy Skovby, H. Lundbeck A/S

PhD Study
Started: November 2017
To be completed: October 2020

Continuous biocatalytic processes

Abstract

There is a growing trend in the field of biocatalysis to shift toward continuous processing for more efficient production and shorter development times. New technology is already helping to overcome some of the barriers that have previously prevented continuous biocatalysis, such as mass transfer limitations and poorly water-soluble substrates and products. However, one challenge that still remains is dependence on cofactors like NADPH which must be continuously supplied to several enzymes of interest. These cofactors are very expensive and so they must be regenerated *in situ* at high rates over prolonged periods of time. As such, the aim of this project is to develop a system that includes a mechanism for cofactor regeneration to facilitate continuous production with these enzymes.

Introduction

Enzymes as biocatalysts are increasingly gaining attention in industry because they are often highly enantio-, regio- and stereoselective which makes them ideal for the production of fine chemicals, especially Active Pharmaceutical Ingredients [1]. They also operate at mild conditions and are produced from renewable resources, allowing for more sustainable processes. This often makes them more attractive than traditional chemical catalysts which frequently have low selectivities, produce many undesirable by-products, require harsh operating conditions and may contain expensive transition metals. In addition to this, recent advances in the fields of protein and metabolic engineering are allowing biocatalysts to be designed to better suit the specific needs of a reaction or process. Despite these advantages, biocatalysts are only rarely implemented at large scales and, when they are, operation is typically limited to batch mode, as is the case in the pharmaceutical industry. The use of batch technologies not only limits the productivities of existing industrial processes but also makes research and development of new processes more time-consuming.

In contrast, the implementation of continuous flow technologies in biocatalytic processes could greatly improve efficiency while reducing costs, compared to equivalent batch processes [2]. This is because continuous flow processes generally have very low reactor downtimes, are highly productive, energy

efficient, and allow reactions to operate under steady state conditions [3]. Continuous flow technologies could also drastically shorten development times because of their reproducibility and efficient control of operating conditions. This allows process parameters to be changed quickly during experiments, simplifying optimization of the system [4].

For these reasons, the development of continuous biocatalytic processes is a rapidly growing field, with some successes already having been made with aldolases, amidases, transaminases, oxidases and peroxidases [4]. However, a number of challenges remain. For instance, some enzymes are dependent on gases or additional cofactors and so ensuring the availability of these compounds is essential. Additionally, the products and substrates of biocatalysts are not always water soluble and so organic phases or co-solvents are sometimes necessary to facilitate adequate mass transfer. To overcome these challenges in a continuous process will require innovative new reactor designs.

Continuous Flow Reactors

A number of reactor types are available for carrying out continuous biocatalytic processes, as shown in Figure 1. The Packed-Bed Reactor is one of the most commonly used systems. However, immobilization of a biocatalyst on the stationary phase could limit the economic feasibility of implementing a process at scale. As such, in some cases it is preferable to use liquid enzyme

formulations in a series of Stirred-Tank Reactors. But, in the absence of an efficient way to recycle the enzyme, these systems are only economical for processes that use low-value biocatalysts or low concentrations of highly active biocatalysts. The Agitated-Cell Reactor overcomes mass transfer limitations by rapidly agitating the reaction media, but the power input required to accomplish this limits its use to smaller scales [5]. Microtube reactors are used to overcome mass transfer limitations between two phases by increasing the available surface area for mass transfer. In the case of the Tube-in-Tube Reactor the two phases are a gas and a liquid while in a Segmented Flow Reactor the phases are organic and aqueous [6,7]. Scale-up of these reactors is limited by pressure drop, however, running parallel reactions in a tube bundle can be a viable alternative [8].

Cofactor-dependence

Many enzymes of interest are dependent on cofactors like Nicotinamide Adenine Dinucleotide Phosphate (NADPH) to catalyze their target reactions. These cofactors are generally far too expensive to feasibly supply them to a process [9]. As such, it is necessary to regenerate them *in situ* as the enzymatic reaction takes place, for which a number of methods are being researched. As of yet, there is no platform that allows the reliable use of cofactor-dependent enzymes in a continuous mode of operation. As such, it will be necessary to develop a system that allows cost-effective and continuous regeneration of the necessary cofactors for prolonged periods of time. Additionally, the cofactors must be regenerated at sufficient rates so as not to limit the overall rate of reaction.

Specific Objectives

The objective of this project is to develop a laboratory scale continuous flow system that allows the use of cofactor-dependent enzymes by continuous regeneration of the necessary cofactors. The following will be required:

- Investigating methods of cofactor regeneration and ascertaining which is most feasible
- Determining whether enzyme recycle or immobilization must be used
- Testing the system with industrially relevant cofactor-dependent enzymes

The overall goal of the research is to determine whether a continuous flow system is a viable means of utilizing cofactor-dependent enzymes for the production of fine chemicals.

Acknowledgments

This project is a collaborative effort between the Department of Chemical and Biochemical Engineering at DTU and H. Lundbeck A/S, who is partly funding the research.

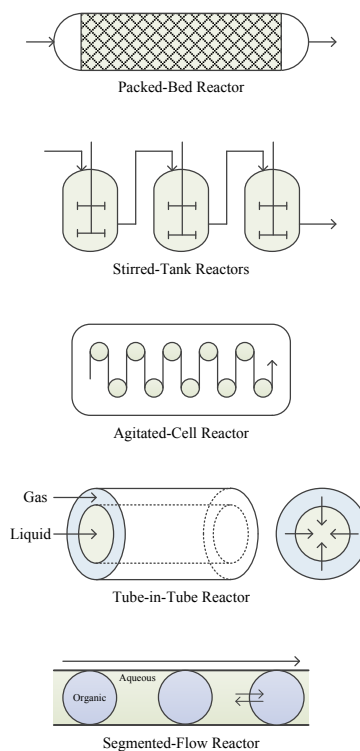


Figure 1: Reactors for continuous biocatalysis

References

1. L. Hajba, A. Guttman, *J. Flow. Chem* 6(1) (2015) 8-12.
2. M. Planchestainer, M.L. Contente, J. Cassidy, F. Molinari, L. Tamborini, F. Paradisi, *Green Chem.* 19 (2017) 372-375.
3. N.N. Rao, S. Lutz, K. Würges, D. Minör, *Org. Process Res. Dev.* 13 (2009) 607-616.
4. J.C. Thomas, M.D. Burich, P.T. Bandeira, A.R.M. de Oliveira, L. Piovan, *Biocatalysis* 3 (2017) 27-36.
5. A.T. Pedersen, T.M. de Carvalho, E. Sutherland, G. Rehn, R. Ashe, J.M. Woodley, *Biotechnol. Bioeng* 114(6) (2017) 1222-1230.
6. R.H. Ringborg, A.T. Pedersen, J.M. Woodley, *ChemCatChem* 9 (2017) 3285-3288.
7. R. Karande, A. Schmid, K. Buehler, *Adv. Synth. Catal.* 353 (2011) 2511-2521.
8. M.S. Thomsen, B. Nidetzky, *Biotechnol. J.* 4 (2009) 98-107.
9. G. Rehn, A.T. Pedersen, J.M. Woodley, *J. Mol. Catal. B: Enzym.* 134 (2016) 331-339.



Xinyan Liu
Phone: +45 45256180
E-mail: xlin@kt.dtu.dk

Supervisors: Rafiqul Gani
Georgios M. Kontogeorgis
Xiaodong Liang
Xiangping Zhang
Suojiang Zhang

PhD Study
Started: September 2016
To be completed: August 2019

Energy efficient hybrid gas separation with ionic liquid

Abstract

For most gas mixtures, the most common separation technology applied is distillation, which consumes large amounts of energy to give the high purity products. Hybrid gas separation processes, combining absorption and membranes together with distillation require less energy and have attracted much attention. With the property of non-volatility and good stability, ionic liquids (ILs) have been considered as new potential solvents for the absorption step. However, the enormous number of potential ILs that can be synthesized makes it a challenging task to search for the best one for a specific hybrid separation. In order to solve this problem, a systematic screening model for ILs is established by considering the needed properties for gas absorption process design. Rigorous thermodynamic model of IL-absorbed gas systems is established for process design-analysis. A strategy for hybrid gas separation process synthesis where distillation and IL-based absorption are employed for energy efficient gas processing is developed and its application is highlighted for a model shale gas processing case study.

Introduction

Gas separation process has been one of the most important technologies in the oil and gas related industries. For most gas mixtures, the most common separation technology applied is distillation, which consumes large amounts of energy to give the high purity products. These distillation columns operate at low temperatures and high pressures and therefore require high energy consumption, leading to negative environmental impacts. Therefore, an alternative scheme, taking advantage of the regions where each individual technology operate best, a hybrid gas separation scheme of combining distillation with absorption separation processes is considered.

Because of non-volatility, good stability, tunable viscosity and designable properties, ionic liquids (ILs) are considered as novel potential solvents and alternative media for gas absorption. Therefore, a strategy for hybrid gas separation process synthesis where distillation and IL-based absorption are employed for energy efficient gas processing has been developed. However, the potentially thousands of ILs that may be applicable, makes it a challenging task to search for the best one for specific gas absorptions in different raw gas systems. Therefore a selection-screening method for ILs is necessary for the development of novel hybrid gas separation process that can be designed.

Methodology

In this work, a three-stage methodology proposed for hybrid gas separation process design and evaluation will be highlighted. The first stage involves IL screening, where a systematic screening method together with a database tool is established to identify suitable ILs. The second stage is process design, where the important design issues are determined and the separation flowsheet is generated. The third stage involves verification and sustainability analysis based on rigorous process simulation of the generated hybrid gas separation process strategy. The gas separation problem for a model shale gas mixture is selected as a case study to highlight the application of this hybrid separation process design method.

This report will highlight the method, the data and applications of the method to generate novel, innovative and sustainable gas separation processes requiring significantly less energy than known processes.

Hybrid gas separation scheme

A generic representation of the natural or shale gas mixtures is developed, consisting of gases A, B, C, D and E, where a gas-A present in small amount is the lightest boiling, gas-B is in the largest amount, and the gases C-E are in small amounts and heavier boiling than gases A-B. A typical distillation train (scheme-1) for their separation is shown in Fig. 1 for a 5-gas mixture

requiring 3 separation steps. An alternative hybrid separation (scheme-2) is shown in Fig.2, where the distillation columns are replaced by absorption followed by flash-evaporation operations. Since the only energy requiring steps in the hybrid scheme of Fig 2 are the flash-evaporation steps, potentially a large reduction of energy consumption is possible by switching from scheme-1 to scheme-2.

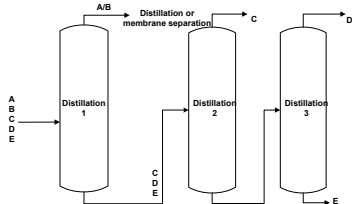


Figure 1: Gas separation with scheme-1

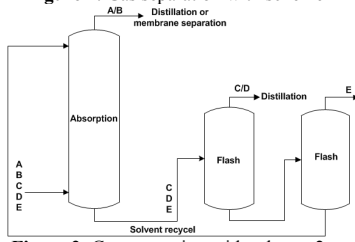


Figure 2: Gas separation with scheme-2

Scheme-2 is based on a new technology for removal of CO₂ from shale gas with IL as the solvent [1]. The first step for application of scheme-2 is the selection of an appropriate IL.

Database of ILs with measured solubility data

A database with collected measured solubility and Henry's law constant data of gases in ILs has been created. The collected data contains measured solubility data at different temperatures as well as Henry's law constant data of many gases in various ILs. It includes 14393 data points covering 16 gases and 136 ILs.

Model for Henry's law constant prediction

Because of the larger amount of data available for solubility of CO₂ in ILs, models to generate additional data were first developed for CO₂. The temperature dependence of the Henry's law constants was described by the following equation.

$$H = \exp[a + b/T] \quad (1)$$

Where, H is Henry's law constant of CO₂ in ILs, in bar. T is the temperature, in K. a and b are coefficients which are regressed by using the experimental data.

Linear fitting of coefficients a and b as a function of carbon atom number on the alkyl chain of different anions of IL, the Henry's law constant model of CO₂ in a specific IL type is established (see Eq.2).

$$H = \exp[c_1 + c_2 \cdot C_n + \frac{c_3 + c_4 \cdot C_n}{T}] \quad (2)$$

Where, C_n is the carbon atom number on the alkyl chain of ILs. c₁, c₂, c₃ and c₄ are parameters estimated

through regression. Through this model, solubility of CO₂ (or other gases with their corresponding models) in new IL can be predicted. In this case study, we established the model for imidazolium-based ILs with [Tf₂N], [BF₄] and [PF₆] as anion.

Besides this group contribution model, other models such as UNIFAC and COSMO-RS model are also taken into consideration to be developed.

Application on database and model library

Based on the measured Henry's law constant data of CO₂ and CH₄, the Henry's law constant of CO₂ versus selectivity of CO₂/CH₄ under different temperature is plotted as in Figure 3.

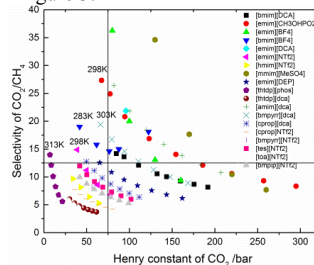


Figure 3 Henry's law constant of CO₂ versus selectivity of CO₂/CH₄ under different temperature

Then the optimal IL is the one which has the lowest Henry's law constant of CO₂ and highest selectivity of CO₂/CH₄. As the temperature increases, both the solubility of CO₂ and selectivity of CO₂/CH₄ decrease. Since [thtdp][phos] shows the lowest Henry constant among others at relative high temperature, which means it may have a lower Henry's law constant and higher selectivity when the temperature decreases, and it was, thus, chosen as the optimal one for the further study.

Conclusion and future work

This work provided a good basis for novel IL-based hybrid gas separation process design. All the predictive Henry's constant models have been found to be in good agreement with experimental data. On the basis of the database and models, a case study for selection of the potential IL-solvent for gas separation by absorption has been highlighted. An IL-based hybrid separation scheme for significantly reduced energy has been introduced and the potential benefits highlighted through a conceptual example.

Future work is necessary to develop a UNIFAC model in more gas-ILs systems. A better solvent and process for shale gas separation will be designed based on the database and model library. Rigorous gas separation simulation and evaluation will be also developed.

References

1. X. Liu, Y. Huang, Y. Zhao, R. Gani, X. Zhang, S. Zhang, Ionic liquid design and process simulation for decarbonization of shale gas. *Industrial & Engineering Chemistry Research*, 55(20) (2016) 5931-5944.



Petter Lomsøy
Phone: +45 2889 7086
E-mail: plom@kt.dtu.dk
Center: Center for Energy Resources Engineering

Supervisors: Kaj Thomsen
Philip Loldrup Fosbøl

PhD Study
Started: September 2017
To be completed: August 2020

Kinetics of scale gormation in oil and gas production

Abstract

Scale formation poses a major challenge for the oil and gas industry. Scale build up on interior piping may cause losses in production, due to loss of internal diameter. Substantial deposition may result in stop of production or failure in critical components. The industry is moving towards deeper exploration, with the tough conditions that involves. Additionally, the development of subsea satellite wells with long tie backs is posing challenges in regards to access for well interventions. Prevention and inhibition of scales, is therefore considered preferable in comparison to removal. This requires reliable thermodynamic models, and experimental data. The understanding of the conditions which results in scaling occurrence, are of great significance for the ability to predict scaling behavior.

Introduction

Scales are inorganic deposits which are occurring in processes, which are producing water. As the produced fluid is transported from reservoir to surface, it experience changes in conditions. Changes in temperature and pressure are inducing the precipitation of for instance CaCO_3 and FeCO_3 . FeCO_3 is found in the completion of the well as corrosion product. Another scenario is due to incompatible mixing of brines. This is occurring when introducing pressure support by sea water injection. The seawater is rich in anions and the formation water is rich in cations. Examples of common scale types found in this scenario are CaSO_4 , BaSO_4 and SrSO_4 . The chemical equilibrium of the formation fluid, may be distressed by the sudden interaction of the injected fluid [1]. The produced water may be oversaturated with scaling components. Additional factors that decide the location and magnitude of scaling occurrence are kinetics, pH, composition and CO_2 content [2].

The target system for this project is iron carbonate, which is commonly found in production equipment, and often as corrosion product in production tubing. This scale mineral has not been investigated to a far extent, as for example calcium carbonate.

Specific objectives

This project aims for contributing in the improvement of integrity of wells, facilities and pipelines. Scale build-up causes decrease of well efficiency, and is considered a

contributing factor for potential loss of well integrity. Improved understanding of observed mechanisms, and development of testing methods for predicting and mitigating scale deposits is essential for optimal recovery of oil reserves.

The purpose of the project is to create a knowledge base which allows for a further model development giving the possibility to better predict scale formation in the future. The objective is to reduce the cost of well workovers by developing methods to predict the rate of scale formation. Existing equipment and methods need to be further developed. Measurements are to be conducted under conditions allowing the determination of scale formation under varying supersaturation conditions, as functions of production fluid properties and composition like sea water fraction as an example. The study of the interaction between brine and surfaces will play a role in the project.

The scale in focus for this study will be FeCO_3 , an oilfield scale which are found in the hydrocarbon production facilities of the North Sea. Due to lack of information regarding the kinetics of FeCO_3 , it seem advantageous to correlate the study with the findings of CaCO_3 . CaCO_3 scaling kinetics has to a certain extent been studied, and reported in open literature.

An experimental setup for determining scaling kinetics, are to be constructed. After establishing the sufficient experimental method, there will be introduced measurements of CaCO_3 scaling precipitation and deposition. The goal is to reproduce the values found in

open literature, for validation of the experimental setup. After this is established, the experimental program for determining FeCO₃ kinetics can commence. The objective will be to determine the kinetics of surface deposition, and bulk crystallization. Enhanced understanding of the properties of the scale in question, will be valuable for the work on avoiding scale deposition. This through active control of the properties of the well, for avoiding/limiting the scaling problem.

Experimental conditions

The following conditions pose as the frame for the experimental campaign:

- CO₂ Partial pressure 0-150 kPa
- Temperature 25-80°C
- Varying supersaturation
- Anoxic conditions

It is important to evaluate the CO₂ partial pressure, since the solubility of FeCO₃ is dependent on it. This is related to the increased solubility of CO₂ gas in the produced fluid, with increased CO₂ partial pressure. With increasing CO₂ partial pressure the content of carbonate in the produced water increase.

Both the temperature range and the introduction of varying supersaturation, are important in order to discover the conditions where scaling occur. These conditions are planned to be investigated in an experimental campaign, which involves anoxic conditions.

Model development

Most models used to describe the kinetics of crystal growth in the bulk, are variations of the Diffusion-reaction theory. The two common versions are:

$$\frac{dC}{dt} = (C_e - C)^2 \cdot k \cdot S \quad R = k(SI^{0.5} - 1)^2$$

To create a model that is able to describe the experimental data, an evaluation of the different types of models are to be conducted. The Diffusion-reaction theory expression are describing the kinetics of crystal growth in bulk phase. However, scales are occurring in bulk phase, on metal surfaces and deposits on top of existing scale layers. Special attention are to be given the kinetics of metal surface deposition. This is the scenario which are causing risk of clogging, hence loss in production. The surface deposition and bulk crystallization are processes, which have different kinetics [3]. How the kinetics of these two processes are behaving in relation to another, are to be investigated.

Conclusion

This PhD study will address problem of scaling, which are substantial to the flow assurance and integrity of wells and equipment. Quantifying the kinetics of FeCO₃ scale surface deposition and bulk crystallization, are to improve future prediction of its occurrence.

References

1. Crabtree, M., Eslinger, D., Fletcher, P., Miller, M., Johnson, A. and King, G.: 1999, Fighting scale - removal and prevention, *Oilfield review* 11(3), p. 30 - 45. URL: <https://pdfs.semanticscholar.org/5ddd/cdc5e89e335bacdf40bd1de0f7768c480ba8.pdf>
2. García, A. V., Thomsen, K. and Stenby, E. H.: 2006, Prediction of mineral scale formation in geothermal and oilfield operations using the extended uniuqac model: Part ii. carbonate-scaling minerals, *Geothermics* 35(3), p. 239–284.
3. Eroini, V., A. Neville, N. Kapur and M. Euvrard. 2013. New insight into the relation between bulk precipitation and surface deposition of calcium carbonate mineral scale. *Desalination and water treatment*, 51(4-6), p.882-891.



Hao Luo
 Phone: +45 4525 2853
 E-mail: haol@kt.dtu.dk

Supervisors: Kim Dam-Johansen
 Hao Wu
 Weigang Lin

PhD Study
 Started: October 2016
 To be completed: September 2019

CFD Simulation of biomass combustion in fluidized beds

Abstract

The project aims at developing an efficient and reliable computational fluid dynamics (CFD) model to simulate biomass combustion in fluidized bed systems. A multi-scale methodology (particle-scale, meso-scale, and reactor-scale) is adopted to simplify such a complex system. A heat transfer corrected isothermal model has been developed for CFD simulation of devolatilization of large biomass particles in fluidized bed.

Introduction

Biomass combustion in fluidized bed is a typical complex heterogeneous reacting system. Conventional chemical reaction engineering (CRE) models (e.g. plug-flow, ideal well-mixed etc.) oversimplifies the hydrodynamic behaviors in fluidized beds. Thus, the effect of hydrodynamic behaviors on biomass particles reaction is not fully understood. Compared to CRE models, CFD models have been widely considered as a useful tool to reveal both hydrodynamic and reaction behaviors in detail, e.g. velocity, pressure and temperature profiles, as well as mixing in fluidized bed combustors. However, the following challenges remain in CFD modeling of biomass combustion in a fluidized bed at different scales, as shown in Fig. 1.

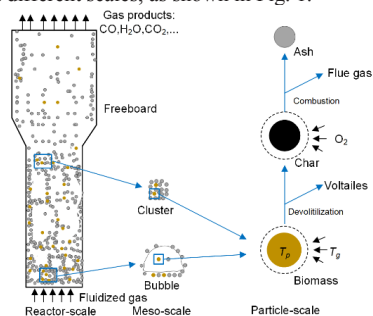


Figure 1: Different scales of CFD modeling biomass combustion in fluidized bed.

(1) Particle-scale: internal heat and mass transfer are usually neglected in CFD simulations, because a computational cell is larger than particles. However, internal transfer has significant effects on reaction at particle scale, especially for large particles [1].

(2) Meso-scale: the meso-scale structures (e.g. cluster or bubble) have significant effects on momentum, and heat and mass transfer between gas and solid phase [2,3]. Current meso-scale structure model should be validated for modeling biomass combustion in fluidized bed.

(3) Reactor-scale: CFD modeling coupled with chemical kinetic models is time-consuming for a large-scale fluidized bed. It is essential to develop reliable and efficient approaches to couple CFD models with chemical reaction kinetics.

Objectives

The objective of this project is to develop an efficient and reliable approach to simulate biomass combustion in fluidized bed systems. Through this project, we can have better understanding of biomass combustion in fluidized bed and the developed method can be used to model biomass combustion both at particle-scale and reactor-scale.

Heat transfer corrected isothermal model

An isothermal particle model is commonly used in CFD modeling of biomass devolatilization in fluidized beds. However, the model is only reasonable for small particles (Biot Number: $Bi < 1$). For large particles, the internal temperature gradient has significant effect on devolatilization. Therefore, a non-isothermal model is favored for modeling biomass devolatilization. However, it is time-consuming when a non-isothermal model is directly coupled with CFD models. To solve the problem, a heat transfer corrected isothermal model is developed by using correction coefficient defined as follows:

H_T : Correction coefficient for heat flux

$$\begin{aligned} Q_{cor-iso} &= Q_{non-iso} = H_T Q_{iso} & (1) \\ H_T &= \frac{Q_{non-iso}}{Q_{iso}} = \frac{h_c (T_g - T_{surf}) + \varepsilon_p \sigma (T_w^4 - T_{surf}^4)}{h_c (T_g - T_p) + \varepsilon_p \sigma (T_w^4 - T_p^4)} & (2) \end{aligned}$$

H_R : Correction coefficient for reaction rate

$$R_{cor-iso,i} = R_{non-iso,i} = H_{R,i} R_{iso,i} \quad (3)$$

$$H_{R,i} = \frac{R_{non-iso,i}}{R_{iso,i}} = \frac{\int_0^R 4\pi f_{r,i} r^2 dr}{f_i V_p} \quad (4)$$

Based on the correction coefficients, a heat transfer corrected isothermal model is derived:

$$c_p \rho_p \frac{dT_p}{dt} = \frac{b}{r} (h_c (T_g - T_p) + \varepsilon_p \sigma (T_w^4 - T_p^4)) H_T - \sum_{i=1}^n \Delta H_{R,i} R_{cor-iso,i} \quad (5)$$

$$R_{cor-iso,i} = f_i V_p H_{R,i} \quad (6)$$

where Q is the heat flux between gas and particle, h_c is convection heat transfer coefficient, R is the reaction rate, f is kinetic model of reaction i . V_p is particle volume. T_w , T_p , T_g , T_{surf} are wall, particle, gas, and particle surface temperature, respectively, ΔH is heat of reaction.

In this way, the non-isothermal and corrected isothermal model can predict similar results and more importantly, the corrected isothermal model can be easily coupled to a CFD software with similar computational time of isothermal model.

Fig 2. shows the conversion history predicted by different models and a comparison to experimental data [4] of a near-spherical particle devolatilized at the single particle combustor. Obviously, the mass loss history predicted by corrected isothermal and non-isothermal model are in good agreement with the experimental data, while the isothermal model underestimates the conversion at the beginning and overestimates the conversion at later time.

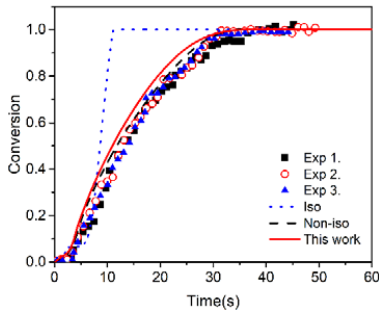


Figure 2: Conversion history of large particle ($d_p=9.5\text{mm}$, $T_g=1050\text{K}$, Moisture=6 wt%, $T_w=1276\text{K}$)

Fig 3 shows a comparison of CFD modeling of biomass particle pyrolysis rate by using corrected isothermal and isothermal model in a batch fluidized bed. At average particle temperature $T_p \sim 600\text{K}$, the particle outer layer temperature is high enough for biomass devolatilization, and this stage corresponds to $H_R > 1$. Therefore, corrected isothermal model shows a higher pyrolysis rate as well as volatiles mass fraction than isothermal model. At average particle temperature $T_p \sim 800\text{K}$, the particle outer layer has high conversion or even totally

converted, this stage corresponds to $H_R < 1$. Therefore, the pyrolysis rate predicted by isothermal model larger than that of corrected isothermal model. In totally, the corrected isothermal model shows that biomass particle starts devolatilization at low particle temperature and ends at higher particle temperature, as compared to isothermal model. The result is consistent what we observed in single particle modeling.

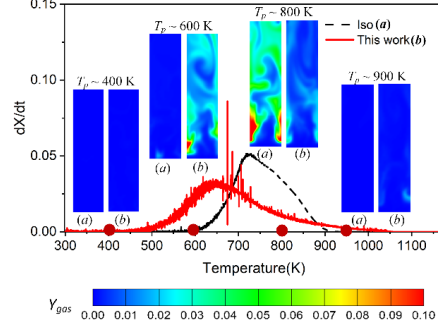


Figure 3: Comparisons of CFD modeling pyrolysis rates versus particle average temperature and contour plot of volatiles mass fraction by using isothermal model and this work.

Conclusion

CFD modeling biomass combustion in fluidized bed dependent on the development of models of different scales (particle scale, meso-scale, and reactor scale). A heat transfer corrected isothermal model is developed to model devolatilization of large biomass particle at particle scale. Two heat-transfer corrected coefficients, H_T -correction of heat transfer and H_R -correction of reaction rates are introduced and correlated as a binary function of heat convection coefficients and a dimensionless particle temperature. The model is validated by experimental data in literatures and implemented in a CFD software.

Future work

In future, it is planned to extend this method to describe char combustion in a fluidized bed. After that, the current meso-scale model (e.g. drag model, heat transfer model etc.) will be validated for CFD modeling biomass combustion in fluidized bed. Finally, we plan to develop a reliable and efficient approach to model large-scale fluidized by coupling CFD and CRE models.

References

1. A. Gómez-Barea, B. Leckner, Prog. Energy Combust. Sci. 36 (2010) 444–509.
2. W. Wang, B. Lu, N. Zhang, Z. Shi, J. Li, Int. J. Multiph. Flow. 36 (2010) 109–118.
3. K. Hong, Z. Shi, W. Wang, J. Li, Chem. Eng. Sci. 99 (2013) 191–202.
4. H. Lu, W. Robert, G. Peirce, B. Ripa, L.L. Baxter, Energy and Fuels. 22 (2008) 2826–2839.



Line Riis Madsen

Phone: +45 2896 0199
E-mail: linmads@kt.dtu.dk

Supervisors: Anne Ladegaard Skov
Ole Hassager

PhD Study
Started: May 2016
To be completed: April 2019

Modelling of thermal breakdown in dielectric elastomers

Abstract

A dielectric elastomer (DE) is a thin elastomer film sandwiched between two compliant electrodes, and upon application of an electrical field the DE increases in area and decreases in height. DEs are soft transducers that can be used as actuators, generators, and sensors. When using DEs multiple types of breakdowns may occur, depending of the operating conditions. The scope of this project is to study the parameters that lead to breakdown by modelling the performance of DEs during operation, with main focus on thermal breakdown.

Introduction

Dielectric elastomers (DEs) are a promising group of materials that can convert electrical energy into mechanical energy and vice versa. Thus, they can serve multiple purposes as actuators, generators, and sensors. DEs are composed of a thin incompressible elastomer film sandwiched between two compliant electrodes. When an external voltage is applied to the electrodes, electrostatic forces are created between the two electrodes which cause the elastomer to decrease in height but increase in the planar directions as shown in Figure 1. When the applied voltage is switch off again, the elastomer regains its original shape.

The thickness of one dielectric elastomer is usually 50 μm , whereas the diameter of the elastomer is in the order of millimeters to centimeters. Usually a stack of DEs are used in products, such that the achievable mechanical force is increased.

Several types of breakdowns can occur during operation of DEs, and they can be categorized based on the required time until breakdown with aging mechanisms being slow mechanisms while breakdown mechanisms are somewhat instantaneously fatal. One of the most important breakdown mechanisms is thermal breakdown since this require less than 10^{-5} seconds for a

breakdown to occur. Thermal breakdown occurs at low electrical fields, and the breakdown occurs when the energy generated within the DE, i.e. from joule heating, is higher than the amount of energy dissipated. This will cause an increase in temperature, which in return causes the thermal conductivity to increase, which again causes the amount of joule heating to increase. Thus, thermal breakdown occurs when the temperature of the material, either locally or macroscopically, increases exponentially.

Thermal breakdown is more prone to occur in a stack of DEs than in a single layer of DE, since when DEs are stacked up, the volume is increased while the surface area of the stack is not increased significantly. Hence, more energy is generated while the amount of heat dissipated away is not increased significantly when DEs are stacked.

Specific Objectives

The aim of this project is to obtain a better understanding of the different breakdown mechanism that can occur in DEs, and furthermore investigate which parameters that affects the ability of a breakdown to take place. The research will be based on modelling of breakdown mechanisms of DEs, with main focus on thermal breakdown.

The obtained model will continuously be validated with experimental data in order to ensure consistency between modelling and experiments. The different electrical, thermal and physical parameters of the DE will be found experimentally, as well as the breakdown strength, which will be measured by using an in-house-built device.

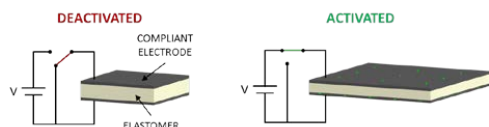


Figure 1: Illustration of the working principle of a dielectric elastomer during actuation [1].

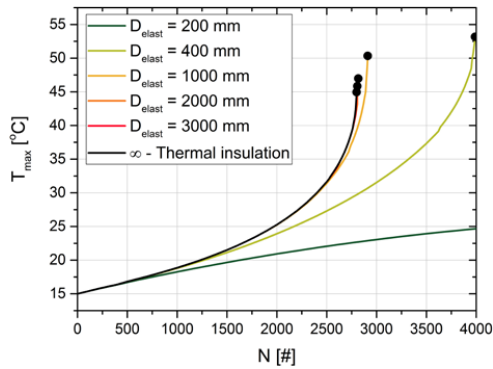


Figure 2: Maximum temperature inside a stack of DEs as a function of the number of layers and the diameter of the stack. The electric field is set to $100 \text{ V}/\mu\text{m}$ and the surrounding temperature is 15°C .

Results and Discussion

An electro-thermal model was setup in COMSOL in order to perform the investigation of how various parameters affect the thermal breakdown of dielectric elastomers. The geometry used was a stack of N discs of DEs each with a height of $50 \mu\text{m}$ and a given diameter, D_{elast} . Natural convection takes place at all surfaces of the stack, and it is assumed that joule heating is the only source of generated heat within the stack.

The first parameter that is examined is the diameter of the stack. From Figure 2 it can be seen that no thermal breakdown occurs when the diameter is small, since the heat transfer taking place at the surface area of the stack is large enough to balance the energy generated within the stack. However, when the diameter increases the maximum amount of layers in the stack is decreased, since the volume in which energy is generated increases more than the surface area of the stack. If the diameter of the stack is very large, it is fair to assume that there is thermal insulation on the curved side of the stack, since heat transfer on this surface is negligible.

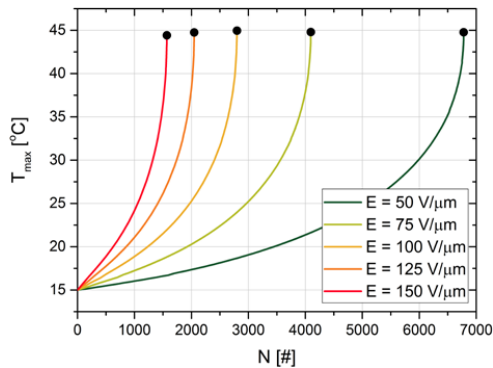


Figure 3: Maximum temperature inside a stack of DEs as a function of the number of layers and the applied electric field. The surrounding temperature is 15°C and with thermal insulation on the curved sides of the stack.

The second parameter that is investigated is the applied electric field. It is found that when the applied electric field increases, the maximum possible number of layers in the stacked DE decreases, as shown in Figure 3. This is due to the amount of energy being generated by joule heating increases with the electric field.

The last parameter that is investigated in this study is the temperature of the air surrounding the stack. In Figure 4 it can be seen that the maximum possible number of layers in a stack of DEs before a thermal breakdown occurs, decreases when the temperature of the surroundings increases. The reason for this is that the driving force for heat transfer at the sides of the stack is given by the temperature difference between the actual temperature at the surface and the temperature of the surroundings. Thus, when the surroundings temperature increases, the driving force for removing heat from the stack decreases, and consequently less discs of DE can be stacked before thermal breakdown occurs.

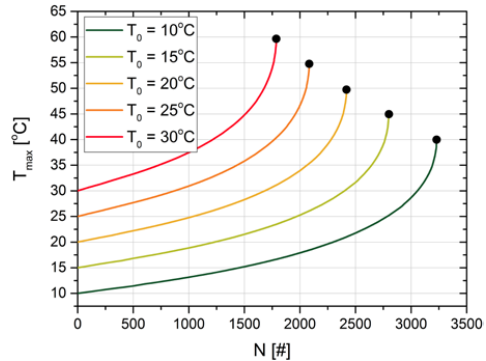


Figure 4: Maximum temperature inside a stack of DEs as a function of the number of layers and the temperature of the surroundings. The electric field is set to $100 \text{ V}/\mu\text{m}$ and with thermal insulation on the curved sides of the stack.

Conclusion

An electro-thermal model for a stack of DEs has been set up in which some of the key parameters leading to thermal breakdown has been studied. It was found that possible number of layers in a stack of DEs before thermal breakdown occurs was increased if the diameter, electrical field, and surrounding temperature were decreased.

Acknowledgements

The author would like to thank Aage og Johanne Louis-Hansens Fond and DTU Chemical Engineering for funding my PhD project.

References

1. L. R. Madsen, O. Hassager, A. L. Skov, Dansk Kemi 10 (2017) 12-15.



Marvin Masche
Phone: +45 9351 1606
E-mail: marv@kt.dtu.dk

Supervisors: Jesper Ahrenfeldt
Maria Puig Arnavat
Peter Arendt Jensen
Sønnik Clausen
Ulrik Birk Henriksen
Jens Kai Holm, Ørsted

PhD Study
Started: January 2016
To be completed: December 2018

Morphology and grindability study of wood and combustion characterization at pulverized-fuel firing conditions

Abstract

Wood pellets will play an important role to replace the use of coal in existing Danish combined heat and power plants. However, compared to coal, wood suffers from several undesired properties, such as a fibrous nature, anisotropy and low energy density. The aim of the project is to improve the understanding and knowledge of milling and combustion characteristics of pellets made of different softwood and hardwood species. The results of current research suggest that power plant operators need to choose pellets with a finer particle size distribution of material within pellets, in order to achieve the desired comminuted product fineness with lower specific energy consumption.

Introduction

Danish energy companies have already converted, or are currently converting their existing suspension-fired power plants from coal to operate 100 % on biomass, mostly wood pellets, in order to reduce greenhouse gas emissions by 20 % by 2020. To mitigate industrial greenhouse gas emissions, retrofitting power plants from coal to wood pellets by utilizing the existing milling equipment and auxiliary infrastructure offers a cost-efficient and practical option at low capital investment [1]. Furthermore, the converted plants preserve grid reliability compared to intermittent renewable energies like wind and solar [2].

The description and analysis of the size reduction process of wood particles in suspension-fired power plants are essential with the purpose of getting desirably combustible properties. Generally, comminuting fibrous and orthotropic elastic wood that is capable of absorbing energy before size reduction requires more energy than brittle coal regardless of mill type [3]. The energy required for milling biomass depends on the feed moisture, particle size reduction ratio, feedstock characteristics, feed rate and mill operating parameters [4]. The comminuted particle size and shape are important properties for suspension-firing, as they influence the particle dynamics, particle heat and mass transfer. To ensure robust future pulverized wood utilization, further research within the areas of wood particle characterization, wood pellet grindability, wood combustion characterization is required.

Aim and Scope

Recent research focuses on the assessment of the milling behavior of industrial wood pellets in coal roller mills at the biomass-converted suspension-fired combined heat and power plant Amagerværket unit 1, Copenhagen. The hypothesis was tested that large-scale pellet comminution in roller mills is affected by the particle size distribution (PSD) of material within pellets (i.e. disintegrated pellets). The results provided can be valuable to optimize the overall milling and combustion process for plant operators facing the problems of changing from coal to biomass pellets.

Material and Methods

Two industrial wood pellet qualities (i.e. I1 and I2 pellets) that conformed to the requirements of industrial pellets according to ISO 17225-2:2014 were tested. The major difference between both qualities is the particle size distribution (PSD) of material within pellets (or internal PSD). I1 pellets featured a 20 % higher mass fraction of particles below 1 mm within pellets compared to I2 pellets.

Pellets were comminuted in three coal mills (type LM 19.2 D, Loesche GmbH, Germany), each equipped with a dynamic classifier. Figure 1 shows a schematic representation of the design features of a coal roller mill and the internal flow of comminuted wood pellet material. The throughput rate for wood pellets is reduced due to their lower energy density compared to coal [1].

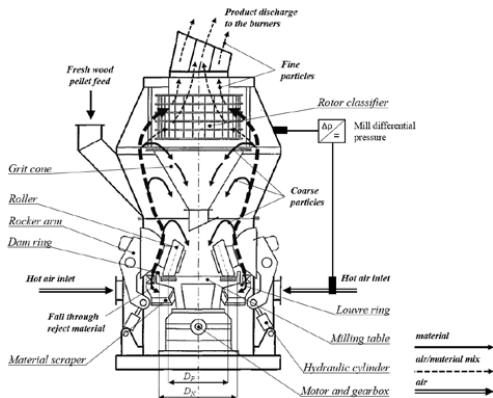


Figure 1: Schematic representation of a large-scale roller mill and the material flow within the mill.

The pellet milling behavior was assessed by determining the specific grinding energy consumption (*SGEC*) and the differential mill pressure (Δp). Furthermore, the size and shape of comminuted wood particles conveyed to the burners were analyzed by using dynamic image analysis (Camsizer[®] X2 operated in X-Jet mode) and sieve analysis, respectively.

Results and Discussion

Figure 2 shows the PSD of comminuted pellets analyzed by sieve analysis and Camsizer[®]X2. Good agreement exists for particles larger or equal 0.5 mm. However, the fraction retained on the 0.25 mm and 0.09 mm sieves seems to be underestimated, possibly due to an increased dust cohesiveness when decreasing the particle size [5], increasing the tendency to block sieve openings by forming agglomerates, which remain on the sieve, and thus diminish the mass of comminuted wood pellets in the finer fraction.

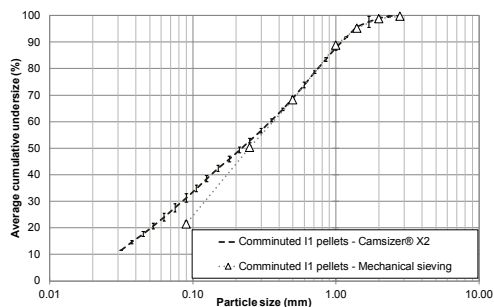


Figure 2: PSD analysis by sieving and Camsizer[®]X2.

Sieve analysis, which is limited to the measurement of one single dimension (i.e. particle width) may be rudimentary, and should be replaced by an image analysis system suitable to characterize the product fineness and shape.

To achieve the desired product fineness, plant operators should be aware that the PSD of the material within pellets is a decisive pellet specification. Figure 3 shows

that, on average, the comminution of I1 pellets is more efficient compared to I2 pellets indicated by finer particles produced at lower *SGEC*.

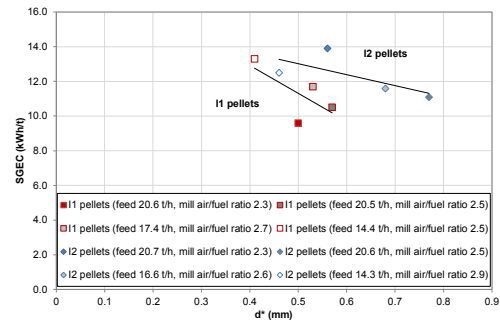


Figure 3: *SGEC* vs. characteristic particle size (d^*).

Conclusions

The following conclusions can be drawn from recent research:

- Traditional sieve analysis may not be suitable to characterize the comminuted product fineness.
- The PSD of material within pellets affects the large-scale pellet milling behavior. Pellets with coarser internal particles require more energy for milling and lead to a higher differential mill pressure
- Roller mills only break pellets down into the original elongated particle shape of the material within pellets, even at changing mill operation conditions.

Acknowledgements

This study is part of the Forskel project “AUPW – Advanced Utilization of Wood Pellets”. The author would like to thank Energinet.dk, Ørsted and HOFOR for co-funding of the study.

References

1. W.R. Livingston, The status of large scale biomass firing: The milling and combustion of biomass materials in large pulverised coal boilers, IEA Bioenergy Task 32: Biomass Combustion and Co-Firing. (2016) 21–23.
2. M. Odenberger, The role of combustion in the future energy system, Presentation at the Nordic Flame Days, in: Stockholm, Sweden, 2017.
3. O. Williams, G. Newbolt, C. Eastwick, et al., Influence of mill type on densified biomass comminution, *Applied Energy*. 182 (2016) 219–231.
4. S. Mani, L.G. Tabil, S. Sokhansanj, Grinding performance and physical properties of wheat and barley straws, corn stover and switchgrass, *Biomass and Bioenergy*. 27 (2004) 339–352.
5. J. Tomas, S. Kleinschmidt, Improvement of flowability of fine cohesive powders by flow additives, *Chemical Engineering and Technology*. 32 (10) (2009) 1470–1483.



Murray P. Meissner

Phone: +45 5029 9315
E-mail: mmeiss@kt.dtu.dk

Supervisors: John M. Woodley
Mathias Nordblad
Gustav Rehn

PhD Study
Started: July 2015
To be completed: July 2018

Biocatalytic Baeyer-Villiger oxidations

Abstract

Baeyer-Villiger oxidations catalysed by Baeyer-Villiger monoxygenases (BVMOs) have become industrially relevant in light of their superior selectivity, use of molecular oxygen, and ability to satisfy new 'green chemistry' process constraints when compared to conventional chemical oxidants. However, the difficulty in characterising such enzymes in reactions featuring poorly water-soluble substrates challenges their industrial implementation. This project aims to detail a generic methodology for dealing with problematic substrates/products for the characterisation and demonstration of enzymes in their often heterogeneous reaction environment. The target reaction, which is the oxidation of an insoluble macrocyclic ketone to its corresponding lactone, will be used to demonstrate and formulate such a protocol. Knowledge from this rational and simple method of evaluating biocatalysts in heterogeneous reaction mixtures will be directly applicable and fundamental to operating these reactions at an industrial scale.

Introduction

The broadening of the industrial scope of bio-oxidation processes beyond pharmaceutical applications to new fine chemicals, nutrition, feed and materials markets has been targeted in light of the EU 2020 goal for industrial biotechnology. One such group of flavin-dependent monoxygenases presents a promising route using Baeyer-Villiger type oxidation reactions to yield numerous products from non-natural substrates. The biocatalytic route allows the substitution of conventional, unsafe and unstable oxidants with molecular oxygen and affords superior regio-, chemo-, and enantioselectivity [1,2].

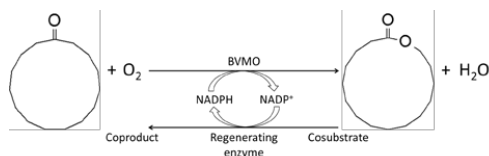


Figure 1: Reaction scheme for the oxidation of cyclopentadecanone to cyclopentadecanolid catalysed by a Baeyer-Villiger monoxygenase (BVMO).

The industrially-relevant target reaction for the BVMO-based process is the conversion of a macrocyclic ketone (exaltone: *cyclopentadecanone*) to its corresponding lactone (Figure 1). The challenge and

novelty of such a reaction lies in the low aqueous solubility of both substrate and product. Indeed, reactions featuring these problematic substrates are ubiquitous in biocatalysis.

Furthermore, industrial processes require high substrate loadings often resulting in media consisting of multiple phases. Although some co-solvent may be required to help bolster solubility, solubilising all substrate at these high concentrations would otherwise necessitate economically and environmentally unfeasible co-solvent demands.

Fundamental to the development of multi-phase biocatalytic processes is the necessity to be able to characterise the enzyme with respect to enzyme kinetics, stability and behaviour of the final formulation in a heterogeneous reaction environment.

Specific Objectives

Employing poorly water-soluble substrates in biocatalysis requires special considerations for how biocatalysts may be characterised, and are typically executed on a case-by-case basis. In addition, there are further analytical and sampling challenges brought about by these heterogeneous reaction mixtures.

The objective of this work is therefore to detail a generic, rational and simple methodology for characterising biocatalysts in reactions with poorly water-soluble components. The methodology required

consideration and development towards different experimental procedures than those used in standard assays due to the heterogeneous nature of reaction.

Results and Discussion

1. Substrate/product physical properties

First, substrate and product physical properties were evaluated (including the affinity of the product for partitioning to the substrate phase).

The solubilities of substrate and product in water at 28 °C were found to be 113 ± 21 and 101 ± 24 μM respectively (mean \pm SD, $n = 3$).

It was found from a simple crystallisation experiment that product forms separate crystals to the substrate particles from an oversaturated solution with product containing a ‘seed crystal’ of substrate within. This perfect separate crystal formation was further verified using gas chromatography. Therefore, when insoluble product is formed during the reaction it will not crystallise on the surface of substrate molecules, despite their similar physical properties, and mass transfer will be unhindered by this phenomenon.

2. Kinetic assays

The next step of understanding the BVMO-based reaction was to perform kinetic assays under single phase, dilute conditions to determine Michaelis-Menten parameters and assess enzyme stability.

Spectrophotometric activity assays revealed the V_{max} of this reaction to be $2.56 \text{ U} \cdot \text{mL}_{\text{CFE}}^{-1}$ and $K_{\text{m,S}}$ was found to be $24 \mu\text{M}$. Therefore, at the substrate saturation of $113 \pm 21 \mu\text{M}$ the reaction will proceed at V_{max} and not be kinetically limited.

For improved accuracy, a different method of performing activity assays by sacrificial sampling of 1 mL reaction mixtures was developed. Substrate and product concentration profiles during the reaction are monitored directly by GC analysis. Measurement error introduced by undissolved substrate/product particles was minimised by operating under dilute conditions and at a slightly elevated temperature of 30 °C. This method is more robust than the standard assay that relies on spectrophotometric measurements of the secondary substrate (NADPH), which is made difficult since it is regenerated during reaction.

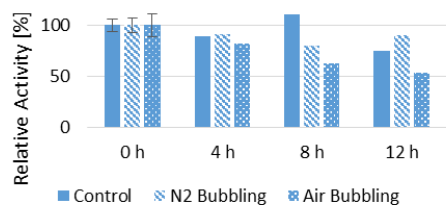


Figure 2: BVMO stability as a function of gas-liquid interfaces (bubbling with N_2 (striped bars)) and oxygen concentration (bubbling with air (dotted bars)). Error bars reflect 95CI ($n = 6$).

Using this activity assay, the stability of the BVMO towards gas-liquid interfaces, and oxygen concentration was assessed (Figure 2). Further stability assessments towards different types of solvents (miscible and immiscible) is ongoing.

3. Reaction work-up

Lastly, work-up of the reaction to a reactor-scale with process control capabilities allowed the study of effects of reaction environment (e.g. temperature, type of co-solvent, fraction of co-solvent) on the biocatalytic reaction.

Reactions at a scale of 150 mL were performed in an aerated stirred tank reactor with dissolved oxygen, pH and temperature control. In order to avoid troubles with representative sampling of the heterogeneous reaction mixture, an analytical method using oxygen mass balance across the gas-phase was validated and demonstrated (Figure 3).

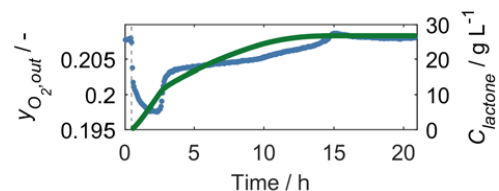


Figure 3: Reaction kinetics of the oxidation of cyclopentadecanone to cyclopentadecanolide by a BVMO. Oxygen fraction in the outlet gas stream is shown in blue, and the predicted concentration of lactone product by oxygen mass balance is shown in green.

Further investigations with this system are planned to evaluate process performance under varying co-solvent fractions and temperatures. Eventually, a primary process limitation can be established and potential strategies to counter this formulated.

Understanding from such a reaction system may be directly scalable to industrial processes.

Acknowledgements

This project falls under EU ROBOX (grant agreement n° 635734): “Expanding the industrial use of robust oxidative biocatalysts for the conversion and production of alcohols.” Any statements herein reflects only the author’s views. The European Union is not liable for any use that may be made of the information contained herein.

References

1. M. Bučko, P. Gemeiner, A. Schenk Mayerová, T. Krajčovič, F. Rudroff, M.D. Miholovič, *Appl. Microbiol. Biotechnol.* 100 (2016) 6585-6599.
2. G. de Gonzalo, M.D. Miholovič, M.W. Fraaije, *Chembiochem* 11 (2010) 2208-2231.

List of Publications

M.P. Meissner, M. Nordblad, J.M. Woodley, *ChemBioChem* (2017) DOI:10.1002/cbic.201700577.



Xianglei Meng
Phone: +45 52909586
E-mail: xmen@kt.dtu.dk

Supervisors: Nicolas vol Solms
Xiaodong Liang
Suojiang Zhang, IPE (Beijing, China)
Xiangping Zhang, IPE (Beijing, China)

PhD Study
Started: Dec. 2015
To be completed: Dec. 2018

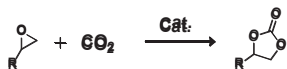
Efficient transformation of atmospheric CO₂ to carbonates by DBU based ionic liquids under mild conditions

Abstract

1,8-diazabicyclo-[5.4.0]undec-7-ene (DBU) based ionic liquids (DBUILs) composed by a protonic acid and multi-nucleophilic sites were designed to catalyze the cycloaddition reaction of CO₂ with epoxides at atmospheric pressure and mild temperature. As a metal-free catalyst, DBUILs could support the transformation of CO₂ to carbonates in excellent yields with broad substrate scope, without the need for time-consuming and co-catalyst. The experimental evidences revealed a greatly improved activity via hydrogen bond activating epoxides by introduced extra hydrogen protons from water.

Introduction

The efficient transformation of CO₂ has attracted remarkable interests from viewpoint of sustainable chemistry, as these may reduce the greenhouse gas and mitigate the effects of climate change, whilst also producing various organic chemical commodity.^[1] However, CO₂ activation requires electrolytic reduction processes or high-energy substrates,^[2,3] due to its thermodynamic stability and kinetic inertness. One of the viable routes to overcome the thermodynamics is the synthesis of five-membered cyclic carbonates by cycloaddition of CO₂ with epoxides (Scheme 1).^[4,5]



Scheme 1: Cycloaddition of CO₂ with epoxides

To date, various catalysts have been developed for the synthesis of cyclic carbonates from CO₂ and epoxides, such as metal catalysts,^[6] salen complexes,^[7] organocatalysts^[8] and ionic liquids.^[9,10] However, most of the catalyst systems often require high energy input, such as high temperatures (>100 °C) and/or high CO₂ pressures, which made this process not so “sustainability”. Recently, great efforts have been focused on the development of more efficient and sustainable catalyst systems that can be carried out at atmosphere CO₂ pressure and ambient temperature conditions.

Specific Objectives

Therefore, the design of efficient, green and metal-free catalysts is still a great challenge toward effective CO₂ conversion under mild conditions. Herein, we demonstrated the use of DBU-based protic ionic liquids (DBUPIs) composed by protonic acid and multi-nucleophilic sites (Figure 1) for the conversion of atmospheric CO₂ with epoxides at mild conditions. The DBUPIs showed high activity in producing carbonates without the need for long reaction time and co-catalyst. Furthermore, the addition of suitable amount of water, a green solvent and hydrogen proton, had a notable effect on the proceeding of the cycloaddition reaction. Thus, this work provides an efficient way for the development of green, low-energy consumption and sustainable process of transformation of CO₂.

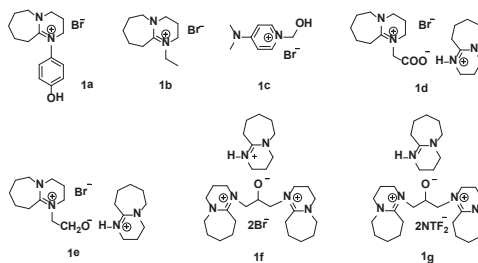


Figure 1: ILs used in this study.

Results and Discussion

We have been proved that Br⁻ is an excellent nucleophilic ion for the cycloaddition reaction in our previous work.^[10,11] Hence, Br⁻ is chosen as the model anion. At the initial of our study, we prepared a series of DBUPIs in one-step by acid-alkali neutralizing reaction (Figure 1). The reaction could be completed in minutes at room temperature. The structures of the ILs DBUPIs were analyzed by NMR study and SEM (Figure 2). Then, the catalytic activity of various DBUPIs was carried out with epichlorohydrin and a balloon of CO₂ in schlenk tube at 30 °C. The results were shown in Table 1.

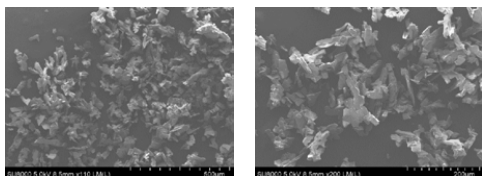


Figure 2: Photographs of **1f**

Table 1: Reaction of CO₂ with epichlorohydrin catalyzed by different ILs^a

Entry	Catalyst	Time (h)	Yield ^b (%)
1	[Bmim]Br	6	23
2	TBAB	6	25
3	1a	6	14
4	1b	6	26
5	1c	6	47
6	1d	6	70
7	1e	6	79
8	1f	6	92
9	1g	10	4
10	1f	2	58

^aReaction conditions: epichlorohydrin (0.5ml), ILs (6mol%), CO₂ (balloon), Temperature (30°C) ^bDetermined by ¹H NMR using 1,1,2,2-tetrachloroethane as an internal standard. TBAB=tetrabutylammonium bromide.

It was found that the common ILs [Bmim]Br (entry 1) had a very low activity in catalyzing the reactions under this room temperature and atmospheric CO₂ condition. As a co-catalyst that regularly used in this cycloaddition reaction, TBAB was investigated a 25% yield of chloropropene carbonate (CPC) (entry 2). Interestingly, DBU-based ILs without protonic acid (**1b**) was observed similar activity with [Bmim]Br and TBAB (entry 4 vs 2 vs 1), which indicated that cation may have little effect on the reaction. However, the DBU-based ILs **1a** with a phenolic hydroxyl group showed lower activity than common ILs (entry 3 vs 1, 2, 4), even though the phenolic hydroxyl group could activate epoxide in previous reports. The negative effects of phenolic hydroxyl group in this work may be induced

by the stereo-hindrance. The 4-dimethylaminopyridine (DMAP) based ILs (**1c**) with a hydroxyl group was also studied (entry 5). **1c** showed promising yield of CPC (47%) for the hydroxyl group activating epichlorohydrin. To our delight, all of the DBUPIs demonstrated much higher activity than **1c** (entries 6-8 vs 5). Possibly because that the protonic acid site of DBUPIs could activate epichlorohydrin more efficiently at room temperature compared with hydroxyl group, besides, as a nucleophilic anion, alkoxy anion might play the same role with Br⁻, which could increase the active site. Then, **1g** without Br⁻ was prepared to identify the catalytic activity of the alkoxy anion. But, the result shown in table 1 (entry 9) was only a 4% yield of CPC, which demonstrated that the alkoxy anion could not catalytic this reaction. For DBUPIs, **1f** with two Br⁻ exhibited much higher activity (92%) than the other two DBUPIs that have only one Br⁻ (entry 8 vs 6, 7). The result illustrated that nucleophilic Br⁻ was very important to promote the reaction. To our surprise, the catalytic activity of **1f** was up to 58% in the initial of the reaction (entry 10). So, **1f** was chosen as benchmark catalyst to investigate influence of reaction parameters.

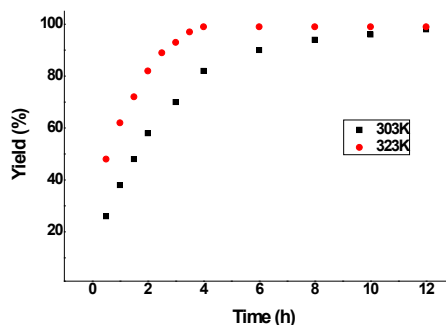


Figure 3: Effects of reaction time and temperature catalyzed by **1f**

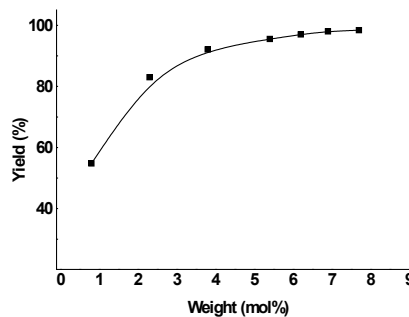
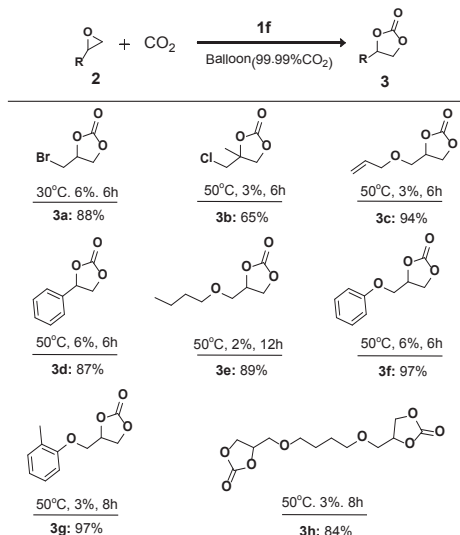


Figure 4: Effects of catalyst dose catalyzed by **1f**

It could be seen from figure 3 that the yield increased rapidly to 82% in the first 4 h at 30°C and then slowly increased to 99% in 12 h. The result indicated an obviously decrease of reaction rate. However, as

temperature was 50°C, the yield increased to 99% sharply in 4h without any obviously slow-growth stages. This might be caused by the increasing viscosity of CPC/1f reaction system with the producing of CPC during the reaction, thus affect the transferring effect of CO₂. The above mechanism was confirmed by the same behavior of the catalyst loading study shown in figure 4, which also had a slow-growth stage with the increasing of 1f.

Table 2: Reaction of CO₂ with substrates catalyzed by 1f



Subsequently, a range of different substituted terminal epoxides were examined under a balloon of CO₂ condition in the presence of 1f ILs. The results were summarized in Table 2. Epibromohydrin (2a) could afford the product 3a in a good yield of 88% at the optimal condition. Then, we found ILs 1f had a very low solubility in the other terminal epoxides at 30 °C. Taking into account of the industrial application, the loading of 1f was reduced, and the reaction temperature was increased to 50°C. However, the carbonate 3b showed much lower yield than 3c at the same condition, which probably due to the high stereo-hindrance effect. Furthermore, Styrene oxide 2d and glycidol derivatived 2e-2h were examined, and all of these epoxides generated the corresponding cyclic carbonates in excellent yields (3d -3h).

Then, 2f was chosen as an optimal terminal epoxide to study the cycling performance of DBUPIILs 1f, because 1f could be easily separated from 3f by adding water. Unexpectedly, when we tried to recycle 1f after the reaction, we found that the yield of 3f decreased obviously (See Figure 5) after it ran 4 times. This might be caused by the reaction of 1f with 2f.

In order to study the reaction mechanism, FT-IR spectra were employed to identify the possible

intermediate under atmospheric CO₂ during the reaction. As shown in Figure 5, there appeared a new band at 1795 cm⁻¹, after the reaction of CO₂ with 1f, which corresponded to the new asymmetric (C=O) vibration of the carbamate salt, presumably implying the activation of CO₂ by the alkoxy anion of 1f.

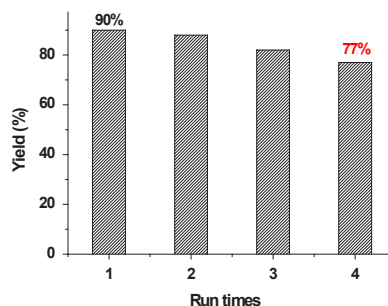


Figure 5: Reaction conditions: catalyst (6 mol%), CO₂ balloon, temperature (50°C).

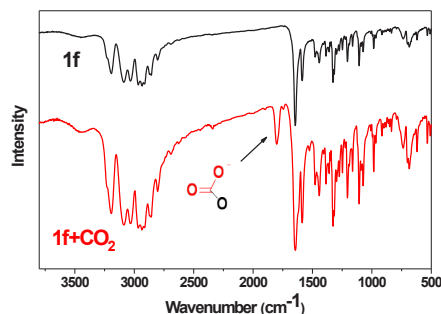
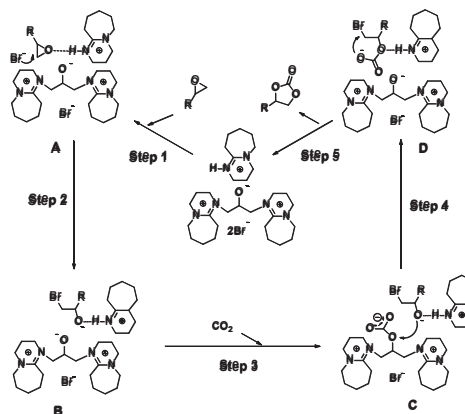


Figure 6: FT-IR spectra of the interaction between 1f and CO₂



Scheme 2: Proposed Mechanism for Cyclic Carbonates Synthesis Catalyzed by 1f

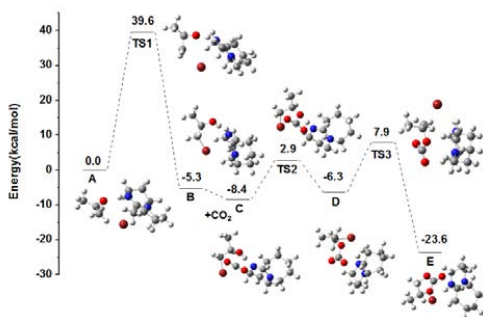


Figure 7: Potential energy surface profiles of **1f**-catalyzed process and the optimized geometries for the intermediates and transition states.

Based on these studies, we proposed a probable mechanism of **1f** catalyzed cycloaddition of CO₂ with epoxide. The detail was shown in Scheme 2. Subsequently, we investigated the mechanism of the **1f**-catalyzed process through DFT study. As shown in Scheme 2 and Figure 7, firstly, **1f** and **2f** interacted to form a complex **A**, and then epoxy ring-opening step made **A** convert into intermediate **B** via transition state TS1 with a barrier of 39.6 kcal/mol. A new complex **C** was formed, when CO₂ was added into the reaction system. Then, nucleophilic attack of the intermediate on the complex **C** produced the alkyl carbonate **D** through TS2 with a lower energy barrier of 2.9 kcal/mol. Finally, the cyclic carbonate was obtained by intramolecular ring-closure and the catalyst was regenerated with an energy barrier of 7.9 kcal/mol (TS3). The study illustrated that the epoxy ring-open step was the rate limiting step with the highest energy barrier of 39.6 kcal/mol (TS1).

Conclusions

In summary, DBU based protic ionic liquids with protonic acid and nucleophilic sites were successfully used as single and metal-free homogenous catalysts in the cycloaddition reaction of atmospheric CO₂ with epoxides at room temperature. DBUPIs showed excellent activity and good substrate compatibility. This work provides an excellent epoxy ring-open catalysts at room temperature conditions, which may be also promising in the other epoxy ring-open reactions.

Acknowledgements

This work is financially supported by National Key R&D Program of China (2017YFB0603301), The National Natural Science Fund for Distinguished Young Scholars (21425625) and Key Research Program of Frontier Sciences CAS (QYZDY-SSW-JSC011). The author is grateful to the support from the Department of Chemical and Biochemical Engineering, Technical University of Denmark.

References

1. X.B. Lu, D. J. Darensbourg, *Chem. Soc. Rev.* 41 (2012) 1462-1484.
2. T. Sakakura, J.-C. Choi, H. Yasuda, *Chem. Rev.* 107 (2007) 2365-2387.
3. P. Jessop, T. Ikariya, R. Noyori, *Chem. Rev.* 95 (1995) 259-272.
4. C. Bruckmeier, B. Rieger, W. A. Herrmann, F. E. Kühn, *Angew. Chem. Int. Ed.* 50 (2011) 8510-8537.
5. B. Schaffner, F. Schaffner, S. P. Verevkin, A. Börner, *Chem. Rev.* 110 (2010) 4554-4581.
6. J. W. Comerford, I. V. Ingram, M. North, X. Wu, *Green Chem.* 17 (2015) 1966-1987.
7. M. North, B.D. Wang, C. Young, *Energy Environ. Sci.* 4 (2011) 4163
8. J. Q. Wang, Y.G. Zhang, *ACS Catal.* 6 (2016) 4871-4876
9. B. H. Xu, J. Q. Wang, J. Sun, Y. Huang, J. P. Zhang, X. P. Zhang, S. J. Zhang, *Green Chem.*, 17 (2015) 108-122.
10. X. L. Meng, Y. Nie, J. Sun, W. G. Cheng, J. Q. Wang, H. Y. He, S. J. Zhang, *Green Chem.* 16 (2014) 2771-2778.
11. X. L. Meng, H. Y. He, Y. Nie, X. P. Zhang, S. J. Zhang, J. J. Wang, *ACS Sustainable Chem. Eng.*, 5 (2017) 3081-3086



Victor Buhl Møller

Phone: +45 4525 2923
E-mail: vibum@kt.dtu.dk

Supervisors: Søren Kiil
Kim Dam-Johansen
Sarah Maria Frankær, Hempel

PhD Study
Started: August 2014
To be completed: December 2017

Degradation and durability of acid resistant organic coatings

Abstract

Acid and abrasive resistant organic coatings have found their uses as cheap alternatives to ceramics and metal alloys as protective measures in the heavy duty industry. But there are still knowledge gaps when it comes to coating degradation in acidic solutions and the combined erosion/corrosion mechanism, which can occur when acidic exposure is combined with erosive forces. To fully map organic coating degradation, coatings are analyzed in diffusion cells, a pilot-scale agitated leaching reactor and in chemical immersion experiments. The dominant degradation mechanisms was found to be acid diffusion, while the chemical environment was found to have significant effect on coating erosion rates in the agitated leaching environment.

Introduction

Acid resistant organic coatings are cheap alternatives to ceramics, like acid bricks, and metal alloys, such as hastelloy. The application of organic coatings is limited in the mineral industry due to the higher risk that comes with using these organic coatings, compared to its inorganic counterparts [1]. Potential application areas include any surface that comes into contact with acidic substances such as pipes, batch reactors and surrounding structures. The research within degradation mechanisms of acid resistant coatings is scarce [2]–[5] and no research has been done on acidic exposure combined with mechanical degradation from erosion.

The purpose of the project is to convert the practical knowhow of current coating solutions into know-why by careful experimentation. This is achieved by mapping the degradation mechanisms of acid resistant organic coatings, using the agitated leaching reactor as a case study. The leaching reactor is a link in mineral extraction and purification process, where fine ($\approx 50 \mu\text{m}$) inorganic particles are mixed with warm ($75\text{--}80 \text{ }^\circ\text{C}$) sulfuric acid ($\text{pH}=1.0$). An environment that provides warm acidic solution combined with hard erosive particles.

Degradation mechanisms

Organic coating degradation mechanisms can be categorized into failure by chemical reaction, mechanical wear and physical diffusion [6]. All 3 mechanisms must be mapped to fully evaluate a coatings performance in acidic environments. These

degradation mechanisms can be observed through testing coatings using 3 different types of experiments.

Pilot scale experiments that combines erosion and acidic exposure, made to mimic the real life conditions that coatings are exposed to. Erosion is observed through reductions in coating film thickness.

Immersion experiments to observe the effects of chemical exposure, and support the pilot plant experiments by removing the erosive element from the equation.

Diffusion experiments determine permeation speeds of chemicals through a coating, and are used to determine diffusion constants and break-through times.

Pilot scale reactor and results

A pilot scale agitated leaching reactor was designed and constructed as part of the project; see Figure 1 for the completed set-up. All equipment is similarly made of acid resistant material to contain the harsh environment. Experiments were performed on a series of coatings, the example shown in Figure 2 is a polyurethane. The coating DFT was tested in the reactor using a water slurry ($\text{pH}=4.0$), and an acidic slurry containing sulfuric acid ($\text{pH}=1.0$), all at elevated temperatures of $75 \text{ }^\circ\text{C}$. Pure chemical immersion experiments were also carried out without the erosive slurry.

The difference between Reactor and immersion experiment, represents the film thickness loss due to slurry erosion. The large uncertainty in Reactor experiments is due to the erosion being inhomogeneous, and varying in intensity across the coating sample.



Figure 1: Pilot scale agitated leaching reactor set-up. Coating test panels can be inserted and removed at will inside the reactor

Figure 2 shows how the film thickness reduction is greater in acidic conditions for polyurethane. The same was true for all coatings tested, including a vinyl ester and an amine-cured novolac epoxy. A vinyl ester had the highest erosion resistance, with a 1000 μm film having a lifetime of approximately 5.9 years in agitated leaching tank conditions.

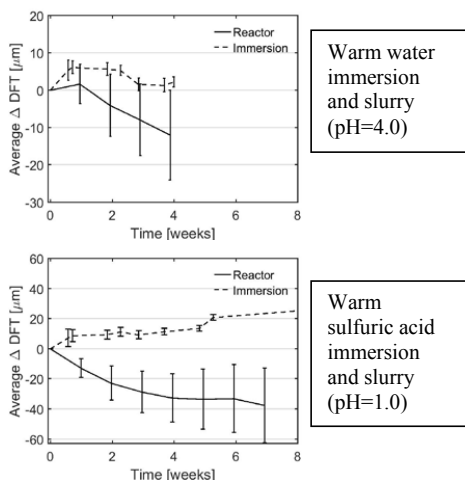


Figure 2: DFT change of polyurethane coating when exposed warm water or sulfuric acid (pH=1.0). Immersion represents pure chemical exposure, while Reactor represent chemical and erosive exposure, with 20 wt% erosives. Temperature of 75 °C and stirring intensity of 1000 rpm.

Diffusion cell setup and results

Ionic diffusion cells were designed and constructed to determine the penetration time of a given acid through the test coatings. It was composed of two chambers separated by a free coating film. A Receiver chamber containing demineralized water, and a Donor chamber containing the acid solution. pH change is monitored in the Receiver chamber using an ion sensitive probe. An example result is shown in Figure 3, where a series of polyurethane films were tested at elevated temperature (68 °C). The Donor chamber filled with pH 1.0 sulfuric acid.

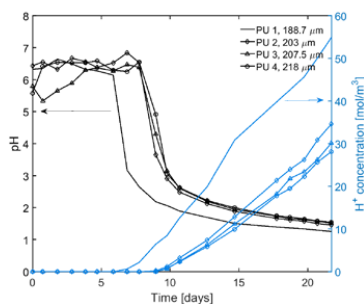


Figure 3: H^+ concentration and pH change of water in the Receiver chamber as caused by sulfuric acid diffusion through polyurethane films at 68 °C.

The data collected using the diffusion cells was used to predict acid breakthrough times of thicker films. Which for a 1000 μm thick polyurethane coating would be 180 days.

Conclusions

Chemical environment can have a significant impact on organic coating erosion rates. For the coatings tested, the main cause of failure in an agitated leaching reactor would be due to acid diffusion through the barrier film.

Acknowledgement

This work is part of the project 'Minerals and Cement Process Technology - MiCeTech' funded by Innovation Fund Denmark, FLSmidth A/S, Hempel A/S, and Technical University of Denmark (DTU).

References

1. G. C. K. Lawrence, Australas. Corros. Eng. 4 (19) (1975) 25-28.
2. C. H. Hare, J. Prot. Coatings Linings 2 (17) (2000) 58-64.
3. C. H. Hare, J. Prot. Coatings Linings 12 (16) (1999) 17-25.
4. C. H. Hare, J. Prot. Coatings Linings 1 (17) (2000) 63-75.
5. H. Hojo, K. Tsuda, M. Kubouchi, and D.S. Kim, Met. Mater 6 (4) (1998) 1191-1197.
6. V. B. Møller, S. M. Frankær, K. Dam-Johansen, and S. Kiil, J. Coat. Tech. Res 14 (2) (2017) 279-306.

**Frederico Montes**

Phone: +45 4525 6194
E-mail: fmon@kt.dtu.dk

Supervisors: Gürkan Sin
Krist Gernaey

PhD Study
Started: April 2016
To be completed: April 2019

Model library development for pharmaceutical process design and simulation

Abstract

Pharmaceutical industry faces several challenges and barriers when implementing new or improving current pharmaceutical processes. High operational costs and low productivity, strict regulations and competition from generics manufacturers are some of the drawbacks in the referred industry. The objective of this work is to collect, develop and integrate a library of reliable pharmaceutical models that can simulate and predict the behavior of the process, even when under uncertainty. To this end, Ibuprofen synthesis was used as case study, for the development of different reaction models and crystallization units. Local sensitivity analysis is also presented at the level of the crystallizer.

Introduction

Although modern pharmaceutical processes study the possibility to operate in continuous, batch processes and “feed-react-empty” concept will always be associated to traditional methods [1]. The batch production brings flexibility to the process, and is easier to adapt to the market needs. However, there is a considerable number of drawbacks of the traditional methods: low understanding, lack of modeling and no optimization of energy/waste production [2]. Although that the Food and Drug Administration (FDA) and European Medicines Agency (EMA) urged and imposed that pharmaceutical companies should emphasize in the process knowledge and integration, there is a lack of tools for process evaluation and simulation. The need of these tools is of even greater importance when creating new processes: there is little patent life-time since the patented API is approved until its patent expires. Within this time, a full operating process needs to be built in order to recover the investment used in the past years. Within so few time, it is no wonder that little knowledge is acquired from other process designs/configurations. Process system engineering (PSE) tools and methods are a great way to study and analyze the process economics, deviations on the product quality requirements, and process optimization under constraints and uncertainty [3]. For both continuous and discontinuous pharmaceutical processes however, there is a lack of such tools, when comparing with other chemical engineering processes and fields (petrochemicals, energy production, fine chemistry...).

Also, there is a lack of trustworthy and reliable dynamic modeling tools for this specific field that include control, monitoring and batch /continuous integration and configuration. Motivated by the new Process Analytical Technology (PAT) [4] trend, a whole new look is given to pharmaceutical industry, and modelling/simulation of this chemical engineering area is blooming.

Specific objectives

The main objective of the developed model library is to be able to simulate, control and optimize pharmaceutical processes under uncertainty, no matter which kind of operation they are being operated: continuous, batch, cyclic-continuous.

The referred library is converted into Matlab/Simulink language, and it includes:

- Kinetic models, specific for certain pharmaceutical APIs
- Operation models, which refer to operation models such as separations (crystallization, Liquid-Liquid separation, distillation), reactions, and transport models.
- Control and sensor models,

Furthermore, monitoring and control strategies will be implemented and analyzed, based on the results of intensive uncertainty and sensitivity analysis performed to chosen integrated processes. This is extremely important for specific sensitive processes, such as cooling crystallization of solvent-adding crystallization.

Case Study – Ibuprofen synthesis

Ibuprofen (1-(4-isobutylphenyl)ethanol) is a world known nonsteroidal anti-inflammatory drug. It was first discovered and synthesized by Boots Company in 1960 by performing 6 reactions steps with isobutylbenzene as the main reagent. Nowadays, the Hoechst path (or green path) [5] is more common, having only three reaction steps: Friedel-Crafts acylation, hydrogenation and carboxylation. The whole process involves liquid, gaseous and solid phases, and many separation units. It has been converted into the model library, as figure.1 shows.

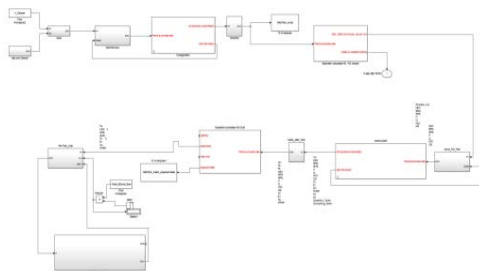


Figure 1: Model of the Ibuprofen synthesis trough Hoescht path. The three reactors are included, as well as a distillation column, a 2-dimension crystallizer model, a decanter and tanks [6,7].

The current library allows the dynamic tracking of the different synthesis steps, and through uncertainty input and statistical methods as Bootstraps and Monte Carlo, the design space of the final crystal population can be studied [8] (figure.2) . Additionally, this case study is the example of an integration of batch and continuous processes, achieving the cyclic-steady-state harmony. (figure.3)

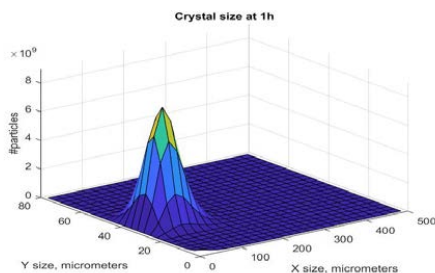


Figure 2: Crystal size distribution in two dimensions growth, of Ibuprofen crystal in an ethanol/water mixture.

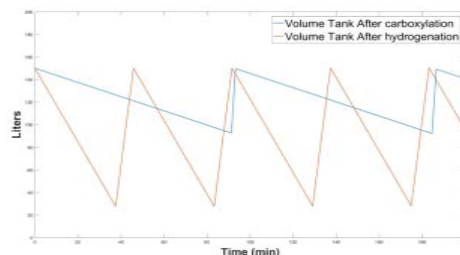


Figure 3: Cyclic-steady-state achieved in the liquid level of the tanks existent after and before the carboxylation reaction.

Conclusion – Future work

The current state of the model library allows the integration of different reliable dynamic process models for reactions, separations and content holders (tanks). Both continuous and batch processes are included, and operating with both in the same flowsheet model is possible and verified. Further work will include control strategies and algorithms for proposed case studies, and in collaboration with industrial partners.

Acknowledgments

This work has received funding from the European Union's Horizon 2020 research and innovation programme under the Marie Skłodowska-Curie grant agreement no.675251.

References

1. C. Jiménez-González, P. Poechlauer, Q. B. Broxterman, B.-S. Yang, D. am Ende, J. Baird, C. Bertsch, R. E. Hannah, P.Dell'Orco, H. Noorman, S. Yee, R. Reintjens, A. Wells, V. Massonneau, and J. Manley, *Org. Process Res. Dev.* 15(4), (2011), 900-911.
2. K. Plumb, *Chem. Eng. Res. Des.*, 83 (6), (2005), 730-738.
3. K. Gernaey, A. Cervera-Padrel, J. Woodley, *Comp. and Chem. Engineering* (42), 2012, 15-29
4. FDA Process Analytical Tools guidance notes, 2004
5. V. Elango, M. Murphy, B.L. Smith, K.G., Davenport, G.N. Mott, E.G. Zey , G.L. Moss, US Patents 4.981.995, 1991
6. S.P. Mathew, M.V. Rajasekheram, R.V. Chaudhari, *Catalysis Today* (49), 1999, 49-56
7. N. Thakar, R. Berger, F. Kapteijn, J. Moulijn, *Chemical Engineering Science* (62), 2007, 5322-5329
8. F. Montes, K. Gernaey, G. Sin, ESCAPE 27, Barcelona, 2017



Caroline Mosbech

Phone: +45 4525 6892
E-mail: carmo@kt.dtu.dk

Supervisors: Anne S. Meyer
Jane Wittrup Agger

PhD Study
Started: May 2016
To be completed: May 2019

Enzymatic cleavage of lignin-carbohydrate complexes (LCCs)

Abstract

Lignin is covalently linked to hemicellulose in lignocellulosic biomass creating lignin-carbohydrate complexes (LCCs). These complexes create challenges when processing lignocellulosic biomass because even after exhaustive polysaccharide degradation the lignin fraction still contains carbohydrates. The aim of this PhD project is to study the enzymology and kinetics of specific enzymes called glucuronoyl esterases proposed to enable targeted cleavage of LCCs and thereby achieve more optimal utilization of both the lignin and the carbohydrate process streams.

Introduction

Lignocellulosic biomass is one of the most important raw materials for energy and chemicals [1]. Polysaccharides and lignin in the plant cell wall are covalently linked forming lignin-carbohydrate complexes (LCC). LCCs are present in low amounts but they play an important role in selective separation and isolation of pure lignin and carbohydrate from lignocellulosic material. [2].

The main types of LCCs found in wood are reported to be phenyl glucoside bonds, benzyl ethers and esters. The main focus in this PhD is the ester linkages present in hardwoods between 4-O-methyl-D-glucuronic acid (MeGlcA) residues in glucuronoxylan and hydroxyl groups of lignin alcohols [2] [4] (See Figure 1). This ester linkage is suggested to be hydrolysed by glucuronoyl esterases (GE) (EC 3.1.1.-) in nature. GEs are part of a fairly new family of enzymes assigned to a class of carbohydrate esterases classified in the Carbohydrate-

Active Enzymes database (CAZy) as the CE15 family. Today the CE15 family contains 182 entries of which only 8 have been characterized using a series of synthetic model substrates and 2 enzymes have their crystal structures determined [5]. The high complexity of the lignocellulosic material and the low concentration of LCCs have made it difficult to demonstrate catalytic activity of GEs on natural substrate and the exact biological activity is still uncertain [1] [6].

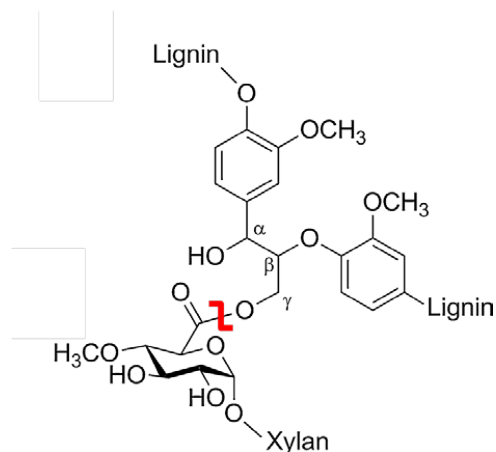


Figure 1: Representative structure of LCC ester linkage connecting lignin alcohols and 4-O-methyl glucuronic acid residues in xylans [6] Enzymatic cleavage site is indicated by red bar.

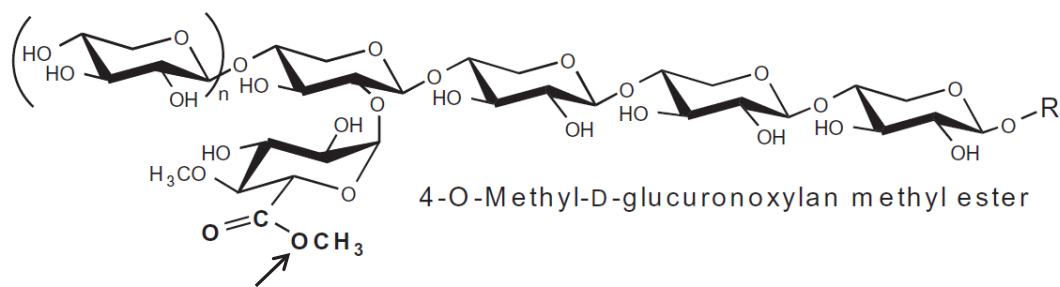


Figure 2: Methyl ester from extracted glucuronoxylan serving as substrate for GEs. Site of attack marked with arrow. [7]

First evidence of GE catalytic activity on polymeric substrate was published in 2015 using methyl ester of glucuronoxylan (See Figure 2). The methyl ester does not occur in nature, but imitates the natural substrate present in plant cell walls. Synthetic substrates mimicking the LCC closer are still not available but essential in outlining the function of GEs [7]. Two attempts to demonstrate activity on natural substrate have been published. d’Errico et al studied the effect of GE on natural corn fiber degradation suggesting improved yield of fermentable sugars with addition of esterase to commercial cellulase and hemicellulase preparations, [8]. Bååth et al. examined reduction in molecular mass of extracted LCC from spruce and birch by size exclusion chromatography [9].

Bioinformatic tools have been demonstrated to be very powerful in enzyme discovery. Recently 1024 new putative GE sequences was identified and grouped based on DNA sequences. A high number of GEs were found in genomes originating from lignocellulose degrading organisms such as white rot and coprophillic fungi, indicating applicability in lignocellulose conversion [10]. However the natural substrate sufficient to examine the correlation between function and grouping is still not available. Putative GE sequences identified in the bioinformatic study will be used in this PhD project to express and characterize novel glucuronoyl esterases.

Objectives

The PhD project is based on the hypothesis that LCC ester linkages are at least partly responsible for the carbohydrate contamination in extensively “polysaccharide-hydrolyzed” lignin fractions and that cleaving the ester linkages will have a positive effect on the overall conversion of biomass.

The aim of the project is to outline the kinetics of CE15 glucuronoyl esterases, on soluble and complex, genuine LCC substrates. Several approaches will be followed including establishing a sufficient analytical method to assess activity of glucuronoyl esterases. CE15 from the white rot fungi *Cerrena unicolor* has been expressed in

Pichia pastoris and demonstrated to be active using the very simple model substrate Benzyl D-glucuronic acid ester (BnzGlcA). Thereby creating a solid ground for demonstration of activity and benchmarking reactions on natural substrate and for further experimental work.

Conclusion

It is hypothesized that GE is a widespread enzyme family in nature that has a natural biological function of targeting ester linkages in LCCs and thereby potentially a potent biocatalysts for efficient enzymatic cleavage of LCCs. By targeted cleavage of LCCs it is presumed that higher purity of lignin can be obtained and that lignin can be utilized, as the only naturally occurring aromatic polymer, as a high value product.

References

1. X. Du, G. Gellerstedt, and J. Li, *Plant J.*, (74), (2013) 328–338.
2. M. Balakshin, E. Capanema, H. Gracz, H. min Chang, and H. Jameel, *Planta*,(6) (2011) 1097–1110
3. T. Q. Yuan, S. N. Sun, F. Xu, and R. C. Sun, *J. Agric. Food Chem.*(19) (2011) 10604–10614.
4. P. Biely, *Appl. Environ. Microbiol.*,(24) (2016) 7014–7018. .
5. V. Lombard, H. Golaconda Ramulu, E. Drula, P. M. Coutinho, and B. Henrissat, *Nucleic Acids Res.* (42) (2014) 490–495..
6. C. d’Errico, J. O. Jørgensen, K. B. R. M. Krogh, N. Spodsberg, R. Madsen, and R. N. Monrad, *Biotechnol. Bioeng.*(5)(2015) 914–922.
7. P. Biely, A. Malovíková, I. Uhliaríková, X. L. Li, and D. W. S. Wong, *FEBS Lett.*, (18) (2015) 2334–2339.
8. C. d’Errico et al., *J. Biotechnol.*, (219) (2016) 117–123.
9. J. Arnlíng Bååth, N. Giummarella, S. Klaubauf, M. Lawoko, and L. Olsson, *FEBS Lett.* (590) (2016) 2611–2618.
10. J. W. Agger, P. K. Busk, B. Pilgaard, A. S. Meyer, and L. Lange, *Front. Microbiol.*, (8) (2017) 1–8.



Phone:
E-mail:

Line Munk
+45 4525 2979
lmun@kt.dtu.dk

Supervisors:

Anne S. Meyer

PhD Study

Started:

October 2012

To be completed:

December 2017

Assessment of laccase catalyzed lignin modifications by Py-GC/MS analysis

Abstract

Lignin consists of a three dimensional mesh of aromatic structures and is currently an underexploited resource in biorefining of plant biomass. Laccases (EC 1.10.3.2) catalyze oxidation of phenolic compounds using O_2 as electron acceptor, but they have also been suggested to induce bond cleavage between phenolic units in lignin in the presence of mediators acting as electron vehicles. This article outlines plausible events occurring upon lignin oxidation by laccases and how the different outcomes can be assessed by means of pyrolysis gas chromatography/mass spectrometry (py-GC/MS).

Introduction

Lignin is a very complex biopolymer, which is found in almost every type of biomass. It fills the spaces in the cell walls between cellulose, hemi-cellulose, and pectin polymers and contributes to the protection of the plant against the surrounding environment. Unlike other biopolymers in lignocellulosic material, lignin is comprised by aromatic, conjugated units and has a very irregular structure [1].

Functionalization of lignin by surface modifications can be obtained with assistance of oxidative enzymes. Treatments of lignin with laccase, activate lignin by oxidizing phenolic subunits in lignin to generate a radical-rich reactive polymer in which different events can occur [2]

in numerous fungi, plants, and bacteria [4]. Laccases catalyze the oxidation of phenolic substrates with the concomitant reduction of O_2 to two molecules of H_2O (Fig 1). The fact that laccases use O_2 as the final electron acceptor rather than H_2O_2 , differentiate them from other lignin modifying enzymes and make them more qualified in potential industrial applications with regard to economy and sustainability.

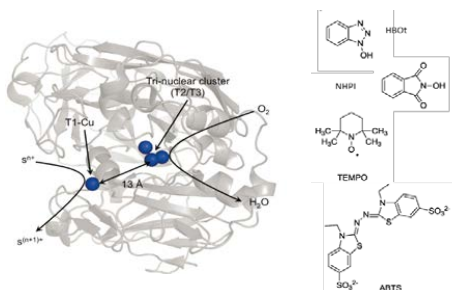


Figure 1: (left) Structure of Laccase from *Trametes Versicolor* [3], (right) Synthetic mediators used in combination with laccase.

Laccases (EC 1.10.3.2) belong to the multicopper oxidase family, a group of enzymes that is widespread

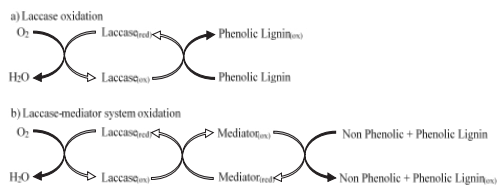


Figure 2: (a) oxidation range for laccase, (b) oxidation range for laccase-mediator systems.

As illustrated in figure 2, use of laccase-mediator systems, may expand the oxidation ability of laccase to include oxidation of aliphatic alcohols in the lignin subunits by enabling oxidation through mechanisms not achievable for the laccase alone. A mediator requires a high stability both in its reduced and oxidized (radical) form [4]. A selection of commonly used mediators is shown in figure 1 (right).

Specific objectives

This PhD project is supported by the Danish National Advanced Technology Foundation via the Technology Platform “Biomass for the 21st century -

B21st⁷. The objective is to elucidate mechanisms of laccase action on lignin, to provide a better understanding of these enzymes. Elucidation of their putative role in lignin modification, may clarify how they can assist in a more sustainable conversion of ligno-cellulosic biomass.

Modification of lignin

Upon studying the current literature within the field of laccase catalysed lignin modification, it has become evident that different events are likely to occur after formation of radical subunits in lignin has been facilitated by laccase catalysis (Fig. 3):

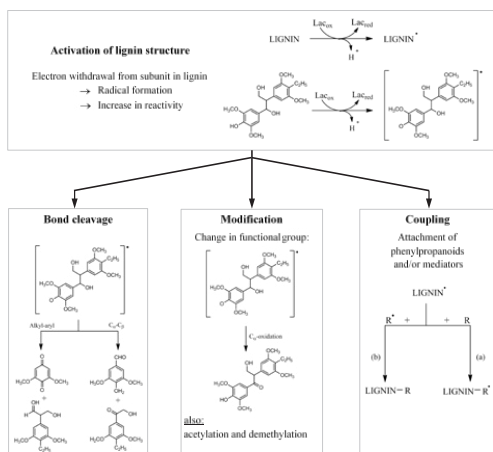


Figure 3: Plausible occurring events in lignin upon laccase oxidation (activation). Modified from [2].

- **Modification**

Activated lignin subunits can be stabilized by delocalization of electrons to areas in the conjugated system where the structure is most stable. This may lead to modifications seen as changes in functional groups.

- **Bond cleavage**

Activated lignin subunits may not be stabilized by above mentioned modifications, but instead result in bond cleavage. Consecutive oxidation of lignin subunits may lead to defragmentation of the lignin.

- **Polymerization**

If an activated lignin subunit react with other aromatic derivatives and initiate a radical chain reaction, it will result in polymerization.

- **Grafting**

If an activated lignin subunit react with other radicals, generated by laccase, it results in endwise coupling, known as grafting [2].

A full comprehension of how to govern the different events to control the outcome has not yet been achieved.

Assessment of lignin modification by Py-GC/MS

The majority of native lignin is insoluble, which renders the analysis of lignin challenging. By use of py-GC/MS, solid material can be pyrolysed to lignin fragments, which are separated and identified. In the

pyrogram of organosolv lignin (Fig 4.), the peaks represent different lignin residues, each being identified and grouped according to syringyl (S) or guaiacyl (G) origin. The relative abundance of all identified residues provides the basis for a semi-quantitative evaluation of potential changes after laccase or laccase-mediator treatment.

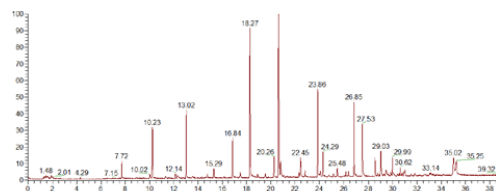


Figure 4: Pyrogram of organosolv lignin. Peaks represent different lignin residues originating from the lignin polymer

Lignin-rich substrates treated with laccases in combination with mediators, as those illustrated in fig. 1, may result in changes in the relative occurrence of individual lignin residues. Grouping of the lignin pyrolysis fragments into aliphatic alkenes, alcohols and carbonyls can then reveal shifts towards a higher occurrence of oxidised lignin fragments after laccase-mediator treatments. Lignin modification facilitated by laccase oxidation, may also be correlated to changes in the distribution of S and G residues, where alterations has been observed after laccase treatments. Finally, it is possible to detect grafting of molecules by py-GC/MS, if they are distinguishable from lignin derivatives. Thus, py-GC/MS provides a method to evaluate lignin types that can be functionalized with molecules applicable to grafting and final function [6].

Conclusion

Laccases oxidation facilitate different events in the lignin structure, which affect the outcome of the reaction. Laccases-mediator treatments have been demonstrated to modify functional groups in lignin, presumably on the lignin surface, towards a more oxidized state. In addition, laccases may be capable of facilitating grafting onto lignin. Assessment of such changes is achieved well by py-GC/MS analysis.

References

1. R. Vanholme, B. Demedts, K. Morreel, J. Ralph, W. Boerjan. *Plant Physiol.* 153(3) (2010) 895–905.
2. L. Munk, A. Sitarz, D. C. Kalyani, J. D. Mikkelsen, A. S. Meyer. *Biotechnol Adv.* 33(1) (2015) 13-24.
3. D. Chakraborty, S. C. Barton. *Journal of the Electrochemical Society* 158(4) (2011) 440-47.
4. A. Virk, *Biotechnol Prog.* 28 (2011) 21-32.
5. S. Coseri. *Catalysis Reviews.* 51(2) (2009) 218-92.
6. L. Munk, A.M. Punt, M.A. Kabel, and A.S. Meyer. *RSC Advances* 7(6) (2017) 3359-68.



Gisela Nadal Rey
Phone: +45 4525 2993
E-mail: gnre@kt.dtu.dk

Supervisors: Krist V. Gernaey
Anna Eliasson Lantz
Sjef Cornelissen, Novozymes A/S

PhD Study
Started: March 2017
To be completed: February 2020

Physiological characterization of the impact of gradients on fermentation processes

Abstract

Heterogeneous conditions in large-scale fermentation processes can lead to suboptimal performance that negatively affects process yields, productivity and product quality. In order to improve scale-up of fermentation processes and prevent the negative influence of heterogeneous fermentation environments on productivity, a thorough characterization of gradients in different scales should be performed from a physiological point of view. A strategy to investigate the practical occurrence and the physiological impact of gradients on pilot- and production-scale fermentation processes is presented. Once this has been executed and validated, improvements of the current scale-up approach can be defined. Unlike traditional scale-up strategies, the physiology of the microorganisms will be considered as a relevant variable for the development and optimization of fermentation processes.

Introduction

Large-scale fermentation processes are widely used in industry for the production of chemicals, proteins (e.g. enzymes) and biomass, amongst others. Unlike bench-scale fermentations, industrial bioprocesses are heterogeneous because of limitations in the mixing and in the mass transfer capabilities of the system [1]. Thus, gradients in relevant reactor parameters such as C-source and nutrient concentrations, pH, dissolved oxygen (DO) and dissolved carbon dioxide are likely to occur in large scale [2]. As cells transition through the various zones of the reactor, they are constantly exposed to oscillatory conditions. Such oscillations can affect cell physiology at several levels. For instance, inducing stress responses, reducing yields, productivity and product quality and causing changes in the cell metabolism and in the physiological properties of the cell [3], [4], ultimately affecting process economics.

Bacillus licheniformis as model organism

Bacillus licheniformis is a non-pathogenic Gram-positive facultative anaerobe mainly used for the production of proteases and amylases due to its capability to secrete large amounts of enzymes over a short period of time into the fermentation broth.

B. licheniformis has a rapid and varied metabolism, characterized by the excretion of a wide array of overflow metabolites [5] when the carbon flow through aerobic routes exceeds the respiratory capacity. The

main by-products are acetate, ethanol, lactate, glycerol, acetoin and, under oxygen-limiting circumstances, small amounts of 2,3-butanediol. While lactate, ethanol and glycerol are produced for cofactor regeneration, acetate directly yields to energy formation. Acetoin and 2,3-butanediol are produced from acetate in order to avoid over-acidification of the fermentation broth and regulate the intracellular pH. The study of the production of these overflow metabolites as metabolic markers formed under suboptimal conditions can facilitate the understanding and quantification of heterogeneities.

In short, *B. licheniformis*' industrial relevance and similarity with the well-studied model organism *Bacillus subtilis*, together with its rapid and varied metabolism which enhances the occurrence of gradients and facilitates their characterization, make it an attractive organism to investigate the physiological effects of gradients on industrial fermentation processes.

Use of Computational Fluid Dynamics (CFD) for the design of scale-down experiments

In order to mimic and improve the comprehension of the industrial fermentation environment, the use of scale-down simulators is recommended. Although there is an extended variety of configurations, two main groups of scale-down systems are distinguished [6] (Figure 1): the pulsed addition systems and the multi-compartment systems. The first are usually performed in a single vessel. After the pulsed addition of a disturbing

agent (e.g. glucose, pH controlling agent), samples are taken rapidly. The main goal of this setup is to study the impact of process disturbances on metabolism and to perform metabolic flux analysis studies. On the other hand, multi-compartment systems aim at resembling the real industrial situation. This can be achieved by placing multiple reactors in series, operating at such different conditions that overall an industrial fermenter is represented.

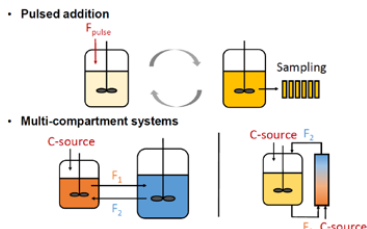


Figure 1: Representation of different types of scale-down simulators.

Until now scale-down experiments have been designed based on intuition or correlations, being an useful tool for metabolic analysis but poorly resembling the industrial fermentation environment [7]. Nevertheless, with the use of Computational Fluid Dynamics (CFD) simulations, detailed information regarding the fermentation environment can be generated and therefore scale-down experiments could be rationally designed. This could be the first step towards a new generation of scale-down systems that can adequately resemble industrial fermentation processes.

Specific Objectives

The aim of this project is to get a better understanding of the practical occurrence and physiological impact of gradients on industrial fermentation processes.

The project will be conducted with the following objectives:

- To identify and study metabolic markers formed under suboptimal conditions, which are for example created due to the formation of gradients in bioreactors.
- To elaborate experimental protocols to rapidly characterize the effect of gradients on the physiology of the host.
- To validate the CFD simulation results currently generated at DTU for bioreactors at different scales.
- To evaluate the current scale-up methodology and define improvements according to the results of this study.

Approach

The study will include the following work packages:

1. Characterization of *Bacillus licheniformis* strain. Quantification of its basic physiological parameters and build-up of a kinetic model.
2. Design of scale-down experiments using Computational Fluid Dynamics (CFD). To start

with, both glucose and oxygen gradients will be studied. After simulating the flow pattern, the glucose and oxygen distributions and the kinetics of the organism, an heterogeneous profile of concentrations of substrate and (by-)products at several time points can be obtained, being the starting point for the scale-down experiments.

3. Performance of scale-down experiments. The configuration that will be used will be based on the results of the CFD simulations.
4. Performance of fermentations at larger scales. Fermentations at larger scales will be run to validate and exploit the results obtained with the scale-down experiments. Spatially-distributed sensors will be used to monitor the process parameters.

By following the above-mentioned steps, an improved comprehension of how the microorganism's physiology is affected by gradients in pilot- and production-scale fermentation processes can be achieved and further improvements of the current scale-up methodology can be defined.

Acknowledgments

This project receives financial support from the Technical University of Denmark and Novozymes A/S.

References

1. G. Larsson, M. Törnkvist, E. Ståhl Wernersson, C. Trägårdh, H. Noorman, and S. O. Enfors, "Substrate gradients in bioreactors: Origin and consequences," *Bioprocess Eng.*, vol. 14, no. 6, pp. 281–289, 1996.
2. A. R. Lara, E. Galindo, O. T. Ramírez, and L. a Palomares, "Living with heterogeneities in bioreactors: understanding the effects of environmental gradients on cells," *Mol. Biotechnol.*, vol. 34, no. 3, pp. 355–381, 2006.
3. S. O. Enfors *et al.*, "Physiological responses to mixing in large scale bioreactors," *J. Biotechnol.*, vol. 85, no. 2, pp. 175–185, 2001.
4. F. Bylund, E. Collet, S. O. Enfors, and G. Larsson, "Substrate gradient formation in the large-scale bioreactor lowers cell yield and increases by-product formation," *Bioprocess Eng.*, vol. 18, no. 3, pp. 171–180, 1998.
5. H. C. Ramos, T. Hoffmann, M. Marino, E. Presecan-siedel, O. Dreesen, and P. Glaser, "Fermentative Metabolism of *Bacillus subtilis*: Physiology and Regulation of Fermentative Metabolism of *Bacillus subtilis*: Physiology and Regulation of Gene Expression," *J. Bacteriol.*, vol. 182, no. 11, pp. 3072–3080, 2000.
6. P. Neubauer and S. Junne, "Scale-down simulators for metabolic analysis of large-scale bioprocesses," *Curr. Opin. Biotechnol.*, vol. 21, no. 1, pp. 114–121, 2010.
7. H. J. Noorman and J. J. Heijnen, "Biochemical Engineering's Grand Adventure," *Chem. Eng. Sci.*, pp. 1–17, 2017.

**Mohammadhadi Nakhaei**

Phone: +45 4525 2853
E-mail: mnak@kt.dtu.dk

Supervisors: Kim Dam-Johansen
Peter Glarborg
Hao Wu
Lars Skaarup Jensen, FLSmidth
Damien Grévain, FLSmidth

PhD Study
Started: May 2015
To be completed: May 2018

Multiphase flow and fuel conversion in cement calciner

Abstract

The main focus of this PhD project is the development of a Computational Fluid Dynamics (CFD) model for simulation of cement calciners firing fossil fuels and/or Refuse Derived Fuels (RDF). Unlike the fossil fuels, RDFs are composed of different waste materials with diverse physical and chemical properties. In order to develop a CFD model that can describe the aerodynamic and conversion of RDF in cement calciners, advanced characterizations of the physical, aerodynamic, chemical, and combustion properties of RDF are carried out. The developed CFD model are compared and validated with pilot-scale and full-scale measurements. The validated CFD model will be applied to evaluate the influences of fuel properties and operating conditions on calciner performance, and to optimize the operation and design of cement calciners.

Introduction

Driven by the demand of reducing fuel cost and CO₂ emission in cement production, there are growing interests in utilizing alternative fuels, such as Refuse Derived Fuels (RDF), in cement plant calciners. Unlike the conventional calciner fuels such as coal and petroleum coke, the characteristics of RDF are very different in physical, chemical, and combustion aspects. They also have large variations depending on their source and processing technology. In order to design and operate RDF-based calciners with high fuel conversion and low pollutant emissions, in-depth knowledge on the multiphase flows and conversion of RDF under calciner conditions is required. This could be obtained by conducting experiments and developing cost-efficient modelling tools, such as Computational Fluid Dynamics (CFD) models. The model could be used to support the process design, trouble shooting, and performance optimization in industrial calciners.

Objectives

The main objective of this project is to achieve new and improved knowledge about aerodynamics of gas-solid flows, calcination, and conversion of fossil fuels and RDFs (i.e. drying, pyrolysis, and char oxidation) in cement plant calciners. A CFD model will be developed and validated for this purpose. This CFD model can support the design and operation of RDF-fired cement plant calciners to achieve a high fuel conversion and low pollutant emissions.

As an important part of the CFD model, physical information of RDF particles as well as validated sub-models for aerodynamics and conversion of these particles should be implemented in the model. Hence, a framework for characterization of RDF particles is developed.

Current results and future work

RDF characterization

RDF is produced from combustible fraction of municipal solid waste or industrial waste using various techniques such as sorting, screening, shredding, and so on [1]. Despite the production processes help RDF to become more uniform in content compared to its original source, there are still a large number of material types in RDF which makes it a heterogeneous fuel. Aerodynamic characterization of different RDF samples has been conducted using a wind sieve. This wind sieve is composed of a vertical hollow tube. Air passes through the tube with a predetermined bulk velocity. The particles are fed from the middle of the tube and are separated into light and heavy fractions based on their aerodynamic behavior inside the wind sieve. Through the wind sieve experiment, a sample of RDF particles is categorized into different groups based on particles terminal velocity. The corresponding mass fraction of each separated group from the wind sieve experiment of a RDF sample is reported in Fig. 1 (left). After the wind sieve test, the physical properties of a sample of individual particles from each group (i.e. weight, size,

and shape) are estimated by weight measurements and taking 2D pictures using a photographing platform. This platform can be seen in Fig. 1 (right).

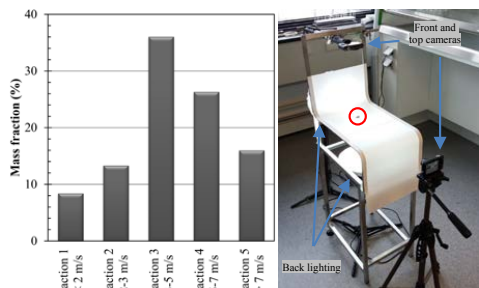


Figure 1: Results of the wind sieve experiment for a RDF sample (left) and the photographing platform for physical characterization (right).

Apart from the physical characterization, the conversion characterization of plastic and biomass particles from RDF samples is studied experimentally using a single particle combustor (SPC). A 1D mathematical model is derived for plastic conversion and the accuracy of the model is tested against the SPC experiments. The conversion of RDF plastic particles in SPC as well as the model predictions are presented in Fig. 2. The plastic conversion model is simplified and will be used as a sub-model in the CFD model.

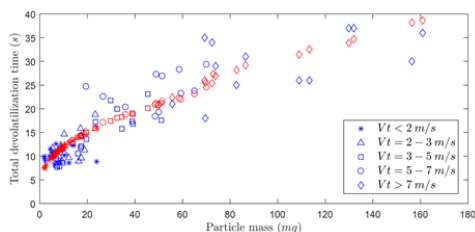


Figure 2: The conversion of a sample of plastic particles in SPC (blue symbols) as well as predictions from the 1D model (red symbols) at reactor condition of 900°C and 0-0.5 O₂ vol. %.

Pilot-scale and full-scale measurements

It is in plan that full-scale measurements will be carried out for a RDF-fired cement calciner. Probing measurements can be conducted to reveal the gas temperature and species concentration in the calciner. Also worthy to mention that there are available measurement data for a fossil fuel-fired calciner. The data from these measurements will be used for validating the CFD model under reacting conditions. The CFD solver is also validated in cold conditions for a pilot-scale calciner at FLSmidth Research Centre Dania.

CFD simulations

CFD simulation of a full-scale coal-fired calciner is carried out using Barracuda virtual reactor software.

Full-scale measurements (i.e. gas temperature and species concentration) at different cross-sections of the calciner are carried out previously. Comparison of CFD predictions and the measurements for the gas temperature are presented in Fig. 3 for two cross-sections of the calciner.

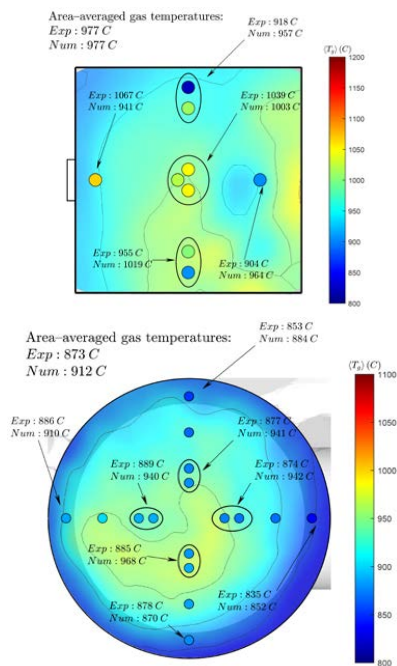


Figure 3: A comparison of the gas temperatures from CFD simulation and the measurements at two cross-sections in the riser (top) and in the bottom calciner (bottom)

Once the CFD model is validated for both coal-fired and RDF-fired calciners, parametric studies will be performed in the following areas:

- Feed positions and flow rate of inlets for raw meal, fuel, and tertiary air.
- RDF properties such as heating value, moisture content, size and shape distribution, etc.
- Scaling of the calciner.

The most important target functions in these parametric studies are fuel burnout and NO_x reduction capability of the calciner.

Acknowledgement

This work is part of the research platform ‘Minerals and Cement Process Technology – MiCeTech’ funded by Innovation Fund Denmark, FLSmidth A/S, Hempel A/S, and DTU.

References

1. D. Lechtenberg, Alternative Fuels and Raw Materials Handbook for the Cement and Lime Industry, Vol. 1. Verlag Bau und Technik, 2012.



Sina Sedaghat Nezhad

Phone: +45 71441440
 E-mail: sisen@kt.dtu.dk

Supervisors: Søren Kiil
 Claus E. Weinell

PhD Study
 Started: September 2017
 To be completed: August 2020

Anticorrosive coatings and pigment engineering

Abstract

Corrosion compromises structure safety and is one of the most noticeable reasons for catastrophic failure in building and equipment. The application of coatings is very useful and economical method for controlling and suppressing corrosion in metals. Paints are the mostly used method for protection of metals against corrosion. Approximately 90 percent of all metal surfaces are covered by organic coatings. The coatings have two main reasons: Functional and aesthetic. The combination of organic coatings and functional pigments can improve the protection ability of the final coats. The aim of this work is to improve the performance of anti-corrosive primers by pigment engineering, such as surface modification, change in particle size and improving connectivity between pigments.

Introduction

Beside the cost of corrosion, the structural failure of the different industrial structures make the protections against corrosion very important and vital especially in the presence of chloride. An anticorrosive coating system usually consists of multiple layers of different coatings with different properties and purposes. Depending on the required properties of the coatings system, the individual coats can be metallic, inorganic or organic. The common system build-up consists of a primer, a mid-coat and a top coat. For better protection against corrosion, some functional pigments are added. The function of the primer is to ensure good adhesion to the substrate and to protect the substrate from corrosion [1].

Corrosion resistant coating systems generally provide some of these characteristics to have a good protection from metal substrate: (i) an impermeable barrier to corrosive species like oxygen and also moistures, (ii) corrosion inhibition utilizing corrosion inhibitors and finally (iii) cathodic protection [1].

The anticorrosive pigments as it is showed in Fig.1, can be divided into three main categories including inhibitive, barrier and sacrificial pigments [2].

Epoxy ester resins play a significant role in the formulation of anticorrosion primers. All studies have indicated that pigment characteristics, such as chemical nature, particle size, state of dispersion, morphology and level of pigmentation, determine the coating properties in its liquid and solid state. The most important ones are: type of binder, type and also the size of pigmentation

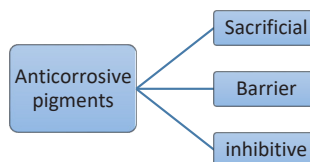


Figure 1: anticorrosive pigments categorizes

particles, film permeability and Λ which is the ratio of pigment volume concentration (PVC) to the critical pigment volume concentration (CPVC) [3], [4], [5].

$$\Lambda = \text{PVC} / \text{CPVC}$$

It is one of the important parameters and has a significant effect on the characteristics of primers.

Zinc chromate and red lead are the most effective inhibitive pigments, but because of their toxicity, some non-toxic alternative should be found. The pigments conventionally categorize into five main groups: phosphates, borates, complex silicates, organic salts and basic ion-exchange pigments (Fig.2) [6].

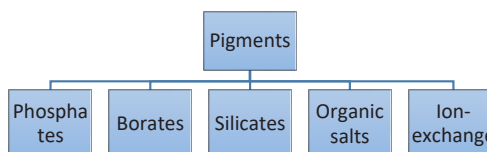


Figure 2: Different pigments family

Permeability and surface modification:

For primers with thermostable binders and with high curing rate, cross-linking density depends on the amount of pigments, so it is not surprising that when the barrier performance of coating is important, a low Λ is usually used. For coating as a barrier, it is important to reduce water, ion and corrosive species permeation to the interface of coating and the substrate, which can be done by increasing cross-linking density and reducing free volume. When $\Lambda > 1$, as pigment volume content increases, new possible paths in the primer can be formed which will increase the coating permeability [3]. By a careful setting of PVC/CPVC ratio of the primer the permeability profile can be controlled. In such a case, sufficient presence of moisture beside the pigments can be expected to dissolve enough inhibitor to maintain the passive film on the metal substrate. It is important to save passivated substrate for as long as possible and without being so much permeable as to let depassivating ions reach the substrate from the environment [3]. In Fig.3, the effect of Λ on different coating parameters is illustrated.

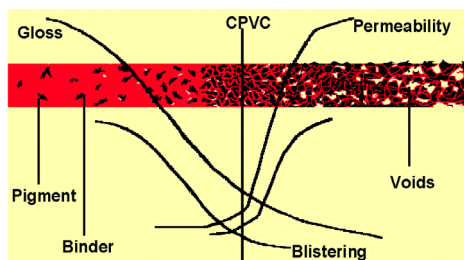


Figure 3: Dependency of coatings properties to Λ

By surface modification of the pigments, the corrosion resistance was improved by means of decreasing zinc electrochemical activity and increasing compatibility between the formed complex layer on zinc surface and binder [7].

Specific objectives:

The main objectives of this project are to increase the functionality of AC coatings and decreasing the price of them, or at least with the same functionality decreasing the price of final coatings by decreasing the amount of pigments in the coatings formulation. The focus of this work will be on the coats with zinc-based pigments.

The AC coatings can be improved by changing different parameters in different layers of the coating. The scopes of this work are related to these possible solutions:

1. Galvanic protection is one of the possible strategies in AC coatings. For having galvanic protection in organic coatings, some functional pigments are added to the coatings. The pigment engineering and changing the functionality of the pigments is one possible solution for improving the functionality of the pigments and finally

the coatings. It is also possible to try different kind of zinc base pigments and to use auxiliary pigments.

2. Barrier effect should be studied deeply; the barrier effect can be improved by changing type of pigments in the coatings formulation. In addition, it is possible to use flake form pigments for increasing the barrier effects.

3. Using chemical inhibitors is another possibility for improving the anti-corrosive effectiveness of the coatings.

Conclusions

The objectives of this project will be:

1. Literature study on AC coatings and pigments
2. Characterization of AC pigments
3. Pigment engineering and modifying coating formulation
4. Surface modifications of pigments
5. Accelerated testing of coated samples

During this work, different parameters of pigments will be studied and different experiments will be done to understand the effect of the main parameters.

References

1. L. H. Hihara, *Electrochemical Aspects of Corrosion-Control Coatings*. Elsevier Inc., 2014.
2. B. N. Popov, "Evaluation of Corrosion," *Corros. Eng.*, pp. 1–28, 2015.
3. D. Y. Perera, "Effect of pigmentation on organic coating characteristics," *Prog. Org. Coatings*, vol. 50, no. 4, pp. 247–262, 2004.
4. A. Kalendová, P. Kalenda, and D. Veselý, "Comparison of the efficiency of inorganic nonmetal pigments with zinc powder in anticorrosion paints," *Prog. Org. Coatings*, vol. 57, no. 1, pp. 1–10, 2006.
5. A. Amirudin, C. Barreau, R. Hellouin, and D. Thierry, "Evaluation of anti-corrosive pigments by pigment extract studies, atmospheric exposure and electrochemical impedance spectroscopy," *Prog. Org. Coatings*, vol. 25, no. 4, pp. 339–355, 1995.
6. G. Blustein, R. Romagnoli, J. A. Jaén, A. R. Di Sarli, and B. del Amo, "Zinc basic benzoate as eco-friendly steel corrosion inhibitor pigment for anticorrosive epoxy-coatings," *Colloids Surfaces A Physicochem. Eng. Asp.*, vol. 290, no. 1–3, pp. 7–18, 2006.
7. J. H. Park, T. H. Yun, K. Y. Kim, Y. K. Song, and J. M. Park, "The improvement of anticorrosion properties of zinc-rich organic coating by incorporating surface-modified zinc particle," *Prog. Org. Coatings*, vol. 74, no. 1, pp. 25–35, 2012.

**Christian Førgaard Nielsen**

Phone: +45 40 87 10 41
E-mail: chrfn@kt.dtu.dk

Supervisors: Anne Meyer
Lene Lange
Jakob Munkholt Christensen

PhD Study
Started: April 2017
To be completed: March 2020

Discovery and engineering of enzymatic biocatalysts for conversion of CO₂ to industrially relevant C1 products

Abstract

Enzymatic conversion of CO₂ to formate, formaldehyde, and methanol has previously been demonstrated in biocatalytic cascade systems based on reverse enzymatic catalysis. However, the conversion performance is far from industrially interesting, and significant improvement of yield, rate and stability is required. The overall aim of this PhD study is to discover, characterize and improve new and existing enzymatic catalysts for CO₂ utilization.

Introduction

The rapid depletion of global fossil-fuel feedstock present a two-sided issue. First of all, use of fossil fuels cause pollution and an increase in global temperature. Here CO₂ is widely recognized as the main contributor to global warming. Secondly, as easily available fossil fuel depots become depleted, cost of extraction increases when less readily available resources, such as shale gas or tar sand, are taken into use.

To avoid the dire consequences of global warming and potential resource depletion, it is of utmost importance to discover and implement alternative sustainable paths to supply global demand for energy and materials currently derived from fossil fuels.

Conversion of CO₂ to commodity chemicals represent a double gain. Not only will part of the sequestered CO₂ remain bound in materials, reducing global CO₂ levels, but CO₂ is renewable and readily available substrate (Perez-Fortes, 2016). Chemical processes, where CO₂ is part of the substrate, may form another pillar under a sustainable carbon economy.

Intense research towards CO₂ capture and utilization has been conducted during the last decade. This has resulted in several different approaches across scientific fields of interest (Goepfert, 2014). For this PhD study, enzymes will be applied as biocatalysts for the production of C1 products.

Specific objectives

While chemical conversion of CO₂ holds many benefits, it remains a major challenge. In practical industrial

applications catalysts are essential to allow any CO₂ conversion to run within reasonable energy use. And here, interest towards natural enzymatic catalysts was developed. Life itself is dependent on the ability of autotroph organisms to convert CO₂ into other materials. With the advantage of efficiently catalyzing processes under mild conditions with limited byproduct formation enzymes are promising catalysts for this exact application.

Results and discussion

In nature, CO₂ is primarily fixed through one of six major pathways (Shi, 2015). It was expected that these pathways would have the highest degree of enzyme variability, making them suitable for enzyme mining. For five of these six pathways, the CO₂ fixation step requires a complex co-substrate making the fixation less likely to be viable when working *in vitro*. The remaining pathway is the Wood-Ljungdahl pathway (Figure 1). Here, formate hydrogenase (FDH) was identified as a strong candidate for enzymatic conversion of CO₂.

By combining FDH (EC 1.2.1.2) with formaldehyde dehydrogenase (FaldDH)(1.2.1.46) and alcohol dehydrogenase (ADH)(EC 1.1.1.1) is has been shown that it is possible to reduce CO₂ to methanol – an enzymatic cascade process that does not occur in nature (Figure 2)(Marpani, 2017a).

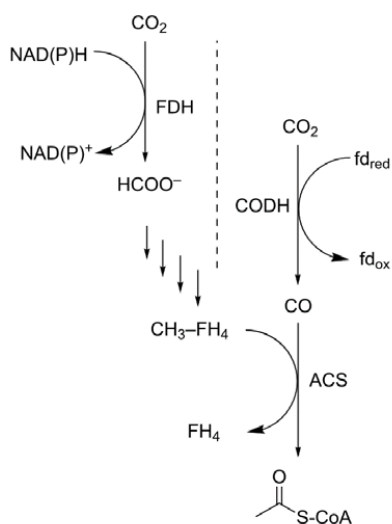


Figure 1: The Wood-Ljungdahl pathway. Acetyl-CoA is generated through the reduction of CO₂ to formate and CO. The key enzyme of interest is the formate dehydrogenase (FDH)(EC 1.2.1.2). Original for this modified figure from Alissandratos 2015.

While this synthetic enzymatic cascade reaction was reported for the first time in 1999 (Obert and Dave, 1999), it has been heavily developed and fine-tuned ever since. Since the reaction requires three mole of NADH per mole of methanol, it was critical to develop a way to regenerate NADH.

Recently, several methods to regenerate NADH were developed. Among these, an interesting example is the application of xylose dehydrogenase (XDH) which catalyzes xylose conversion to xylonic acid, whilst regenerating NADH. Xylonic acid is significantly more valuable than xylose, and has been categorized by the US Department of Energy to be among the top 30 potential basic precursors relevant for synthesis of high value chemicals and fuels in the carbon economy (Figure 3)(Marpani, 2017b)

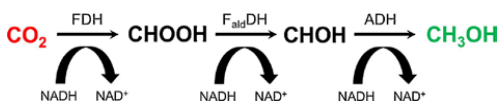


Figure 2: Reverse reaction cascade pathway from CO₂ to methanol. Formate dehydrogenase (FDH), formaldehyde dehydrogenase (FaldDH) and alcohol dehydrogenase (ADH) each require an NADH molecule as the reducing equivalent for the specific reaction.

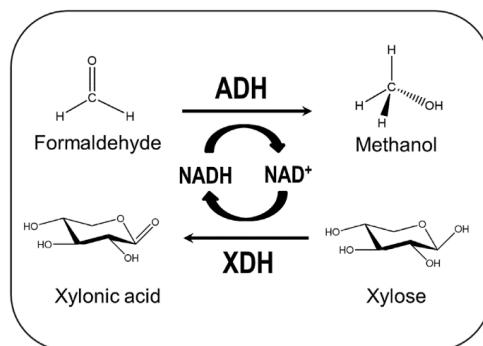


Figure 3: NADH regeneration by converting xylose to xylonic acid. This reaction is facilitated by xylonic acid dehydrogenase (XDH) (EC 1.1.1.175)

By modeling the kinetics of the simultaneous forward ADH reaction and the XDH catalyzed xylose conversion to balance the NADH consumption and formation, this reaction allowed for a biocatalytic productivity rate of 24 μmol MeOH/U³h during a six hour reaction. While the experiment was only conducted with the last step in the reaction cascade - formaldehyde to methanol - it still represents a plausible NADH regeneration methodology.

Despite promising results for CO₂ conversion and NADH regeneration, the productivity and stability of the individual enzymes is still far from optimal. Nonetheless, optimism prevails.

Conclusions

The use of enzymatic catalysts for CO₂ conversion represents an interesting strategy for approaching the need to utilize CO₂ as an alternative carbon source. However, while recent results are promising, there is a need for further process and enzyme development.

References

1. M. Perez-Fortes et al., Applied Energy 161 (2016) 718-732
2. A. Goepfert et al., Chem Soc Rev 43 (2014) 7995-8048
3. J. Shi et al., Chem Soc Rev 44 (2015) 5981-6000
4. F. Marpani et al. Biochem. Eng. 127 (2017a) 217-228
5. R. Obert and B.C. Dave, J. Am. Chem. Soc. 121 (1999) 12192-12193
6. F. Marpani et al., Biotechnology and Bioengineering (2017b) 1-9
7. A. Alissandratos, C.J. Easton, Beilstein Org. Chem. 11 (2015) 2370-2387



Henrik Lund Nielsen

Phone: +45 4525 2886
E-mail: hluni@kt.dtu.dk
Center: Center for Energy Resources Engineering

Supervisors: Philip Loldrup Fosbøl
Peter Glarborg
Søren Kiil
Kaj Thomsen

PhD Study
Started: July 2015
To be completed: June 2018

Measuring and modelling of chemical sulfur corrosion mechanisms in marine diesel engines

Abstract

When large ships engines are run at reduced load, "cold corrosion" has turned out to be a considerable problem. Cold corrosion occurs from mechanical wear in combination with acidic flue gas species condensing at the liner surface inside of the engine cylinder. For the purpose of investigating the electrochemical corrosion rates and mechanisms of the liner material in the engine cylinder environment, an electrochemical test set-up has been designed. Results will help us better understand the mechanisms behind the corrosion phenomena and identify the process-governing conditions and/or mechanisms.

Introduction

In the next 5-10 years stricter regulations on ships' fuel sulfur content and pollution are coming into force. A consequence is that ships engines, and in particular their operation will change due to alteration of the market requirements. With regard to this, prevention of "cold corrosion" in the engines is a major challenge. This phenomenon happens mainly when "slow-steaming" (i.e. sailing at reduced speeds). "Cold corrosion" is a mixture of acid attack and mechanical wear in the engine that occurs because the sulfur components like sulfuric acid (H_2SO_4), SO_2 , and SO_3 to a greater extent condense on the cylinder walls in the engines at conditions of slow-steaming where the engine runs at a reduced load. Expensive lube oil which has a specific high content of dissolved limestone is continuously added to the cylinders to neutralize the acid generated, but the efficiency of this procedure is not always optimal. The life time of certain components is reduced by a factor 5-10.

This PhD project is a part of a large project, SULCOR, involving DTU Chemical Engineering, DTU Mechanical Engineering, and MAN Diesel and Turbo A/S. The overall objective is to develop a multi-zone model that can identify and predict the corrosion occurring from combustion of Sulphur-containing fuels. This PhD project addresses the corrosion mechanisms taking place right at the cylinder liner surface. Other PhD/Post doc projects in the SULCOR framework provide data/models for other "zones", serving as boundary conditions for this work. These are mainly the

cylinder bulk gas and the lube oil film that covers the cylinder wall.

Specific objectives

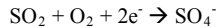
- Literature study covering electrochemical theory, relevant techniques and equipment as well as existing studies of SO_x corrosion, mechanisms and reactions.
- Design and conduct experiments that reveal the nature of the corrosion phenomena. The experiments are aimed at measuring the current densities that are governing the corrosion rate. These data can be used for estimating the rate and extent of metal dissolution from the cylinder liner at given engine operation conditions. Key variables to consider are temperature, pressure, concentrations, oil film properties as well as steel type, surface structure, piston movements and wear.
- The experiments conducted as well as literature and results from the other SULCOR PhD/post-doc projects are basis for creating a mathematical model describing the corrosion process. Expressing the current densities at various relevant conditions will likely be a basis for the model.

Results and discussion

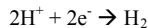
Not much information about the role of SO_2 on electrochemical corrosion is found in literature. Several studies claim that SO_2 is significantly enhancing the corrosion rate, but these studies are dealing with

conditions far from those found in marine engine cylinders – mainly atmospheric conditions, pipelines for transportation of supercritical CO₂ and high temperature gaseous corrosion. In addition, most studies report observations of increasing corrosion but do not propose actual mechanisms.

Some studies suggest that SO₂ is able to accept an electron from the metal surface, e.g. [1]



This reaction is believed to proceed in addition to the well-known cathodic reduction of H⁺:



resulting in an overall increased cathodic current.

For the purpose of investigating the corrosion phenomena, an electrochemical test set-up has been designed and constructed. The set-up consists of a 1 L thermostated glass cell containing an aqueous solution to be investigated.



Figure 1: The electrochemical set-up consists of a glass cell containing a solution and a cylinder electrode mounted to a rotating shaft.

The cylinder-shaped test specimen, made of the actual cast iron material, is mounted to a rotating shaft – a so-called rotating cylinder electrode (RCE) – and submerged into the solution. This enables us to control the mass transport conditions around the electrode. Thus, the effect of hydrodynamic conditions of the environment can be investigated.

The RCE is connected to a potentiostat along with a reference and counter electrode in order to control and

monitor the electrochemical properties of the metal/solution system. These properties can reveal valuable information about corrosion rate and mechanisms.

In connection with the electrochemical cell, a set-up with a number of mass flow controllers will enable us to introduce various gasses to the cell and thereby simulate the gaseous environment inside the engine cylinder. Furthermore, a device applying sliding wear to the RCE is to be installed.

Preliminary results show that there is a very limited effect of the hydrodynamic conditions on the corrosion of cast iron at high H₂SO₄ concentrations (1M). At low concentration (0.002M), however, there is a strong dependence on the mass transport conditions.

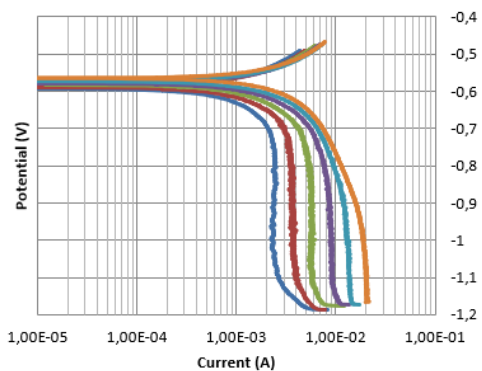


Figure 2: Potential-current curves measured at different rotation rates showing significant differences in diffusion limiting current (vertical slope region). Curves from left: 25 rpm; 50 rpm; 100 rpm; 200 rpm; 500 rpm; 1000 rpm.

Conclusion

A valuable output of the work will be identifying the limiting mechanisms of the corrosion process. In this way, focus can be put on the conditions that lead to further limiting of the corrosion rate. Limitations could be thermodynamic, kinetic or related to diffusion (e.g. protective films or precipitate).

The aim of the developed model is to fit into the large multi-zone model of the SULCOR project. In this way it serves to provide valuable information about the core corrosion mechanism.

References

1. K. Barton and Z. Bartonova. Über den beschleunigenden Einfluss von Schwefeldioxid und Wasser auf die atmosphärische Korrosion von verrosteten Eisen. *Werkstoffe und Korrosion* 20(3) (1969) 216-221.



Elisa Ogliani

Phone: +45 91485400
E-mail: eliogl@kt.dtu.dk

Supervisors: Anne Ladegaard Skov
Liyun Yu
Søren Hvilsted

PhD Study
Started: January 2017
To be completed: December 2019

Investigation of thermal degradation mechanisms of silicone elastomers

Abstract

In this study, the thermal degradation mechanisms and thermal degradation products of cross-linked silicone elastomers are investigated. Thermogravimetric analysis (TGA) performed in inert atmosphere is carried out on PDMS networks synthesized with different stoichiometric ratios. In order to determine to which extent the thermal degradation is influenced by the sol fraction of the silicone elastomers, extraction of the samples in heptane is exploited to remove unreacted PDMS chains. Furthermore, long-term thermogravimetric measurements at constant temperatures are performed with the aim of recovering and analyzing the degradation products of the thermally treated elastomers.

Introduction

Polydimethylsiloxane (PDMS) is the most extensively used polymer among silicones. It finds application in an unlimited number of fields such as medical implants, soft robotics, microfluidic devices, automotive and electronic industry, and many commodity products. These applications include use in high temperature environments, and PDMS meets these demanding requirements, due to its excellent thermal stability [1]. It is crucial to understand the thermal degradation mechanism of PDMS, in order to ensure the reliability of silicone based devices employed in high temperature applications. The thermal degradation mechanism of linear PDMS occurs by a molecular mechanism or a radical mechanism depending on the temperature and the heating rate [2,3]. Nevertheless, even though the thermal degradation mechanism of linear PDMS is well understood, the thermal degradation mechanism of cross-linked PDMS networks has not been studied yet. Therefore, the goal of this study is the elucidation of the thermal degradation mechanisms of cross-linked silicone elastomers, through the investigation of their thermal degradation behavior and thermal degradation products.

Materials

As shown in Figure 1, silicone elastomers were synthesized by a hydrosilylation reaction between a hydride cross-linker (HMS-301, $M_w = 1950 \text{ g mol}^{-1}$) and a vinyl-terminated PDMS (V35, $M_w = 49500 \text{ g mol}^{-1}$). The elastomers were prepared using different

stoichiometric ratios (r) as a reference, namely 1, 1.5, and 2.

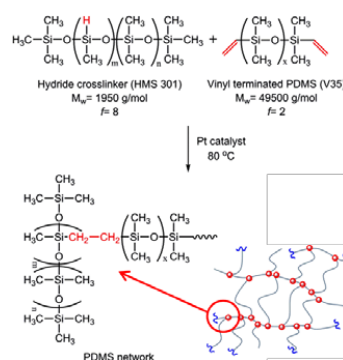


Figure 1: Schematic representation of the hydrosilylation reaction used to synthesize the silicone elastomers.

Specific objectives

TGA was carried out on the pristine silicone elastomers under N_2 flow, from room temperature to $700 \text{ }^\circ\text{C}$, at a heating rate of $10 \text{ }^\circ\text{C min}^{-1}$. The main scope of this first step is the inspection of the general degradation behavior.

Subsequently, the elastomers were extracted in heptane in order to remove the sol fraction.

Thermogravimetric measurements were repeated on the extracted elastomers, to determine to which extent the thermal degradation is influenced by the sol fraction. In the last step, thermal treatment of the samples was performed by isothermal TGA at 300 and 400 °C, in inert atmosphere for 12 hours. The isothermal treatment aimed at analyzing the thermal degradation products. In particular, soluble degradation products were collected by means of extracting the thermally treated elastomers in heptane.

Results and Discussion

Figure 2 shows the comparison of the 1st derivative of the weight loss curves of linear PDMS (V35) and the silicone elastomers. The linear PDMS underwent one degradation stage, which took place at 540 °C and presumably corresponds to the formation of the volatile cyclic oligomers [2]. Whereas, the cross-linked PDMS elastomers showed two distinct degradation stages, which occurred at different temperatures, with respect to different stoichiometric ratios.

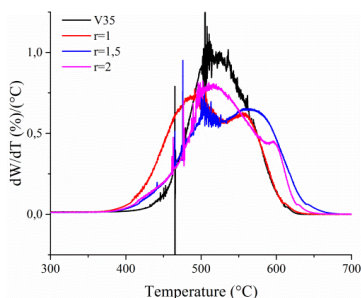


Figure 2: Plot of the 1st derivative of the weight loss curves of linear PDMS (V35) and the silicone elastomers with stoichiometric ratios 1, 1.5, and 2.

Subsequently, silicone elastomers were extracted in heptane in order to remove un-reacted PDMS chains. By increasing the stoichiometric ratio of the elastomers, the sol fraction of the samples decreases, and, consequently, the number of dangling chain decreases. Hence, as expected, the elastomer with ratio 1 was found to have the highest amount of sol fraction.

Then, the thermal degradation behavior of the extracted elastomers was screened by TGA. As shown in Figure 3, the derivative thermogravimetric plots drastically change, after extracting the elastomers. Only one degradation stage was detected, which occurred at ~510 °C for all the extracted samples.

Subsequently, isothermal TGA was performed on the linear PDMS and the elastomer with $r=1$ before and after extraction (Figure 4). After the thermal treatment at 300 and 400 °C, respectively, the elastomers were extracted in heptane and soluble degradation products were collected. Then, the liquid of extraction was analyzed by size exclusion chromatography (SEC) in order to determine weight and number average molecular weights of the degradation products.

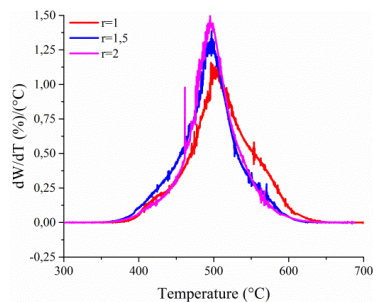


Figure 3: Plot of the 1st derivative of the weight loss curves of silicone elastomers with stoichiometric ratios 1, 1.5, and 2 after extraction in heptane.

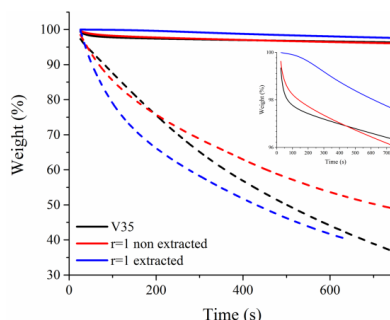


Figure 4: Plot of the %weight losses of the samples as a function of time at a constant temperature of 300 °C (solid line) and 400 °C (dashed line).

Conclusions

In this preliminary phase, a new experimental procedure has been designed in order to investigate thermal stability and thermal degradation products of cross-linked silicone elastomers. It is found that the sol fraction significantly affects the thermal degradation process. In particular, the isothermal treatment of the samples allows collection and analysis of thermal degradation products, characterization of which is currently on going by using diverse analytical techniques, such as nuclear magnetic resonance (NMR) and Fourier-transformed infrared spectroscopy (FT-IR). In future investigations, volatile thermal degradation products will be collected and analyzed.

Acknowledgements

The author is grateful to Villum Fonden for founding this project.

References

1. K. Chenoweth, S. Cheung, A. C. T. van Duin, W. A. Goddaard III, E. M. Kober, *J. Am. Chem. Soc.* 127 (19) (2005) 7192-7202.
2. G. Camino, S. M. Lomakin, M. Lageard, *Polymer* 43 (2002) 2011-2015.
3. N. Grassie, I. G. Macfarlane, *Eur. Polym. J.* 14 (1978) 875-884.

**Merve Öner**

Phone: +45 91849864
E-mail: meon@kt.dtu.dk

Supervisors: Gürkan Sin
Jens Abildskov
Stuart M. Stocks, LEO Pharma A/S
Michael F. Freitag, LEO Pharma A/S
Getachew S. Molla

PhD Study
Started: January 2017
To be completed: December 2019

Scale-up modeling and analysis of a pharmaceutical crystallization process

Abstract

This research project aims to develop a scale-up model of a pharmaceutical batch cooling crystallization process via a compartmentalization approach. In this work, computational fluidic dynamics (CFD) is used to study the mixing behavior in the large-scale system. The compartmental volumes, location and flux connections are extracted from CFD data analysis to define the interconnected compartment network. The scaled-up process model containing multiple compartments is implemented and simulated in MATLAB/Simulink. The influence of the fluid dynamics on the simulated process performance in terms of crystal size distribution and final average crystal diameter is investigated by comparing the multi-compartment model with a single-compartment well-mixed model.

Introduction

Prediction of the influence of the crystallizer scale on the process behavior and process performance is one of the major challenges in the design of industrial crystallization processes. Fluid dynamic conditions of industrial scale crystallizers are far from well-mixed behavior. This leads to spatial variations of critical crystallization process variables such as temperature, super-saturation, particle concentration, etc. within crystallizer geometry [1]. Consequently, crystallization process models based on the assumption of well-mixed behavior are not representative for a scaled-up process, and therefore not credible for the use in supporting optimal design of industrial crystallizers. Therefore, a more detailed insight into mixing conditions and its consequences for local crystallization phenomena must be taken into account in order to achieve reliable process design and scale-up [2, 3].

Specific Objectives

The main objective of this study is to develop a predictive scale-up model of a pharmaceutical batch cooling crystallization process based on a compartmental modelling approach.

Methodology

Compartmental modeling is a trade-off approach to overcome the limitations of well-mixed models, by considering local mixing, heat transfer and fluid dynamics separately from crystallization kinetics within a crystallizer [2, 3]. Application of compartmental

modelling to pharmaceutical batch cooling crystallization requires the division of the crystallizer into a finite number of compartmental volumes. Minimized or negligible gradients *e.g.* in temperature, crystal distribution, super-saturation and energy dissipation should exist within individual compartmental volumes. However, the fundamental challenge is the characterization of these compartmental zones, mass and energy fluxes between adjacent zones as well as the affected properties due to non-ideal fluid mixing. The predictive capability of the model (by means of the critical phenomena in the process) strongly depends on the quality of this characterization [1, 4]. Seeded-batch cooling crystallization of paracetamol (active pharmaceutical ingredient – API) from ethanol (solvent) [5, 6] is chosen as a case study in this work. In the model, a linear cooling with a cooling rate of 0.4 °C/min is applied to the initial solution, which has an initial concentration of 0.2617 kg paracetamol / kg ethanol and an initial temperature of 40 °C, for 50 min. The liquid volume in the crystallizer is 220 L and impeller stirrer speed is 100 rpm. To determine the compartmental zones within the volume of industrial-scale crystallizer equipment, primarily the fluid dynamics, mixing and heat transfer are studied by means of CFD simulations. The compartmental volumes, location and flux connections are extracted from data analysis to define the interconnected compartment network as shown in Figure 1. The crystallization process modelling based on compartmental approach is implemented in

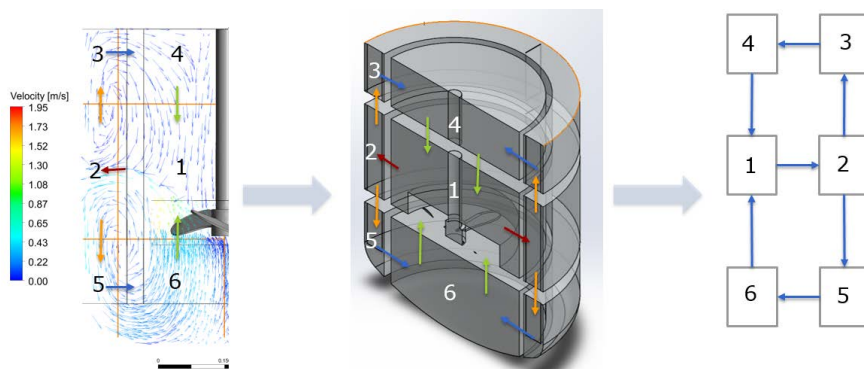


Figure 1: Characterization of compartmental zone network (location, volume, flux connections).

MATLAB/Simulink, where every individual compartments are modelled as Mixed Suspension and Mixed Product Removal (MSMPR) crystallizer (Figure 2). The same set of model equations and model parameters are defined in order to solve the conservation balance equations for crystallization process system (e.g. population, mass) for every compartment. However, spatial variations in the crystallizer modelled by different temperature gradients result in different rates of crystallization kinetics (e.g. nucleation, growth) between the individual compartments, which represents the deviation from the ideal case.

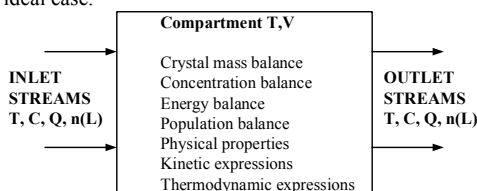


Figure 2: Single compartmental model [7].

Results and Discussions

The performance of the pharmaceutical batch cooling crystallization process has been analyzed in terms of crystal growth rate, crystal size distribution and final average crystal size. The multi-compartment model has been compared with a single-compartment well-mixed model to examine the influence of the non-uniformly distribution of related process variables on the process performance. CFD simulations have shown that there is a difference in average temperature over time between different locations in the crystallizer vessel so called in the different compartments. Hence, crystals are subjected to different growth and nucleation rates in different compartments. This leads to a wider final crystal size distribution and less growth with a final average crystal diameter of 113 μm compared to the single-compartment model (final average crystal diameter is 135 μm) as shown in Figure 3. It can be clearly observable that fluid dynamics plays an important role in scaled-up systems, since it determines the transport processes in the system. Therefore, it

should be taken into account in modeling of large systems. This study has shown that mixing has a significant impact on the simulated crystal growth, nucleation and consequently final crystal size distribution as well as final average crystal diameter.

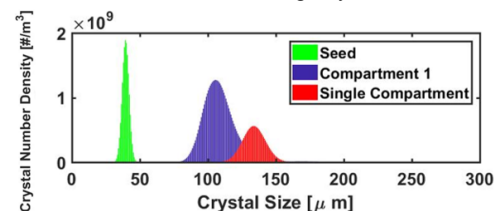


Figure 3: Final crystal size distribution in multi-compartment model and single-compartment model.

Acknowledgement

We would like to thank the Danish Council for Independent Research (DFR) for financing the project with grant ID: DFF-6111600077B.

References

1. H.J.M. Kramer, S.K. Bermingham and G.M. van Rosmalen, *Journal of Crystal Growth*, 198/199 (1999) 729-737.
2. H.J.M Kramer, J.W Dijkstra, P.J.T Verheijen, and G.M van Rosmalen, *Powder Technology*, 108 (2-3) (2000) 185-191.
3. D. Green. *Handbook of Industrial Crystallization*, Butterworth-Heinemann, 2002, p. 181-199.
4. F. Bezzo, S. Macchietto and C.C. Pantelides, *Computers & Chemical Engineering*, 28 (2004) 501-511.
5. C. Fernandes. Effect of nature of the solvent on the crystallization of paracetamol, accepted for 14th International Symposium on Industrial Crystallization (ISIC 14), 1999.
6. N.A. Mitchell (2013), *Numerical Modeling of Cooling Crystallisation*. PhD thesis.
7. E. Kougoulos, A.G. Jones and M. Wood-Kaczmar, *Chem. Eng. Comm.*, 193 (2006) 1008-1023.



Stylianos Pachitsas

Phone: +45 4525 2830
E-mail: stylpac@kt.dtu.dk

Supervisors: Stig Wedel
Jytte Boll Illerup
Kim-Dam Johansen
Lars Skaarup Jensen, FLSmidth A/S

PhD Study
Started: May 2015
To be completed: May 2018

Control of Hydrogen Chloride (HCl) emission from cement plants

Abstract

HCl is a gaseous industrial pollutant with significant environmental impact and one of the major acid gases emitted from cement plants. The main purposes of this project are the prediction of HCl emission from cement plants and optimization of the HCl control during cement manufacturing process, using optimal operating conditions. The project is focused on the study of HCl absorption mechanism by cement raw meal in cement manufacturing process which comprises the evaluation-understanding of HCl absorption in cement plant units, e.g., raw mill, particles filter, and development of a reliable prediction model for the HCl emission from cement plants. The evaluation of the raw meals HCl absorption capacity and absorption affecting parameters was conducted, using TGA-FTIR and Fixed-Bed reactor – FTIR set ups.

Introduction

The E.U. and U.S. environmental regulations in combination with maintenance issues require the further decrease of HCl emissions from cement plants and effective control of HCl levels in cement manufacturing process. Industrial measurements indicate that HCl can be formed in the cement preheater upper cyclones and fuel combustion zones (Fig.1). [1, 2] The fuel originated HCl is absorbed by calcined raw meal in calciner, however, it can contribute to HCl emission through Bypass system.[2] This project does not consider the Bypass contribution, albeit its significance. In addition, industrial measurements disclosed the presence of HCl absorption phenomena in raw mill and particles filter units in the temperature range 90-300°C. As it is illustrated in Fig. 2, project basic assumptions are the presence of one HCl release zone (preheater upper cyclones), and one HCl absorption zone, which comprises the gas condition tower, raw mill and particles filter.

The HCl release mechanism in the cement preheater is unknown. On the other hand, CaCO_3 chlorination is considered responsible for HCl absorption effect, however, the affecting parameters and optimal operating conditions are not clearly identified.

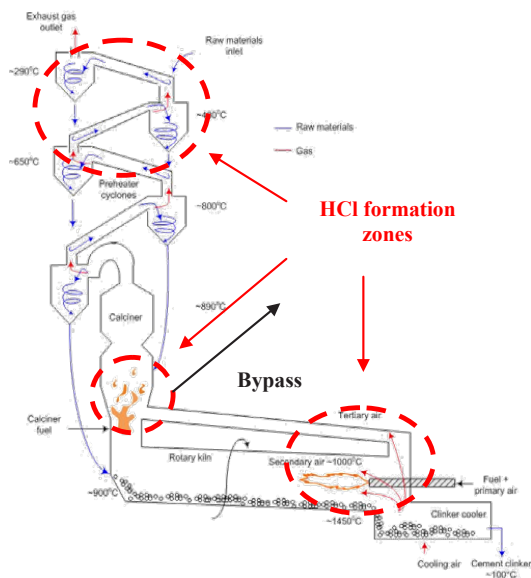


Fig. 1: Schematic presentation of preheater – kiln system and HCl formation zones.

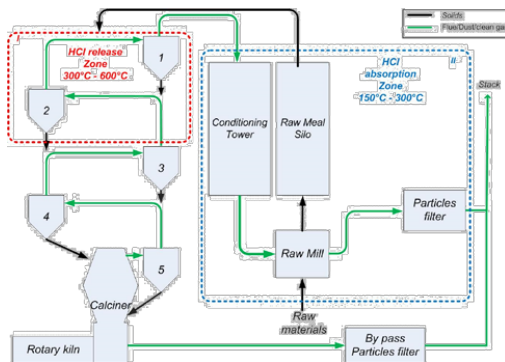


Fig. 2: Typical cement plant layout and the zones of interests.

Objectives

The project objectives can be summarized as follows:

- Understanding of HCl absorption mechanism by raw meal at cement plant conditions
- Identification of HCl absorption affecting parameters (physical properties and solids-gas phase composition)
- Determination of cement plant optimal operating conditions
- Prediction model for HCl emission from cement plants

Experimental Activities – Modelling

The research activities were focused on the study of HCl absorption mechanism using a standard TGA-FTIR set-up for ramping temperature experiments and a Fixed-Bed reactor-FTIR set-up for isothermal experiments. Furthermore, the HCl absorption in cement plant units was modeled based on appropriate conceptual reactor models for the operating conditions considering first reaction order with HCl.

The reaction rate [$\text{mol}/(\text{m}^2_{\text{CaCO}_3\text{S}})$] was expressed by eq. 1, where k is the reaction constant, k_w is the water effect factor, and C_{HCl} is the gas phase HCl content [mol/m^3].

$$r_{\text{HCl}} = k(T) \cdot k_w \cdot C_{\text{HCl}} \quad (1)$$

The gas conditioning tower (GCT) was modeled as a PFR or a PFR- CSTR system in serial configuration base on the operation mode.

The raw mill model (Fig.3) comprises (i) three PFRs in serial configuration, (ii) two gas-solids separation points, and (iii) a separated grinding system where no gas mass transference occurs from PFRs. Moreover, the solid material recirculation is considered in calculation of dust actual specific surface area in each PFR reactor.

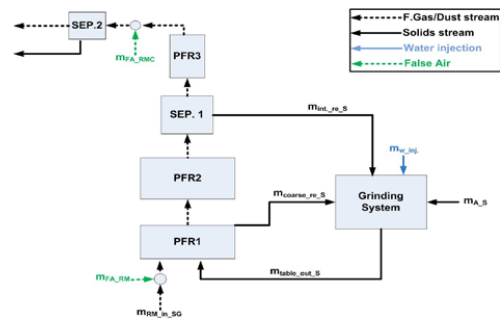


Fig.3: Schematic presentation of the raw mill section model.

The bag filter model considers the filter bags as PFRs in parallel configuration. Furthermore, bag filters are categorized into groups of characteristic dust layer thickness based on the filter unit operating conditions and construction specifications.

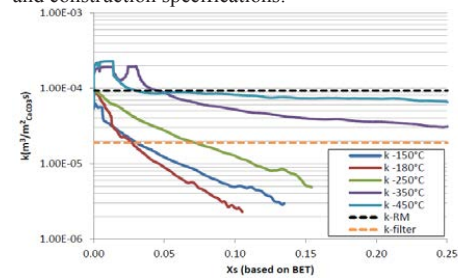


Fig.4: k values from experimental data, and particle filter and raw mill (RM) models vs CaCO_3 particles external surface layer conversion assuming one calcite unit cell thickness.

Fig.4 shows the experimentally determined and calculated by models k values, using as input industrial data. It is clearly seen that there is not coherence between the modeling based and experimental k values.

Conclusions

The conducted experimental activities outlined the temperature, gas phase composition, and raw meal component effects on HCl absorption mechanism. The modeling of HCl absorption in cement plant units showed that the HCl absorption by raw meal is not first order relative to HCl concentration and not independent on raw meal conversion degree.

Acknowledgements

This project is part of the research platform ‘Minerals and Cement Process Technology – MiCeTech’ funded by Innovation Fund Denmark, FLSmidth A/S, Hempel A/S, and DTU.

References

1. Emission measurements of cement plant A, Internal report FLSmidth, Copenhagen, 2012.
2. Emission measurements of cement plant B, Internal report FLSmidth, Copenhagen, 2013.

**Soheila G. Parto**

Phone: +45 4525 2842
E-mail: Sohg@kt.dtu.dk

Supervisors: Anker Degn Jensen
Jakob Munkholt Christensen
Lars Saaby Pedersen, Haldor Topsøe

PhD Study
Started: November 2014
To be completed: January 2018

Catalytic liquefaction of lignin to value-added chemicals

Abstract

Solvothermal conversion of lignosulfonate in ethanol and ethylene glycol mediums was investigated over Ni/SiO₂ catalyst at 250 °C. Similar oil yields up to 32 wt% were observed in both reaction mediums. However, there was considerable difference in solubility of the solid fractions in THF, which indicated that solvents have different capabilities in end-capping reactions. Moreover, conversion of lignosulfonate over NiMo/Al₂O₃ in ethanol medium was investigated at 260-310 °C. The oil yield increased to 67 wt% at 310 °C. The oil yield could be further increased to 88 wt% by doubling the mass of catalyst.

Introduction

Lignin is the second most abundant organic matter on earth. Lignin is a promising source of chemicals. It is composed of phenylpropane building blocks connected via C-O and C-C bonds. Different pretreatment methods are applied for separation of cellulose and hemicellulose from lignin, such as Kraft pulping, sulfite pulping, soda pulping, organosolv extraction, etc. During pretreatment, some inter-connecting bonds are cleaved while new bonds are formed. Therefore, depending on the pretreatment pulping method, different lignin structures can be obtained from the same type of biomass. Degradation of lignin to monomeric building blocks is of interest.

Specific objectives

Lignosulfonate is a byproduct from sulfite pulping, mainly produced by the company Borregaard. Compared to the other types of technical lignins, degradation of lignosulfonate is rarely studied. Solvothermal degradation assisted by a heterogeneous catalyst is a promising method for conversion of lignin. A major challenge for catalytic degradation of lignin is the presence of sulfur, which can adsorb on the catalytic active phases, leading to permanent deactivation. Two types of catalyst were investigated for conversion of lignosulfonate: Home-synthesized supported Ni and commercial NiMo/Al₂O₃ catalysts. Ni is a hydrogenation catalyst, which was reported to be resistant to sulfur deactivation [1]. Ni promoted molybdenum catalyst (NiMo) is widely used in industry for hydrotreating purposes, including hydro-

desulfurization (HDS). NiMo catalyst should generally be activated prior to use by sulfidation and formation of the NiMoS phase. The sulfur can be removed from feedstock through sulfur vacancies on the catalyst. The role of solvent was evaluated using ethylene glycol (EG) and ethanol (EtOH) in the tests with Ni catalyst. EtOH inhibits repolymerization of degraded compounds by alkylation reactions and acts as a hydrogen donor [2]. EG is a good solvent for lignosulfonate due to formation of hydrogen bonds between EG and lignin, and also has end-capping capabilities. Herein, we present the main outcomes from our research.

Experimental

Spruce based sodium lignosulfonate, provided by Borregaard, was used as lignin source. Sodium lignosulfonate was ion-exchanged to proton-lignosulfonate (H-LS). The sulfur content of H-LS is 3.1 wt%. A 300 ml Parr 4560 batch reactor was used. In catalytic tests using Ni/SiO₂ catalyst (containing 5 wt% Ni), 7.5 g lignin, 0.75 g catalyst and 75 ml solvent were used. The reactor was charged with 50 barg hydrogen at room temperature, and heated to 250 °C. The Ni/SiO₂ catalyst was initially reduced by treating at 350 °C with 1 Nl/min H₂ flow for 2 h in the batch reactor.

An amount of 1 g catalyst, 10 g lignin and 100 ml ethanol was used in the catalytic conversion of lignosulfonate with NiMo. Two temperatures of 260 and 310 °C were tested. The reactor was filled with 25 barg hydrogen at room temperature. In some experiments, NiMo was presulfided overnight using 10 ml dimethyl

disulfide (DMDS) with 30 barg hydrogen (loaded at room temperature) at 400 °C. The reaction time was 3 hours in all experiments with Ni/SiO₂ and NiMo catalysts.

At the end of each experiment, solid and liquid products of the reactions were separated by filtration. Hereafter, two different methods were applied for separation of liquefied products from solvents. When EtOH was used, the liquid phase was subjected to vacuum evaporation at 35 °C and 5 mbar for isolation of light and heavy liquid fractions. The heavy liquid phase remaining unevaporated was regarded as bio-oil. However, separation of EG from the bio-oil by evaporation was not possible due to its high boiling point. Therefore, an extraction method was applied using water and ethyl acetate for separation of products in the reactions with EG. It was assumed that EG will be transferred to the water phase while depolymerized lignin compounds will end up in ethyl acetate. Ethyl acetate was further evaporated using rotary evaporation. GC-MS was used for identification of the compounds in the oil fractions. The molecular weight distribution of the oil and solid phases was determined using size exclusion chromatography (SEC). Gaseous products were analyzed by GC. Elemental analysis (Eurovector EuroEA3000) was used for quantification of organic C, H, N, S and O content of the oil and solid fractions.

Results and discussions

Conversion of lignosulfonate over Ni/SiO₂

Some of the results from catalytic conversion of lignosulfonate over Ni/SiO₂ catalyst are presented in Table 1. The yields of oil fractions were almost similar in the two mediums. The solid phases were dissolved in THF. Only 16 wt% of the solid from tests in EtOH were dissolved in THF while 45 wt% of the solid from EG test was soluble in THF. These results indicate the capability of EG in end-capping the degraded radicals and preventing formation of highly crosslinked solid chars. Guaiacol was the main identified compound originating from lignin in the oil from reaction in EG. For reaction in EtOH, guaiacol and 4-hydroxy-3-methoxy benzoic acid ethyl ester were the major identified compounds. Formation of monomeric esters in EtOH is possibly taking place by reaction of in-situ produced aromatic carboxylic acid compounds from degradation of lignosulfonate and ethanol.

Table 1: The results from conversion of lignosulfonate over Ni/SiO₂ catalyst at 250 °C and reaction time of 3 h. 0.75 g catalyst, 7.5 lignin, 75 ml solvent

Entry	Solvent	Oil yield wt%	THF soluble solid wt%
1	EtOH	31	16
2	EG	32	45

While EtOH remained stable at the reaction conditions, the GC-MS analysis of the liquid fractions from EG tests confirmed formation of diethylene glycol (DEG),

triethylene glycol (TEG), tetraethylene glycol (TTEG) and pentaethylene glycol (PEG), which were formed by self-reaction of ethylene glycol.

Conversion of lignosulfonate over NiMo

NiMo catalyst was used in oxide and sulfide form. It was assumed that sulfur in the structure of lignosulfonate may activate the catalyst, *in-situ*. The oil and solid yields are shown in Figure 1. As can be seen, the oil yield increased from 17 % without catalyst to 29 wt% at 260 °C over Non-sulfided NiMo. The oil yield increased from 25 wt% in non-catalytic condition to 67 wt% at 310 °C.

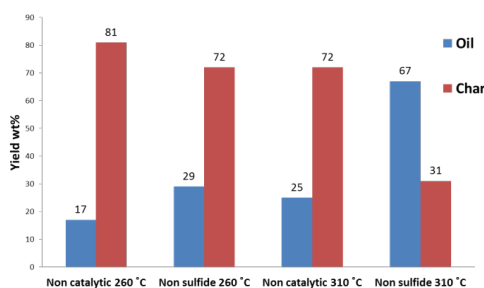


Figure 1 The solid and oil yields from conversion of lignosulfonate over NiMo at 260 and 310 °C.

In some tests, the catalyst was presulfided overnight in the presence of DMDS and tested at 260 and 310 °C. While similar oil yields were observed at 310 °C, the oil yields at 260 °C increased to 52 wt%. This indicates that at 310 °C, *in-situ* sulfidation of catalyst takes place by cleavage of C-S bonds and deposition of sulfur on sulfur vacancies. The oil yield increased further to 88 wt% by doubling the mass of catalyst; however the oil yield did not change by further increase of the catalyst mass to 3 g. The catalyst showed reusability for at least two times without any pretreatment.

Conclusion

According to our results, the nature of catalyst and solvent has great impact on the liquefied and solid fractions. EG has superior activity compared to EtOH in terms of end-capping activity, however, it is converted to higher glycols in the reaction condition.

Acknowledgement

This project is part of Biovalue SPIR platform and in collaboration with Haldor Topsøe and Borregaard companies. The support from the companies are very much appreciated.

References

- F. Wang, J. Xu, Q. Song, and J. Xu, Chem. Commun 48, (2012) 7019-7021.
- X. Huang, T. I. Korányi, M. D. Boot, and E. J. M. M. Hensen, Green Chem.17 (11) (2015), 4941–4950.



Morten Nedergaard Pedersen

E-mail: monepe@kt.dtu.dk

Supervisors: Kim Dam-Johansen
Peter Arendt Jensen
Sønnik Clausen
Lars Skaarup Jensen, FLSmidth A/S

PhD Study
Started: March 2015
To be completed: April 2018

Burners for Cement Kilns

Abstract

Waste derived fuels are increasingly being used in the cement industry as a way to reduce cost. However, the shift from traditional fossil fuels is difficult, due to the widely different physical and chemical properties of the alternative fuels. New burners are therefore required in the cement industry, in order to best deal with the challenges imposed by the use of alternative fuels. This project aims to increase the knowledge of the combustion process in the cement rotary kiln by video imaging at large scale cement plants firing high amounts of alternative fuels. Another goal is to model the rotary kiln flame with various fuels in order to assess the influence of a high degree of alternative fuels and propose guidelines for how the use can be increased.

Introduction

Alternative fuels are increasingly being used in the cement industry, primarily as a method to reduce the cost of the energy intensive manufacturing process [1]. If the fuels are partly biogenic and substitute fossil fuels, net CO₂ emissions from the industry can also be reduced [1]. Solid Recovered Fuel (SRF), which is produced by sorting the combustible fraction of municipal solid waste [2], is one type of fuel receiving much interest.

The use of alternative fuels introduces various challenges, since the fuels are very different from the fossil fuels. Compared to coal or petcoke, SRF is difficult to mill [3] and has a larger particle size. The water content is also higher and the heating value is lower [2]. This makes it difficult to ignite the fuel and obtain the high temperatures required for efficient heat transfer in the cement rotary kiln [4].

To overcome these challenges a new development in kiln burners is required. FLSmidth A/S has recently developed the JETFLEX burner, shown in Figure 1. The burner is equipped with a powerful swirl channel and rotatable jet nozzles, which can be used to shape the flame depending on the quality of the available SRF.



Figure 1: The FLSmidth JETFLEX burner.

Specific Objectives

The project considers two parts

- 1) Measurements at a full-scale cement plant
- 2) Mathematical model development of a rotary kiln flame

The objective of part 1 is to gain increased knowledge of the combustion process in the near burner region of the rotary kiln and support the development of FLSmidth's new burner.

The objective of part 2 is to formulate a model that can predict the temperature and heat transfer in the rotary cement kiln using fossil fuel or SRF. The model can then be used to create guidelines on how to increase the share of alternative fuels at a given cement plant.

Results and Discussion

Only some of the results of Objective 1 will be covered here. A prototype of the JETFLEX burner has been installed at a European cement plant, where it is undergoing an extensive test program. The plant is a dry kiln with a 5-stage preheater and has a daily production capacity of approx. 3500 ton clinker. The plant fires a mix of SRF and petcoke in the kiln burner, with the SRF contributing up to 70 % of the energy.

Special camera equipment has been developed at DTU, which can withstand the high temperatures (1000 °C) and dusty environment in the cement rotary kiln hood. Using the camera, it is possible to make a detailed study of e.g. fuel behavior and ignition in the near burner zone of the cement kiln. Detailed information of this work has recently been published in [4], while some of the highlights will be presented here.

The images in Figure 2 and 3 compare the flames from the old burner installed at the test plant with the JETFLEX burner. The images in Figure 2 show a petcoke flame and the images in Figure 3 show a cofired flame with 70 % energy input from SRF and the remainder petcoke.

The image in Figure 2 shows that petcoke gives a wide dark flame plume. The ignition point for the old burner is outside the image at 5-6 m from the burner tip. With the JETFLEX burner, ignition occurs 4 m from the burner tip.

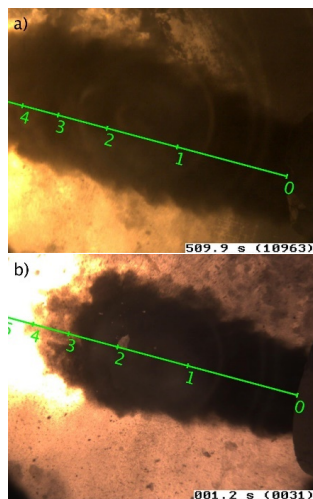


Figure 1: Petcoke flame in cement kiln for (a) old burner and (b) JETFLEX burner.

Cofiring with SRF gives a narrower flame plume, which is also lighter in color, and the ignition is delayed. For the old burner the ignition point is far from the burner, and no ignition is observed in the image. For the new burner the ignition point is also pushed away from the burner to between 5-6 m. Some ignition of fuel can be seen in the upper left corner of Figure 3b and below the fuel plume.

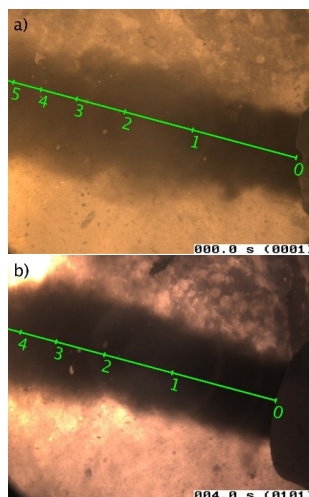


Figure 3: Cofiring of 70 energy % SRF with petcoke for (a) old burner and (b) JETFLEX burner.

Conclusions

The special high temperature camera equipment developed at DTU gives an opportunity to closely study the near burner zone in the cement kiln. This has been used to compare burner performance at a cement plant.

The recorded videos show how it is easier to ignite both a petcoke flame and a cofired flame using the JETFLEX burner, compared to the old burner at the test plant. This is caused by the jet design and powerful swirl channel of the JETFLEX burner. In combination, the two features can help to mix the fuel and hot secondary air, which leads to an early ignition, of the otherwise hard to ignite SRF. An early ignition is required to create a high temperature zone at the kiln exit, which ensures a high cement clinker quality [4].

Acknowledgments

This work is part of the research platform ‘Minerals and Cement Process Technology – MiCeTech’ funded by Innovation Fund Denmark, FLSmidth A/S, Hempel A/S, and DTU.

References

1. A. A. Usón, A. M. López-Sabirón, G. Ferreira, E. Llera Sastresa, *Renewable and Sustainable Energy Reviews*, 23 (2013) 242–260.
2. L. F. Diaz, G. M. Savage, L. L. Eggerth, *Solid Waste Management*, United Nations Environment Program (UNEP), 2005, pp. 295–302.
3. J. Maier, A. Gerhardt, G. Dunnu, in: P. Grammelis (Ed.), *Solid Biofuels for Energy*, Springer-Verlag, London, 2011, pp. 75–94
4. M.N. Pedersen, M. Nielsen, S. Clausen, P.A. Jensen, L.S. Jensen, K. Dam-Johansen, *Imaging of Flames in Cement Kilns To Study the Influence of Different Fuel Types*, *Energy & Fuels*. 31 (2017) 11424–11438.

**Olivia Ana Perederic**

Phone: +45 42725918
E-mail: oper@kt.dtu.dk

Supervisors: John M. Woodley
Georgios M. Kontogeorgis
Rafiqul Gani
Bent Sarup, Alfa-Laval

PhD Study
Started: September 2015
To be completed: September 2018

Systematic computer aided methods and tools for lipids process technology

Abstract

Lipids are represented by a large number of complex compounds and they can be used as additives, emulsifiers, surfactants or intermediary compounds in a wide range of applications such as food, health care, fuels, coatings and many more. Accurate and consistent prediction of lipids pure compounds properties, as well as, lipids mixture properties and phase equilibria are very important when process synthesis, design, optimization, along with energy, economic and environmental impact analysis are performed through model-based tools. Recently a new systematic identification method for data analysis and phase equilibria modelling for lipids systems was developed and applied for different type of UNIFAC models (e.g.: Original, Linear, Modified and Dortmund UNIFAC). In this work the most important results of method application are presented.

Introduction

Lipids, also known as fats and oils, are organic compounds of biological origin which are belonging to different classes such as: fatty acids, fatty esters, mono-, di- and triglycerides, sterols, waxes, etc.[1]. Lipids-based industries employ processes such as, fat splitting, esterification, epoxidation, hydrogenation, etc., where different types of phase equilibria play important roles.

GC based methods can provide a wide range of properties for pure compounds and their mixtures, making them an indispensable tool for process design when no data or only few data is available. Limited experimental data availability and poor performances of currently available GC based methods for lipids compounds is therefore an obstacle for obtaining the necessary information for systems with lipids. For this reason, a systematic identification-regression method for regression of selected model parameters applied for phase equilibrium property modelling was developed [2]. The method provides a detailed approach for data selection and a regression procedure for binary interaction parameter estimation for group contribution based models. The aim is to offer support for a faster assessment and solution of the identification-regression problem. The method has the following characteristics: inclusion of a detailed algorithm for data selection, which complements personal judgment and available expertise; use of an efficient calculation sequence, which can be further exploited for planning

experimental data collection in order to fill in the gaps within the binary interaction matrix and to make possible the step by step estimation of the binary group interaction parameters; the regression problem formulation and solution for each regression step.

Specific Objectives

The identification method is applied to estimate binary group interaction parameters for the different UNIFAC models dedicated to lipids systems. The objective is that the new set of parameters must be able to improve the performance of different UNIFAC models with published parameters quantitatively as well as qualitatively by eliminating the prediction inaccuracies and/or uncertainties. The identification method uses the SPEED Lipids database as a source for experimental data and models for estimation of pure compound properties of lipids.

Results and discussion

The systematic identification-regression method [2] is applied for following models: Original, Linear, Modified and Dortmund UNIFAC. The new parameters performances for each model are compared with the published ones by performing the validation on VLE data and by extrapolation to SLE prediction. The results are given in Table 1.

All four models perform better with the lipids based parameters. In general, the Linear UNIFAC model with lipids-based group-interaction parameters show the best

Table 1: UNIFAC models performance with Published and Lipids parameters for VLE and SLE.

UNIFAC model		ARD(%)	
		VLE data ^a	SLE data ^b
Original	Published [3]	21.7	1.2
	Lipids [2]	13.9	1.1
Linear	Published [4]	16.9	1.4
	Lipids [5]	9.9	1.4
Modified	Published [6]	18.4	1.9
	Lipids [5]	10.9	1.8
Dortmund	Published [7]	20.7	1.3
	Lipids [5]	9.9	1.7

$$a \quad ARD(\%) = \frac{1}{N} \sum_{i=1}^N \left| \frac{P_{\text{experimental}} - P_{\text{calculated}}}{P_{\text{experimental}}} \right| \cdot 100, \quad N - \text{number of data points}$$

$$b \quad ARD(\%) = \frac{1}{N} \sum_{i=1}^N \left| \frac{T_{\text{experimental}} - T_{\text{calculated}}}{T_{\text{experimental}}} \right| \cdot 100, \quad N - \text{number of data points}$$

performance as it has the lowest deviation for VLE prediction. The Dortmund UNIFAC model is the second best model when lipids-based parameters are used. The cumulative deviation for Original UNIFAC model with lipids and published parameters is presented in Figure 1. An example of quantitative and qualitative improvement of VLE prediction is presented in Figure 2 for monocaprylin – palmitic acid system.

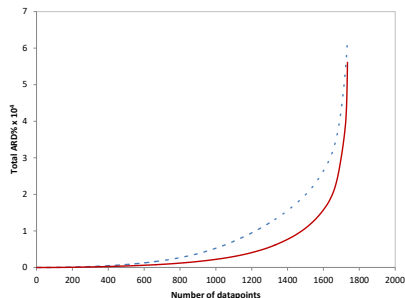


Figure 1: Cumulative ARD(%) for VLE prediction using Original UNIFAC model with published (- -) and lipids parameters (-).

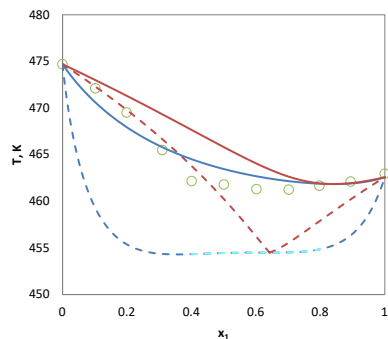


Figure 2. VLE prediction using Original UNIFAC model with published (- -) and lipids based (-) parameters for monocaprylin (1) – palmitic acid (2) system at 2.50 kPa [8] (o)

When extrapolated for SLE prediction, a slight overall improvement is noticed for Original and Modified UNIFAC models using the lipids-based group-

interaction parameters compared to the published parameters. An example of Original UNIFAC performance on SLE prediction is presented in Figure 3.

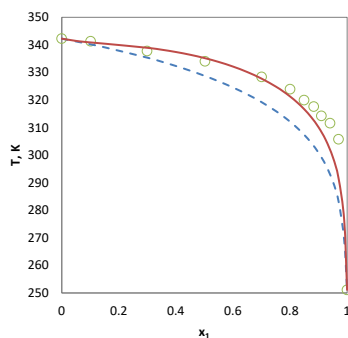


Figure 3. SLE prediction using Original UNIFAC model with published (- -) and lipids based (-) parameters for stearic acid – trilinoleine [9] (o).

Conclusions and future work

The method application for Original, Linear, Modified and Dortmund UNIFAC models using SPEED Lipids Database provides new sets of parameters for lipids mixtures which offer better performance of the models quantitatively as well as qualitatively. The validation of the parameters is done using VLE data. The prediction capabilities of the parameters are checked by extrapolation to SLE, where small improvements are achieved for lipids based parameters compared to the published parameters. The main drawback in developing and extending the predicting capabilities of the model remains the amount and quality of the available data. Further the parameters performances on LLE prediction will be checked.

The next step within the project is to apply and test the performances of the presented GC models in a lipids related process, such as solvent fractionation of Shea oil, which lead to added value products with application in confectionary fats industry as cocoa butter equivalents and cosmetic industry.

References

1. E. Fahy, S. Subramaniam, R.C. Murphy, M. Nishijima, C.R.H. Raetz, T. Shimizu, F. Spener, G. Van Meer, M.J.O. Wakelam, E.A. Dennis, *J. Lipid Res.* 50 (2009) 9–14.
2. O.A. Perederic, L.P. Cunico, S. Kalakul, B. Sarup, J.M. Woodley, G.M. Kontogeorgis, R. Gani. *J. Chem. Thermodyn.* (2017).
3. A. Fredenslund, R. Jones, J.M. Prausnitz. *AIChE J.* 21 (1975) 1086–99.
4. H. K. Hansen, B. Coto, B. Kuhlmann. Internal report. 1992.
5. D. Damaceno, O.A. Perederic, R. Ceriani, G. Kontogeorgis, R. Gani. *Fluid Phase Equilib.* (2017).
6. B. Larsen, P. Rasmussen. A. Fredenslund. *Ind. Eng. Chem. Res.* 26 (1987) 2274–86.
7. U. Weidlich, J. Gmehling. *Ind. Eng. Chem. Res.* 26 (1987) 1372–81.
8. L.P. Cunico, D.S. Damaceno, R.M. Matricarde Falleiro, B. Sarup, J. Abildskov, R. Ceriani, R. Gani, *J. Chem. Thermodyn.* 91 (2015) 108–15.
9. K. Nishimura, K. Maeda, H. Kuramochi, K. Nakagawa, Y. Asakuma, K. Fukui, M. Osako, S. Sakai, *J. Chem. Eng. Data.* 56 (2011) 1613-16.



Valentina Perna

E-mail: valper@kt.dtu.dk

Supervisors: Anne Meyer
Jane Agger

PhD Study
Started: December 2015
To be completed: November 2018

Laccase structure-function relations for enzymatic lignin modification

Abstract

With the increase of biofuel production, lignin is becoming a large by-product which is nowadays burned to produce energy. Lignin is composed by a large network of aromatic compounds and potentially very valuable and therefore a more sustainable way of using it could be to turn it into valuable chemicals through enzymatic reaction with laccase. In this work purification of a laccase from a white-rot fungi *Ganoderma lucidum* is studied and optimized with the final aim of obtaining a highly pure enzyme that can be used for crystallization and 3D structure determination.

Introduction

Lignocellulosic materials are employed in the production of biofuels. One of the major components of these feedstocks is lignin (20-30%), a hydrophobic biopolymer built of phenylpropanoid units, acting as a waterproof, protective shield in plant cells.

Unfortunately, due to the complexity, high degree of polymerization and hydrophobicity, lignin is the least exploited biomass component. The most common way to use lignin is by burning it for energy production but considering the fact that it is the only biopolymer exclusively composed of aromatic units [1], it could potentially be exploited to produce other valuable compounds and thereby contribute to the develop an efficient enzymatic conversion of lignocellulose.

Lignin modification in Nature can occur by different enzymes such as peroxidases, oxidoreductases and oxidases, but the best known lignin modifying enzyme is laccase (benzenediol: oxygen oxidoreductase, EC 1.10.3.2). Laccases belong to the multi-copper oxidase family and are produced by fungi, plants, insects and bacteria. The different origins of the enzymes result in laccases with different properties, e.g. activity and red-ox potential. However, all of them are able to catalyze phenol oxidation using O_2 as final electron acceptor and generate only H_2O as a harmless co-product, in contrast to peroxidases where hydrogen peroxide is also used.

Modification of lignin by laccase is not entirely understood since there are evidences that laccases are able to both polymerize and depolymerize [2, 3, 4]. One aim of the project is to investigate the ability of a laccase from white-rot fungi, i.e. *Ganoderma lucidum*, to modify lignin. As first steps production and

purification of the laccase has to be performed in order to characterize the enzyme both with respect to activity and 3D structure.

Specific objectives

In this part of the project purification and characterization of a laccase from *Ganoderma lucidum* a white-rot fungi is investigated. A two-step purification system has been developed and consists of anion exchange chromatography and size exclusion. Such a purification protocol results in a highly pure enzyme, suitable for crystallization.

Results and Discussion

Ganoderma lucidum laccase was produced in house using heterologous expression in *Pichia pastoris*.

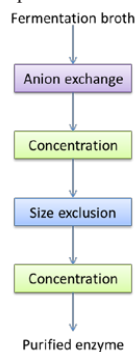


Figure 1: Flow chart of the enzyme purification.

In order to perform crystallization and thereby determine the enzyme's 3D structure, high purity enzyme has to be produced. Due to the presence of copper in the enzyme His-tag cannot be taken into consideration, His-tag purification column contains a nickel based resin which can interact with copper ion in the enzyme and inactivate the enzyme. The use of other tag has, moreover, to be avoided due to subsequent problem in the crystallization step. Therefore a two-step purification strategy was developed (Figure 1).

Anion exchange purification step is used as a step to remove all the native *Pichia pastoris* protein and salts from the fermentation broth. After anion exchange the protein solution is weak in concentration and needs to be concentrated. Hereafter, size exclusion is performed to remove salts from the anion exchange and to polish smaller impurities from the enzyme. The purification results in an increase in the specific activity (Table 1).

Optimization of the purification was achieved by optimizing the injection volume in both anion exchange and size exclusion, resulting in a higher yield of enzyme after anion exchange and good peak resolution in the size exclusion, all in all allowing higher enzyme purity (Figure 2).

Table 1: The table text is placed above the table.

Purification step	Total protein	Specific activity
	[mg]	[U/mg]
Culture filtrate	14.7	0.035
Anion exchange	3.5	0.040
Size exclusion	2.1	0.061

All fractions showing laccase activity after anion exchange were pooled and concentrated (as shown in Figure 1) prior size exclusion, in order to inject in the latter the highest protein concentration possible.

Purification quality was verified by running an SDS-page and shows the presence of a single band after size exclusion (Figure 2).

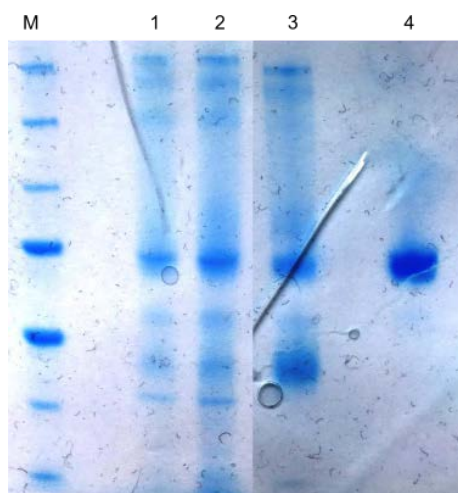


Figure 2: SDS page showing the purification steps. M: marker, 1: *G. lucidum* 1, 2: *G. lucidum* 2, 3: sample after anion exchange and 4: sample after size exclusion.

References

1. Ragauskas *et al.*, Science 344, (2014).
2. Munk *et al.*, Biotechnol Adv. , (2015) .
3. Sitarz *et al.*, Crit. Rev. Biotechnol., (2014)
4. Cañas *et al.*, Biotechnol Adv., (2010)

**Leander A.H. Petersen**

Phone: +45 8136 0919
E-mail: leape@kt.dtu.dk

Supervisors: Krist V. Gernaey
Anna E. Lantz
Ib Christensen, Unibio A/S

PhD Study
Started: October 2016
To be completed: October 2019

A biochemically structured model for *Methylococcus capsulatus*

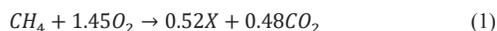
Abstract

To utilize *Methylococcus capsulatus* in a stable commercial scale production of single cell protein (SCP) a more sophisticated model for the apparent metabolic diversity is needed. A structured dynamic model able to account for the catabolic, anabolic, maintenance and co-metabolic processes is proposed and the uncertainty is investigated through Monte Carlo simulations with parameters from literature. The Monte Carlo uncertainty analysis showed that a satisfactory model prediction could not be achieved with the parameter values and standard model derivations found in literature. It is therefore necessary to carry out experiments and re-estimate the parameters.

Introduction

The methanotrophic bacterium *Methylococcus capsulatus* is capable of assimilating methane and oxygen into a protein rich biomass (up to 70% of the total dry weight content).

The process has historically been described by a combination of steady state stoichiometric coefficients (1) and unstructured Monod-like kinetics (2) [1]:



$$q_x = \mu_{max} \frac{[CH_4]}{K_{CH_4} + [CH_4]} \cdot \frac{[O_2]}{K_{O_2} + [O_2]} X \quad (2)$$

While this approach is not without merit for steady state operation, it offers little to describe (and thereby predict) deviations from ideal growth conditions under dynamic conditions.

It is a well-described phenomenon that ammonia (NH_3), the nitrogen source of choice, is readily oxidized to nitrite (NO_2^-) by *Methylococcus capsulatus* even at low extracellular concentrations if methane is not largely in excess [2,3]. This co-metabolic reaction not only makes the nitrogen source inaccessible for biomass production by the microorganism, but is also detrimental to the bioreaction as a whole because nitrite will act as an inhibitor.

To utilize *Methylococcus capsulatus* in a stable commercial scale production of single cell protein (SCP) a more sophisticated model for the apparent metabolic diversity is needed. Here, we propose a

structured model for the growth and co-metabolism of *Methylococcus capsulatus*.

The model is capable of predicting a dynamic transition from methane oxidation and cell growth to co-metabolism and nitrite production. Contrary to recent trends of making increasingly complex metabolic models for microorganisms, we have tried to keep the model as simple as possible, to allow applicability for both steady state and transient state operation while keeping computational time low, and to allow for the model to be used for process control applications.

Specific objectives

The model of the microbial metabolism of *Methylococcus capsulatus* must be able to accurately account for

1. A series of catabolic reactions in which methane (CH_4) is oxidized to carbon dioxide (CO_2) yielding energy in the form of ATP and/or reducing equivalents (eg. $NADH + H^+$)
2. A series of anabolic reactions in which the energy generated in the catabolic processes is used for maintenance and to assimilate carbon, oxygen and nitrogen into new living cells.
3. Finally a co-metabolic reaction resulting in oxidation of the nitrogen source due to molecular structural similarities between the CH_4 and NH_3 .

Results and Discussion

4 global reactions describing, catabolism, anabolism, maintenance and co-metabolism could be used to describe the 3 objectives. The 4 reactions can be seen in Table 1.

Table 1: Stoichiometric equations

Catabolism	$CH_4 + \frac{4}{3}O_2 + \frac{4}{3}NAD^+ + \frac{1}{3}H_2O \xrightarrow{q_s} CO_2 + \frac{4}{3}NADH + \frac{4}{3}H^+$
Anabolism	$CH_4 + (\frac{4}{3} + \frac{1}{2}\alpha)O_2 + \frac{1}{4}NH_3 + (\frac{19}{24} + \alpha)NADH + (\frac{19}{24} + \alpha)H^+ \xrightarrow{q_x} X + (\frac{19}{24} + \alpha)NAD^+ + (\frac{7}{6} + \alpha)H_2O$
Maintenance	$\frac{1}{3}NADH + \frac{1}{3}H^+ + \frac{1}{6}O_2 \xrightarrow{q_m} \text{maintenance} + \frac{1}{3}NAD^+ + \frac{1}{3}H_2O$
Co-metabolism	$\frac{1}{3}NADH + NH_3 + \frac{5}{2}O_2 \xrightarrow{q_n} NO_2^- + \frac{1}{3}NAD^+ + \frac{2}{3}H^+ + \frac{4}{3}H_2O$

Applying a pseudo steady-state assumption (common practice when modeling bioreactions) on the $NADH + H^+$ production and consumption would only lead to an unconstrained increase in methane oxidation to support the increased need for reducing equivalents when co-metabolism occurs, and this is not in agreement with reality.

An individual rate expression is therefore needed for each reaction and since multiple substrates can be limiting at different time points, extended Monod expressions are used [1,4]. The reaction rate expressions can be seen in Table 2.

Table 2: Rate equations

$$q_s = v_{CH_4} \cdot \min \left(\frac{\left(\frac{[CH_4]}{K_{CH_4}} \cdot \left(1 + \frac{[NH_3]}{K_{NH_3}} \right) + \frac{[CH_4]}{K_{CH_4}} \cdot \frac{[NADH]}{K_{NADH} + [NADH]} \right)}{\frac{[O_2]}{K_{O_2} + [O_2]}} \right) \cdot X$$

$$q_x = \mu_{max} \cdot \min \left(\frac{\left(\frac{[CH_4]}{K_{CH_4}} \cdot \left(1 + \frac{[NH_3]}{K_{NH_3}} \right) + \frac{[CH_4]}{K_{CH_4}} \cdot \frac{[NADH]}{K_{NADH} + [NADH]} \right)}{\frac{[O_2]}{K_{O_2} + [O_2]} \cdot \frac{[NH_3]}{K_{NH_3} + [NH_3]}} \right) \cdot X$$

$$q_m = m \cdot X$$

$$q_n = v_{NO_2} \cdot \min \left(\frac{\frac{[NH_3]}{K_{NH_3}} \cdot \frac{[NADH]}{K_{NADH} + [NADH]}}{\frac{[O_2]}{K_{O_2} + [O_2]} \cdot \left(1 + \frac{[CH_4]}{K_{CH_4}} + \frac{[NH_3]}{K_{NH_3}} \right)} \right) \cdot X$$

Values and standard derivation for each individual parameter in the stoichiometric equations and rate expressions were found in literature and supplemented with expert knowledge. A simple fed batch experiment with constant dilution rate was chosen as framework for model evaluation. Mass balances were set up for both the liquid and the gas phases. The initial conditions for the fed batch experiment were chosen based on expert knowledge.

The uncertainty of the model prediction was assessed using Monte Carlo simulations [5] through the steps recommended by [6]. A uniform uncertainty distribution was assumed. Results can be seen in Figure 1.

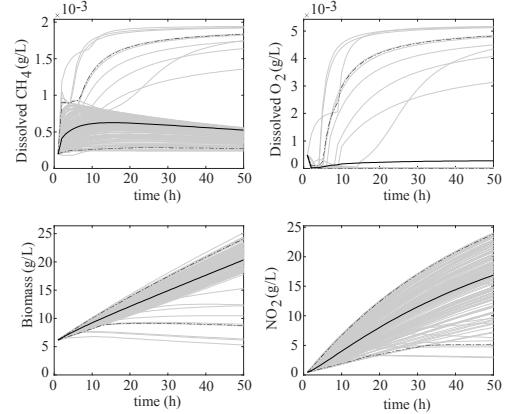


Figure 1: Results (gray), mean (black) and 95% confidential intervals (dash dotted) generated by the Monte Carlo simulations. The results were generated using 150 samples from the input space, using the Latin Hypercube sampling technique.

Conclusions

The uncertainty of a kinetic model for the microbe *Methylococcus capsulatus* with kinetic parameters found in the literature has been investigated through Monte Carlo simulations.

The Monte Carlo uncertainty analysis showed that a satisfactory model prediction quality could not be achieved with the parameter values and standard derivations found in the literature. It is therefore necessary to carry out the experiment and re-estimate the parameters.

References

1. J. Villadsen, J. H. Nielsen, and G. Lidén, *Bioreaction Engineering Principles*, 3rd ed. Springer US, 2011.
2. H. Dalton, "Ammonia oxidation by the methane oxidising bacterium *Methylococcus capsulatus* strain bath," *Arch. Microbiol.*, vol. 114, no. 3, pp. 273–279, 1977.
3. H. N. Carlsen, L. Joergensen, and H. Degn, "Applied Microbiology Biotechnology ©," pp. 124–127, 1991.
4. R. J.A, *Energetics and kinetics in biotechnology*. Elsevier Biomedical Press, 1983.
5. N. Metropolis and S. Ulam, "The Monte Carlo Method," *J. Am. Stat. Assoc.*, vol. 44, no. 247, pp. 335–341, 1949.
6. G. Sin, K. V. Gernaey, M. B. Neumann, M. C. M. van Loosdrecht, and W. Gujer, "Uncertainty analysis in WWTP model applications: A critical discussion using an example from design," *Water Res.*, vol. 43, no. 11, pp. 2894–2906, 2009.



Bo Pilgaard

E-mail: bpil@kt.dtu.dk

Supervisors: Lene Lange
Anne Meyer
Casper Wilkens

PhD Study

Started: August 2016

To be completed: July 2020

Systematic enzyme discovery, targeted to fungal and algal biomass

Abstract

Fungal and algal biomass has great potentials in the nutraceutical area and as health promoting alternate sources of foodgrade protein and glucan. Enzyme mediated bioprocessing is the best option for controlling and directing the specific product formation, however knowledge of the complete enzymatic degradation of these specific biomasses is lacking. This PhD study aims to elucidate various decomposition strategies in nature using state of the art bioinformatic and proteomic analysis, combined with molecular methods.

Introduction

Fungal biomass are worldwide an abundant by-product of several industries. Spent yeast cells from the brewing and insulin industry, excess mycelia from the mushroom industry and spent filamentous fungal biomass from the enzyme industry are some of the most prevalent examples. The biorefineries of the new and upcoming bio-economy era will also lead to significant growth in volume and diversity of fungal biomass. This is generally considered a low value by-product and currently used for medium priced animal feed or low priced biogas. However, both fungal polysaccharides and proteins have potential for high value food and feed ingredients; furthermore the interest in fungal polysaccharides and peptides is growing since studies suggest that they can play important roles as antifungal agents, in immunization against pathogens and having antitumor activity [1]. The standard methods of extracting the fungal polysaccharides consist of treating the biomass with high temperature and mild alkaline solutions and solvents, which only solubilizes a part of the constituents [2]. In order to elevate the whole fungal biomass to high-value products and to control the solubilisation, more research into the enzymatic breakdown is needed. Through evolution Fungi have developed unique compositions of their cell walls, metabolism and storage materials. It is a complex web of several types of polysaccharides and proteins. The complex synergy of enzymes going into the decomposition is further complicated by the variance of composition and structure of the cell walls both across and within the major fungal phyla of Ascomycota, Basidiomycota, Chytridiomycota and Zygomycota.

Furthermore the specific mode of attack from the antagonists can be various combinations of hyphal penetration, chemical and enzymatic attacks [3]. Overall this dynamic is poorly understood and the bulk of the current molecular research lies within the area of fungal mycoparasite host interactions, more specifically within certain *Trichoderma* species although mycoparasites also exists in the bacterial, oomycetes (stramenopile) and in all of the fungal phyla.

Macro-algae biomass is produced in even greater quantities for food purposes and like the fungal biomass there are great potentials in upgrading, not only the whole biomass, but also any potential waste streams from the new Blue (marine) Biorefineries to higher value products. The cell wall of macro-algae is likewise a recalcitrant and intricate web of polysaccharides, different from both plant and fungi, but with similarities to both [4]. For example both algae and fungi have an affinity for 1-3 and 1-6 β -glycosidic bonds in the glucan part of their cell wall, unlike the characteristic 1-4 bond known in the plant cell walls. Information of active enzymes for these polysaccharides are also lacking in the public databases and proper resolution of the decomposition strategies of saprobic and ectoparasitic organisms is imperative for gaining the necessary insights.

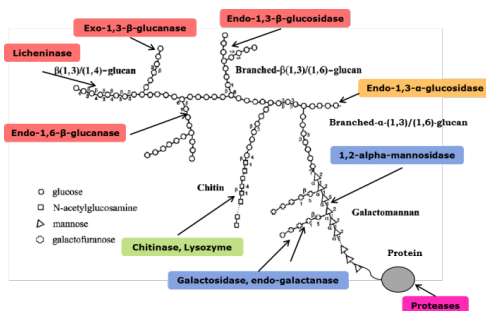


Figure 1: An approximation of some of the various polymers of the fungal cell wall [5] and some of the enzyme classes that targets them.

Specific Objectives

- To obtain a comprehensive understanding of the necessary enzymatic synergy for decomposition of the fungal/algal cell wall.
- To select and investigate specialized organisms from the bacterial, fungal and animal kingdom with the focus of highlighting each unique decomposition strategy.
- To shed light on the specific role of some of the more under-evaluated enzyme classes necessary for decomposition by expressing and characterizing members of these classes.
- To evaluate the use of these enzymes on spent fungal and algal biomass in an industrial process perspective.

Hypotheses

- Discovery of the diversity of enzymes breaking down fungal and algal cell wall and storage components will give basis for design of new processes for new types of value added products
- Fungal/algal cell wall degrading organisms across kingdoms and phylae vary in their enzyme repertoire and therefore also in their decomposition strategies.
- Effective Fungal/algal cell wall decomposition is possible solely via enzymatic reactions.
- The existing knowledge of the relevant enzymes is far from exhausted. Discovery of new context based reactions, novel enzymes and perhaps even new types of enzymes, will be a result of thorough analyses.

Current results and discussions

An extensive overview of carbohydrate active enzymes needed for complete fungal cell wall degradation has been established (figure 1) through literature studies and exploration of curated databases. Based on the same study, various obligate parasitic and mycophagous fungus strains and bacteria have been selected for screening of growth and enzyme production in laboratory. Similarly several marine fungi have been selected for the study of algal cell wall degrading enzymes. After selecting promising candidates they will undergo genomic and proteomic analysis, which will be the basis of a larger selection of target enzymes to express and characterize.

References

1. Wasser, S. Applied Microbial Biotechnology 60 (2002) 258–274.
2. Pinto, M. et al. Carbohydrate Polymers 116 (2015) 215–222.
3. Jeffries, P. Canadian Journal of Botany 73 (1995) 1284–1290.
4. Deniaud-Bouët, et al. Annals of Botany 114 (2014) 1203–1216.
5. Bernard, M., and Latgé, J.-P. Medical Mycology 39 (2001) 9–17.

**Katrin Pontius**

Phone: +45 4525 6194
E-mail: kpon@kt.dtu.dk

Supervisors: Anna Eliasson Lantz
Ivan Hundebøl
Krist Germaey

PhD Study
Started: December 2015
To be completed: January 2019

Auto-sampling and monitoring of bioprocesses

Abstract

Fermentations provide a highly demanding environment for reliable, stable and noise-free measurements and the measurements must provide demonstrable benefits without compromising the process. Consequently, fermentation production reactors are normally rather sparsely instrumented and typically only involve standard sensors such as pH, temperature and dissolved oxygen. Furthermore, robust, automatic sampling systems maintaining a sterile barrier and including a sampling preparation unit facilitating real-time analysis by more advanced methods like flow cytometry and NMR are increasingly under development on the market today. In order to allow further optimization of industrial fermentations, this project investigates and evaluates tools for process on-line monitoring devices that will supplement traditional on-line process data. It focuses on spectroscopy and image analysis as rapid and rather uncommonly used techniques acquiring real time fermentation data with respect to two different case studies.

Introduction

The establishment of economically viable processes through increasing product yields and reducing operating cost are one of the primary objectives of industrial bioprocess research and development. Industry is focusing increasingly on the development of more efficient and less time-consuming methods to monitor and control their fermentation processes at optimal conditions. By supplementing the standard monitoring tool-box only including pH, temperature and oxygen sensors with generic, robust and easy to use and apply monitoring devices it is possible to gain profound control regarding productivity and product quality. In order to select among the huge variety of potential on-line monitoring strategies proposed in literature including spectroscopy (IR, NIR, Raman, Fluorescence, NMR), flow-cytometry, image analysis and HPLC, two industrial production processes demonstrating state of the art protein production via recombinant microorganisms are considered as particular cases: a protease production process by *Bacillus* sp. as well as an insulin production process by yeast.

Specific objectives

The two particular case studies under investigation are:
Case study 1: Monitoring of phosphate and ammonium in the fermentation broth of an enzyme production

process by *Bacillus* evaluating vibrational spectroscopic techniques (IR, IR, Raman) in combination with partial least-square modelling.

Case study 2: Monitoring of the physiological state of an insulin producing yeast strain combining digital time-lapse microscopy and image analysis.

Case study 1

Phosphates and ammonium are central nutrients in media for *Bacillus* fermentations and need to be present in relevant levels to promote growth and enzyme production. Besides, there are also major challenges associated with phosphate and ammonium. Both species impose additional costs on downstream wastewater treatment if more is added to the medium than needed by the microorganism during the fermentation. Spectroscopic techniques are increasingly used for the monitoring of fermentation processes due to their ability to monitor a wide array of organic species including biomass, nutrients, metabolites, proteins and cofactors [1-5].

This case study focuses on the determination of phosphate and ammonium concentrations in a *Bacillus* enzyme production process. IR, NIR and Raman spectroscopy in combination with partial least square regression (PLS) are being employed in this work. Finally, the spectroscopic technique leading to the best results regarding both analyst will be selected and developed into an at-line set up for fermentation

monitoring. To minimize the complexity associated with spectroscopic measurements on fermentation broth and decouple natural correlations of parameters, synthetic samples spiked with phosphate or ammonium in addition to real fermentation samples were applied in the model development process. Thereby, regions of IR, NIR and Raman spectra tied to phosphate and ammonium were appropriately identified and selected. Exemplary the spectral region correlated with phosphates in varying concentrations is shown in figure 1.

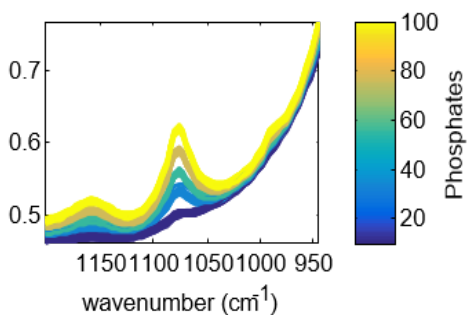


Figure 1: Section of an IR spectrum corresponding to different phosphate concentrations colored from blue (10 mM) to yellow (100 mM).

Case study 2

We want to take advantage of the recent advances in microscopy image analysis and evaluate its potential for on-/ at-line monitoring of yeast morphology during an insulin production process. In yeast cultures, cell size (distribution) has been shown to be correlated with cell viability (dead/alive⁶, osmotically stressed⁷) and growth rate⁸. Furthermore, the cell size was recently correlated to the accumulation of an internal product (fatty acids) in microalgae⁹. Consequently, image analysis seems to be a promising tool for getting a snapshot of the physiological state of a yeast culture during a production process.

The lately developed oCelloScope instrument¹⁰ enables rapid imaging and image analysis of a growing yeast culture. An example image with yeast cells identified is presented in figure 2. By analyzing images over the cultivation time we investigate the distribution dynamics of single cells, budding cells and cell aggregates, aiming at correlations between these morphological features and process performance. Reference data sets stating process performance are traditional fermentation data obtained by HPLC measurements (glucose, ethanol, glycerol, acetate, insulin) and off-gas analysis (CO₂). The method developed in case study two is taken into account to supplement this data set further with information about phosphate and ammonium uptake. We want to develop a real-time monitoring tool that may be used in industrial bioprocess set-ups. Within this approach, methodologies for automatic distinction between image

objects (single cells, budding cells, cell aggregates) are developed and first time trends of the morphology dynamics of an insulin production process have been achieved.

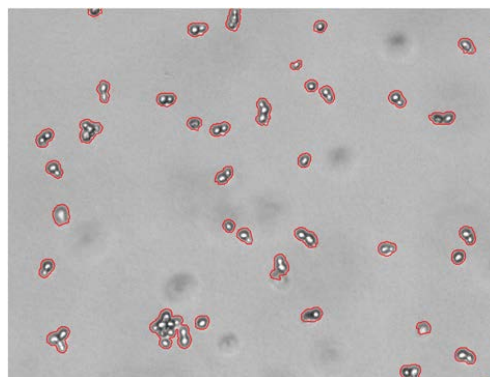


Figure 2: Image of a yeast culture showing with different objects (single cells, budding cells, cell aggregates) identified (red boundaries) by the image analysis software.

References

1. Harry L.T. Lee a, Paolo Boccazzib, Nathalie Gorreth, Rajeev J. Rama, Anthony J. Sinskeyb, In situ bioprocess monitoring of Escherichia coli bioreactions using Raman spectroscopy. *Vibrational Spectroscopy* 35: 131–137 (2004)
2. Marose S, Lindemann C, Ulber R and Scheper T, Optical sensor systems for bioprocess monitoring. *Trends Biotechnol* 17: 30–34 (1999).
3. Vaccari G, Dosi E, Campi AL, Gonzalezvara A, Matteuzzi D and Mantovani G, A near-infrared spectroscopy technique for the control of fermentation processes - an application to lactic-acid fermentation. *Biotechnol Bioeng* 43:913–917 (1994).
4. Boehl D, Solle D, Hitzmann B and Scheper T, Chemometric modelling with two-dimensional fluorescence data for claviceps purpurea bioprocess characterization. *J Biotechnol* 105:179–188 (2003).
5. Ronnest NP, Stocks SM, Lantz AE and Gernaey KV, Introducing process analytical technology (PAT) in filamentous cultivation process development: comparison of advanced online sensors for biomass measurement. *J Ind Microbiol Biotechnol* 38:1679–1690(2011).
6. Tibayrenc, P., Preziosi-Belloy, L., Roger, J. M. & Ghommidh, C. Assessing yeast viability from cell size measurements? *J. Biotechnol.* (2010).
7. Camisard, V., Brienne, J. P., Baussart, H., Hammann, J. & Suhr, H. Inline characterization of cell concentration and cell volume in agitated bioreactors using in situ microscopy: Application to volume variation induced by osmotic stress. *Biotechnol. Bioeng.* (2002).
8. Tyson, C. B., Lord, P. G. & Wheals, A. E. Dependency of Size of Saccharomyces cerevisiae Cells on Growth Rate. *J. Bacteriol.* 138, 92–98 (1979).
9. Marbà-Ardébol, A.-M., Emmerich, J., Neubauer, P. & Junne, S. Single-cell-based monitoring of fatty acid accumulation in Cryptocodinium cohnii with three-dimensional holographic and in situ microscopy. *Process Biochem.* 52, 223–232 (2017).



Carlos Eduardo Ramírez-Castelán

Phone:
E-mail: cara@kt.dtu.dk

Supervisors: Jakob K. Huusom
Anker D. Jensen
Angélica Hidalgo-Vivas, Haldor Topsøe
Jacob Brix, Haldor Topsøe

PhD Study
Started: November 2014
To be completed: February 2018

Optimal model-based monitoring of tubular reactors

Abstract

Achieving high quality information online is a challenge for a large range of processes in the chemical and biochemical industry. Even if it is possible to implement online sensors on the process, it constitutes a cost which requires the companies to optimize the sensor selection. This is especially true for processes with spatial variations as for the concentration and temperature in tubular reactors. Such processes are examples of nonlinear processes which require that the operator can get information of the nonlinear transient and profile in the system. Real time information of the state of the process is paramount in terms of online optimization through control and for ensuring product quality as well as a safe and reliable process operation.

Introduction

Modern refinery operations cover a wide and complex variety of processes, since the crude stills are the first major processing units, distillation processes are used to separate the crude oils by into fractions according to boiling point so that each of the processing units following will have feedstocks that meet their particular specifications. Higher efficiencies and lower costs are achieved if the crude oil separation is accomplished in two steps: first by fractionating the total crude oil at essentially atmospheric pressure; then by feeding the high-boiling bottoms fraction (topped or atmospheric reduced crude) from the atmospheric still to a second fractionator operated at a high vacuum.

Nevertheless, specific chemical reactions are vital for further refining stages such as hydrotreating, catalytic cracking, hydrocracking, hydroprocessing and hydrodesulfurization; terms that are used rather loosely in the industry because, in the processes hydrodesulfurization and hydrocracking, cracking and desulfurization operations occur simultaneously and it is relative as to which predominates.

Despite that, hydrotreating refers to a relatively mild operation whose primary purpose is either to saturate olefins, reduce the sulfur and nitrogen content of the feed, or both. It refers to a process in which petroleum products are catalytically stabilized and/or objectionable elements are removed from products or feedstocks by reacting them with hydrogen. Stabilization usually involves converting unsaturated hydrocarbons such as olefins and gum-forming unstable diolefins to paraffins.

Objectionable elements removed by hydrotreating include sulfur, nitrogen, oxygen, halides, and trace metals. Hydrotreating is applied to a wide range of feedstocks, from naphtha to reduced crude. When the process is employed specifically for sulfur removal it is usually called hydrodesulfurization. Catalytic hydrotreatment is essential to obtain fuels with improved quality and low polluting compounds content (sulfur, nitrogen, aromatics). Catalytic cracking is the most important and widely used refinery process for converting heavy oils into more valuable gasoline and lighter products over 1 million tons/day of oil processed in the world [1].

In the case hydrotreating, and other large scale processes, it is not always possible to directly measure the important state variables online which are needed by the operator to judge if the plant is behaving as planned or not. If these cannot be determined by indirect measurements, then the information can be constructed by means of a state estimator using a process model and the available measurements from the system. Examples of such systems are the spatial concentration and temperature profiles inside tubular reactors, more specifically trickle-bed reactors that play an important role in the overall refinery flow.

Trickle bed reactors

A unique characteristic of trickle-bed reactors compared to other types of three-phase reactors is, in general, the catalyst particle is filled with liquid while the outer surface may not be completely wet or covered by the

flowing liquid which leads to a more direct contact between the gas phase and the catalyst [2].

The operation conditions of trickle-bed reactors are too hostile or fouling for sensors to work. In such cases, the system measurements must be made whether by sampling and lab analysis, which results are issued with significant delay, or using state estimators that may also incorporate information of known disturbances from feed mixture analysis or upstream data. For these reasons, trickle-bed reactors are difficult to operate due to the coupling between transfer phenomena, non-linear kinetics and their distributed nature which can lead to temperature hot spots in the catalytic bed or formation of an undesired compound. In that sense, online information of the current state of the process is important for the operator or any model based control algorithm for process optimization. Especially when a system may be operated close to a process constraint or the operator needs to avoid an unstable region which may lead to run away or undesired reactions.

Given known process inputs the model can predict online what the state of the process is and what the sensors should measure. By comparison between actual and predicted measurements, corrections in the model predictions can be made through a systematic algorithm which utilizes the statistical uncertainty of the measurements. Linear state estimators such as the Kalman filter is in wide-spread use but advanced monitoring of nonlinear process behavior in tubular reactors by nonlinear state estimators could reduce the risk of having a product that does not meet specifications significantly or conditions that reduce the performance of the catalytic bed.

For that reason, if the reaction rate depends on the liquid reactant, the wetting efficiency leads to reduced global reaction rates, on the other hand, if the reaction rate is controlled by the gas phase, the global reaction rate is higher since the resistance to mass transfer in the non-wetted surface is lower than in the covered surface [3]. Figure 1 shows the concept of trickle flow.

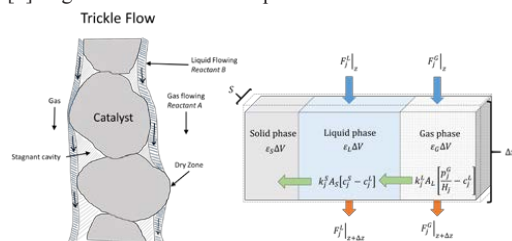


Figure 1: Trickle flow in fixed bed reactors

A model of the trickle-bed reactor is derived from the mass and energy equations according to the law of conservation to a small element of volume. The focus of interest is the nonstationary volume element, fixed in space, through which a fluid and gas are flowing and chemical reactions taking place only in the solid phase. The model of a trickle-bed reactor can be validated with

experimental data [4], and will allow to develop the state estimation of representative real case studies aiming towards the implementation of optimal model-based monitoring.

Current status

The petroleum feedstock contains a complex mixture of hydrocarbon compounds, therefore the phase distribution must be addressed to accurately describe the temperature and concentration profiles in the reactor. The model, solved using a finite differences scheme in MatLab, is able to describe the dynamic concentration and temperature profiles along the reactor. In order to describe the phase change, the simulation of the system is achieved by developing a framework that allows the information exchange between MatLab and ProII. Using the database available from ProII for petroleum streams, the framework consists in a dynamic model of a trickle-bed reactor, solved in Matlab, coupled with a flash calculation carried out in also ProII. This approach reduces the complexity of the numerical solution compared to the solution of a model that considers vaporization of complex petroleum Feedstocks. The objective is to apply this simulation framework to a real large-scale hydrotreating process.

Objectives

The aim of this project is to develop a generic optimal-model based monitoring framework suited for a wide range of tubular reactor applications of industrial relevance but the results may also be extended to other process system with similar characteristics.

Acknowledgements

This project is being developed with the collaboration of Haldor Topsøe A/S and founded by Consejo Nacional de Ciencia y Tecnología (CONACyT), Mexico.

References

1. James H. Gary, Glenn E. Handwerk, Mark J. Kaise Petroleum Refining: Technology and Economics, Fifth Edition, 2007.
2. AlDahhan, M. H.; Larachi, F.; Dudukovic, M. P.; Laurent, A. High-Pressure Trickle-Bed Reactors: A Review. *Ind. Eng. Chem. Res.* 1997, 36 (8), 3292-3314.
3. Herskowitz, M. Trickle-Bed Reactors: A Review. *AIChE Journal* (Vol. 29, No. 1) January, 1983.
4. Mederos, Fabián. Ancheyta, Jorge. Mathematical modeling and simulation of hydrotreating reactors. *Applied Catalysis*, 332 (2007) 8-12.



Kristian Viegaard Raun

E-mail: krvie@kt.dtu.dk

Supervisors: Anker Degn Jensen
Martin Høj
Max Thorhauge, Haldor Topsøe A/S
Jan-Dierk Grundwaldt, KIT

PhD Study

Started: October 2015
To be completed: September 2018

Next generation methanol to formaldehyde selective oxidation catalyst

Abstract

Formaldehyde (CH₂O) is one of the most important industrial intermediate chemicals, with an approximate production of 52 million ton in 2017 [1]. Formaldehyde is synthesized by selective oxidation of methanol over an iron-molybdate (Fe-Mo) oxide catalyst. The average lifetime of the industrial catalyst is only 1-2 years depending on the operating conditions. This work presents a study of the continuous deactivation behavior and structural changes in the Fe-Mo catalyst during selective oxidation of methanol to formaldehyde, determined by prolonged activity tests and comprehensive characterization of spent catalyst.

Introduction

Formaldehyde (CH₂O) may be synthesized industrially by selective oxidation of methanol over an iron-molybdate (Fe-Mo) oxide catalyst according to:



The reaction is normally carried out in a multitubular reactor with excess of air at 250-400 °C (yield = 90-95 %), known as the Formox process [2]. The average lifetime of the industrial catalyst is only 1 – 2 years depending on the operating conditions. The catalyst consists of a bulk phase of Fe₂(MoO₄)₃ and a surface layer phase of MoO₃. The MoO₃ surface is selective towards formaldehyde while the iron in the sublayer increases the activity of the catalyst [3]. Pure MoO₃ in itself has low activity. Literature from the last decades agrees that the major reason for the deactivation is loss of molybdenum from the catalyst. Molybdenum forms volatile species with methanol and migrate along the reactor bed, which can leave behind Mo poor zones. The catalyst is usually prepared with excess MoO₃ (Mo/Fe > 1.5) to counter the loss of Mo.

Ivanov and Dimitrov [4] performed an experiment at industrial conditions over several months to investigate the deactivation of iron-molybdate catalyst. Over time they observed axial changes in the composition of the catalyst through the test-reactor. The molybdenum content was decreased significantly in the initial zone of the reactor and slightly increased in the subsequent

zone. This shows that during operation of the catalyst molybdenum species migrate along the catalyst bed.

As the molybdenum migrate away from the initial zone of the reactor, the molybdenum rich phase of the catalyst surface changes and iron rich phases are exposed. The iron rich catalyst surface decreases the selectivity towards formaldehyde due to formation of CO and CO₂.

This work presents a study of the deactivation behavior of Fe-Mo oxide catalyst during selective oxidation of methanol to formaldehyde in a period of 600 hours. The structural changes after 10, 100, 250 and 600 hours on stream in a fixed bed reactor have been determined by comprehensive characterization including: XRD, Raman spectroscopy, XPS, SEM-EDX and STEM-EDX.

Specific Objectives

The objectives of the project are to:

- Develop improved iron molybdate catalyst synthesis, by exploring novel catalyst preparation methods and by addition of promoters.
- Obtain a complete understanding of the reaction mechanism and kinetics of methanol selective oxidation over iron molybdate catalyst.
- Understand catalyst deactivation and molybdenum transport through the catalyst bed.

Results and Discussion

Fe-Mo oxide with Mo/Fe molar ratio = 2.0 was prepared by hydrothermal synthesis. The fresh catalyst was characterized by ICP-OES, XRD, Raman spectroscopy, XPS, SEM-EDX and STEM-EDX. The catalyst (150-250 μm) was tested in a fixed-bed reactor. The feed gas consisted of 10 % O_2 and ~5 % MeOH in N_2 . Before each experiment the catalyst was thermally treated at 400 $^\circ\text{C}$ in air for two hours. The reactors were heated to 375 $^\circ\text{C}$ during operation. The spent catalyst from the fixed-bed experiment was characterized by XRD, Raman spectroscopy, XPS, SEM-EDX and STEM-EDX.

Figure 1 shows the conversion of MeOH, the selectivity towards formaldehyde and the reversible product DME, and the catalyst bed temperature, for the catalyst tested in the fixed-bed reactor.

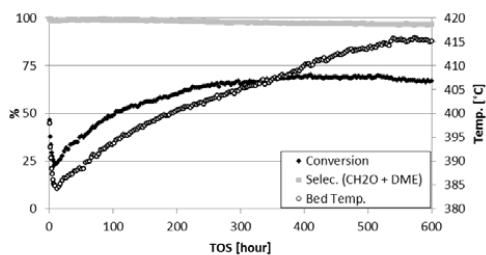


Figure 1. MeOH conversion, combined formaldehyde and DME selectivity, and catalyst bed temperature in the fixed bed reactor. Operating conditions: 25 mg catalyst diluted in 170 mg SiC, ~157.5 NmL/min gas feed: 10 % O_2 , ~5 % MeOH in N_2 . Other products: CO and CO_2 .

The results of the activity test shows an initial deactivation period of 10 hours, where the methanol conversion decreased as a function of time from 47 – 24 %). In this period the combined selectivity towards formaldehyde and DME is high (>98 %). The initial deactivation period where followed by a period up to ~250 hours where the conversion increased slowly to 64 %. In the period between 250 and 600 hours only small changes in the conversion was observed. At 530 hours the conversion starts to decrease slightly. Throughout the experiment CO and CO_2 are formed. At ~150 hours both CO and CO_2 increase slowly in the remaining period of the experiment. As a result of the CO and CO_2 formation the product selectivity decreased to 97 % at the end of the experiment. The initial bed temperature were 398 $^\circ\text{C}$ and decreased to 384 $^\circ\text{C}$ during the first 10 hours followed by and increase to 416 $^\circ\text{C}$ through the remaining experiment. The varying temperature is due to the exothermic oxidation reactions and the catalyst activity towards CH_2O , CO and CO_2 respectively.

The structural changes in the catalyst after 10, 100, 250 and 600 hours on stream was determined by comprehensive characterization as follows.

The XRD data confirm that the fresh catalyst consist of ferric iron molybdate phase ($\text{Fe}_2(\text{MoO}_4)_3$) and MoO_3 . After 10 hours on stream no MoO_3 is detected in the catalyst which must be due to the sublimation of the MoO_3 under reaction condition. The iron molybdate phase is not subject to molybdenum loss due to replenishment from the former excess MoO_3 phase. After 100 hours on stream some of the initial ferric iron molybdate phase ($\text{Fe}_2(\text{MoO}_4)_3$) has been reduced to the less molybdenum rich ferrous phase (FeMoO_4). After 250 hours on stream more of the ferrous phase has been formed. After 600 hours the catalyst is subject to significant degrees of molybdenum loss. None of the initial ferric phase is detected and a significant amount of hematite is present in the catalyst. The surface chemical compositions of the fresh and spent catalysts were studied by XPS. After 600 hours on stream the surface Mo/Fe ratio was reduced to 0.38, which is significant under stoichiometric ($\text{Fe}_2(\text{MoO}_4)_3 = 1.50$). However, the selectivity at this point in the activity test is rather high (combined formaldehyde and DME selectivity = 97 %). This shows that even small amounts of molybdenum present at the catalyst surface yield a rather selective catalyst.

Conclusions

In the present study iron molybdate catalyst (Mo/Fe = 2) were tested under reaction conditions for up to 600 hours on stream. During operation the activity and compositional changes in the catalyst have been investigated by comprehensive characterization. Most of the excess MoO_3 sublimate during the initial 10 hours under reaction, which result in a 2 fold activity decrease of the catalyst. While the excess molybdenum phase is present in the catalyst it has a replenishing effect on the iron molybdate phase. In the period following the initial sublimation of MoO_3 , the iron molybdate phase becomes subject to leaching of molybdenum leading to less selective iron rich phases (FeMoO_4 and Fe_2O_3). However, the catalyst surface remains molybdenum rich in some degree due to segregation of molybdenum from the crystal bulk. The selectivity does only decrease slightly through the activity test even at significant loss of molybdenum.

Acknowledgements

This project is a collaboration between the CHEC research center at DTU Chemical Engineering and Haldor Topsøe A/S. Financial support from The Independent Research Council (DFF – 4184-00336) is gratefully acknowledged.

References

1. Merchant Research & Consulting Ltd, World Formaldehyde Production to Exceed 52 Mln Tonnes in 2017, (2016).
2. C. Brookes et al. ACS Catal. 4 (1) (2014) 243-250.
3. M. Rellán-Piñeiro and N. López. ChemSusChem. 8 (13) (2015) 2231-2239.



Giulia Ravenni
Phone: +45 93511592
E-mail: grav@kt.dtu.dk

Supervisors: Ulrik Birk Henriksen
Jesper Ahrenfeldt
Zsuzsa Sárosy
Benny Gøbel, Ørsted

PhD Study
Started: December 2015
To be completed: December 2018

Tar conversion for gas cleaning in biomass gasification by using biochar

Abstract

This project investigates the potential of repurposing residual gasification char to clean and upgrade biomass producer gas. At first, the interaction between tar model compounds and the surface of chars has been investigated on a laboratory scale, using dedicated setups at DTU and at TU Berlin. Promising results on the decomposition of model tars have led to the design of a larger reactor, to test the effectivity of a char bed in cleaning producer gas with high tar load (30 g/Nm³). The gas was generated in a 100kW_{th} Low Temperature Circulating Fluid Bed (LT-CFB) gasifier at DTU, Risø. Preliminary results suggest that the use of residual char is promising for gas treatment.

Introduction

Biomass producer gas is rich in heavy and easily condensable hydrocarbons (tars) that cause problems in downstream processes, hindering the catalytic conversion of syngas to sustainable fuels. The carbonaceous products of gasification or pyrolysis (chars) and active carbons (AC) have been found effective in adsorbing aromatics [1] and active as a catalyst for tar conversion [2]. Therefore they may be applied to gas cleaning: particularly, the use of residual char from gasification would represent a favourable solution for downstream tar removal in biomass producer gas. Char is continuously produced and once it is spent it can be recycled in the system along with fresh feedstock. Moreover, residual char is currently considered as waste, therefore its repurposing would represent an economic benefit, especially for small-scale gasifiers.

The char produced in the TwoStage gasifier (also known as “Viking” gasifier) presents interesting properties, somehow similar to commercial AC. Indeed, the Viking char has a Brunauer–Emmett–Teller (BET) specific surface area over 1000 m²/g, and a pore volume of 0.7 cm³/g, according to the Density Functional Theory (DFT) method. Moreover, it contains inorganics (mainly Ca, Si, K) which are well dispersed on the surface. These characteristics suggest that this material could act as a catalyst to reform tar into stable gases (H₂, CO, CH₄), if used for treating biomass producer gas. The application of carbonaceous materials for removal of tars has been reported by several authors

[2]–[5]. Particularly, the effectivity of this solution appears to be higher when coupled with partial oxidation of the producer gas prior to the passage to a fixed bed of char [6].

However, further research is needed in order to determine which are the char characteristics and the reaction conditions that can guarantee a stable and effective removal of tars.

Specific objectives

This work is aimed at demonstrating the feasibility of using residual gasification char for cleaning and upgrading producer gas. Laboratory tests have been used to evaluate the effect of Viking char on model tar compounds. Experiments were designed also to compare its performance with ACs and, in general, to identify the processes involved in the interaction between aromatic molecules and the surface of chars. The results of tar adsorption and decomposition experiments at different temperatures were used to design a test reactor for real biomass producer gas, generated by the 100kW_{th} Low Temperature Circulating Fluidized Bed (LT-CFB) gasifier at DTU, Risø. The tests on actual producer gas will be used to verify the feasibility of the char-based cleaning system and to optimize the operational parameters such as temperature and excess air ratio (λ) for the partial oxidation step.

Experimental activity

A laboratory setup was built at DTU laboratories to test the effect of a char bed on tar model compounds at

different temperatures. A flow of N_2 (1 l/min), entrained with a model compound (phenol or naphthalene) was passed in a heated reactor, containing the char bed. The gaseous stream was sampled before and after the passage through the bed, using Solid Phase Adsorption (SPA) technique.

Further experiments were performed by using a similar setup developed at TU Berlin (Fig. 1). This system was equipped with a syringe pump to add a mix of toluene and naphthalene to a N_2 flow. The gas was then passed in a heated tubular reactor housing a char bed. The concentration of tar model compounds were continuously monitored with a Gas Chromatograph with Flame Ionization Detector (GC-FID), and the permanent gas composition was measured with a micro GC: both instruments automatically sampled the gas flow in regular time intervals.

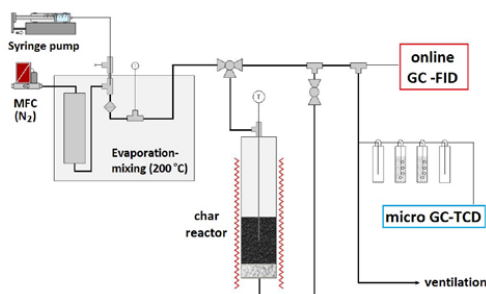


Figure 1: Diagram of experimental setup at TU Berlin

The setup was used for testing three different chars (Viking char and 2 different ACs) in the temperature range 250 to 800 °C.

For the larger scale tests at the LT-CFB gasifier, a reactor has been designed and connected to the producer gas outlet pipe. The reactor contained a grate to support a fixed bed of char, and was equipped with an air inlet to partially combust the gas prior to the passage through the bed. The quality of the LT-CFB producer gas has been assessed in detail before and after the passage through the cleaning step. Producer gas analysis included tar quantification and analysis, stable gas composition, presence of S and Cl compounds. Preliminary tests were run with a 300g char bed and a producer gas flow of 30 l/min, with and without air injection.

Results and Discussion

Results from the laboratory setup at DTU suggest that the char bed is able to efficiently remove aromatics from a gaseous stream at 250 °C, 500 °C and 600 °C. However, the nature of the interaction between char and model tars is probably limited to physical adsorption at these temperatures. This is confirmed by the diminished effect on naphthalene at higher temperature (600 °C). Preliminary results from the setup at TU Berlin showed that the performances of the three chars in adsorption

test are comparable. The H_2 production was observed starting from 600 °C. At 800 °C, also CH_4 was produced in the reactor (Fig.2).

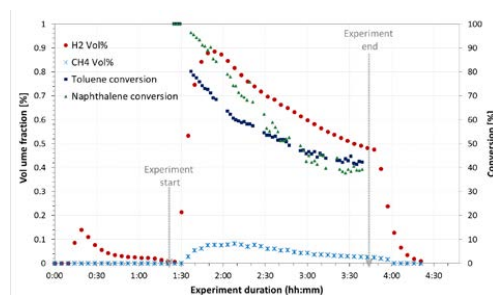


Figure 2: Results from “Viking” char test at 800 °C

In general, the presence of char in the reactor favored the cracking of toluene and naphthalene as showed by an increase of the H_2 concentration at the outlet, in comparison with empty reactor condition.

Preliminary results from the tests on real producer gas showed a significant tar reduction after the passage through the char reactor. At the same time, a marked increase in H_2 , CO, and CH_4 was observed in comparison with the raw producer gas. The effect of the char bed was stable for the whole experiment duration (90 minutes). Further tests on a longer time scale will verify the long term stability of the char bed for cleaning and upgrading biomass producer gas.

Acknowledgments

This work is financially supported by Innovation Fund Denmark as part of the project “Synfuel - Sustainable synthetic fuels from biomass gasification and electrolysis”

Special thanks to Dr.-Ing. Y. Neubauer and Ing. O.H. Elhami for the fruitful collaboration during the external research stay at the Institute for Energy Engineering of TU Berlin.

References

1. A. M. Mastral, T. García, R. Murrillo, M. S. Callén, J. M. Lopez, M. V Navarro, J. Galbán, *Energy & Fuels*, 16, 669–676, 2003.
2. D. Fuentes-Cano, A. Gómez-Barea, S. Nilsson, P. Ollero, *Chem. Eng. J.*, 228, 1223–1233, 2013.
3. S. Hosokai, K. Kumabe, M. Ohshita, K. Norinaga, C. Li, J.-I. Hayashi, *Fuel*, 87, 13–14, 2914–2922, 2008.
4. N. Klinghoffer, M.J. Castaldi, A. Nzihou, *I&Ec*, 13113–13122, 2012.
5. X. Nitsch, J.-M. Commandré, J. Valette, G. Volle, E. Martin, *Energy & Fuels*, 28, 6936–6940, 2014.
6. S. Zhao, Y. Luo, Y. Zhang, Y. Long, *J. Anal. Appl. Pyrolysis*, 112, 262–269, 2015.

**Łukasz Ruszczyński**

Phone: +45 4525 2912
E-mail: lrus@kt.dtu.dk

Supervisors: Jens Abildskov
Gürkan Sin
Alexandr Zubov

PhD Study
Started: May 2016
To be completed: April 2019

Thermodynamic modelling and data evaluation for life sciences applications

Abstract

In the case of available experimental data for the systems containing biomolecules, there is a strong need for reliable data as well as for validation of their consistency. It was shown that for solid- and liquid-liquid equilibria data, validation using fluctuation solution theory (FST) could be applied. Substantial part of work is devoted to the development of the methodology for data validation, which includes development of the correlation models, production of initial guesses for parameter estimation and evaluation of the model parameters, including their uncertainty as well as criteria for discrimination among reliable and questionable data. We have reported the initial steps for validating the temperature dependence of binary LLE. For considered FST-based model uncertainties of parameter estimates and predicted compositions are provided using information related to the covariance matrix of the estimation problem.

Introduction

The reliable knowledge of thermodynamic properties of multicomponent systems is of the central importance in chemical engineering. Solid- and liquid-liquid equilibria (SLE and LLE, respectively) are important thermodynamic phenomena in a wide range of downstream separations and formulated products. Hence, over past decades much research has led to useful thermodynamic models for prediction of properties from limited data. However, most models require determination of a number of physical properties and several model parameters, compared to the available data. Moreover, the measured values are often uncertain and many measurements are required to build reliable data sets for parameter identification. Lack of interaction parameters between biomolecules (such as drugs) and solvents, as required in group contribution methods, makes the conductor-like screening (COSMO)-based activity coefficient models [1, 2] attractive. Predictions can be made prior to as well as in the absence of experimental data, which renders this class of models fully predictive. Although and because many relevant data are published, there is a strong need for reliable data as well as their evaluation [3, 4]. We have explored and refined a methodology for correlation and validity checks for solid- and liquid-liquid equilibria, SLE [5] and LLE [6] based on the fluctuation solution theory. We have formulated LLE with the unsymmetrical convention for normalizing activity

coefficients of dilute species. An inherent part of the method is the estimation of initial guesses for parameter estimation and evaluation of obtained parameters. For that purpose, graphical representation method as well as the molecular predictive models like COSMO-SAC [1] model was applied, since parameters in the model are connected to the other measurable thermodynamic properties. In addition, uncertainties of parameter estimates as well as of predicted compositions are provided using information related to the covariance matrix of the estimation problem.

Specific objectives

The focus of this PhD project is a thermodynamic modelling of systems containing biomolecules or in general organic compounds whose structure includes more than one functional group such as active pharmaceutical ingredients (APIs) and equilibria between them and molecular solvents or ionic liquids.

Crucial part of the work is the improvement database of measurements including solid-liquid and liquid-liquid equilibria with systems relevant for life sciences (e.g. pharmaceuticals) including uncertainty analysis. Therefore, there is a need for reliable data as well as their evaluation. It was shown that for SLE data validation using FST (fluctuation solution theory) could be applied [5, 7]. In the developed FST model for SLE parameters are 2-parameter temperature dependence for activity coefficients at infinite dilution and 1-parametr

expression for solute non-ideality relative to infinite dilution. Important and inherent part of this task is the estimation of initial guesses for parameter optimization and evaluation of obtained model parameters. The natural extension is the development of the FST model to LLE validation. So far, model for binary Tx LLE correlation and validation outside the critical region has been formulated.

Modelling methodology

The binary LLE problem consists of solving a set of two equilibrium equations (isofugacity criterion).

We use different standard states for the components in both phases α and β , assuming that phase α is rich in component 1 and phase β is rich in component 2 and introduce unsymmetrically normalized activity coefficients γ_i^* .

FST provides the expansion of the unsymmetrical activity coefficient for the components in both phases (each with one c parameter) and the infinite dilution activity coefficient is a function only of temperature and is usually modelled with 2 parameters for each phase, a and b . The final model (with potentially six parameters in total) is represented by the following equations:

$$\ln x_1^\alpha - \frac{c^\alpha}{T} (1 - x_1^\alpha)^2 = \ln x_1^\beta + \frac{c^\beta}{T} [2x_1^\beta - (x_1^\beta)^2] + a^\beta + \frac{b^\beta}{T} \quad (1)$$

$$\ln (1 - x_1^\alpha) + \frac{c^\alpha}{T} [1 - (x_1^\alpha)^2] + a^\alpha + \frac{b^\alpha}{T} = \ln (1 - x_1^\beta) - \frac{c^\beta}{T} (x_1^\beta)^2$$

We have applied two steps for parameter estimation. First is to regress the (a , b) parameters in both phases, with fixed c^α and c^β parameters, provided by COSMO-SAC model. We minimize an objective function defined as the sum of the squared differences between the experimental and calculated phase mole fractions. After that, one can regress simultaneously all six parameters. For the initial guesses, the graphical representation was applied. Values of c need to be negative, liquid-liquid split occurs only in systems with positive deviation from ideality [6].

Results and discussion

The developed procedure has been tested in several binary LLE cases including systems with ionic liquids and water or classical solvents commonly used in downstream separations. The overall performance in data fitting (absolute average relative deviation) was found to be approximately 5%. Comparisons with results from the NRTL model indicate mostly similar reliability within 95% confidence limits.

Regression of all six parameters showed that c is hard to identify, especially when a miscibility gap for considered system is very wide [6].

The initial guesses obtained from a graphical representation of experimental data were successfully used in a parameter regression. Prediction of a , b and c by the COSMO-SAC model is only qualitative.

In data evaluation, it was assumed that those experimental points, which lies inside a calculated 95% confidence intervals on the predicted by model molar

fractions are recommended. Those outside are questionable.

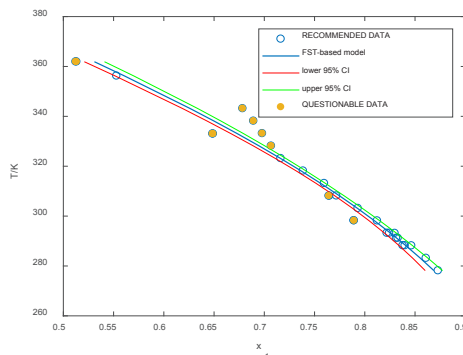


Figure 1: LLE data validation in [bmim][PF₆] (1) / butan-1-ol (2) system [8].

Conclusions and future work

A model has been constructed and tested for the correlation of binary LLE data over ranges of temperature. At least four parameters are needed, which is similar to current models. Depending upon the relative solubilities, additional parameters may be needed. A model is applicable for data validation. The future work will be to develop the criteria for further data validation as well as an extension to three component systems.

Acknowledgements

This project has received funding from European Union's Horizon 2020 research and innovation programme under the Marie Skłodowska-Curie grant agreement No. 675251.

Web-link: <http://www.modlife.eu>

References

1. S.T. Lin, S.I. Sandler, *Ind. Eng. Chem. Res.*, 2002, 41, 899.
2. A. Klamt, *J. Phys. Chem.*, 1995, 99, 2224.
3. M. Frenkel, *J. Chem. Thermodynamics*, 2015, 84, 18.
4. V. Diky, J.P. O'Connell, J. Abildskov, K. Kroenlein, M. Frenkel, *J. Chem. Eng. Data*, 2015, 60, 3545.
5. L.P. Cunico, R. Ceriani, B. Sarup, J.P. O'Connell, R. Gani, *Fluid Phase Equilibria*, 2014, 362, 318.
6. Ł. Rusczyński, A. Zubov, J. P. O'Connell, J. Abildskov, *J. Chem. Eng. Data*, 2017, 62, 2842.
7. Ł. Rusczyński, A. Zubov, G. Sin, J. Abildskov, *Proceedings of the 27th European Symposium on Computer Aided Process Engineering - ESCAPE 27*, 2017, 247.
8. Ana B. Pereiro, A. Rodriguez, *J. Chem. Eng. Data*, 2007, 52, 1408.

**Vickie Schultz-Falk**

Phone: +45 61893003
E-mail: vjen@kt.dtu.dk

Supervisors: Peter Arendt Jensen
Mette Solvang, ROCKWOOL International A/S
Lars E. Hansen, ROCKWOOL International A/S

PhD Study
Started: August 2016
To be completed: July 2019

Optimized waste recycling in an integrated melting furnace (IMF) for stone wool melt production

Abstract

Stone wool waste is generated either during the production process or when buildings are renovated or demolished. This project aims at understanding the behavior of stone wool waste that is recycled back into the melting unit of the stone wool production process. The goal is to optimize the process and increase the recycling amounts. This will be done by obtaining fundamental knowledge of the melting behavior of conventional raw materials and stone wool waste, by conducting full scale tests on existing melting furnaces, and development of a model of the process.

Introduction

Stone wool is produced by melting raw materials and subsequently spinning the 1500 °C melt into fibers using a cascade spinner [1]. Conventional raw materials are mineral materials obtained from quarries. It is also possible to use secondary raw materials i.e. waste materials from other industries and thus re-cycling material that would otherwise have been landfilled. This is also possible for direct recycling of stone wool waste back into the stone wool production process. Stone wool waste is generated either during production, where shaping of the products leads to waste, but also when buildings are renovated or demolished.

This PhD study focuses on a new cyclone based melting technology; the IMF. In the IMF conventional stone wool raw materials and stone wool waste is blown tangentially into a melting cyclone along with coal, oxygen and natural gas. This generates a swirling motion inside the cyclone in which combustion of the fuel and heating of the feed takes place. The cyclone motion results in the separation of molten particles and the flue gas.

Specific Objectives

The aim of the project is to understand the behavior of recycled stone wool waste in the IMF. This will be done through the following steps:

- (i) Material characterization of a conventional stone wool charge and recycled stone wool waste
- (ii) Particle sampling and full scale tests on an IMF production plant
- (iii) Building a mechanistic process model

Results and Discussion

A series of samples comprising 0%, 25%, 50%, 75% and 100% conventional stone wool charge and 100%, 75%, 50%, 25% and 0% stone wool waste, respectively, are investigated using three different techniques [3]. X-ray Diffraction (XRD) is used to determine the crystalline content of the samples after different heat treatments. Hot Stage Microscopy (HSM) is used to obtain visual indications of the melting temperatures of the samples. The results are seen on Figure 1, showing that stone wool waste melts at lower temperatures than the conventional raw material mix. Simultaneous Thermal Analysis (STA) is used to obtain heat capacity curves of the samples as they are heated up [2]. The heat capacity curves allows for integration and calculation of the total energy requirement for heating and melting the samples. The obtained energy requirements are seen on figure 2. From this, it is clear, that the stone wool waste requires ~20% less energy for heating and melting than the conventional mix of raw materials.

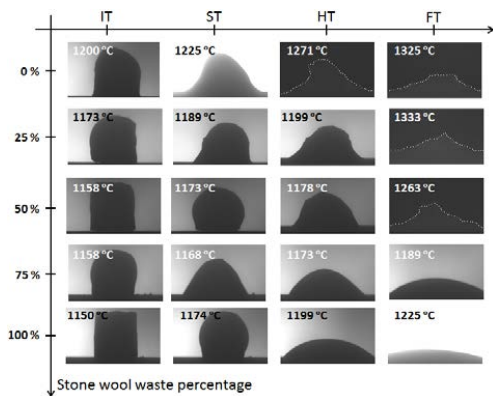


Figure 1: Samples comprising conventional stone wool charge and stone wool waste is analyzed using HSM [3]. The following characteristic shapes are identified during the measurements: Initial Deformation (IT), Spherical Temperature (SP), Hemispherical Temperature (HT) and Flow Temperature (FT). The heating rate was 5 K/min.

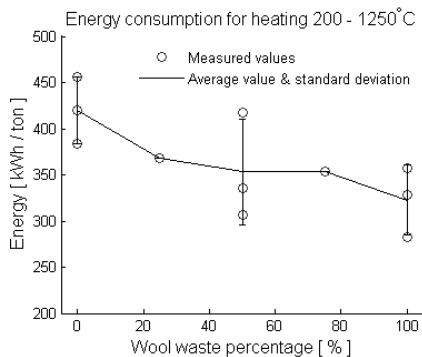


Figure 2: Energy consumption associated with heating, and melting samples of varied recycled stone wool waste content [3].

Conclusion

The melting behavior and melting energies have been investigated for samples comprising mixtures of a conventional stone wool feed and recycled stone wool waste. The study shows that the stone wool waste melts at lower temperatures than the conventional charge, and also that the stone wool waste requires less energy for melting, making stone wool waste recycling desirable for both environmental and economical purposes.

Future Work

The next step in this project is to understand the behavior of the stone wool waste when recycled back into the IMF plant. This part of the study will include particle sampling from within the IMF flue gas stream.

It is planned to use two different types of probes, as seen on Figure 3: a simple deposit probe and a more advanced isokinetic particle suction probe. The deposit probe is a water cooled pipe that is inserted into the flue gas. The material build-up on the probe during the measurement is extracted and analyzed. The isokinetic suction probe functions by suctioning out a stream of the flue gas with a velocity corresponding to the IMF flue gas velocity. Particles entrained in the flue gas passing through the probe are separated out in a dust cyclone for analysis.

The understanding of the materials that has been obtained during the first part of the study will help towards understanding the characteristics of the sampled particles from the full scale experiments.

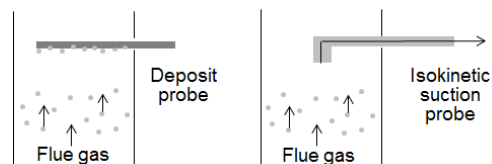


Figure 3: Probes for sampling entrained particles in the flue gas from the IMF. A simple deposit probe (left) and an isokinetic suction probe (right).

Acknowledgements

This project is a collaboration between the CHEC research center at DTU Chemical Engineering and ROCKWOOL International A/S. The financial support from Innovation fund Denmark under Grant number 5189-00019B is gratefully acknowledged.

References

1. B. Sirok, B. Blagojevic, P. Bullen, Mineral wool: production and properties, Elsevier, 2008
2. G. W. H. Höhne, W. F. Hemminger, H.-J. Flammersheim, Differential Scanning Calorimetry, Springer, 2003
3. V. Schultz-Falk, P. A. Jensen, K. Agersted, M. Solvang, "Melting Behavior of Raw Materials and Recycled Stone Wool Waste", Manuscript in preparation



Max Schumann

Phone: +45 53336877
E-mail: maxsch@kt.dtu.dk

Supervisors: Anker Degn Jensen
Jakob Munkholt Christensen
Jan-Dierk Grunwaldt (KIT)

PhD Study
Started: January 2017
To be completed: December 2019

Sustainable production of higher alcohols from CO and CO₂

Abstract

C₂-oxygenate (C₂-O) formation from syngas has been studied over supported metallic Rh catalysts. Preparation was carried out through wet impregnation of Rh(NO₃)₃ on different metal oxides (SiO₂, TiO₂, ZrO₂). Initial catalytic activity tests confirm a strong support dependence for the formation of acetaldehyde (AcH). The activity in producing AcH follows Rh/ZrO₂ > Rh/TiO₂ >> Rh/SiO₂. Rh(OH)₃ impregnation on SiO₂ recreates the active sites which can produce AcH during CO exposure and subsequent temperature programmed hydrogenation. The observed pattern corresponds to that as obtained from TiO₂- and ZrO₂-supported Rh after catalytic CO/H₂ reaction.

Setting the scene

The high energy density of liquid alcohols (e.g. EtOH) and the possibility to integrate those into existing energy systems are big advantages over other sustainably producible energy carriers, e.g. CH₄ or H₂. Conversion of H₂ with CO or concentrated CO₂ streams towards higher alcohols is a highly favorable reaction in that context. Single-metal supported Rh catalysts are known for their ability to produce C₂-oxygenate compounds [1] (mainly acetaldehyde and ethanol) from CO/H₂ and are chosen as starting point of this project.

Background

Rhodium is a good single metal catalyst for CO hydrogenation since it allows CO to adsorb in both, a molecular and a dissociative way. Both steps are required for the production of C₂-O compounds. Narrow product distribution and high selectivities for AcH and EtOH are advantages over other catalyst systems and make metallic Rh an attractive model system for this reaction [2]. In H₂-containing reaction atmosphere, the synthesis of C₂-O competes with the complete hydrogenation, which mainly produces CH₄. This limits the CO conversion range wherein moderate C₂-O selectivity levels are gained (ca. 70 – 80 %) to 10 – 15 %. For any commercial application, it will be necessary to push beyond the limitation of low conversion ranges while keeping low metal Rh loadings.

Mechanistic introduction

There are two common viewpoints onto the reaction mechanism that can explain the observation of Rh to

either behave like a pure methanation catalyst or a system that selectively forms C₂-O products.

One approach that is widely followed in Density-Functional Theory calculations is based on the distinction between the different Rh crystal facets. Rh(211) step sites have a high activity for the CO dissociation whereas Rh(111) terrace sites cannot break the C-O bond but show a high selectivity in forming C₂-O compounds [3]. From this, it would be assumed that the Rh step sites dominate and CH₄ evolves as main product. One approach to explain the observed ability of Rh to form AcH is a selective blocking of the Rh step sites (via doping or support interaction). This can shift the product distribution from CH₄ as main product towards high C₂-O selectivity levels at the expense of overall activity.

Another approach focuses on the interplay of Rh with support metal oxide sites and different surface intermediates. Herein, the insertion of a CO species into C₁-compounds that originate from CO dissociation is widely assumed as the rate determining reaction step. Different species, e.g. acetate, formyl and carbene, were suggested as kinetic relevant intermediates based on isotopic labelling and chemical trapping experiments [4-6]. A mechanism that involves active composite centers

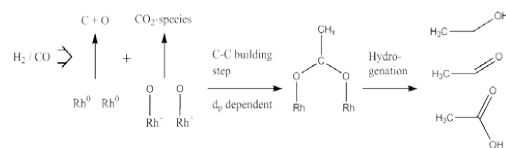


Figure 1: Key steps in reaction mechanism.

which consist of interfacial sites between partially oxidized Rh and metal cations connected via support oxygen atoms, $\text{Rh}^{\delta+}\text{-O-Me}$, was proposed by Liu et al. [6]. These sites may stabilize intermediates that can then be hydrogenated to AcH (see Figure 1).

Tailoring a catalyst that provides the right balance between metallic Rh^0 which can dissociate CO and vicinal interfacial $\text{Rh}^{\delta+}\text{-O-Me}$ islands that enable CO-insertion into CH_x , is hypothesized to lead to an optimum $\text{C}_2\text{-O}$ yield. The addition of dopants (e.g. Fe, Mn and Ce) can significantly shift the product distribution. Different effects, e.g. selective blocking of Rh(211) step sites or providing Lewis-acid sites that assist the build-up active composite centers are related hereto. This PhD project aims to merge the different models on active sites into one consistent image and to identify the optimum synthesis and operational conditions that favor the formation of described interfacial active site centers.

Specific objects

- 1) Investigation of the reaction mechanism
- 2) Topological changes of Rh via support interactions
- 3) Role of oxidized Rh sites

Object 3) is more elaborated on in the preliminary results section.

Mechanistic investigations

Combined temperature programmed desorption (TPD), hydrogenation (TPH) and surface reaction experiments will be combined with IR-vibration spectroscopy and applied to normal and model catalysts. One type of experiment will be to impregnate Rh with speculated intermediates (e.g. formyl, acetate) and expose this model catalyst to CO atmosphere. If subsequent TPH reproduces the same AcH formation-pattern as for catalysts after normal CO/H_2 reaction, this will be a strong evidence for the involvement of these species.

Dynamic topological behavior of Rh in CO atmosphere

TiO_2 can migrate onto noble metals under reducing conditions and form a crystalline overlayer. Such strong-metal support interaction states can alter the catalytic properties. The reverse phenomenon of Rh nanoparticles that disintegrate and form isolated Rh islands on the support was reported for small Rh nanoparticles [7]. FTIR experiments relate this to the formation of Rh(I)-gem-dicarbonyl ($\text{Rh}^I(\text{CO})_2$) under ambient CO pressure. Such species form on isolated Rh^+ sites.

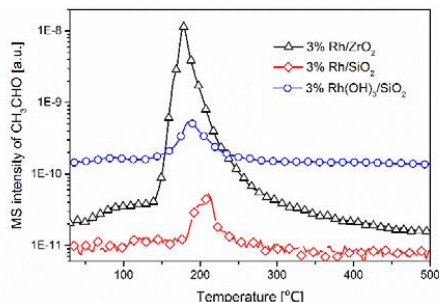
The catalytic properties of $\text{Rh}^I(\text{CO})_2$ for the CO hydrogenation and their ability to be stabilized under reaction conditions are unclear. ZrO_2 is an interesting candidate hereby. Combined catalytic reactor studies and imaging techniques (e.g. environmental pressure TEM) are aimed to exploit the potential of this feature.

Preliminary results and discussion

Role of oxidized Rh sites

The impregnation of $\text{Rh}^{\text{III}}(\text{OH})_3$ onto SiO_2 is intended to probe a possible correlation between catalytic

properties and the oxidation state of Rh. Reduced 3% Rh/SiO_2 showed no significant production of AcH in CO/H_2 . 3% $\text{Rh}(\text{OH})_3/\text{SiO}_2$ was preadsorbed with CO at 100 °C and subjected to TPH afterwards. A significant amount of AcH was formed hereby. Peak temperature (200 °C) and pattern agree well with that as it was observed for a 3 % Rh/ZrO_2 catalyst that was treated in CO/H_2 reaction atmosphere at 250 °C before



(see Figure 2).

Figure 2: MS signal for AcH ($m/z = 43$) as a function of temperature during TPH (5 °C/min). 3% Rh/SiO_2 and 3% Rh/ZrO_2 were calcined (550 – 400 °C) and reduced in H_2 (400 °C). 1% ZrO_2 was treated for 120 min in CO/H_2 (1:2) at 250 °C and 3 % Rh/SiO_2 for 45 min. Catalysts were cooled down to 30 °C in CO/H_2 and subjected to TPH afterwards. 3% $\text{Rh}(\text{OH})_3/\text{SiO}_2$ was kept in He at 100 °C for 30 min, exposed to 9.5 % CO in Ar at 100 °C for 30 min, flushed with He for 30 min and cooled down, subjected to TPH afterwards.

$\text{Rh}(\text{OH})_3$ can recreate required reaction sites that form AcH on SiO_2 as a significantly less active support in forming $\text{C}_2\text{-O}$. The results supports the assumption that $\text{C}_2\text{-O}$ can be formed on oxidized Rh sites as illustrated in Figure 1. The adsorption of AcH on pure (ca. 1 mm sized) Rh particles and subsequent AcH desorption via a TPD was used as a control experiment. Independent from the pretreatment (oxidative/reductive) of the Rh, AcH desorbed around 75 °C in both cases. Similar AcH desorption patterns were observed for $\text{Rh}(\text{OH})_3$ and pure TiO_2 support. This hints towards the desorption of physisorbed AcH and the requirement of elevated temperatures (200 – 250 °C) to make the AcH formation a kinetically relevant pathway.

References

1. M. Ichikawa, Bull. Chem. Soc. Jap. 51 (8) (1978), 2273-2277.
2. H. Luk et al., Chem. Soc. Rev. 46 (5) (2017), 1243-1636.
3. N. Yang et al., JACS 138 (2016), 3705-3714.
4. A. Takeuchi et al., J. Phys. Chem. 86 (13) (1982), 2438-2441.
5. A. Kiennemann et al., J. Chem. Soc., Faraday Trans. 1 83 (1987), 2119-2128.
6. J. Liu et al., Proc. 9th Int. Congr. Catal. V2 (1988), 735-742.
7. S. M. McClure et al., PNAS 108 (3) (2011), 931-936.



Lars Schwarzer

Phone: +45 4525 2837
E-mail: laschw@kt.dtu.dk

Supervisors: Peter Arendt Jensen
Peter Glarborg
Kim Dam-Johansen
Jens Kai Holm (Ørsted)

PhD Study
Started: December 2015
To be completed: January 2019

Biomass particle ignition in mill equipment

Abstract

The share of renewable energy can readily be increased by using biomass instead of coal on existing pulverized fuel power plants. However, biomass is much more susceptible to self-ignition than coal before it reaches the burner, e.g. in power plant mills and storages. The mechanism behind this is currently not well understood, and consequentially, predictions based on available models are not very accurate.

In this study, ignition was found to be a process dominated by the heterogeneous oxidation of the solid material. A slow decomposition can transition to a faster reaction regime, leading to a complete burnout. Flaming appears as separate, alternative regime to the ‘fast’ heterogeneous oxidation. The relation between these reaction modes and parameters influencing their onset are currently investigated further.

Introduction

Denmark is among the countries pioneering a replacement of coal by renewable energy sources for heat and power generation. Biomass combustion is expected to play a significant role, especially for use in combined heat and power (CHP) plants. Existing pulverized coal fired CHP plants are currently being converted to biomass firing. Typical fuels used are wood pellets, but also the use of non-conventional pellets, made from agricultural residues, is being investigated.

Spontaneous ignition events have been observed in both on-site storages and pulverizers (mills). Such ignition events are likely due to combustible material left at elevated temperatures and/or thermally isolated, which then undergoes self-heating. Figure 1 illustrates where such dusts may accumulate in mills.

Besides raising safety concerns, self-ignition causes economic losses due to plant downtime, loss of fuel, and possible damage to the equipment. Methods for

predicting self-heating and thermal runaway are based on simple models developed for mixtures of explosible gases, and rely on extensive lab-scale testing and/or extrapolation. However, the behavior of solid organic fuels is more complex than that of gas mixtures. It has been shown that the extrapolation of simple *heat generation vs. heat dissipation* models may result in inaccurate or even erroneous risk assessments [1, 2].

Objectives

This study aims at a better understanding of self-ignition, both qualitatively and quantitatively. Laboratory experiments are carried out on different scales, reaching thermogravimetric analysis (TGA) to sample amounts in range 10–40 g in lab-scale heating experiments. Results from these measurements are used to identify the relevant reaction, heat transfer and mass transfer mechanisms. The second part of this study is concerned with finding parameter values for a new and improved model of self-heating and self-ignition, which better represents the underlying physical processes.

Experimental Methods

1. Materials

Experiments reported here were carried out on a selection of (mainly) lignocellulosic biomasses and a bituminous coal. Selected composition information is given in Table 1. Additional tests were carried out on lignin, cellulose, and xylan, a hemicellulose compound. All materials were tested in pulverized form.

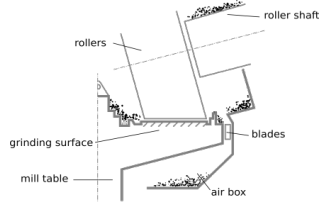


Figure 1: Settled dusts are an ignition hazard.

Table 1: Materials used in this study.

Material	Water [wt-%]	Volatiles [wt-%]	Ash [wt-%]
Beech wood	8.4	70.6	2.5
Pine wood	5.6	80.8	0.3
Wheat straw	8.0	71.2	3.9
Sunflower husk	9.2	68.6	4.7
Bituminous coal	6.6	33.9	8.8

2. Single particle reactor

Experiments in the single particle reactor allowed to visually observe the onset of ignition. The materials investigated were pressed to pellets of ca. 250 mg and inserted into a pre-heated oven (240–500 °C).

3. Fixed-bed experiments

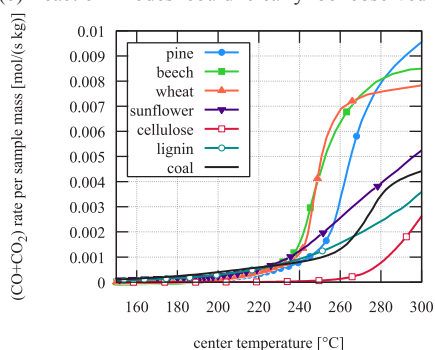
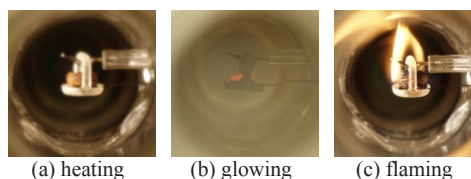
Experiments in this part were carried out by slowly heating 10–40 g of samples at 1 K/min from ambient temperatures to 300 °C. Reaction progress was evaluated by measuring CO and CO₂ concentrations in the off-gases, and scaling them by sample mass.

Results and Discussion

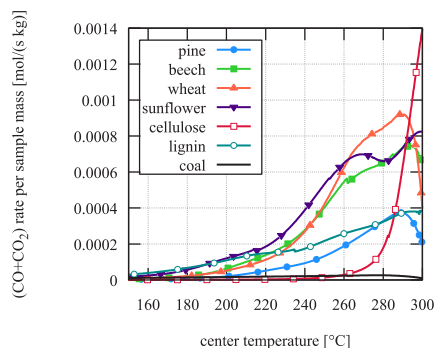
Experiments carried out in the single particle reactor allowed to characterize different reaction modes, Fig. 2. Heating (2a) corresponds to a mild, slightly exothermic decomposition, during which the sample temperature temporarily exceeds the surrounding temperature (+20 K), but does not completely burn out. However, the sample appears slightly discolored, loses mass, and releases CO and CO₂.

Given a sufficiently high ambient temperature (>250 °C), the sample will switch to a regime leading to complete burnout (2b), where large a temperature overshoot (>100 K) is observed. At sample temperatures above ~500 °C, the material emits a faint glow.

To reach flaming (2c), the heating rate seen by the sample must be much higher, which is achieved by higher oven temperatures (>400 °C) in this pulse ignition experiment. A transition from glowing to flaming has not been observed in these experiments. It should however be noted that the sample size is small, and that volatiles needed for homogeneous combustion are easily purged in this experiment. From the fixed-bed experiments, the transition between the slow (a) and fast (b) reaction modes could clearly be observed under

**Figure 3:** Reaction transition under 20% O₂**Figure 2:** Reaction modes (Pine, 25% O₂ atmosphere). Blur in (a, b) due to volatile gases and tars.

oxygen atmosphere, Fig. 3. For beech, wheat and pine, this occurs in the region of 240–260 °C. Considerable amounts of CO and CO₂ are already detected at around 100 °C (see [3]). Comparison with experiments carried out under inert atmosphere (Fig. 4, note the ordinate scaling) demonstrates that the observed off-gases are mainly the result of oxidation reactions across the whole temperature range. Interestingly, the behavior of the different materials could not be linked directly to amount of volatiles or explained by catalytic effects of minerals (as ash).

**Figure 4:** CO and CO₂ released while heating in N₂

Conclusions

Low-temperature reactions are dominated by heterogeneous oxidation, undergoing a change from slow to rapid reactions. The reactivity of different materials appears to be determined by a combination of several factors. Transition to flaming is likely governed by both heat and mass transfer, in addition to reaction kinetics.

Acknowledgements

The author would like to thank Ørsted and Energinet.dk for co-funding of this work; and especially the laboratory of Inorganic Chemistry at Åbo Akademi, Finland, for welcoming the author Oct.–Dec. 2017.

References

1. J.C. Jones, *Combust. Flame* 124 (1–2) (2201)
2. B.F. Gray, J.F. Griffiths, S.M. Hasko, *J. Chem. Tech. Biotechnol.* 34A (1984) 453–463.
3. L. Schwarzer, P.A. Jensen, P. Glarborg, J.K. Holm, K. Dam-Johansen. Biomass ignition in mills and storages – is it explained by conventional thermal ignition theory? *Nordic Flame Days 2017, Stockholm*

**Daria Semenova**

Phone: +45 45 25 29 58
E-mail: dsem@kt.dtu.dk

Supervisors: Krist V. Gernaey
Alexandr Zubov
Ulrich Krühne

PhD Study
Started: August 2014
To be completed: February 2018

Advanced mathematical data interpretation methods for the description of the processes inside microbioreactors and biosensors

Abstract

The interest in downscaling within industrial biotechnology has increased significantly in the last decade. It has resulted in the development and further implementation of small scale reactors such as microbioreactors (MBRs). The design and development of MBRs with integrated sensors and parallel operation is an adequate solution for rapid, high-throughput, and cost-effective screening, with considerably reduced reagent usage and waste generation^[1]. The successful application of MBR technology will only be possible if it can rely on appropriate software and automated data interpretation of the MBR experiments. The development of such tools should allow maximizing the exploitation of MBR platform capabilities on delivering information-rich experiments on the one hand, and on extracting as much information as possible from the obtained experimental data on the other hand. This can be achieved by designing model based state and parameter estimators that can provide reliable on-line information about the biological variables and model parameters.

Introduction

Industrial biotechnology processes rely on screening programs for achieving high yields and volumetric productivities, which are crucial to economic viability. High-throughput screening is a feasible approach to identify interesting, refined production strain candidates. However, a significant problem – both in screening and in large scale biotechnological processes – is state estimation. The design of model based state and parameters estimators that could provide reliable on-line information on the biological variables and model parameters has always been under discussion. Thus, there is a clear need for systems that enable rapid testing, optimization, control and bioprocess development in low sample volumes, allowing parallel cultivations with setup and run-time efforts, both in terms of time and resource consumption, that remain nearly independent of the number of bioreactors. MBR technology with integrated sensors is an adequate solution for rapid, high-throughput, and cost-effective screening. It allows, in principle, continuous measurement and control of various biological parameters, despite the low reactor volumes.

Methodology

Performing experiments at microscale will generate a considerable amount of data, and in the end operating

such a microscale system with multiple functions in parallel will cause difficulties to interpret all generated data using traditional tools such as a spreadsheet program. Therefore, this project will be focused on streamlining the data interpretation. The first part of the work is based on describing biocatalytic processes at microscale by mechanistic models of both reaction and reactor systems, either based on ordinary differential equations (ODEs) or partial differential equations (PDEs). Modeling of the enzymatic oxidation of glucose with different operation of the reactor model was chosen as a case-study. Moreover, a mechanistic model approach is also used to develop a generic mathematical model for the transient behavior of a multilayer enzymatic biosensor. Based on an existing MatlabTM toolbox developed at DTU, the work will be continued for the further application of uncertainty and sensitivity analysis for the developed models with the aim to use the analysis results for proposing new experiments in order to collect informative experiments with the experimental microbioreactor/biosensor set-up using as few experiments as possible.

Mechanistic model

Modelling of biocatalytic processes has resulted in the development of models with different levels of details such as catalyst, reaction, reactor and process model^[2].

In this project a mechanistic model was used for the description of the enzymatic reaction of glucose oxidase and glucose in the presence of catalase inside a microfluidic platform (Figure 1).

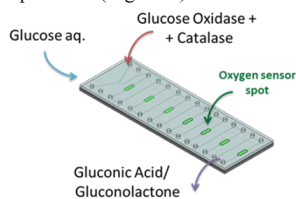


Figure 1: The experimental set-up for studying the enzymatic reaction inside the MBR platform.

The model was validated based on the experimental data produced by integrated into the MBR optical sensors. The on-line monitoring of the reaction was possible by quantifying the oxygen production during catalyzed decomposition of hydrogen peroxide (3), obtained during the glucose (1) transformation into gluconic acid (2), as shown in Figure 2.

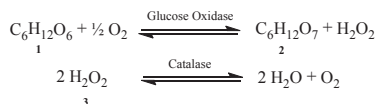


Figure 2: Enzymatic reaction of glucose oxidase and glucose in the presence of catalase.

The developed model showed a good agreement with the obtained experimental data (Figure 3).

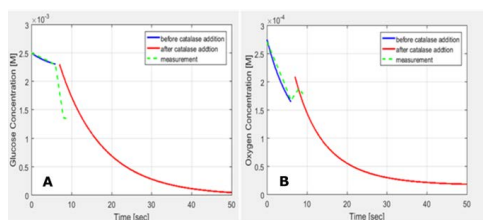


Figure 3: Comparison of concentration profiles for glucose and oxygen in a MBR: simulation results (solid line) vs. experimental data (dashed line).

Electrochemical Biosensors

Biosensors, being compact and relatively cheap, have found application in different fields such as medicine, food industry, defense technologies, etc.^[3]. The first generation amperometric glucose biosensor was chosen as a case study for the mechanistic model development and further integration inside the microfluidic platform. The mathematical description of the mediated enzymatic reaction inside the biosensor involved solving non-linear second order PDEs, which combined diffusion fluxes of the substrate and the mediator, electrochemical reaction of the species, as well as the biocatalytic kinetic term (Figure 4).

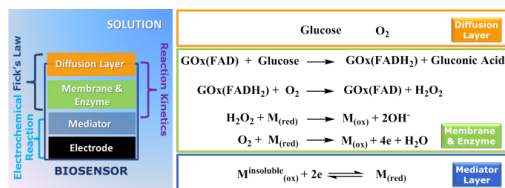


Figure 4: Schematic representation of the biosensor design and operation: $GOx(FAD)/GOx(FADH_2)$ – oxidized/reduced forms of glucose oxidase, M_{ox}/M_{red} – oxidized/reduced forms of mediator.

The general idea underlying this study was the development of a novel mathematical tool for amperometric biosensor operation and design optimization. To achieve this goal, we used, as a first step, the combination of a mechanistic model for cyclic voltammograms (CV) with experimental multi-analytical studies. The developed model showed a good qualitative and quantitative agreement with experimental voltammograms (Figure 5), for various biosensor designs and operating conditions.

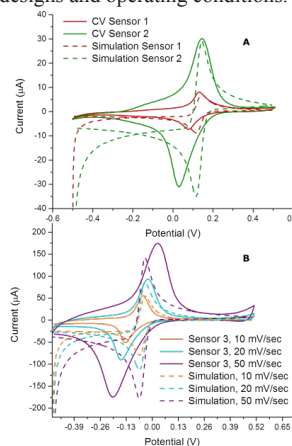


Figure 5: Simulation results (*dashed line*) compared vs. experimental data (*solid line*) for CVs obtained for glucose biosensors from different batches (A) - *sensor 1* to *sensor 3*; and at various scan rates (B).

Acknowledgements

The funding for this project was received from the People Programme (Marie Curie Actions) of the European Union's Seventh Framework Programme FP7/2007-2013/ under REA grant agreement n° 608104 (EUOMBR). The article represents only the authors' views and the European Union is not liable for any use of the information presented here.

References

1. Z. Zhang et al., JALA 12 (2007), 143-151.
2. R. L. Fernandes et al., Adv. Biochem. Eng. Biotechnol. 132 (2013), 137-166.
3. A. Sadana and N. Sadana, Handbook of Biosensors and Biosensor Kinetics, Elsevier, Oxford, 2011.



Peng Shen
Phone: +45 50391888
E-mail: psen@kt.dtu.dk

Supervisors: Peter Szabo
Anders Egede Daugaard
Suojiang Zhang, IPE-CAS

PhD Study
Started: December 2016
To be completed: December 2019

Monolithic Thiol-ene materials with drastically different mechanical properties

Abstract

Thiol-ene materials are a series of materials that can easily be crosslinked using suitable photo-initiator and UV light source. An advantage of thiol-ene materials is that they can be tailored, to have specific mechanical properties, by controlling the stoichiometry of the mixtures. By combination of different material systems it is therefore in principle possible to prepare monoliths with greatly varying mechanical properties, essentially from the same material.

Introduction

The possible application of polymer materials with distributed mechanical properties are many. Figure.1 illustrates one such example. Thiol-ene materials can be obtained through traditional thermal conditions with common azo-species such as 2,2-azobis(isobutyronitrile) (AIBN) or via with little or no added

condensation polymerizations, thiol-ene polymers form in a stepwise manner but their formation is facilitated by a rapid, highly efficient free-radical chain-transfer reaction. Thus, crosslinked thiol-ene polymerizations proceed very rapidly but will not reach the gel-point until relatively high functional group conversions[4], which results in a material with very low shrinkage and

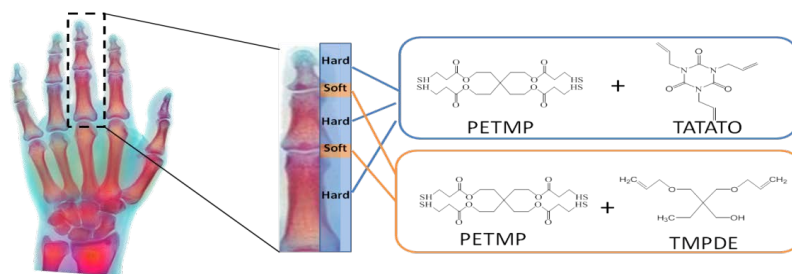


Figure.1 Artificial fingers with hard-soft alternate thiol-ene materials

photoinitiators' photochemical thiol-ene reaction methods[1]. During the last century, thiol-ene material is a global focus because of the highly efficient reactions of thiols with reactive C=C bonds, has widely application in hydrogel drug delivery, coatings, adhesives, optical applications, dendrimer synthesis, all-solid-state electrolyte, high strength laminates, dental resins and electroluminescent films[2]. In particular, two thiol reactions emerged, thiol-ene free-radical addition to electron-rich/electron-poor C=C bonds, and the catalyzed thiol Michael addition to electron-deficient C=C bonds [3]. Unlike typical chain-growth free-radical polymerizations or step-growth

inherent stresses.

Specific Objectives

In this project, the purpose is to prepare new monolithic thiol-ene materials with drastically different mechanical proportion, which is formed via a free radical based thiol-ene addition reaction. Products will show the different mechanical proportion by controlling the kind of reaction compound (thiol and ene with different number of functional groups), the ratio of reactants (the reaction conditions (ultraviolet light and heating)). Through use of different reactants hard and brittle (H, TATATO and PETMP) to soft and flexible materials (S,

PETMP and TMPDE) will be prepared as shown in Figure 1.

Results and Discussion

The mechanical properties of polymers are intimately related to their molecular structure, one of the most important mechanical properties is rheological behavior, which can be measured by shear rheometry and filament stretching rheometer (FSR).

The thermal properties of hard and soft polymer were characterized using the differential scanning calorimeter (DSC). The DSC measurement shows that the glass-transition temperature (T_g) of the hard segment (H) is 55.74°C and the soft (S) is -35.35°C , respectively. (Figure.2)

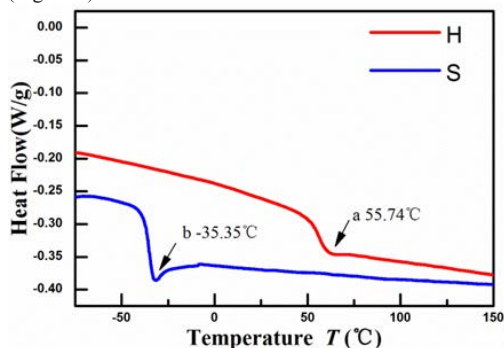


Figure. 2 DSC curve of (a) hard segment and (b) soft segment

To get the sandwich structure column shape sample, we made the hard segment and soft segment polymer, respectively. The hard polymer liquid was prepared by using the ratio (1:1) of PETMP to TATATO. Two chemicals were mixed by the SpeedMixer at the speed of 3000r/min for 2 mins, in addition, all processes should be carried out in total darkness for preventing the mixture prematurely polymerize. The soft liquid was obtained in the same way except for replacing the TATATO with PMDPE.

It is very important that the first two steps of the polymerization process should strictly control the reaction time, the hard polymer liquid and soft polymer liquid are mixed together in a shorter illumination time.(Figure.3)

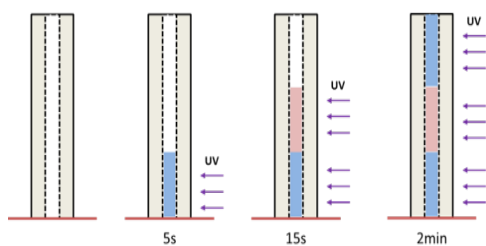


Figure. 3 The production process of hard-soft alternate sample

The extensional stress was measured by a filament stretching rheometer (FSR) to get the Force-Time curve

(Figure.4) and the 40mm-soft segment material can be thought of as the total soft material, because it only has 3cm hard segment in the both end. It can be seen that the new structure materials improved tensile property by 20 percent.

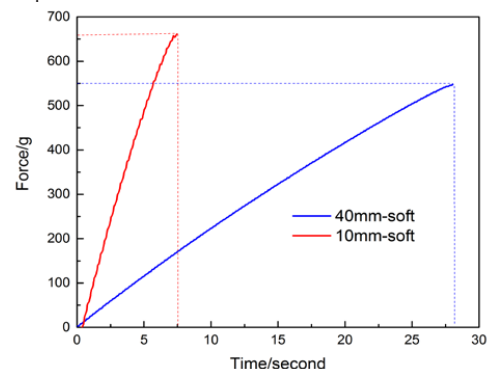


Figure.4 The Force-Time curve of 10mm soft segment and 40mm soft segment

The high-speed camera recorded the images of fracture process. (Figure.5), the crack was generated in the soft segment surface not in the interface of the hard and soft material, so it was the ductile fracture belong to the Mode I crack.

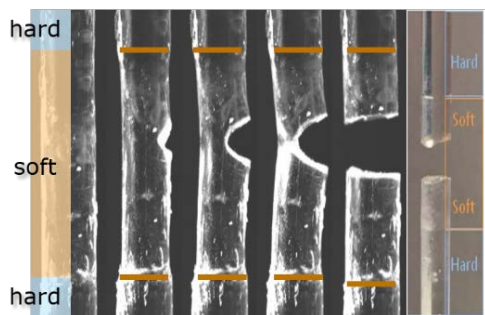


Figure.5 image of 10mm soft segment Hard-Soft material fracture process(bread bond is the interface of hard and soft materials)

Future work

- Future experiment with the different length soft segment materials such as 1mm, 2.5mm and 5mm will be made for the extensional stress test and studying the fracture behavior.
- The bending stress and fatigue test should be done by TA Instruments Electroforce 3200, the most suitable material, which has the optimal performance, will be selected.

References

1. P. Alagi, Y. J. Choi, J. Seog, S. C. Hong, Industrial Crops and Products 87(2016), 78-88.
2. K. Aoki, R. Imanishi, M. Yamada, Progress in Organic Coatings 100 (2016) 105-110
3. J. Bae, Y. Yang, Journal of Non-Crystalline Solids 357(2011) 3103-3107.
4. J. W. Bartels et al., Acs Applied Materials & Interfaces 3(2011)2118-2129



Sigyn Björk Sigurðardóttir

Phone: +45 4525 6184
E-mail: sigsig@kt.dtu.dk

Supervisors: Assoc. Prof. Manuel Pinelo
Assoc. Prof. Andreas Kaiser

PhD Study
Started: June 2017
To be completed: May 2020

High performance immobilization of enzymes in inorganic membranes

Abstract

Enzyme immobilization is an efficient method for improving the stability and reusability of enzymes, which greatly facilitates their use in industrial processes. Enzyme immobilization can be achieved by a number of different methods and on different carriers, the selection of which is based on the enzyme and process conditions in question, as well as on the balance between enzyme activity and stability upon immobilization. The objective of this project is to design optimal biocatalytic inorganic membrane systems by studying the enzyme/carrier interactions and the effects of the membrane processing methods on these interactions. This knowledge should enable the fabrication of membranes with optimal properties that fit the needs of the specific enzymes in question.

Introduction

The importance of enzymatic catalysis in industrial processes has seen a significant increase in recent years, following the shift of focus towards more environmentally friendly processing and production methods along with advances in enzyme engineering [1]. One of the main complications involved in industrial enzymatic catalysis is the often rapid decay in enzyme activity. In this regard, enzyme immobilization can offer increased enzyme stability as well as reusability, thus prolonging the useful life of the biocatalyst. Membranes can be used as carriers for enzyme immobilization, exploiting the advantages of both enzymes and membranes, i.e. the high efficiency and selectivity of the biocatalyst and the process intensification brought about by the membrane [2]. Inorganic membranes offer several advantages over polymeric membranes, such as high chemical and mechanical stability, microbial resistance and longer lifetime [3]. In this project, the interactions between the inorganic membranes and the enzymes will be studied from the perspective of material sciences and enzyme technology with the aim of designing optimal biocatalytic inorganic membrane systems that can be applied to multiple enzymatic processes.

Theoretical Background

Enzyme immobilization is an established method by now and is achieved by several different methods, the most common ones being physical adsorption, covalent

bonding, encapsulation and enzyme cross-linking. These

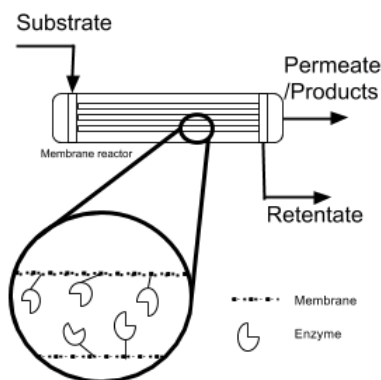


Figure 1: The enzymatic membrane reactor with immobilized enzymes allows simultaneous reaction and product separation, as well as reuse of the biocatalyst in multiple reaction cycles or its use in a continuous process.

methods differ in their complexity and advantages/disadvantages offered to the system. Physical adsorption is the most simple method, the immobilization is a result of non-covalent bonds, e.g. hydrogen bonds, van der Waals forces or electrostatic

forces between the enzyme and the carrier. This method can offer high enzyme activity retention while the stability and reusability are hampered by enzyme leakage due to the relatively weak bonds. On the contrary, covalent bonding provides the strongest interactions between enzyme and carrier, and thereby offers high stability and reusability of the catalyst while the activity retention can be negatively affected by the conformational changes in the enzyme structure upon the formation of covalent bonds. Covalent bonding is a multi-step process in which the enzymes are attached to the carrier through functionalizing and activating agents, where 3-aminopropyltriethoxysilane (APTES) and glutaraldehyde are undoubtedly the most common functionalizing and activating agents, respectively [4]. The functionalizing agent is attached to the inorganic surface through hydroxyl groups present on the surface. Depending on the type of inorganic carrier, the surfaces must often be activated as a first step of the immobilization strategy in order to enhance the number of hydroxyl groups. Inorganic surfaces are typically highly hydrated by nature, while for ceramic materials, surface activation is usually required nevertheless, since the surface area and activity (number of hydroxyl groups) decreases as a result of the fabrication method, e.g. high temperature sintering or calcining [5], [6]. A high surface area and activity are important factors that allow high degree of functionalization and subsequently high enzyme loading.

Specific objectives

The overall objectives of this project are:

- To design optimal membrane systems for efficient immobilization of enzymes
- Understanding and optimizing the interaction between inorganic surfaces and enzymatic proteins
- Method validation by measuring enzyme productivity and membrane performance.

Having identified the most promising immobilization methods as well as membrane materials, the immobilization will be carried out on raw ceramic powders initially, and later on membranes that will be fabricated from the same powders by our project collaborators from DTU Energy. This allows the evaluation of the processing methods used for the fabrication of the ceramic membranes and their influences on the interactions between the carrier and the enzyme.

Four different starting materials have been identified; SiC, TiO₂, Al₂O₃ and yttria stabilized zirconia (YSZ). The characterization of the materials includes surface area measurements, zeta potential, particle size distribution and sedimentation tests. All these parameters greatly affect the success of the immobilization and the influence on the enzyme properties upon immobilization, notably activity, stability and reusability. The system and methods chosen will be validated by studying the enzyme

properties prior to and after immobilization, as well as the shelf life of the catalytic membrane. Moreover, the possibilities of cleaning and reuse of the inorganic membranes will be investigated.

Conclusions

Enzyme immobilization on ceramic membranes is an attractive option in the design of energy efficient and environmentally friendly industrial processes. A systematic study of the enzyme/carrier interactions and the effects of the membrane processing methods on these interactions should enable the fabrication of membranes with properties tailored to fit the needs of the enzyme. An optimized system has many advantages, such as improved enzyme stability and reusability compared to the soluble enzyme and both the enzyme immobilization as well as the use of ceramic membranes contribute to a prolonged lifetime of the system.

References

1. U. T. Bornscheuer, G. W. Huisman, R. J. Kazlauskas, S. Lutz, J. C. Moore, and K. Robins, "Engineering the third wave of biocatalysis," *Nature*, vol. 485, no. 7397, pp. 185–194, 2012.
2. X. Dong, W. Jin, N. Xu, and K. Li, "Dense ceramic catalytic membranes and membrane reactors for energy and environmental applications." pp. 10886–10902, 2011.
3. G. Ranieri, R. Mazzei, Z. Wu, K. Li, and L. Giorno, "Use of a ceramic membrane to improve the performance of two-separate-phase biocatalytic membrane reactor," *Molecules*, vol. 21, no. 3, 2016.
4. P. Zucca and E. Sanjust, "Inorganic materials as supports for covalent enzyme immobilization: Methods and mechanisms," *Molecules*, vol. 19, no. 9, pp. 14139–14194, 2014.
5. N. Carlsson, H. Gustafsson, C. Thörn, L. Olsson, K. Holmberg, and B. Åkerman, "Enzymes immobilized in mesoporous silica: A physical-chemical perspective," *Adv. Colloid Interface Sci.*, vol. 205, pp. 339–360, 2014.
6. W. Wan, Y. Feng, J. Yang, S. Xu, and T. Qiu, "Preparation of mesoporous silica ceramics with relatively high strength from industrial wastes by low-toxic aqueous gel-casting," *J. Eur. Ceram. Soc.*, vol. 35, no. 7, pp. 2163–2170, 2015.



Ting Song
Phone: +45 50251205
E-mail: tison@kt.dtu.dk

Supervisors: Peter Szabo
Anders Egede Daugaard
Suojiang Zhang, IPE, CAS

PhD Study
Started: November 2015
To be completed: October 2018

The modification of PSf membranes with ionic liquids used for CO₂ separation

Abstract

The PhD project focuses on the separation of CO₂ from CH₄ or N₂ with ionic liquid-based membrane. Commercial PSf membrane is a good candidate to act as the substrate membrane due to its specific properties. This is the first time to polymerize ionic liquid on the surface of a commercial membrane through atom-transfer radical-polymerization (ATRP). In order to get better performance of CO₂ separation, the ionic liquid counter ion on the as prepared membrane can be exchanged to CO₂-philic anion, such as bis(trifluoromethylsulfonyl)imide ([NTf₂]), etc. The introduction of butyl acrylate helps improve the flexibility of the ionic liquid modified PSf membrane.

Introduction

Carbon capture and utilization are regarded as one of the major challenges in the 21st century. Carbon dioxide (CO₂) can be commonly found in natural gas streams, biogas, flue gas and product of coal gasification [1]. The presence of CO₂ and other acid gases reduce the thermal efficiency and make the gas streams become acidic and corrosive, which in turn reduces the possibilities of gas compression and the transport within the transportation systems [2]. Therefore, it is urgently necessary to develop new technologies for CO₂ separation with high efficiency, low energy consumption. Membrane separation is a promising technology for CO₂ capture due to its energy efficiency, simple process design, low cost and environmentally friendliness [3]. Recently, ionic liquids (ILs) have attracted great attention for their potential as alternative media for CO₂ separation due to their unique properties. However, it is difficult to realize industrialization using ILs to capture CO₂ due to their high viscosity. The high viscosity of ILs will lead to its low heat transfer and mass transfer performance, which may not only affect the speed of absorption regeneration, but also increase the cost of energy consumption of transport, and operation. Immobilization of ILs in membranes has been extensively investigated to combine the advantages of membranes and ILs and to overcome their disadvantages for CO₂ capture [2]. Polysulfone (PSf) membranes can be used as platform for gas separation because it has many excellent properties such as a high mechanical, chemical and thermal resistance. Moreover,

its separation and plasticization properties are also in an acceptable range [4]. In order to obtain a membrane with high CO₂ permeability and selectivity, we plan to modify the surface of commercial polysulfone membrane with poly(ionic liquids) (PILs).

Here, imidazole-based IL was polymerized and grafted on the surface of PSf membrane via atom-transfer radical-polymerization (ATRP). The thickness of the poly(IL) layer can be controlled by controlling the reaction time. In order to overcome the brittle property of imidazole grafted PSf membrane, butyl acrylate was introduced in and copolymerized with N-vinylimidazole on the surface of PSf membrane.

Methodology and results

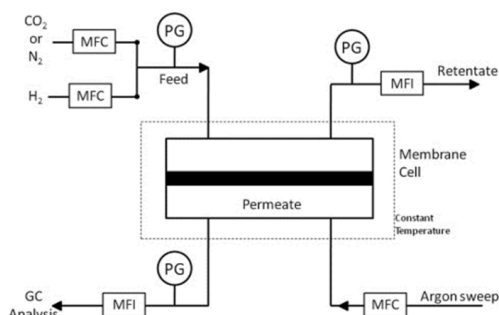


Figure 1. Brief diagram of the mixed gas constant pressure variable volume apparatus.

The mechanism of gas separation with membranes is showed in Figure 1. CO₂ can go through the membrane priority over other gases when the mixture gas of CO₂ and CH₄ or CO₂ and N₂. The permeate gas can be test by GC (Gas Chromatography). The membrane used for CO₂ separation is based on the solution-diffusion mechanism. There are two parameters, permeability and selectivity, to evaluate the performance of membranes used for gas separation.

IL is for the first time polymerized on the surface of PSf through Atom-transfer radical-polymerization (ATRP) (Figure 2a, 2b, 2c). The thickness of PILs layer can be controlled by controlling the ATRP reaction time. Additionally, membranes with different properties in terms of CO₂ affinity can be obtained by changing the counter ion of the ionic liquid as shown in Figure 2d.

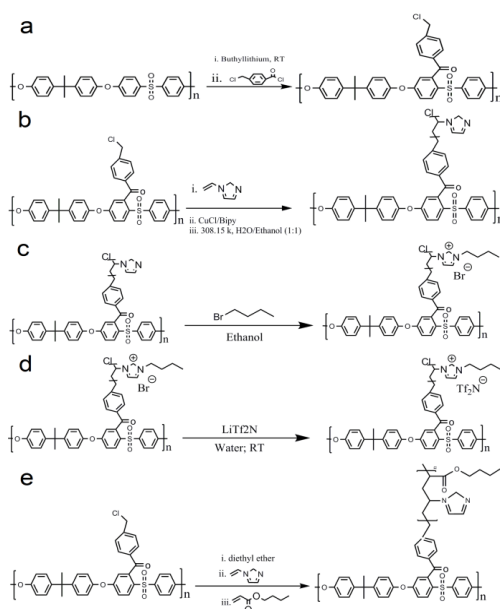


Figure 2. The synthesis of IL modified PSf membrane (a, b, c); anion exchange process (d); N-vinylimidazole and butyl acrylate copolymerized on the PSf membrane (e).

The as prepared N-vinylimidazole modified PSf membrane is brittle, since the poly(N-vinylimidazole) is a glassy polymer. In order to overcome this problem, butyl acrylate, to provide softness, was introduced in (Figure 2e). The result turns out that the membrane becomes more flexible after the introduction of butyl acrylate.

FT-IR (Figure 3) and WCA (Figure 4) of membranes I prepared were tested to confirm that all the reactions here happened successfully.

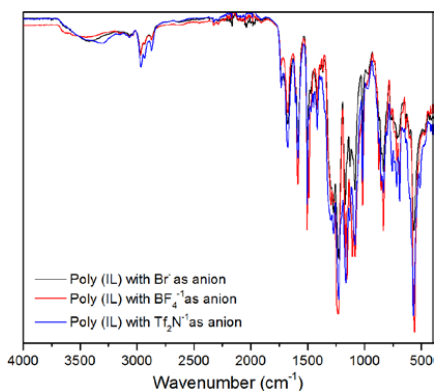


Figure 3. FT-IR of different kinds of membranes.

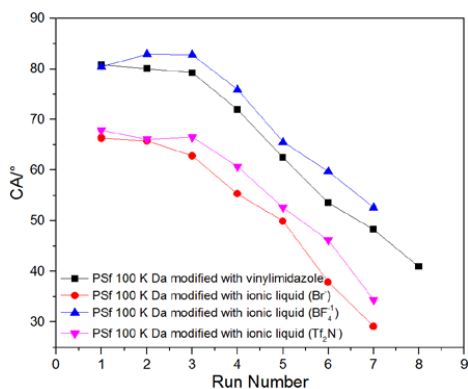


Figure 4. WCA of different kinds of membranes.

Conclusion

In order to improve the gas separation performance of commercial PSf membrane, N-vinylimidazole and butyl acrylate are copolymerized on its surface. The introduction of butyl acrylate helps overcome the shortcoming of the ionic liquid modified PSf membrane, which is very brittle. All the reactions have been confirmed by FTIR and WCA. The gas separation performance will be tested afterwards, and the experimental conditions can be optimized according to the results of gas separation test.

References

1. Y. Zhang, J. Sunarso, S. Liu, R. Wang, *Int. J. Greenh. Gas Control.* 12 (2013) 84–107.
2. J. Deng, L. Bai, S. Zeng, X. Zhang, Y. Nie, L. Deng, S. Zhang, *RSC Adv.* 6 (2016) 45184–45192.
3. S. Rafiq, L. Deng, M.-B. Hägg, *ChemBioEng Rev.* 3 (2016) 68–85.
4. T. Chittrakam, Y. Tirawanichakul, S. Sirjarukul, C. Yuenyao, *Surf. Coatings Technol.* 296 (2016) 157–163.
5. Matthew G. Cowan; Douglas L. Gin; Richard D. Noble, *Acc. Chem. Res.* 2016, 49, 724-732;



Robert Spann

Phone: +45 4525 6194
 E-mail: rosp@kt.dtu.dk

Supervisors: Gürkan Sin,
 Krist V. Gernaey
 Anna Eliasson Lantz
 David Kold, Chr. Hansen

PhD Study
 Started: August 2015
 To be completed: July 2018

Bioprocess risk assessment using a mechanistic modelling framework

Abstract

Process system engineering methods relying on mechanistic models are more and more applied for the development, optimization, monitoring, and control of biotechnology manufacturing processes. The aim of this PhD project is to apply and validate a risk assessment method using a mechanistic modelling approach for aerotolerant lactic acid bacteria fermentations. In the present study, the model is applied to: i) monitor the fermentation process; and, ii) to predict pH gradients in the bioreactor. The impact of the uncertainties in the model and on-line measurements on the model outputs is there quantified by applying Monte Carlo simulations. In the end, this methodology will feed into the toolbox of the BioRapid project that will enable effective and rapid development of novel bioactive molecules.

Introduction

Process system engineering methods relying on mechanistic models are more and more applied for the development, optimization, monitoring, and control of biotechnology manufacturing processes. First principles models are increasingly applied because the understanding of chemical, physical, and biological processes has reached an advanced level. However, the models, the input variables, the on-line measurements, and the parameters need to be checked for reliability using tools such as identifiability, uncertainty, and sensitivity analysis [1,2]. In addition, computational fluid dynamic (CFD) modelling is a strong tool to predict concentration gradients that occur in large-scale

bioreactors due to insufficient mixing. Combining biokinetic and CFD modelling allows a better understanding of the fermentation process than traditional homogeneous modelling approaches.

Specific Objectives

The objective of this PhD study is to apply and validate a risk assessment method for a mechanistic, first principles model for lactic acid bacteria fermentations (Fig. 1). To this end, i) a probabilistic soft sensor to monitor the fermentation is designed; and, ii) the pH gradients in the bioreactor are quantified using CFD simulations.

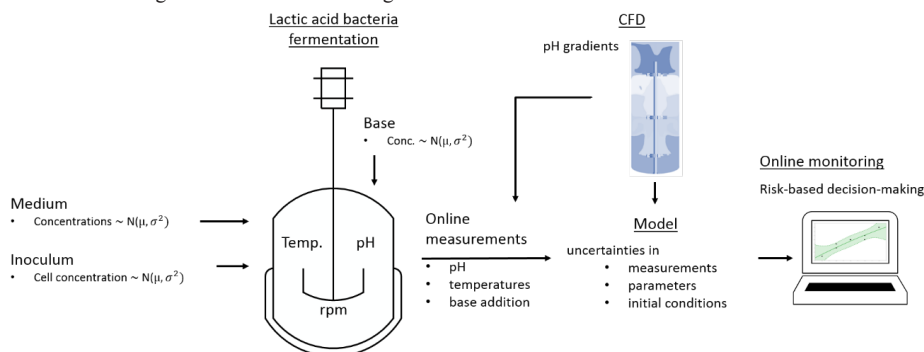


Figure 1: A robust on-line monitoring tool for risk-based decision-making. Uncertainties in the media, inoculum, and base concentration, as well as uncertainties in the on-line measurements and model parameters are considered. Furthermore, pH gradients occurring in the large-scale bioreactors will be included in future applications.

Results and Discussion

Soft sensor

The soft sensor to monitor the homolactic lactic acid bacteria fermentation is based on a mechanistic model describing the biomass growth, lactic acid production, and substrate consumption [2]. In addition, the pH is predicted using a mixed weak acid/base model [3]. A comprehensive model validation and the design of the soft sensor are presented elsewhere [4]. In the soft sensor, the available on-line measurements, the amount of base addition and pH, are used as inputs in order to predict the current state of the cultivation and the future course of the fermentation (Fig. 2). There, uncertainties in the input variables, on-line measurements, and model parameters are considered using Monte Carlo simulations, and providing therefore a probability distribution of the state variables.

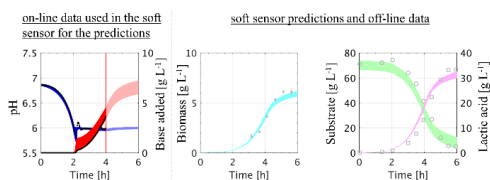


Figure 2: Soft sensor predictions during the fermentation. On-line measured variables (left), and not measured variables such as biomass, substrate, and lactic acid (middle and right).

This monitoring system supports the plant operators, who can now see biological variables such as growth in real time instead of relying on process parameters like base addition. Furthermore, this system could be used for plant scheduling since it is capable of predicting the end time of the fermentation, and improve thereby the full utilization of the production plant for an economical production.

pH gradients

A CFD model of a 700 L pilot-scale bioreactor was first validated with mixing experiments, and then used to predict pH gradients during a non-aerated lactic acid bacteria fermentation [5]. There, the biological model is incorporated in the CFD simulation, and pH gradients between 5.9 and 6.3 are predicted and measured near the baffles. However, a much higher pH is predicted in the close vicinity of the inlet where the base solution is introduced to the bioreactor (Fig. 3).

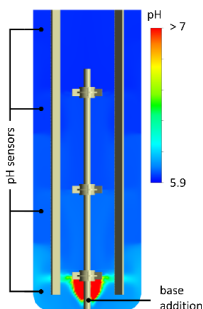


Figure 3: pH prediction during the exponential growth phase of a not-aerated lactic acid bacteria fermentation using a one-phase CFD model.

Cells that travel through the bioreactor are exposed to continuously changing environmental conditions (e.g. the pH), which might lead to productivity loss especially at large scale, since they need more energy in order to cope with these changing conditions. However, the effect of pH gradients on the bacteria is beyond the scope of this study. Quantifying gradients in simulations is crucial since measurements are mostly not available. This knowledge can then be transferred and used for the design of bioreactors and scale-down systems enhancing process development and production.

Future studies need to use the information obtained from the CFD simulation to propose compartment models that are able to run e.g. in MATLAB. This would allow running monitoring and controlling systems on-line considering gradients in the bioreactor. The CFD simulation is too slow to be applied directly on-line. On-line control considering pH gradients is particularly interesting, as the controller could then be tuned to minimize gradients in the bioreactor improving the productivity of the fermentation.

Conclusion

A mechanistic model describing a lactic acid bacteria fermentation was first applied as an on-line monitoring system using the very limited on-line measurements. This allows the plant operators to follow biological variables like biomass growth in real time, and to plan batches more economically. Second, the model was used to predict pH gradients during a fermentation using a CFD simulation. It shows that cells face pH gradients while they travel through the bioreactor but the impact of the gradients on the microbial growth is not investigated in more detail.

Acknowledgement

This project has received funding from the European Union's Horizon 2020 research and innovation programme under the Marie Skłodowska-Curie grant agreement No 643056. We are thankful for the cooperation with Chr. Hansen A/S.

Web-link: <http://www.bio-rapid.com/>



References

1. R. L. Fernandes, V. K. Bodla, M. Carlquist, A.-L. Heins, A. E. Lantz, G. Sin, K. V. Gernaey, *Adv. Biochem. Eng. Biotechnol.* 123 (2012) 137-166.
2. R. Spann, C. Roca, D. Kold, A. Eliasson Lantz, K.V. Gernaey, G. Sin, *Proc. 27th Eur. Symp. Comput. Aided Process Eng. - ESCAPE 27.* (2017) 3042-2047.
3. E.V. Musvoto, M.C. Wentzel, R.E. Loewenthal, G.A. Ekama, *Systems. Water Res.* 34 (2000) 1857-1867.
4. R. Spann, C. Roca, D. Kold, A. Eliasson Lantz, K.V. Gernaey, G. Sin, (2017) submitted.
5. R. Spann, J. Glibstrup, K. Pellicer Alborch, S. Junne, P. Neubauer, C. Roca, D. Kold, A. Eliasson Lantz, K.V. Gernaey, G. Sin, U. Krühne, (2017) submitted.



Magnus Zingler Stummann

Phone: +45 4525 2957
E-mail: mazi@kt.dtu.dk

Supervisors: Anker Degn Jensen
Martin Høj
Peter Arendt Jensen
Jostein Gabrielsen, Haldor Topsøe A/S

PhD Study
Started: October 2015
To be completed: October 2018

Hydrogen assisted catalytic biomass pyrolysis for green fuels

Abstract

Catalytic hydrolypyrolysis of biomass is a promising technology for production of sustainable liquid fuels. In this project we have shown that it is possible to produce a hydrocarbon oil with oxygen content below 100 ppmw at yields up to 22 wt. % resulting in energy recovery up to 53 %.

Introduction

The transportation sector accounts for one fifth of the world's total energy consumption [1]. Currently, transportation fuels are mainly produced from crude oil, however, these reserves are depleting and the need for alternative fuels increases [2]. In order to decrease the CO₂ emission future fuels must come from renewable energy sources [3].

During the last years there has been an increasing interest in converting biomass to liquid fuels. Biomass can be converted to bio-oil by flash heating the biomass to 350-500 °C in an inert atmosphere [4]. Unfortunately, bio-oil is very different from crude oil, due to high oxygen and water content in the bio-oil. The bio-oil is unstable and has a heating value approximately half the heating value of crude oil and further hydroprocessing of the bio-oil is necessary [5]. However, since the bio-oil is very reactive, rapid catalyst deactivation, because of coking, is common [5]. Recent research has shown that conducting the pyrolysis in a hydrogen atmosphere at elevated pressure instead of using an inert atmosphere can significantly improve the properties of the bio-oil, thus making the further upgrading much easier [6].

The PhD study is part of the project "H₂CAP – Hydrogen assisted catalytic biomass pyrolysis for green fuels" (see also Trine Marie Hartmann Dabros, pg. 39 - 40).

Specific Objectives

- Commissioning and running a bench scale setup for catalytic hydrolypyrolysis in a fluid bed reactor with a downstream fixed bed HDO reactor.
- Synthesis and characterization of hydrolypyrolysis catalysts suitable for fluid bed operation.

- Performing an experimental investigation of hydrolypyrolysis of different biomass sources with systematic variation of process parameters.
- Performing detailed physical and chemical analysis of bio-oil products using e.g. elemental analyzer and GC-MS.

Results and Discussion

The experimental work is conducted on the newly constructed H₂CAP unit. The setup consists of a pressurized biomass feeding system, a fluid bed reactor, where the catalytic hydrolypyrolysis takes place, and a fixed bed reactor, where complete hydrodeoxygenation takes place. Experiments have been performed with 50 g of CoMo/MgAl₂O₄ catalyst in the fluid bed reactor and 173 g of NiMo/Al₂O₃ catalyst in the HDO reactor. The catalysts were sulfided prior to the experiments. The catalyst in the fluid bed reactor was replaced after each experiment, while the catalyst in the HDO reactor was reused. Hydrolypyrolysis of beech wood was performed at 25 barg with gas composition 470 ppm H₂S, 6 % N₂ balance H₂. The effect of varying the temperature and pressure has been studied. The effect of bypassing the HDO reactor has also been investigated. Varying the temperature in the fluid bed reactor changed the product distribution as shown in Figure 1. Increasing the temperature in the fluid bed reactor mainly decreased the char yield, while increasing the gas yield, in agreement with the results obtained with IH²® process. The organic yield including condensed organics and C₄₊ gasses increased when the temperature increased from 365 to 400 °C above which it remained constant within the experimental uncertainty.

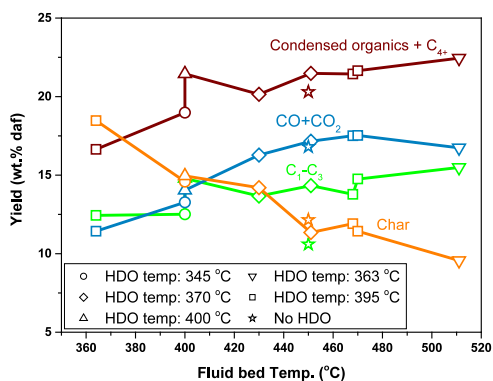


Figure 1: Effect of varying the fluid bed temperature on the product distribution.

The influence of pressure on the product distribution is shown in Figure 2. Increasing the total pressure did not affect the liquid organic yield, but decreased the CO and CO₂ yield. The hydrogen consumption also increased from 35 g/kg biomass at 15 barg to 46 g/kg biomass at 25 barg, but did not increase further when the pressure increased to 35 barg. The char yield also increased with increasing pressure.

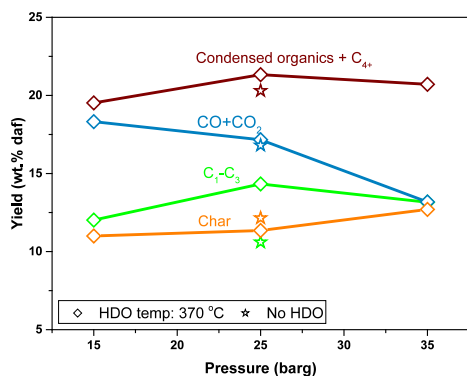


Figure 2: Effect of varying the total pressure on the product distribution

Oxygen specific GC-AED showed that when the HDO reactor was bypassed the total oxygen content in the condensed organics was 1.8 wt. % and that the main oxygenates were different phenols. When the HDO reactor was used the oxygen content was below 100 ppmw and only traces of phenols, naphthol, and dibenzofurans were detected in the condensed organics.

The energy recovery was calculated on the basis of the amount of biomass fed to the setup and the heating value of the different phases. The resulting energy recoveries for each product are shown in Figure 3. The energy recovery for the condensed organics and C₄₊ was between 40 and 53

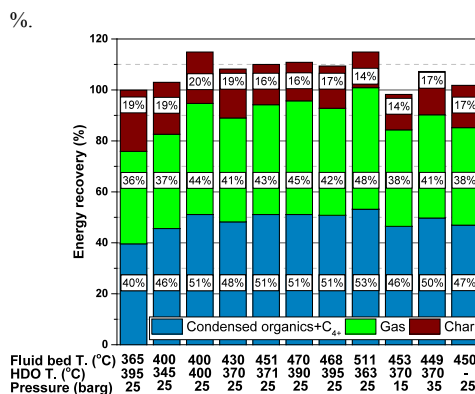


Figure 3: The effect of the process conditions on the energy recovery.

Conclusion

This study confirms that catalytic hydropropylolysis with hydrodeoxygenation is an attractive route for biomass to liquid transportation fuels. Most of the hydrogenation takes place in the fluid bed reactor, but it is necessary to use the HDO reactor in order to achieve an oxygen free oil.

Acknowledgements

This work is part of the Combustion and Harmful Emission Control (CHEC) research center at the Department of Chemical and Biochemical Engineering at DTU. The project is funded by the Danish Council for Strategic Research (project 1305-00015B), The Programme Commission on Sustainable Energy and Environment.

References

1. B. van Ruijven and D. P. van Vuuren, "Oil and natural gas prices and greenhouse gas emission mitigation," *Energy Policy*, vol. 37, no. 11, pp. 4797–4808, 2009.
2. S. Sorrell, J. Speirs, R. Bentley, A. Brandt, and R. Miller, "Global oil depletion: A review of the evidence," *Energy Policy*, vol. 38, no. 9, pp. 5290–5295, 2010.
3. R. K. Pachauri, L. Meyer, J.-P. Van Ypersele, S. Brinkman, L. Van Kesteren, N. Leprince-Ringuet, and F. Van Boxmeer, *Climate Change 2014 Synthesis Report*. 2014.
4. a. V. Bridgwater, "Review of fast pyrolysis of biomass and product upgrading," *Biomass and Bioenergy*, vol. 38, pp. 68–94, 2012.
5. P. M. Mortensen, J.-D. Grunwaldt, P. A. Jensen, K. G. Knudsen, and A. D. Jensen, "A review of catalytic upgrading of bio-oil to engine fuels," *Appl. Catal. A Gen.*, vol. 407, no. 1–2, pp. 1–19, Nov. 2011.
6. M. Linck, L. Felix, T. Marker, and M. Roberts, "Integrated biomass hydropropylolysis and hydrotreating: A brief review," *Wiley Interdiscip.*

**Li Sun**

Phone: +45 4525 2876
E-mail: lsun@kt.dtu.dk
Center for Energy Resources Engineering

Supervisors: Georgios M. Kontogeorgis
Xiaodong Liang
Nicolas von Solms

PhD Study
Started: October 2016
To be completed: September 2019

Modeling Tetra-n-butyl ammonium halides aqueous solution with the Electrolyte CPA Equation of state

Abstract

Tetra-n-butyl ammonium halide is the most widely used promoter for semi-clathrate hydrates. Accurate modeling of tetra-n-alkyl ammonium halides aqueous solution is crucial for industrial applications. In this work, the mean molal activity and osmotic coefficient of tetra-n-butyl ammonium halides aqueous solution at 298.15 K are modeled with the electrolyte Cubic-Plus-Association equation of state. The molalities are up to 10, 10, 1.6 mol/kg of TBAB, TBAC and TBAF, respectively. The mean relative deviation of mean molal activity coefficient are 9.4%, 9.5% and 6.6%, and the mean relative deviation of osmotic coefficient are 7.6%, 6.1% and 3.4% for the TBAB, TBAC and TBAF systems, respectively.

Introduction

Semi-clathrate hydrates have been considered as a possible medium for gas separation and CO₂ capture. Quaternary ammonium salts are the promoters for semi-clathrate hydrates, and Tetra-n-butyl ammonium halide, generally denoted TBAX (with X being bromide, chloride, fluoride, nitrate, etc.) is the type of promoters most applied.

Tetra-n-butyl ammonium cation (TBA⁺) is hydrophobic organic cation, the linear formula of TBA⁺ is [CH₃(CH₂)₃]₄N⁺. Figure 1 shows the structural formula of TBA⁺, the large alkyl groups sterically inhibit the close approach of the positive nitrogen to the anion radical.

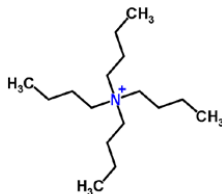


Figure 1: Structural formula of TBA⁺.

The phase behavior of tetra-n-butyl ammonium halide + water system is complex. Some thermodynamic experimental studies (especially the activity and osmotic coefficient) have been published [1, 2, 3].

Model Theory

Maribo-Mogensen et al. proposed a new electrolyte equation of state [4, 5]. In their work, the Cubic-Plus-Association (CPA) Equation of State (EoS) is extended to handle mixtures containing electrolytes by including the electrostatic contributions from the Debye-Hückel [6] and Born terms [7] using a self-consistent model for the static permittivity.

In electrolyte CPA (e-CPA) model, the residual Helmholtz energy is extended to account for the electrostatic interactions and the Gibbs energy of hydration using the Debye-Hückel and Born models:

$$A^r = A^{SRK} + A^{ASSOC} + A^{DH} + A^{Born} \quad (1)$$

Where the first two parts are contributions from CPA, and the remaining two contributions are from Debye-Hückel [6] and Born terms [7].

Maribo-Mogensen et al. [4, 5] presented a new model for the prediction of the static permittivity for aqueous salt mixtures. The new model uses the Wertheim association framework [8] to account for the effect of dielectric saturation, and it enables modern EoS to use a term to take into account hydrogen-bonding/association to predict the static permittivity of multicomponent mixtures. The model is based on the polarizability, dipole moment, and three angles within the molecular structure.

The classical mixing rules are not used for ion-solvent interactions, but will typically be used for mixtures of solvents. For the ion-solvent interactions instead the

Huron-Vidal/NRTL (HV/NRTL) infinite pressure mixing rule is used:

$$\frac{a}{b} = \sum_i x_i \frac{a_i}{b_i} - \frac{g^{E,\infty}}{\ln 2} \quad (2)$$

Where a_i , b_i are pure component SRK EoS parameters, and the excess Gibbs energy at infinite pressure $g^{E,\infty}$ is calculated with the modified HV/NRTL equation [9].

Parameters Prediction and Estimation

It is assumed that there is no contribution from ion association in the residual Helmholtz energy, so there is no ion-ion interaction parameter. The Soave-type temperature dependent SRK parameters are set to zero. Moreover, the NRTL non-randomness factor is set to zero [4, 5].

There is no hydration free energy experimental data for TBA^+ , so for the Born term, the Born radius of TBA^+ is estimated using the Latimer-Pitzer-Slansky equation [10]. In this modeling work, the hard-sphere radii of TBA^+ is set to 3.81 \AA [11], and the polarizability of TBA^+ is $35.03 \times 10^{-40} \text{ C} \cdot \text{m}^2/\text{V}$ from Soffer's work [12]. The CPA co-volume parameter of TBA^+ and HV/NRTL interaction parameters are treated as the adjustable parameters in this modeling.

Results and Conclusions

This modeling work uses the same parameters of water and halide ions as Maribo-Mogensen [4, 5]. Table 1 lists the regression parameters, b_{TBA^+} is the CPA co-volume parameter of TBA^+ , u_{0ij} is the interaction parameter between salt and water at 298.15 K. γ_{\pm} is the mean molal activity coefficient, Φ is the osmotic coefficient.

Table 1: e-CPA parameters for TBAX + H₂O binary systems.

Salt	b_{TBA^+} [cm ³ /mol]	u_{0ij} [K]	RAD γ_{\pm}	RAD Φ
TBAB		-116.35	9.4%	7.6%
TBAC	130.03	-192.81	9.5%	6.1%
TBAF		-392.53	6.6%	3.4%

There are 36 data points for TBAB + H₂O, the molality is up to 10 mol/kg; 27 data points for TBAC + H₂O, the molality is up to 10 mol/kg; 13 data points for TBAF + H₂O, the molality is up to 1.6 mol/kg.

The mean relative deviation of mean molal activity coefficient are 9.4%, 9.5% and 6.6%, and the mean relative deviation of osmotic coefficient are 7.6%, 6.1% and 3.4% for the three systems, respectively.

In this work, the same value is used for the co-volume parameters of TBA^+ for all the three systems. It can be seen in figure 2, the experimental data have the correct order in terms of halide ion size. And the order of the absolute value of the interaction parameter u_{0ij} follows the opposite order of halide ion size. This can be explained by that the smaller radius of halide ion, the bigger interaction with water molecules is expected. The e-CPA model with few adjustable parameters can fit rather satisfactorily the mean molal activity and osmotic coefficient of TBA^+ aqueous solution

The TBA^+ cation is a relative big, soft and irregular organic cation, and it is not clear which diameter reflects the physical fact more accurately. Hydrophobic hydration effect (ion pairing) of TBA^+ may also need to be considered in the future. The selection of crystal radius and effective Born radius for TBA^+ is critical for the thermodynamic modelling. TBA^+ is a relative big, irregular organic cation, which has soft alkyl chains. So, the radius value of TBA^+ which is used in electrostatic calculation needs to be revised.

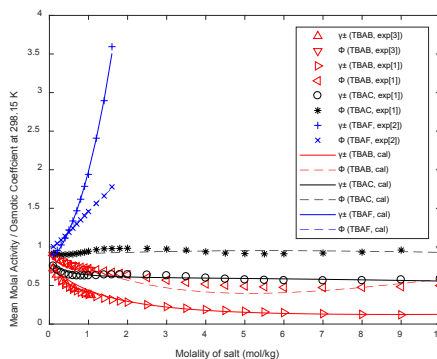


Figure 2: Mean molal activity and osmotic coefficient of TBAB + H₂O, TBAC + H₂O and TBAF + H₂O binary systems at 298.15 K.

References

- Lindenbaum, S., & Boyd, G. E. (1964). The Journal of Physical Chemistry, 68(4), 911-917.
- Wen, W., & Saito, S. (1965). The Journal of Physical Chemistry, 69(10), 3569-3574.
- Amado, G. E. A., & Blanco, L. H. (2005). Fluid Phase Equilibria, 233(2), 230-233.
- Maribo-Mogensen, B. (2014). Development of an electrolyte CPA equation of state for applications in the petroleum and chemical industries. Department of Chemical and Biochemical Engineering, DTU.
- Maribo-Mogensen, B., Thomsen, K., & Kontogeorgis, G. M. (2015). AIChE Journal, 61(9), 2933-2950.
- Hückel, E. (1924). Zur Theorie der Elektrolyte. In Ergebnisse der exakten Naturwissenschaften (199-276). Springer Berlin Heidelberg.
- Born, M. (1920). Zeitschrift für Physik, 1(1), 45-48.
- Wertheim, M. S. (1984). Journal of Statistical Physics, 35(1-2), 19-34.
- Breil, M. P., Kontogeorgis, G. M., Behrens, P. K., & Michelsen, M. L. (2011). Industrial & Engineering Chemistry Research, 50(9), 5795-5805.
- Latimer, W. M., Pitzer, K. S., & Slansky, C. M. (1939). The Journal of Chemical Physics, 7(2), 108-111.
- Masterton, W. L., Bolocofsky, D., & Lee, T. P. (1971). The Journal of Physical Chemistry, 75(18), 2809-2815.
- Soffer, N., Bloemendal, M., & Marcus, Y. (1988). Journal of Chemical & Engineering Data, 33(1), 43-46.



Casper Stryhn Svith

Phone: +45 2077 2056
E-mail: cassvi@kt.dtu.dk

Supervisors: Kim Dam-Johansen
Hao Wu
Weigang Lin

PhD Study
Started: September 2016
To be completed: September 2019

Cyclone reactors: experimental and modeling study

Abstract

The main objective of this study is to obtain fundamental knowledge needed for utilization of cyclone reactors for different applications. This is done through experimental work in pilot- and industrial-scale cyclone reactors, as well as through modeling work based on chemical engineering models and computational fluid dynamic (CFD) models.

Introduction

Cyclone reactors are used in various industries for different applications, such as ore refining in the metals industry, raw meal preconditioning and emission reduction in the cement industry, and flue gas cleaning in the power industry.

A cyclone itself is a continuous and versatile separation device. The simple design makes it popular for application in harsh environments with extreme temperature, abrasion and corrosion.

The use of the cyclones as reactors provides an opportunity for process intensification. Furthermore, the highly turbulent swirling flow of the gas phase provides intense mixing as well as separation of the solid phase from the gas phase. A cyclone reactor can be used for both homogenous and heterogeneous reactions in and/or between the gas and solid phase. The main principle of a cyclone reactor for a gas-solid system is sketched in Figure 1. Compared to entrained flow reactor types, a cyclone reactor has the inverse relationship between the residence time of gas phase and solid phase. An increase in gas flowrate would reduce the gas mean residence time but increase the solid residence time [1]. This makes a cyclone reactor especially interesting for application involving gas solid reactions where secondary reactions of the gaseous products should be minimized, for example in flash pyrolysis.

Extensive research has been carried out for cyclones as separators. However, despite the various application of cyclone reactors in industry, the literature on the subject is scarce and only few authors have developed generalized reactor models for cyclone reactors, which generally have not been validated for different cyclone geometries.

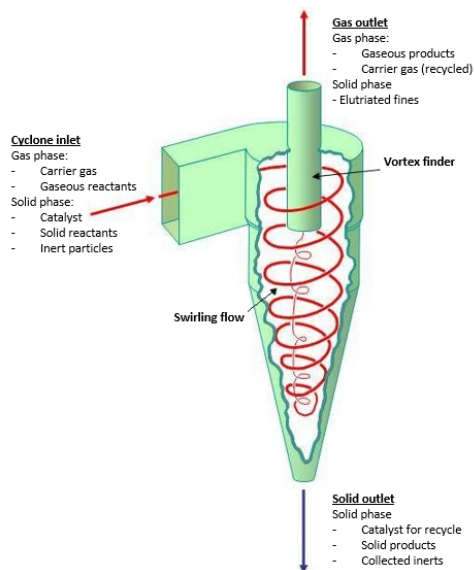


Figure 1: Cyclone reactor principle for gas solid systems

Specific objectives

The main objective of the PhD project is to study the important phenomena, such as gas phase mass transfer, mixing and gas-solid interactions in cyclones through pilot- and full-scale experimental work and modeling.

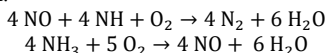
Based on the data collected and knowledge obtained through the experimental and modeling work, reactor models for cyclone reactors will be developed

and validated, and will be used for designing and optimizing cyclone reactors.

Results and discussion

The first part of the PhD project is to investigate the gas phase mixing in cyclone reactors using a model reaction with a known kinetic model. Pilot-scale experiments are conducted. Ideal reactor models (CSTR and PFR) and a residence time based model [2] are used to simulate the experimental data. Basic insight into the mixing pattern can then be achieved based on the differences between the experimental and the model results for a wide variety of operation conditions such as inlet gas velocity, concentration, temperature and particle concentration.

The SNCR reaction [3], with the global reaction mechanism shown below, has been chosen as the model reaction.



This is an existing application in combustion plants such as circulating fluidized bed boilers etc. Therefore, it provides possibility for industrial scale measurements later in the project.

After initial measurements using an existing pilot plant it was refitted to assure the operational stability and quality of the measurements. The setup in its current condition is shown in Figure 2.



Figure 2: Cyclone reactor pilot setup

After the refitting of the setup, experiments have commenced. The initial experimental results compared with modeling results can be seen in Figure 3.

From Figure 3 it can be seen that the obtained conversion is lower than what is predicted by the simple reactor models and the residence time model. However, it is clear that the trend is closer to a mixed reactor than a plug flow reactor or the residence time model.

The experimental work with a wide range of operational conditions is ongoing parallel to the

modeling, where a new residence time model is under development from using available data.

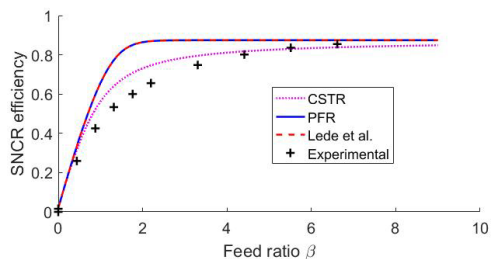


Figure 3: Preliminary experimental and modeling results using simple reactor models and kinetics. With inlet temperature of 975 °C and NO concentration of 200 ppm on dry basis

Future work

The steps to follow in the future is:

- To implement a concentration profile measurement inside the reactor to obtain more detailed information of the mixing pattern
- To use the knowledge obtained through the pilot-scale experiments and modeling to start measurements in industrial-scale
- To start the work with mixing studies using CFD modeling based on well-established practices for CFD modeling of cyclone separator flow fields
- Prepare the pilot setup for residence time distribution (RTD) measurements

Conclusions

There is a gap in the knowledge available about cyclones behavior as a reactor and what is needed for meaningful modeling of cyclone reactors for design and optimization purposes.

An experimental setup for investigating the reactor studies has been made operational and the data gathering has started, while the testing of simple models is being performed, showing limited success and the need for new models.

Acknowledgements

The research is carried out at the Center for Combustion and Harmful Emission Control (CHEC). The author would like to thank the Department of Chemical and Biochemical Engineering for funding this study.

References

1. J. Lede, H.Z. Li, F. Soullignac, J. Villermaux, Chem. Eng. Process 22 (1987) 215-222.
2. J. Lede, H.Z. Li, J. Villermaux, Chem. Eng. J. 42 (1989) 37-55
3. W. Duo, K. Dam-Johansen, K. Østergaard, Can. J. Chem. Eng. 70 (1992) 1014-1020

**Tannaz Tajsleiman**

Phone: +45 4525 2986
E-mail: tantaj@kt.dtu.dk

Supervisors: Ulrich Krühne
Krist V. Gernaey
Jakob Kjøbsted Huusom

PhD Study
Started: August 2015
To be completed: October 2018

Automating experimentation in miniaturized reactors

Abstract

In the present agile society, chemical and biochemical industries face growing pressure to reduce their development costs while accelerating development procedures. Introducing different scale down approaches to mimic large scale processes in miniaturized bioreactors is a big step toward this goal. Using miniaturized bioreactors within an automated high throughput platform provides the possibility of rapid screening and analysis of several parallel processes in a controlled environment. However, design of informative experiments has remained as one of the biggest challenges towards economic and sustainable process development. This project aims at developing an automated strategy to optimize the experimental designs in miniaturized bioreactors and high throughput platforms. The developed routine is simultaneously supported by historical data and predictions of mathematical models such as mechanistic models, computational fluid dynamics (CFD) and compartment models in order to optimize individual experiments.

Introduction

During the last decades, the application of industrial scale biotechnological production processes has seen a significant growth, for example in the pharmaceutical industry. In this perspective, competitive forces drive companies to design robust, efficient and economic processes in order to reach high quality products within the shortest possible operating time. The focus on cost control applies not only to manufacturing but also to the early stages of research and development. In the majority of cases, this early stage is the most resource demanding part of a development procedure, which desires efficient and fast scientific strategies. By development of advanced micro-bioreactors (MBR), a promising opportunity to study multiple parallel processes was delivered within high throughput designs. Moreover, integration of efficient monitoring platforms with miniaturized bioreactors has provided the possibility of on-line monitoring and defining a high level of control on process conditions [1]. However, optimizing experimental designs to achieve the highest level of information from each set of experiments is still one of the main challenges toward an economic, robust and fast process development.

The first step towards a well-designed process is characterizing its behavior. Modelling techniques are mathematical tools to formulate process behavior in

order to make it predictable under various operating conditions. For a successful model structure identification and system parameter estimation, sets of experimental data are required. Moreover, the capability of a model to predict a process behavior needs to be carefully validated by additional data sets. The general procedure of running an experiment and the subsequent data extraction can be significantly speeded up by reducing the reactor size within a controlled high throughput environment. The level of required information from experimental data is a function of problem complexity. From a modelling point of view, this is typically related to the number of parameters, which can easily end up to be a resource consuming exercise in terms of time, economical and computational burden even at a miniaturized scale. Therefore, there is an essential need to use a systematic approach to maximize the level of information acquired from each experiment while minimizing the load of analyses.

This project is going to tackle the mentioned challenges by introducing a new generic design of experiment (DoE) strategy with focus on system characterization and process modelling. In this routine, each experimental design is supported by not only the available historical data but also the predictions of studying model candidates to provide a better overview of probabilities, uncertainties and ultimately the process behavior under various conditions.

Framework and methodology

This work presents a new predictive model development strategy joined with a compound Model based Design of Experiment (M-DoE) approach [2]. Within this routine, a dynamic DoE strategy is applied through an iterative algorithm. At each iteration, one or a set of experimental settings is designed subject to the level of information required for mathematical model structure identification, model parameter estimation and model validation. Each proposed design originates from three serial analysis blocks: 1. prior analysis; 2. DoE criterion analysis and 3. posterior analysis: **Prior analysis** is to take an overall perspective of the design restrictions. Analysis of design operating ranges and historical data or initial standard designed experiments gives an overview of the possible candidate structures corresponding to the studied process. The second block, **DoE criterion analysis**, is to optimize the design criterion 'C' based on analysis of available data and prediction of candidate models. The introduced criterion is a non-linear function of two other criteria 'D' and 'E'. The focus of criterion D is on maximizing the discrimination power among the candidate models while criterion E mostly has emphasis on increasing the level of information with respect to parameter estimation. Hence, the focus of the compound criterion C varies between model candidate discrimination to parameter estimation according to the stage of model development. The extracted experimental data from the designed setting needs to be imported to the last block, **posterior analysis**, for further investigations. In this block, the candidate models are updated and models with inferior performance need to be identified and eliminated. The updated models and probabilities are used for the next iteration of designs until the final validated model is achieved.

The developed routine was successfully tested on the case of mechanistic modelling of a sample reaction. Within this case study, the number of required experiments was minimized to a limited number of the most informative experiments. This goal was mainly achieved by building an efficient interaction between candidate model predictions and mathematical analysis during the model development. Therefore, it is expected to achieve relatively better designs by employing more complex models such as computational fluid dynamics (CFD) with a higher level of detail in the predictions, particularly for complex processes. However, with respect to the calculation time and demands, integration of the DoE routine with a CFD model is not feasible. A compartment model is an alternative technique to improve the resolution of predictions compared with mechanistic models, but within a reasonable calculation time.

Developing a representative compartment model is a big challenge in most of the case studies. Within this project, a novel automated toolbox was developed in order to extract compartment model specifications (compartment volumes, connections and interface fluxes between each set of adjacent compartments) from its

corresponding CFD simulation results. By the developed strategy, a network of compartments is identified with respect to a target parameter. The target parameter can vary within a specific tolerance range for each zone. The assumption of having well-mixed conditions in each compartment is the main key toward simplifying CFD models, thereby significantly reducing the calculation demands while the model is still capable of predicting the gradient present in the control volume. The overall transformation of a CFD result into a compartment map is shown in figure 1.

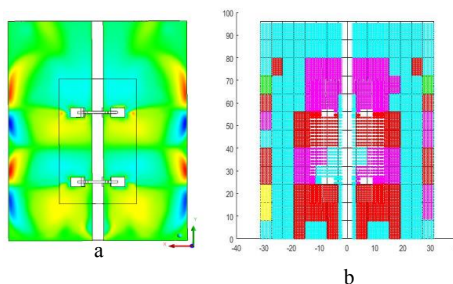


Figure 1. CFD based compartment mapping with target parameter vertical fluid velocity. a. CFD simulation of a 250 ml stirred tank, b. extracted compartment map

Conclusion

This project shows the potential of DoE strategies to minimize the number of required experiments in a research and development stage. Furthermore, a generic M-DoE approach was introduced which benefits from the predictive capacity of different models to characterize unknown processes and designs. The main goal of each proposed design is to specify the experimental settings that can deliver the highest level of target information.

Acknowledgements

This project has received funding from the European Union's Horizon 2020 research and innovation programme under the Marie Skłodowska-Curie grant agreement No 643056.

References

1. Anon 2002 Novel miniaturized systems in high-throughput screening *Trends Biotechnol.* **20** 167–73
2. Tajssoleiman T, Semenova D, Fernandes A, Huusom J, Gernaey K V. and Krühne U 2017 An efficient experimental design strategy for modelling and characterization of processes 2017 *27th European Symposium on Computer Aided Process Engineering* (Elsevier Science)

**Mauro Torli**

Phone: +45 50 15 59 12
E-mail: mtor@kt.dtu.
Center: Center for Energy Resources Engineering

Supervisors: Philip Loldrup Fosbøl
Georgios Kontogeorgis

PhD Study

Started: June-2016
To be completed: May-2019

Thermodynamics, design, simulation and benchmarking of biofuel processes

Abstract

Biofuels production as conventional gasoline is increasing worldwide. Of this, ethanol alone makes up a large share. Conventionally, ethanol is produced from readily fermentable carbohydrates such as sugars and starches. The availability of agricultural feedstocks is limited, because of competition with food production, arable land usage, and water availability. Consequently, forest residues, trees from plantations, straws, grasses and other agricultural residues may become a viable feedstocks for bio fuel production. However, the very heterogeneous nature of these lignocellulosic materials makes them inconvenient for bioconversion.

An alternative bioconversion technology is biomass gasification to syngas followed by fermentation to biofuel. The products from this process consist of ethanol, n-butanol or chemicals such as acetic acid, butyric acid and the like.

Introduction

Syngas fermentation is an indirect conversion process for the production of alcohols, organic acids and other chemicals; it is referred to as an indirect fermentation because the feedstocks are not directly fed in the bioreactor to form products, but are first gasified into syngas, which is then cleaned and cooled before it is fed to the reactor. Synthesis gas is mainly a mixture of CO, CO₂, and H₂; however depending on the type of feedstock and gasification system used, small amounts of tars, CH₄, C₂H₂, C₂H₄, H₂S, NH₃, COS and HCN and nitric oxide are also detected. Some of these impurities may interfere with the fermentation process; selection of conventional technologies suitable for syngas cleanup includes: cyclones, tar cracking, electrostatic filters and scrubber and an absorber-desorber system. Conventional feedstock may include agricultural residue, municipal solid wastes, energy crops, coal, and petroleum coke. The fermentation step itself also faces a number of technical challenges including scale-up and mass transfer limitations. Other important parameters are the metabolic performance and product selectivity of the bacterial strains that converts syngas into the desired biochemical. Compared with traditional fermentations, syngas fermentation has lower reported production concentration, therefore more energy is potentially required for downstream product recovery. LanzaTech, Synata Bio (formerly Coskata), and INEOS Bio are among the companies that are

currently pursuing commercialization of syngas fermentation for biofuels production [1].

This PhD project is part of a large innovation action, SYNFERON, whose technology focuses are: fermentation of syngas to liquid and gaseous (methane) biofuels, design of novel bioreactors, pressure control and use of suitable surfactants for increasing the gas/liquid mass transfer efficiency, use of biomimetic membranes and development of diabatic distillation for gentle and cost-efficient purification of liquid biofuels and development of an optimized process design and comparison with existing technologies.

Specific Objectives

This PhD project is encompassed in the fourth work package of SYNFERON; and the objectives are: investigation of the current technologies in syngas fermentation for fuel production, develop and validate a thermodynamic model parameter base, optimized for the biofuel processes, collecting data and models from literature and from the other team members and implement them in the process simulations, conduct simulation of different possible layouts and perform pinch analysis for determining the highest possible efficiency. The global aim is to compare several different syngas fermentation designs and benchmarking the performance of the various technologies from a mass, energy, economic and engineering point of view.

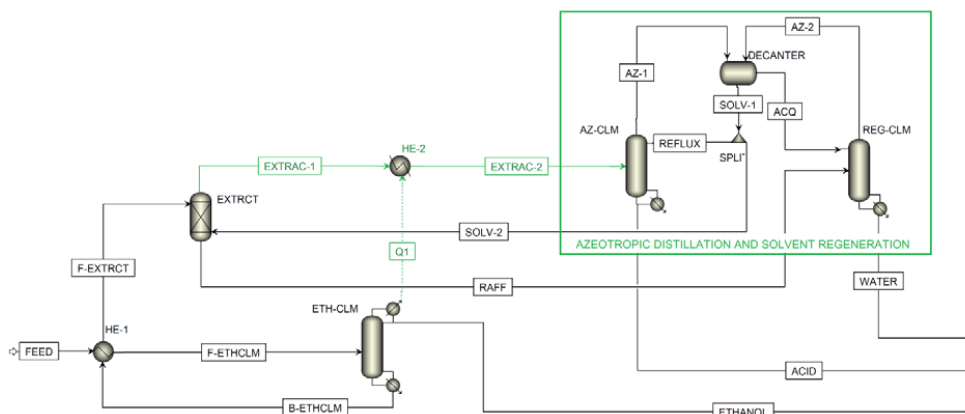


Figure 1: Simplified flowsheet of ethanol distillation followed by MTBE extraction and azeotropic distillation for acetic acid recovery

Results and Discussion

A benchmarking study for different ethanol recovery methods from diluted aqueous solution has been performed with the commercial process simulator Aspen Plus. Among the cases considered are: traditional atmospheric distillation, mechanical vapor recompression and multi-effect distillation. Feed concentration tested ranges from 0.6 to 5 wt% in ethanol and up to 1 wt% acetic acid.

The most recurrent byproduct of syngas fermentation to ethanol is acetic acid: irrespective to the layout chosen when distillation only is applied as mean of separation, the acid is completely recovered as bottom product of the ethanol column, within the water. Although some designs show direct recirculation of this stream to the bioreactor, it is known that accumulation of acetic acid may lead to inhibition of bacteria and ultimately to cessation of substrate conversion. A possible way to partially recover acetic acid from the water before recycling the medium back to the fermenter is extraction followed by azeotropic distillation and solvent regeneration [2].

Typically the most important factors which dictate the solvent selection are the distribution coefficient and separation factor. Due to the low concentration of acetic acid in the fermentation medium, the specific energy requirement for the azeotropic distillation and solvent regeneration may be substantial; therefore properties such as normal boiling point and heat of evaporation become predominant parameters for the choice of the ideal extractant. Among the various solvents tested MTBE showed the best performance: thanks to a boiling point as low as 55°C it is possible to use the heat removed from the condenser of the ethanol column (~78°C) to completely evaporate the extract stream before it enters the azeotropic distillation and regeneration section (Fig. 1, heat and material stream in green).

Fig. 2 shows for all the concentrations tested that a higher acetic acid recovery corresponds to lower

specific energy consumption (MJ per kg of acetic acid recovered); attesting a more efficient use of the waste heat. Basically the heat recovered from the condenser allows the recirculation of a higher flow of solvent, resulting in a higher amount of acid recovered, with little or any increase in the net energy requirement for the azeotropic distillation and solvent regeneration.

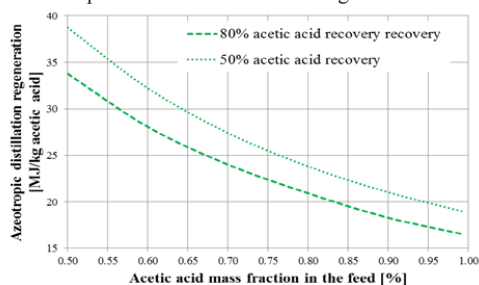


Figure 2: Heat requirement for azeotropic distillation and solvent regeneration per kg of acetic acid recovered

Conclusion

A thermodynamic package optimized for biofuel processes based on γ - ϕ approach has been developed and validated against VLE and LLE data of relevant systems. Different layouts and combinations of conventional separation technologies have been simulated for the recovery of syngas fermentation products, with particular focus to heat integration.

References

1. J. Daniell, M. Köpke, S. D. Simpson, *Energies* 5 (2012) 5372-5417
2. K. L. Li, I. L. Chien, C. L. Chen, *Design and Optimization of Acetic Acid Dehydration Processes*, 5th International Symposium on Advanced Control of Industrial Processes, 2014 Hiroshima



Burak Ulusoy

Phone: +45 4525 2800
E-mail: bulu@kt.dtu.dk

Supervisors: Kim Dam-Johansen
Weigang Lin
Wu Hao

PhD Study
Started: September 2016
To be completed: August 2019

NO_x formation and reduction in fluidized bed combustion of biomass

Abstract

The focal point of this PhD project is to understand the NO_x formation and reduction mechanisms in fluidized bed combustion of biomass. Comprehensive experimental and modelling work will be conducted on both laboratory- and pilot-scale with the ultimate goal of minimizing NO_x emissions during combustion. The initial part of the project will mainly deal with the NO_x formation and reduction during char combustion, which is lesser understood compared to the gaseous NO_x chemistry. Following this, pilot-scale fluidized bed combustion experiments and full-scale CFD modelling will be performed to facilitate the minimization of NO_x emissions.

Introduction

Fluidized bed combustion of biomass is a promising technology for heat and power production from biomass. Due to the possibility of fuel-flexibility, high combustion efficiency, and low pollutant emission, the application of fluidized bed technology in the gasification and combustion industry has increased at a fast pace [1]. However, incentives for further reducing the NO_x emission from fluidized bed combustion are driven by the harmful environmental impact and strict emissions regulations. It has been well established that upon release to the atmosphere, NO_x compounds contribute to global warming, photochemical smog production, and acid rain formation.

In a fluidized bed combustor, the final NO emission is determined by the competing formation and reduction reactions. The NO primarily stems from the fuel bound nitrogen either through volatile or char nitrogen oxidation. Analogous to the formation reactions, NO is reduced through homogeneous thermal DeNO_x reactions or heterogeneous reduction over char [2]. Controlling the NO emissions requires a thorough understanding of the underlying mechanisms, which is the primary goal of this work.

Objectives

The main objective of this project is to minimize NO_x emissions from fluidized bed combustion of biomass. To do this, a fundamental understanding of the underlying mechanisms in NO_x formation and reduction will be acquired through experimental studies in laboratory- and pilot-scale. Mathematical and computational modelling work will also be conducted to

describe the experimental data, which could then serve as predictive tools or as sub-models in large-scale simulations.

Experimental Work

Combustion and NO reduction reactivity of pine wood, straw (S), waste wood, bran (B), DDGS, and sunflower seed chars was investigated in a fixed bed reactor, shown in Figure 1. Prior to charring, the biomasses were demineralized (DM) using 1 M HNO₃ at 60°C for one hour. Subsequently, charring was performed in a horizontal oven at 800°C under a N₂ flow of 2.5 NL/min for 10 min.

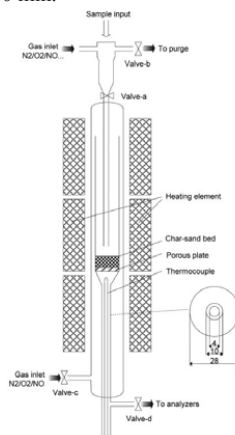


Figure 1: Schematic illustration of the fixed bed reactor.

The reactor is equipped with a solid feeding device, thereby allowing sample admission at a desired temperature and gas composition. In the reduction study, 50 mg char was mixed with 1.70 g silica sand and introduced into the reactor at 800°C and a NO inlet concentration of 400 ppmv. The combustion experiments were performed at 800°C at an inlet O₂ concentration of 10 vol%. In both experiments, the outlet concentrations of NO, O₂, CO, and CO₂ were continuously monitored.

Kinetic Modelling

The steady state fixed bed reactor design equation (Eq. 1) was employed to extract kinetic information from the NO reduction experiments. Assuming the carbon mass based reactivity, R_{NO} (mol/kgC/s), is first order with respect to NO, Eq. 1 integrates to Eq. 2.

$$\frac{dX_{NO}}{dW} = \frac{R_{NO}}{F_{NO,0}} \quad \text{Eq. 1}$$

$$-\ln(1-X_{NO}) = k_{NO} \cdot W/v_0 \quad \text{Eq. 2}$$

Here, X_{NO} (-) is the conversion of NO, W (kg) the instantaneous carbon mass in the bed, F_{NO,0} (mol/s) the flow rate of NO at the inlet, k_{NO} (m³/kgC/s) the first order carbon mass based reaction rate constant, and v₀ (m³/s) the volumetric flow rate. Calculating the instantaneous mass of carbon in the bed using the CO and CO₂ outlet concentrations, the transient behavior of the first order reaction rate constant can be determined.

Results and Discussion

Figure 2 illustrates the selectivity of NO formation from combustion of the biomass chars. A decreasing tendency in the selectivity is observed for the DM chars as the char nitrogen content increases. This has previously been reported [3], however, the reasoning for this behavior remains unknown. Due to the underlying mechanism of NO release from combustion, the char nitrogen content conceivably affects the formation and reduction reactions of NO. The decrease in selectivity was more pronounced for the DM chars wherein the catalytic influence of ash forming elements was diminished.

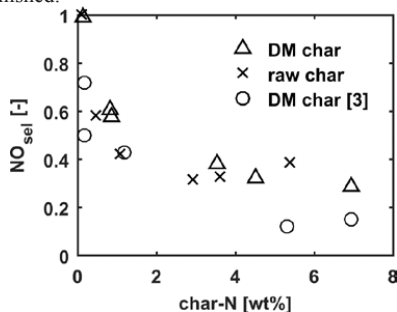


Figure 2: NO selectivity versus char nitrogen content for raw and DM biomass chars. Results of Karlström et al. [3] shown for comparison.

The reduction of NO over chars was examined, with selected results depicted in Figure 3, showing the transient first order carbon mass based reactivity. Of the

raw chars, straw exhibited the highest reactivity towards NO, followed by DDGS and bran. On the other hand, the DM samples in general exhibited little discrepancy with DM straw being the most reactive followed DM DDGS and DM bran. No clear correlation was observed between reduction reactivity and char nitrogen content for both the raw and demineralized chars.

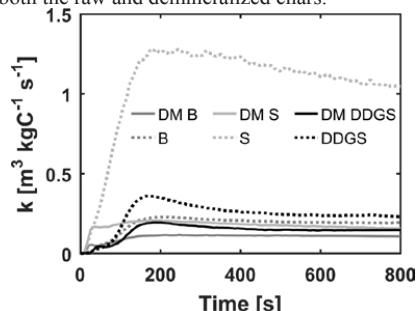


Figure 3: Transient first order reactivity of select chars towards NO. Conditions, T=800°C and C_{NO,0}=400 ppmv.

The explanation of the observed trends can be elucidated from the chemical compositions of the chars. Although, bran was noted to contain a larger potassium content (69610 mg/kg) relative to straw (50769 mg/kg), it exhibited a considerably lower reactivity towards NO. This could be caused by the high phosphorus content in the bran (49429 mg/kg), thereby forming KPO₃ that is catalytically inactive in NO reduction.

Conclusion

It was noted that the char nitrogen content influenced the NO selectivity upon combustion of biomass chars. Examining the reduction behavior of the chars towards NO showed no clear tendency between reduction reactivity and char nitrogen content.

The observed reactivity difference between straw and bran chars indicated that the main controlling factor of reactivity is the content and chemical association of the ash forming elements.

Future work

Experiments will be carried out in a pilot-scale fluidized bed combustor to investigate the emission of NO_x under well-defined operating conditions. To minimize NO_x emissions, the influence of fuel type, secondary air inlet, bed material, and additives will be examined. CFD simulations will be performed in combination with skeletal NO_x models to describe the freeboard of an industrial-scale fluidized bed boiler, thereby providing a simplified gas phase model, useful in industrial applications.

References

- R.I. Singh, A. Brink, M. Hupa, Appl. Therm. Eng., 52 (2) (2013) 585-614.
- P. Glarborg, A.D. Jensen, J.E. Johnsson, Prog. Energy Combust. Sci. 29 (2003) 89-113.



Justina Vaičekauskaitė
E-mail: jusvai@kt.dtu.dk

Supervisors: Anne Ladegaard Skov
Piotr Mazurek
Liyun Yu

PhD Study
Started: July 2017
To be completed: July 2020

Insight into the dielectric breakdown of elastomers

Abstract

The scope of the project is to capture macroscopic changes taking place during the breakdown process of dielectric elastomers. The dielectric breakdown strength measurement is one of the most common methods to evaluate stability of polymers in an electric field. In this work, elastomer movements are recorded with fast speed camera in order to clarify elastomer behavior during breakdown and thereby hopefully gain insight into the underlying breakdown phenomena.

Introduction

Dielectric elastomers find more and more uses as energy transducers but nevertheless the fundamentals behind the electrical breakdown of these thin and elastic films are still not fully understood and elucidated. When a voltage (below the electrical breakdown voltage) is applied to dielectric elastomer they expand reversibly due to the electro-attraction of the compliant electrodes. Dielectric breakdown measurements are commonly used to evaluate stability of polymers in an electric field. The breakdown test has been extensively used over many years and is still gaining on importance, due to an increasing demand of novel polymeric materials applied in large electric fields, such as: dielectric or transport layers, robotics or flexible electronics [1]. There are only few theoretical models, assessing the underlying physical or chemical phenomena which occur during a breakdown process, for example: the hole-induced breakdown model, the electron-trapping breakdown model, the resonant-tunneling-induced breakdown model and the filamentary model [2]. Unfortunately, experimental studies have been conducted to achieve an understanding of what is happening on a microscopic scale in a sample during breakdown. In this work, a high-speed camera is coupled to electrical breakdown measurement in order to capture macroscopic processes taking place during the dielectric breakdown to verify if the time-scale and behavior of the electrical breakdown can elucidate the underlying behavior.

Results and Discussion

In this work, electrical breakdown of thin elastomers were measured. Elastomer film thickness varied from $52\mu\text{m}$ to $60\mu\text{m}$. First polymer film was cut into

rectangle shaped $3 \times 9,5$ cm size form and afterwards placed on the plastic frame with twelve $0,8$ cm size holes. This frame with film on it subsequently was placed into breakdown instrument between the electrodes. The gap between the electrodes was fixed to be the same as the thickness of the film sample (Figure 1). Afterwards, 20kV voltage was applied until polymer film break down. In the meantime, breakdown process was recorded with high-speed camera system (FASTCAM Mini UX100 - Photron).

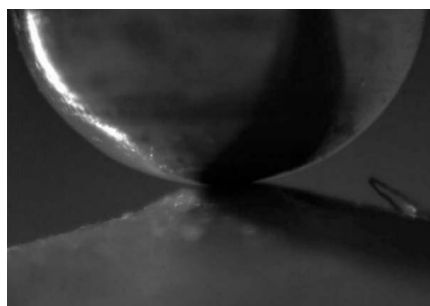


Figure 1: Film sample between electrodes, before breakdown. Electrode diameter: 2mm.

It was observed, that when the voltage is applied, polymer films starts to move (wrinkle) and, depending on which type of film samples is used: with or without filler, it forms, respectively, “bubble” or “ring” like structures. These structures seems to disappear directly after a breakdown (Figure 2 A and B). Blok and Legrand explained such behavior as so-called electro-mechanical breakdown. They stated the hypothesis, that polymer films are never completely smooth, and when

an electric field is applied, the electrical field and thus electrical forces are largest at the thinnest spot of the film. For that reason the film sample starts to deform the most at the thinnest spot and when the electric strength is reached there, breakdown occurs [3]. This is also referred to as electro-mechanical instability and has been extensively studied by modelling [4], [5].

Breakdown is sudden process and when it occurs, it can be spotted with high-speed camera, in a shape of electrical discharge (Figure 3).

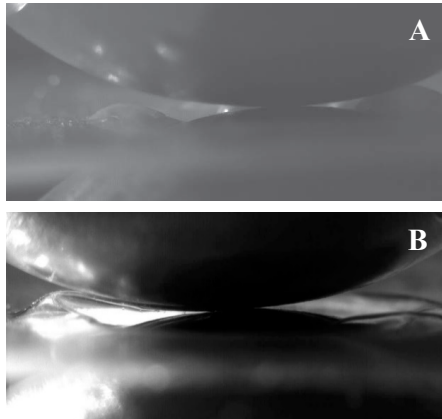


Figure 2: Film movement on the electrode when the voltage is applied. A – film sample with filler creates “bubble” like structures, B – film sample without a filler creates “ring” like structures. Electrode diameter: 20mm.

When the breakdown starts, all structures that were visible during breakdown (“bubble” and “ring”) are gone, and the film returns to its original dimensions. However, in some cases, film sample touches upper electrode in one spot and breakdown occurs in this exact spot (Figure 4).

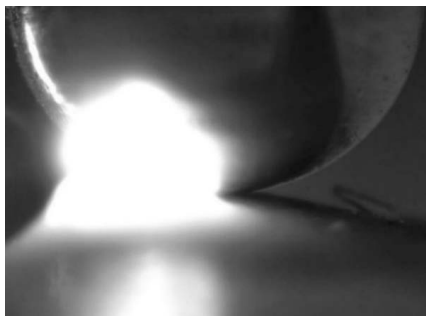


Figure 3: Film sample during breakdown. Electrode diameter: 2mm.

Breakdown lasts until film sample breaks and a hole on the film sample appears (Figure 5). Hole varies in size from few micrometers to a few millimeters and the shape do not change in time.

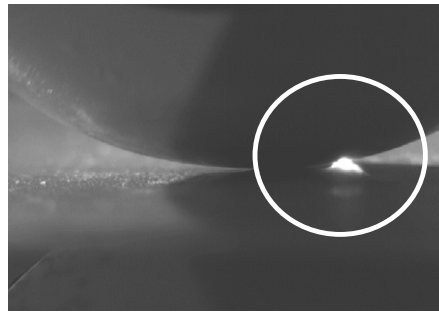


Figure 4: Film sample touching electrode, right before breakdown (marked with a white circle). Electrode diameter: 20mm.



Figure 5: Film sample with a hole, after breakdown (marked with a white circle). Electrode diameter: 2mm.

Conclusions

Although breakdown is widely used to state the quality of a given dielectric elastomer, unfortunately the breakdown phenomenon is not clearly studied. As we can see from our results, there are many different things and film wrinkling movements happening during breakdown. Therefore, this method needs further investigation and experimentation until it is fully understood. With the underlying mechanisms and phenomena elucidated, a design guideline towards more electrically robust dielectric elastomers can be made.

References

1. V. A. Zakrevskii and N. T. Sudar, ‘Electrical Breakdown of Thin Polymer Films’, *Phys. Solid State*, vol. 47, no. 5, p. 961, 2005.
2. A. Belkin, A. Bezryadin, L. Hendren, and A. Hubler, ‘Recovery of Alumina Nanocapacitors after High Voltage Breakdown’, *Sci. Rep.*, vol. 7, no. 1, p. 932, 2017.
3. J. Blok and D. G. Legrand, ‘Dielectric breakdown of polymer films’, *J. Appl. Phys.*, vol. 40, no. 1, pp. 288–293, 1969.
4. X. Zhao and Z. Suo, ‘Theory of dielectric elastomers capable of giant deformation of actuation’, *Phys. Rev. Lett.*, vol. 104, no. 17, pp. 1–4, 2010.
5. X. Zhou et al., ‘Electrical breakdown and ultrahigh electrical energy density in poly(vinylidene fluoride-hexafluoropropylene) copolymer’, *Appl. Phys. Lett.*, vol. 94, no. 16, pp. 92–95, 2009.



Andre Vinhal
Phone: +45 4525 2876
E-mail: anpi@kt.dtu.dk
Center: Center for Energy Resources Engineering

Supervisors: Georgios Kontogeorgis
Wei Yan

PhD Study
Started: May 2015
To be completed: April 2018

Application of advanced thermodynamic models to simultaneously describe phase equilibrium and critical properties of fluid mixtures

Abstract

Mean-field or classical equations of state (*EoS*) are models extensively applied in chemical and petroleum engineering to represent the properties of fluids. However, due to their analytical character, they can only accurately describe the behavior of these systems far away from the critical point. In the near-critical region, fluids behave non-analytically and can only be correctly represented if density fluctuations are incorporated into the classical *EoS*. An improved description of the phase behavior of fluids far from and close to critical point requires the utilization of an advanced thermodynamic model (crossover *EoS*) that bridges the gap between the analytical and singular behavior of fluids. In this work, we utilize a crossover *EoS* to represent the properties of methanol/n-alkanes binary mixtures.

Introduction

Mean-field thermodynamic models are analytical expressions relating the variables that describe the state of a fluid: pressure, temperature, volume and composition. These models are also called classical *EoS* and are designed by considering that the species interact via an average potential. This simplification is useful because it allows the development of expressions that can precisely represent the behavior of fluids far away from the critical point, where the fluctuations of the thermodynamic properties are negligible [1].

In the vicinity of a critical point, fluids possess an asymptotic/singular behavior, which is different from the one implied by a classical model. This contrast is due to the long-range interactions between the system's particles and, since the classical *EoS* do not take into account the density inhomogeneities that arise close to the critical point, they are unable to correctly describe the singular feature of the thermodynamic properties.

Although the limitations of the classical *EoS* in the critical region are known for decades, these models are still widely applied in chemical and petroleum engineering. However, the accurate representation of the properties of fluids in a wide range of conditions requires the use of advanced thermodynamic models.

In this work, we have applied a recursive procedure to correct the representation of the Cubic-Plus-Association (*CPA*) *EoS* in the near-critical region. This model is capable of representing the phase behavior of hydrocarbons and associating molecules, like methanol,

far from the critical region. Additionally, we compare the classical formulation with the crossover *CPA* in the description of phase equilibrium and critical properties.

Thermodynamic Models

The *CPA EoS* is a mean-field thermodynamic model broadly applied in the Oil & Gas industry and other sectors [2]. The pressure explicit relation for this model is given by:

$$P = \frac{RT}{v-b} - \frac{a}{[v(v+b)]} - \frac{RT}{2v} \left(1 - v \frac{\partial \ln g}{\partial v} \right) \sum x_i \Sigma (1 - X_{A_i}) \quad (1)$$

where R is the gas constant, T is temperature, v is molar volume a and b are the attractive repulsive term constants, respectively, x_i is the mole fraction of the associating component, g is the radial distribution function and X_{A_i} is the monomer fraction. The first two right-hand terms correspond to the physical interactions between the molecules of the system, i.e. repulsion and attraction, respectively. Furthermore, the third term explicitly takes into account the association between species due to the hydrogen bonds.

As any other classical *EoS*, *CPA* is unable to represent the behavior of fluids close to the critical point, since it does not incorporate the density inhomogeneities. Thus we applied a recursive procedure in which the long (Ω_n^l) and short (Ω_n^s) range interactions are added to the free energy density (f) via the recursive procedure described by the following expressions:

$$f^{cross} = f^{CPA} + \sum \delta f_n \quad (2)$$

$$\delta f_n = -K_n \ln(\Omega_n^s/\Omega_n^l) \quad (3)$$

$$K_n = kT/2^{3n}L^3 \quad (4)$$

$$\Omega_n^{\lambda} = \int_0^{\min(\rho, \rho^{max})} dy \exp(-G_n^{\lambda}/K_n) \quad (5)$$

$$G_n^{\lambda}(\rho, y) = 0.5[\bar{f}_n^{\lambda}(\rho + y) + \bar{f}_n^{\lambda}(\rho - y) - 2\bar{f}_n^{\lambda}(\rho)] \quad (6)$$

$$\bar{f}_n^l(\rho) = \bar{f}_{n-1}^l(\rho) + a\rho^2 \quad (7)$$

$$\bar{f}_n^s(\rho) = \bar{f}_{n-1}^s(\rho) + 2^{-2n}\phi a\rho^2 \quad (8)$$

where ρ is density, k is the Boltzmann's constant, the superscripts l and s represent the long and short range correlations, ϕ and L are two additional parameters and f^{CPA} is the free energy density calculated with Eq. 1.

The application of the recursive relations (Eq. 2 to 7) modifies the *CPA EoS*, allowing the correct description of the properties of fluids in the critical region [3].

Phase Equilibrium and Critical Point Description

The *CPA* and the crossover *CPA (CCPA)* *EoS* were applied in the description of the phase behavior and the critical properties of binary mixtures containing methanol and n-alkanes (from n-hexane to n-decane).

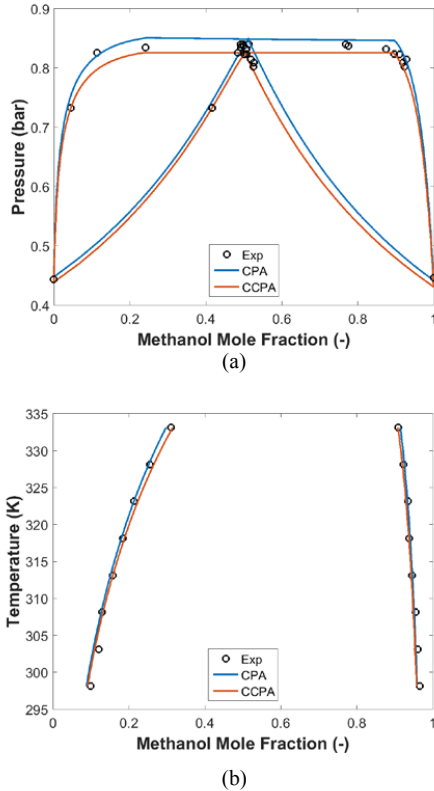


Figure 1: Methanol/n-hexane VLE diagram at 318.15K (a) and methanol/n-nonane LLE diagram at 1.0325bar (b). The open circles represent experimental data, while the blue and red lines are the calculations with the *CPA* and *CCPA*, respectively.

Figure 1 shows the methanol/n-heptane Vapor-Liquid equilibrium (VLE) diagram at 318.15K and the methanol/n-nonane Liquid-Liquid equilibrium (LLE) diagram at 1.0325bar. From the plots is possible to conclude that both models are able to accurately describe the systems far from the critical point.

The critical points of the methanol/n-hexane systems were calculated with the two models and compared with experimental data. Figure 2 shows that the classical model over-predicts the experimental critical points of the system, while *CCPA* precisely predicts them.

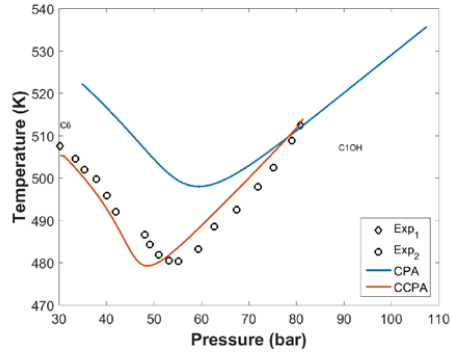


Figure 2: Critical lines of the methanol/n-hexane system. The open circles represent experimental data, while the blue and red lines are the calculations with the *CPA* and *CCPA*, respectively.

Additionally, Table 1 shows that *CCPA* gives an improved overall description of the phase equilibrium and critical properties for the methanol/n-alkane systems studied (methanol and n-hexane to n-decane).

Table 1: Overall deviations of the phase equilibrium and critical properties using *CPA* and *CCPA*.

<i>EoS</i>	Overall Deviations	
	Phase Eq. (%)	Crit. Prop. (%)
<i>CPA</i>	2.6	8.5
<i>CCPA</i>	3.0	5.0

Conclusions

The application of the recursive procedure to the *CPA EoS* corrects the behavior of the classical model in the near-critical regions allowing a precise description of the phase behavior of methanol/n-alkane systems far from and close to the critical point. This is useful for the description of the properties of fluids in a wide range of process conditions.

References

- L. Salvino, J. White, J. Chem. Phys. 96 (1992) 4559-4568.
- G.M. Kontogeorgis, et. al., Ind. Eng. Chem. Res. 35 (1996) 4310-4318.
- X. Xu, Y. Duan, Fluid Phase Equilib. 241 (2010) 229-235.



Guoliang Wang

Phone: +45 4525 2890
E-mail: guow@kt.dtu.dk

Supervisors: Peter Arendt Jensen
Hao Wu
Flemming Jappe Frandsen
Peter Glarborg
Bo Sander, Ørsted Bioenergy & Thermal

PhD Study
Started: October 2014
To be completed: February 2018

K-capture by Al-Si based additives at suspension-fired conditions

Abstract

The reaction between K-salts and kaolin or coal fly ash was investigated by EFR experiments and equilibrium calculations. The results showed that under the studied conditions, kaolin and coal fly ash can effectively capture gaseous K-salts. The kaolin K-capture amount firstly increased and then decreased when reaction temperature increased from 800 °C to 1450 °C. Kaolin captured KCl more effectively than coal fly ashes. K-capture level of AMV coal fly ash was slightly higher than ASV2 coal fly ash at 1300 °C and 1450 °C probably due to a lower melting point or a relatively higher Si concentration.

Introduction

Combustion of biomass in suspension-fired boilers can produce renewable, CO₂-neutral electricity and heat with a higher efficiency and flexibility compared to grate-fired boilers. However, the high content of alkali species in biomass may lead to severe ash deposition, corrosion and SCR catalyst deactivation problems in biomass-fired boilers [1].

One option to tackle these ash-related problems is the injection of additives into boilers for transforming harmful gaseous alkali compounds (e.g. KCl, KOH, K₂CO₃, K₂SO₄) into ash species with higher melting point. Kaolin and coal fly ash are effective additives for biomass combustion and have been studied in laboratory-scale experiments. However, most the previous studies were conducted in fixed bed reactors or specially designed micro-gravimetric reactors [1-3], where the conditions were obviously different from that in suspension fired boilers.

Specific Objectives

The objective of the present work is to develop an experimental method using the EFR to study the K-capture reaction under suspension-fired conditions. The impact of the type of additives, reaction temperature, additive particle size, K-concentration/molar ratio of K/(Al+Si) in reactants, type of K-salts was investigated. Based on the experimental results, a mathematical model describing the K-capture process by solid additives will be developed. Recommendations for choosing and optimal utilization of additives in biomass suspension-fired boilers will be provided.

Experimental

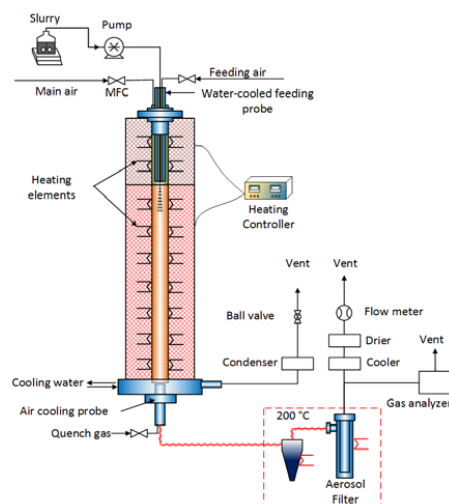


Figure 1: Schematic of Entrained Flow Reactor (EFR).

The EFR employed in this study is shown schematically in Figure 1. K-species (KOH, K₂CO₃, KCl, K₂SO₄) and solid additives were mixed with deionized water, to make a homogeneous slurry. The slurry was fed in and atomized in the EFR. K-species reacted with the solid additives in the EFR and the solid products were collected by a cyclone and a metal filter.

The collected solid samples were analyzed with ICP-OES (Inductively Coupled Plasma Optical Emission Spectrometry) to determine the amount of potassium captured by additives. Two parameters are defined and calculated basing on the ICP-OES analysis: K-conversion (X_K) and K-capture level (C_K). X_K is the percentage of the injected K-salt reacted with additives and transformed into water-insoluble K-aluminosilicate (%), while C_K is defined as the mass of K captured by 1 g solid additive during the reaction (g K/g additive). The mineralogical composition and the morphology of products were studied with XRD (X-ray Diffraction) and SEM-EDX (Scanning Electron Microscopy-Energy-dispersive X-ray spectroscopy) analysis.

Results and Discussion

The experimental K-capture level (C_K) at different K-concentration/molar K/(Al+Si) ratio in reactants and temperature by kaolin was compared with the equilibrium calculation results in Figure 2. The C_K increased when K-concentration/molar K/(Al+Si) ratio increased from 50 to 500 ppmv. However, it did not increase when the KOH concentration further increased to 750 and 1000 ppmv. This is probably because all the Si has transferred into K-aluminosilicate and the increased KOH stayed unreacted.

The results at different temperatures show that C_K firstly increased when temperature increased from 800 °C to 1300 °C. However, it decreased when temperature increased to 1450 °C. This is probably because at 800 °C the reaction was to some extent kinetically controlled. And at 1450 °C, mullite was significantly formed, which is less reactive towards KOH-capture compared to other kaolin minerals. The XRD analysis shows that at 1300 °C and 1450 °C, crystalline kaliophilite was formed, while at lower temperatures amorphous K-aluminosilicate was formed.

Results of KCl-capture by coal fly ash show that kaolin can capture KCl more effectively than the two coal fly ashes. C_K of AMV coal fly ash is lower than ASV2 coal fly ash at 800-1100 °C. However, AMV coal fly ash captured KCl more effectively than ASV2 coal fly ash at 1300 °C and 1450 °C, probably due to a lower melting point and a relatively high Si concentration.

Conclusions

K-capture by kaolin and coal fly ash was studied in the CHEC entrained flow reactor (EFR). The results showed that kaolin and coal fly ash can capture K-salts effectively at suspension fired conditions. K-capture level (C_K) increased significantly when K-concentration increased from 50 ppmv to 500 ppmv. The K-capture level firstly increased and then decreased when reaction temperature increased from 800 °C to 1450 °C. Coal fly ash captured KCl less effectively than kaolin. C_K of AMV coal fly ash is higher than ASV2 coal fly ash at 1300 °C and 1450 °C, probably due to a lower melting point or relatively higher content of Si.

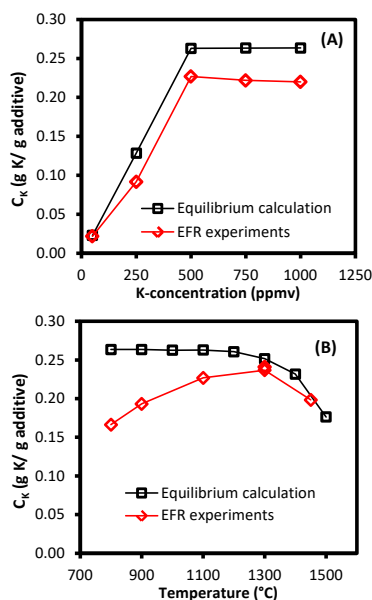


Figure 2: KOH-capture level (C_K) by kaolin at different K-concentration (1100 °C) (A), and different temperatures (500 ppmv KOH) (B). Residence time was 1.2 s for all experiments. Equilibrium calculation results included for comparison.

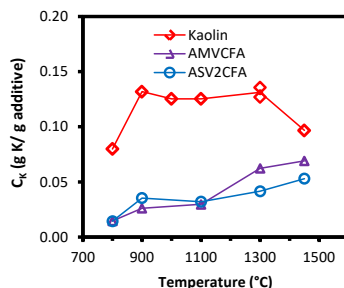


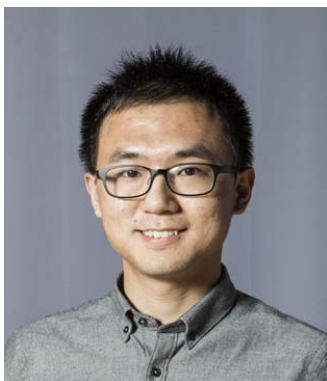
Figure 3: KCl capture level (C_K) by kaolin and coal fly ash at different temperature (500 ppmv KCl, residence time is 1.2 s).

Acknowledgements

This work is part of the project 'Flexible use of Biomass on PF fired power plants' funded by Energinet.dk through the ForskEL program, Ørsted Bioenergy & Thermal Power A/S and DTU.

References

1. Y. Zheng, P.A. Jensen, A.D. Jensen. *Fuel* 87 (15-16) (2008) 3304-3312.
2. W. A. Punjak, M. Uberoi, F. Shadman. *AIChE Journal* 35 (7) (1989) 1186-1194.
3. K.Q. Tran, K. Lisa, B.M. Steenari, et.al. *Fuel* 84 (2-3) (2005) 169-175.



Ting Wang
Phone: +45 4525 2952
E-mail: tinwan@kt.dtu.dk

Supervisors: Søren Kiil
Claus E. Weinell
Kim Dam-Johansen
Erik Graversen, Hempel A/S
Juan José Segura, Hempel A/S

PhD Study
Started: September 2017
To be completed: August 2020

Coating interlayer adhesion loss

Abstract

Weak interlayer adhesion between an epoxy and polyurethane coating can result from improper curing of polyurethane topcoat, which can be caused by the migration of small OH-molecules from the epoxy primer to the topcoat and react with the isocyanate component. The aim of this project is to figure out the interlayer adhesion loss mechanism. The difference in reactivity between different alcohols is regarded as the main cause for the intercoat adhesion loss. Isocyanates are believed to react faster with butyl alcohol than with polyols. Moreover, the diffusion of methanol in organic coatings is investigated. A decreasing diffusion rate of methanol across organic coating film is observed.

Introduction

Corrosion protection of steel structures, such as ships, wind turbines, bridges and oil rigs, is almost exclusively done by the use of anticorrosive coating systems. [1] This multilayer coating system typically consists of a primer such as an epoxy primer, directly on the steel substrate, followed by an intermediate epoxy coating to build up a substantial protective coating thickness. Finally, a top coat of polyurethane is applied for protection against sun light and to provide an aesthetically pleasing surface. Such a coating system can, in many cases, provide corrosion protection for more than 20 years. However, coating systems can fail due to weak interlayer adhesion that causes the top coat detach from the system, which significantly minimize the service life of coating films.

The weak adhesion of the polyurethane topcoat to the underlying epoxy coating can be caused by migration of critical chemicals from the epoxy primer. Due to short overcoating interval, the OH-molecules in the epoxy primer are not completely evaporated before applying the polyurethane topcoat. Small OH-solvents from the epoxy primer can migrate to the polyurethane topcoat and react with the isocyanate component. This induces improper curing of polyurethane topcoat. The adhesion between polyurethane topcoat and epoxy primer is reduced and the topcoat can be easily removed. One way to solve this problem is to find new OH-resins offering proper hardness development of the topcoat.

Specific objectives

The focus of the project will be to investigate the mechanisms of adhesion loss. One main goal is to find

out an OH-resin giving the best hardness development of the polyurethane topcoat even if OH-molecules migrate from the epoxy primer. The OH-resins should enable long-overcoat intervals and have competitive prices. Meanwhile, the diffusion of OH-molecules in organic coating will be also studied. This will help to understand the adhesion loss mechanism due to the migration of OH-molecules.

Results and Discussion

The results from the literature search on the reactivity of different alcohols with isocyanates will be presented in this section. Previous studies on methanol diffusion will be also included.

Reactivity of alcohols:

The formation of polyurethane from isocyanates and alcohols is a nucleophilic addition reaction. Any electron-withdrawing group attached to the OH group of alcohols will reduce the electron density on the oxygen atom, thereby decreasing the reactivity of the alcohol towards isocyanate groups. Sivakamasundari and Ganesan [2] investigated the influence of the alcohols structure on the reactivity of alcohols with isocyanates and the results are presented in Table 1. The reactions involving methyl, ethyl, n-propyl, and n-butyl alcohols have almost constant values of k_2 and E_a , suggesting the length of the alkyl group has little effect on the reactivity of the alcohols. The electron-releasing inductive effect of the alkyl group can increase the electron density on the oxygen atom to enhance the reactivity but increasing the alkyl length has limited effect. However, the activation energies for the

reactions involving allyl alcohol and methoxyethanol are about $10 \text{ kJ} \cdot \text{mol}^{-1}$ higher than the four alkyl alcohols. This is due to the electron-attracting nature of the ally and methoxy groups, reducing the electron density and nucleophilicity of the oxygen atom.

Table 1: Kinetic parameters for the reaction between phenyl isocyanate and some alcohols in benzene medium at 20°C [2]

Alcohol	$10^4 k_2, \text{M}^{-1}\text{s}^{-1}$	$E_a, \text{kJ/mol}$
Methyl alcohol	1.84	37.7 ± 0.5
Ethyl alcohol	2.08	36.0 ± 0.7
N-propyl alcohol	1.89	36.8 ± 0.3
N-butyl alcohol	1.93	36.8 ± 0.5
Allyl alcohol	0.18	50.2 ± 0.7
Methoxyethanol	0.12	47.7 ± 0.5

Figure 1 shows an example of an OH-acrylic resin that can react with isocyanates to form polyurethane coatings. The electron-withdrawing ester group are considered to reduce the nucleophilicity of the oxygen atom. Therefore, the reactivity of the alcohol group of the acrylic resin to the isocyanate would be reduced. This should be further proved by performing experiments in the future.

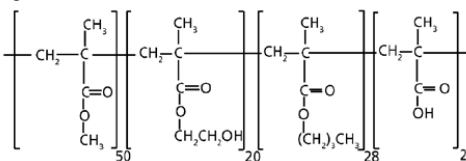


Figure 1: Example of an OH-acrylic resin

Alcohol diffusion experiments:

A one-chamber diffusion cell was designed and constructed to monitor the diffusion of alcohols across the organic coating films. The scheme of the diffusion cell is shown in Figure 2. The diffusion cell monitors the diffusion rate of alcohols across the coating film using the gravimetric method. Alcohols inside the aluminum cup can diffuse across the coating film, decreasing the weight of the whole set-up. The weight loss of the cell is measured intermittently on an analytical balance.

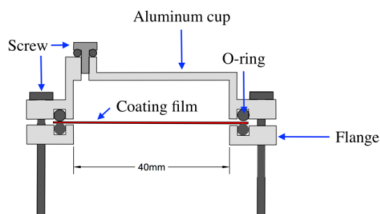


Figure 2: Schematic cross-section of the one-chamber diffusion cell for alcohol diffusion experiments.

Methanol diffusion experiments were performed to evaluate the performance of the diffusion cell. The weight loss profiles of diffusion cell were shown in Figure 3. The methanol diffuses across the polyurethane film very fast, with a 4-hour break-through time. As

shown in Figure 4, the diffusion rate of methanol across the polyurethane film is initially increased rapidly, reach the highest peak after 8 hours, and then is gradually reduced. Generally, it is believed that a steady-state will be achieved after the maximum diffusion rate is reached [3]. However, a decreasing diffusion rate was observed (see Figure 4). One possibility that may explain this decrease would be a change on the properties of the coating, for example, the crosslink density of the coating might be increased due to the plasticization effect of methanol. The cause of the decreasing diffusion rate should be further explored in future research.

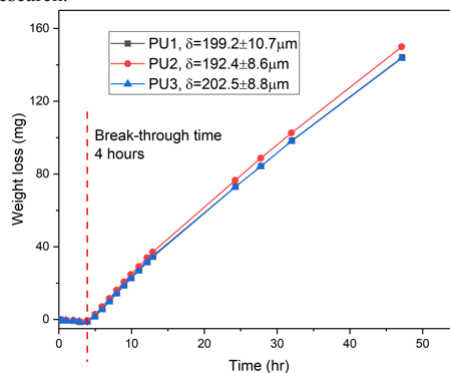


Figure 3: Weight loss profiles of methanol diffusion experiments on polyurethane films at room temperature and ambient environment.

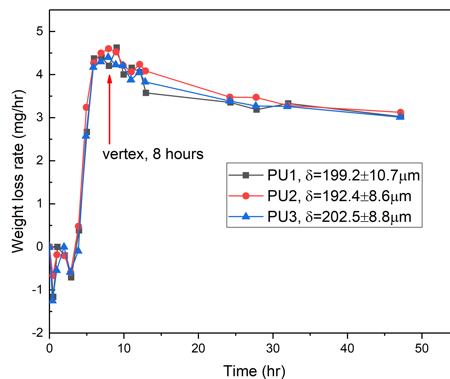


Figure 4: Diffusion rate of methanol across polyurethane films at room temperature and ambient environment.

Conclusions

OH-acrylic resins are considered to react slowly with isocyanates due to the electron-withdrawing effect of the ester group. Kinetic studies should be performed to prove the postulation. The designed diffusion cell successfully monitors the diffusion rate of the methanol across the organic coatings. And it should be further investigated for the reason of the decreasing diffusion rate.



Xueting Wang
Phone: +45 4525 2890
E-mail: xewa@kt.dtu.dk

Supervisors: Søren Kiil
Stefan Møller Olsen, Hempel A/S
Kenneth Nørager Olsen, Maersk Line
Kim Dam-Johansen

PhD Study
Started: August 2015
To be completed: July 2018

Low friction anti-fouling coating for high fuel efficiency

Abstract

To achieve high fuel efficiency for marine vessels applied with antifouling coatings, the coating surface roughness should be decreased as much as possible to diminish the frictional resistance during sailing. A potential approach to decrease the coating surface roughness is improving leveling property of the coatings. The main objective of the project is to understand leveling behavior and improve leveling of antifouling coatings. Besides, effects of coating surface and welding seams on drag resistance were determined and compared.

Introduction

Marine biofouling is known as the undesirable accumulation of marine species, such as bacteria, algae, slime, seaweed, barnacles and tubeworms, on any surfaces immersed into seawater [1]. It will decrease the sailing speed due to the added drag resistance. Otherwise, to maintain the speed, more fuel will be consumed. Consequently, the emission of harmful gases and cost will be increased and the maneuverability of marine vessels will be decreased. All in all, it is of primary importance to prevent biofouling.

Fouling control coatings (FCCs) have been applied to underwater ship hull surfaces as the most successful approach to prevent biofouling. Two major fouling control coating technologies have been developed over the years. The conventional biocide based antifouling (AF) coatings release active compounds into seawater in a controlled manner; whereas the so-called fouling release (FR) coatings, which possess low surface energy, flexible mechanical properties and have smooth surfaces, minimize the adhesion between marine organisms and coating surface so that the marine organisms can be removed by hydrodynamic forces during sailing or an occasional scrubbing.

However, the surface roughness condition varies among different antifouling coatings, where rough coating surfaces will increase the possibility of biofouling and frictional resistance when it is still free of biofouling. Hence, antifouling coating surfaces are preferred to be as smooth as possible in order to diminish frictional resistance. A smoother surface could be potentially achieved by improving leveling property of coating film.

Leveling is a surface phenomenon where the coating film levels out itself driven by surface tension and surface tension gradient during post-application process of coatings. However, the final coating surface is still not even for some reasons, such as high amount of pigment, quick drying and high viscosity. Leveling has been studied theoretically since 1920, however, limited works have been found due to the complexity of the phenomenon. Based on literature [2], various parameters can affect leveling and those parameters are interrelated and changing during the drying process.

Specific objectives

The main objective of the project is to understand leveling behavior and improve leveling of AF coatings and thereby the surface roughness and frictional resistance can be decreased. A 3D profilometer will be used to record the surface data along coating drying. Surface roughness and waviness can be obtained after applying cut-off length or filters. Rheological data (mainly viscosity behavior and viscoelastic properties) of the coatings can be obtained by using a Discovery Hybrid Rheometer (DHR-2).

Another objective is to determine and compare the effects of coating surface and large surface irregularities on drag resistance. One typical large surface irregularity is welding seam formed on ship hull surfaces during ship construction process. The drag resistance can be measured using a pilot-scale rotary setup as shown in Figure 1. Besides, the effects of water absorption of newly-applied AF coatings and FR coatings on drag resistance are aimed to be investigated and compared.



Figure 1: The full pilot-scale rotary setup for drag resistance measurements (left) and the flexible rotor with six artificial welding seams (the grey parts in the photo) on the outer surface (right).

Results and Discussion

The effects of welding seam height and density on drag resistance were investigated using a designed flexible rotor as shown in Figure 1. Welding seam density is seen to have a strong influence on the drag resistance, especially at high speeds in Figure 2. It can be seen from Figure 3 that the effects of welding seam height on drag resistance are less significant when the height is below 5 mm than above 5 mm.

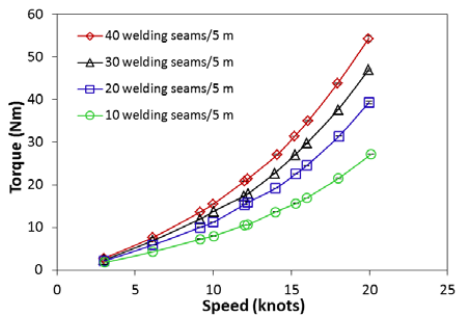


Figure 2: Torque values of different welding seam densities with a welding height of 9 mm as a function of tangential speed.

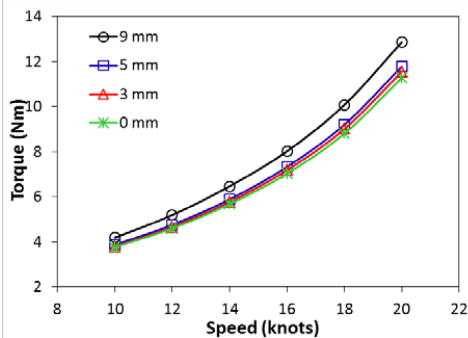


Figure 3: Interpolated torque values of different welding seam heights at full-scale welding seam density (one welding seam per 5 m ship side) as a function of tangential speed.

It can be seen in Figure 4 that at full-scale welding seam density, the torque values of all rotors with FCCs are higher than those of smooth rotors with welding seams when welding seam height is below 5 mm. Furthermore, when welding seam height is 9 mm, the torque values of all rotors with FCCs are still equal to or higher than those of smooth rotors with welding seams except for Hempaguard X7 (FR). Therefore, considering that the welding seam height is normally not above 5 mm, when following the European shipyard standard, both AF coatings and FR coatings will cause more drag resistance than welding seams at full-scale conditions. This is a consequence of the larger surface area taken up by coatings relative to welding seams.

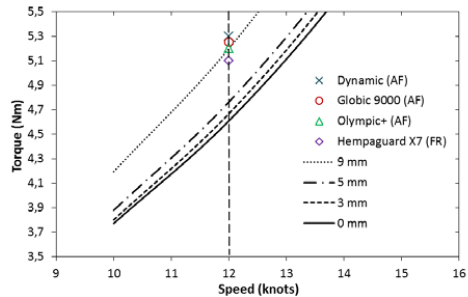


Figure 4: Comparison between torque values for different welding seam heights at full-scale welding seam density (one welding seam per 5 m ship side) and the experimental torque values of different FCCs (in the absence of welding seams) at a tangential speed of 12 knots (indicated by the dashed line).

Conclusions

It is suggested that welding seam height should be controlled to less than 5 mm when ships are constructed in shipyards. This will minimize the negative effects from both welding seam height and density, especially for ships scheduled to sail at high speeds. Accordingly, considerable economic benefits can be achieved. Furthermore, when welding seam height is below 5 mm at full-scale conditions, FCCs were found to result in a higher drag resistance than that of welding seams at a tangential speed of 12 knots. On real ships, welding seams can be ground, which will bring significant economic savings from drag reduction for welding seams of heights above 5 mm.

Acknowledgements

This project is conducted under the partnership of Blue INNOship. Financial support from Innovation Fund Denmark, the Danish Maritime Fund, Hempel A/S and A.P. Møller - Mærsk A/S is gratefully acknowledged.

References

1. D.M. Yebra, S. Kiil, K. Dam-Johansen, *Prog. Org. Coatings* 50 (2004) 75–104.
2. S.E. Orchard, in: *Appl. Sci. Res.*, Imperial Chemical Industries Limited, paints Diviaion, Bucks, England, 1962, pp. 451–464.



Sara Lindeblad Wingstrand

Phone: +45 2890 5680
E-mail: saliwi@kt.dtu.dk

Supervisors: Ole Hassager
Peter Szabo

PhD Study
Started: Sept 2014
Completed: Sept 2017

Extensional rheology and final morphology of polymeric fibers

Abstract

Presence of an ultra-high molecular weight (UHMw) fraction in flowing polymer melts is known to facilitate formation of oriented crystalline structures significantly. The UHMw fraction manifests itself as a minor tail in the molar mass distribution and is hardly detectable using standard characterization methods. In this study, alternatively, we demonstrate how the nonlinear extensional rheology reveals to be a very sensitive characterization tool for investigating the effect of the UHMw-tail on the structural ordering mechanism. Samples containing an UHMw-tail relative to samples without, exhibit a clear increase in extensional stress that is directly correlated with the crystalline orientation of the quenched samples.

Introduction

The morphology and thus mechanical properties of semicrystalline polymeric products is highly dependent on the deformation history during processing [1]. It is known from studies in shear flows, that presence of an UHMw-tail changes the flow-induced morphology significantly [2]. That is, even if the fraction is so small that it is undetectable using standard characterization methods [3]. Due to experimental challenges, studies investigating the effect of the UHMw-tail in extensional

flows on crystallization are quite limited [5,6] despite the fact the many industrial polymer processing unit operations like fiber spinning, blow moulding etc. comprise mainly extensional flows.

In this study we investigate the coupling between extensional flow dynamics and crystallinity of linear polymeric systems with and without an UHMw-tail.

Experimental

We compare a blend of 1% UHMw polyethylene (UHMwPE; $M_w = 4000$ kg/mol) in a matrix of commercial HDPE, high density polyethylene (632-D1 from Dow, $M_w = 156$ kg/mol), with the pure matrix, referred to as the “UH-blend” and the “matrix”, respectively. The molar mass distribution of the two systems is nearly identical (see Fig. 1).

The extensional flow behavior is studied above $T_m = 138$ in controlled uniaxial extension at 140 °C using a filament stretch rheometer (Fig. 2) [7]. Where we measure the extensional stress given by

$$\sigma_{zz} - \sigma_{rr} = (F - \frac{1}{2}mg)/\frac{\pi}{4}D(t)^2 \quad (1)$$

where F is the normal force, m is the mass of the sample and g is the gravitational acceleration, during deformations of constant Hencky strain rates $\dot{\epsilon}$. Here the strain (ϵ) is given by [8]:

$$\epsilon(t) = -2 \ln(D(t)/D_0) \quad (1)$$

with $D(t)$ and D_0 being the mid-filament diameter at time (t) and the initial diameter, respectively. All

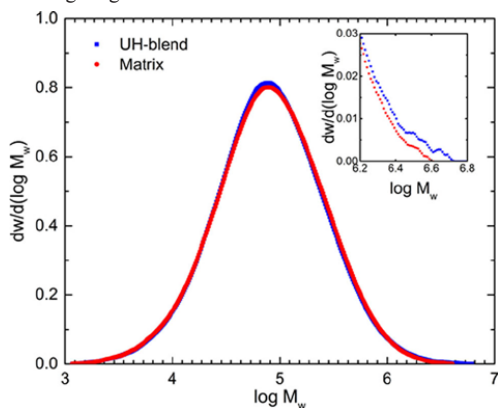


Figure 1: Molar mass distribution of the UH-blend (blue) and the matrix (red). The inset shows a magnification of the UHMw-fraction [4].

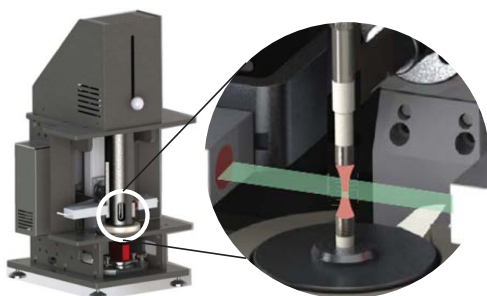


Figure 2: (A) Sketch of the entire filament stretch rheometer (FSR) (B) Lose-up of the stretching section of the FSR, with the sample (red) placed between two plates and a laser sheet (green) measuring the diameter in the mid-filament plane [8]

samples are quenched to room temperature at a Hencky strain of $\epsilon = 5.5$ and small-angle X-ray scattering (SAXS) patterns for the quenched samples are collected ex situ (see Fig. 3).

Results and Discussion

The nonlinear extensional response (Fig. 3), reported in terms of the extensional stress growth coefficient $\eta_E^+ = (\sigma_{zz} - \sigma_{rr})/\dot{\epsilon}$ shows a clear difference between the two samples. Although both samples strain harden

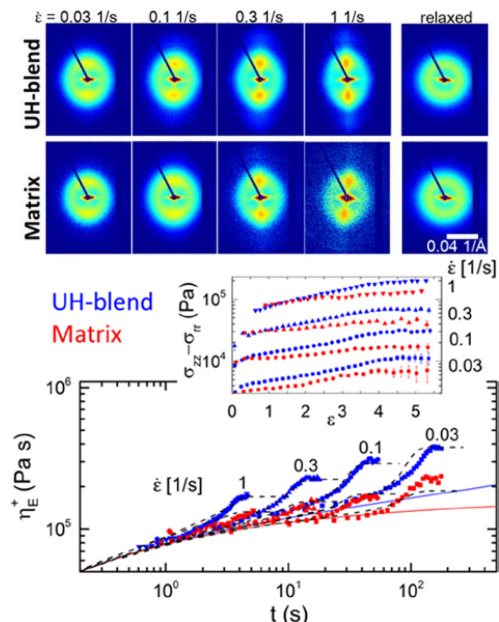


Figure 3: Top: Ex situ SAXS patterns of the quenched filaments. Bottom: Extensional response of the UH-blend (blue symbols) and the matrix (red symbols) at 140 °C together with the linear viscoelastic envelope (blue and red lines) and HMMSF model-prediction (black dashed lines) using the nonlinear fitting parameter $GD = 350$ Pa (see text). Inset: extensional stress vs Hencky strain [4].

i.e. an upwards departure from the linear viscoelastic envelope (LVE), the extent of strain hardening is much larger for UH-blend relative to the matrix. Initially, all samples follow the LVE prediction and overlap at small t . Prior to quench at $\epsilon = 5.5$, all samples reach steady elongational flow (Fig. 3 inset).

We use Herman's orientation factor F_H extracted from SAXS patterns (Fig. 3 top) as a measure for the average degree of crystalline orientation (see van Erp *et al.* [9] for information on the extraction of F_H from SAXS data). For $F_H = 0$ the orientation of crystalline domains are completely random while $F_H = 1$ indicates complete orientation along a given macroscopic direction in this case, the uniaxial extension direction.

Fig. 4 Shows the Herman's orientation factor versus the stress at quench. It is seen that data points both from UH-blend and matrix fall onto the same mastercurve. Hence the increased stress at quench for the UH-blend relative to the matrix is directly reflected in the increased final orientation [9].

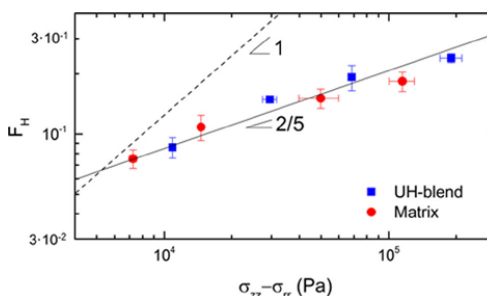


Figure 4: Herman's orientation factor vs steady stress for the UH-blend (blue) and matrix (red). Black solid and dashed lines show the apparent slope of 2/5 and the expected trend for amorphous systems, respectively [4].

Conclusion

We have shown that a very small fraction of UHMW-component in a semicrystalline polymer melt changes the extensional rheology as well as the final morphology significantly and that the link between extensional rheology and enhanced formation of oriented structures lies in their mutual inherent sensitivity to chain stretch.

References

1. B.A.G. Schrauwen, *et al.*, *Macromolecules* 37 (23) (2004) 8618.
2. S. Kimata, *et al.*, *Science* 316 (2007) 1014
3. M. Seki *et al.* *Macromolecules* 35 (2002) 2583.
4. S.L. Wingstrand *et al.*, *ACS Macro Lett.* (2017) 1268
5. C. Hadinata *et al.*, *J. Rheol.* 51 (2007) 195.
6. K. Cui *et al.*, *Macromolecules.* 45 (2012) 5477.
7. J. M. Román Marín *et al.*, *J. Nonnewton. Fluid Mech.* 194 (2013) 14.
8. <http://rheofilament.com>. Accessed: 2017-02-12.
9. T. B. van Erp, *Polymer (Guildf)*, 53 (2012) 5896.
10. S.L. Wingstrand *et al.*, *Macromolecules.* 50 (2017) 1134.



Jifeng Yang
Phone: +45 4525 2817
E-mail: jifyan@kt.dtu.dk

Supervisors: Ulrich Krühne
Krist V. Gernaey
Mikkel Nordkvist, Alfa Laval

PhD Study
Started: December 2015
To be completed: November 2018

A measurement-based cleaning-in-place recycle system

Abstract

The conventional measurement-based cleaning-in-place (CIP) approach is to measure the pollution level in the liquid phase, and to end the cleaning once the liquid has reached the desired water quality. Sometimes, however, such a measurement-based CIP approach is not safe enough, meaning there could still be undetected traces of pollution on the equipment surface even though the liquid measurements show “clear” signals. Nonetheless, the measurement of the liquid quality can be used to switch the drainage and recovery of cleaning liquid, which helps to reduce the volumetric consumption of fresh water during cleaning. Therefore, this study proposes a three-stage partial recovery approach using turbidity measurements to evaluate the water quality. The proposed measurement-based partial recovery is able to save up to 30-70% of the cleaning costs.

Introduction

Cleaning-in-Place (CIP) is commonly applied throughout food and pharmaceutical industries. Depending on the extent to which the cleaning fluids are recycled or not, typical CIP systems can be divided into single use, partial recovery and full recovery.

The current CIP monitoring system normally consists of conductivity probes, flow meters and temperature probes, etc., with the purpose to ensure the system is under control. If a recovery process is applied, the recovery starts when the conductivity output at the return flow reaches a set point or after the detergent has been added for a specific period of time (Tamime, 2008).

The removal of fouling from a surface displays a tailing effect. That is, most of the fouling can be removed in the beginning and then the removal rate decreases until no more fouling is removed. As a result, the cleaning liquid contains lots of impurities in the beginning, and becomes clearer and clearer towards the end of the operation. Therefore, instead of only controlling the cleaning time, it is possible to further reduce water consumption by designing efficient recovery plans. In other words, the initial liquid with high pollution load can be sent to drain and only the clear liquid should be recycled and recovered. In this way, most impurities can be avoided and will not accumulate in the recovery tank.

As a consequence, the lifetime of the cleaning liquid can be prolonged and the total volumetric loss of water is reduced at the same time.

This study investigates the measurement-based CIP with special consideration of water recovery. Turbidity measurement is used as a tool to evaluate the quality of the bulk cleaning liquid, which is a popular technique studied by many researchers. The ultimate purpose of this study is not only to reduce the cleaning time, but also to prolong the lifetime of the cleaning liquid for saving water consumption.

Methods

A pilot scale tank was studied with mustard as model soil. Tap water was used as the cleaning agent. Two cleaning approaches were tested: (1) a single use approach where fresh cleaning water was used and the cleaning water was not recycled, (2) a three-stage partial recovery approach where the reused water was used for rinsing (first stage) and circulation (second stage), and fresh water was subsequently used with recovery (third stage).

The costs of cleaning consisted of the consumption of fresh water, heat, and electricity, as well as the treatment of wastewater. If recovery was applied, the cost of water that was initially filled in the reused water tank was averaged into each operation by being divided

by the number of times that the water is reused. Besides, we needed to consider the time cost when cleaning limited the production yield, the quality risk if cleaning failed, and other costs like capital investment.

Four scenarios were defined in order to compare the cleaning costs by using different cleaning strategies:

Scenario 1 - Single use: The cleaning liquid was once used without recovery or reuse. The cleaning was performed by using fresh water and rinsing for 15 minutes.

Scenario 2 – Full recovery: The cleaning was performed by circulating for 10 minutes. A final rinse was followed by rinsing with fresh water for 5 minutes. All liquid was recovered.

Scenario 3 – Time-based partial recovery: The three-stage partial recovery approach was performed. But there was no turbidity measurement to determine the rinsing time. The first stage and third stage rinsing times were both 5 minutes, which made sense because in industrial practice this time was set based on experience and the value was larger than the real demand. The circulation time was 10 minutes.

Scenario 4 – Measurement-based partial recovery: The three-stage partial recovery approach used turbidity measurement to determine the rinsing time. The third stage rinsing time equaled the first stage rinsing time.

Results and discussions

The comparisons of resource consumption and costs for cleaning in the different scenarios are summarized in Table 1 and Figure 1. Increasing the number of water reuse cycles is able to reduce the operation costs, which, however, become less sensitive when the reuse cycles reach a certain value. For all of the studied reuse cycles, the operation costs for the single use approach is much higher than for the recovery approaches, even though it has to be emphasized that it has the biggest potential to reduce cross contamination and spore formation. The measurement-based partial recovery scenario has the lowest cleaning cost, because it results in the lowest fresh water consumption and wastewater generation. It has been tested that the surface can be well cleaned when the rinsing time is over 15 minutes regardless using fresh water or reused water. Therefore, even though the time-based partial recovery has a wider margin of safety than the measurement-based partial recovery, especially due to the longer rinsing time, the real consumption in the time-based approach is actually more than needed. The operation cost can be actually reduced in confidence.

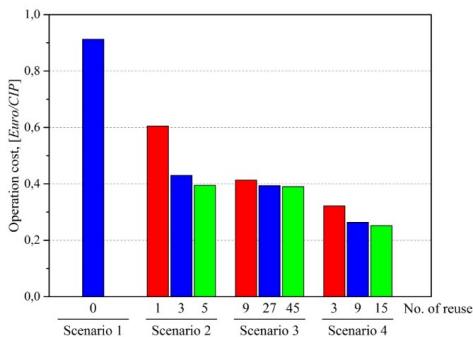


Figure 1: The cleaning operation costs by different scenarios for the tank cleaning at flow rate 1.5 m³/h. The selection of the number of reuse cycles are approximations based on industrial cases and tank capacities.

Conclusions

A three-stage measurement-based partial recovery approach is proposed in this study. Four scenarios are studied to compare the operation costs by conducting single use or recovery approaches. The results reveal that the proposed measurement-based partial recovery allows savings between 30-70% of the cleaning costs. Even though the proposed approach is developed by only using water as medium, it is possible to apply this approach to other cleaning procedures, where solutions of chemicals are used. Especially, the proposed procedure can be used for processes where cleaning downtime does not restrict the production efficiency.

Acknowledgements

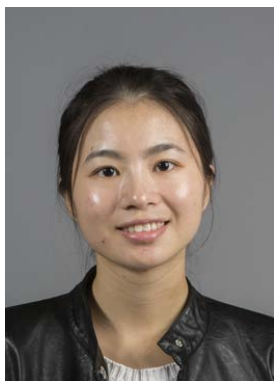
This research results from the DRIP (Danish partnership for Resource and water efficient Industrial food Production) project and is partly funded by the Innovation Fund Denmark (IFD) and Technical University of Denmark.

References

Tamime A., *Cleaning-in-Place: Dairy, Food and Beverage Operations*, Blackwell, Ayr, U.K., 2008.

Table 1: Comparison of the cleaning by different scenarios

Scenario	Cleaning time	Reused water			Operation cost
		Volume	Turbidity	Lifetime	
1	Short	-	-	-	High
2	Short	Increased	Highly increased	Short	Middle
3	Long	Unchanged	Very slowly increased	Very long	Middle
4	Middle	Unchanged	Slowly increased	Long	Low



Ying Zeng
Phone: +45 4525 2952
E-mail: yzen@kt.dtu.dk

Supervisors: Søren Kiil
Claus Erik Weinell
Kim Dam-Johansen
Louise Ring, Hempel

PhD Study
Started: October 2016
To be completed: October 2019

Novel testing methods for intumescent coatings

Abstract

The thermal shield of intumescent coatings is an effective way to protect the structural steel in the event of a fire. This project involves design and validation of a lab-scale setup for fast and reliable fire tests, and evaluation of the effect (or synergic effect) of different concentrations of the ingredients on the performance of intumescent coatings based on a basic hydrocarbon formulation. The evaluation is for understanding the roles of ingredients thoroughly by linking their responses in the fire tests with the char characterizations and mapping the intumescent mechanism.

Introduction

The protection of structural steel on exposure to a fire has become paramount to prevent the loss of lives and assets with increasing use of structural steel as a material to create the shape of construction projects. Structural steel only retains 60% of its original strength when its temperature reaches a critical value and loses its bearing ability under full design load [1]. For regular loaded structural components, such as onshore platforms, 550°C has been selected as a standard critical temperature for steel. While for heavily loaded structural components, such as offshore platforms, 400°C has been selected as a standard. This critical temperature is also known as “failure temperature”, and the time for reaching it in the event of a fire is called the “failure time” [2].

An efficient way to protect the building structure and prolong the time before the failure temperature is reached is by intumescent coatings. At elevated temperature, intumescent coatings swell to a multicellular char layer, which acts as a physical barrier to slow heat and mass transfer between gas and condensed phase and thereby protects the underlying substrate. The most effective intumescent coatings are the ones that have best fire-resistance performance and therefore can provide longest failure time for the substrate in the fire tests.

Instead of natural fire that has varied relationships between temperature and time, usually fire tests refer to the tests under standard fires for which the fixed temperature-time responses are imposed in order to roughly simulate the evolution of natural fires and meanwhile facilitate the normalization of fire test procedure. Depending on the source of fuel, most of the

standard fires are classified into two types: cellulosic fire (ISO 834) and hydrocarbon fire (e.g. UL 1709). Their corresponding intumescent coatings are called cellulosic intumescent coatings and hydrocarbon intumescent coatings. The latter is the focus of the present project, as it is the most challenging type used for high-risk environments such as petrochemical complexes and offshore platforms.

Generally, intumescent coatings consist of three essential ingredients: acid source (e.g. ammonium polyphosphate), carbon source (e.g. dipentaerythritol), and blowing agent (e.g. melamine). Other ingredients are incorporated into the formulation as well to improve its function (e.g. composite fibers). All the ingredients are bound together by a polymeric binder. The physical and chemical interactions among these compounds are complex and have not been fully quantified in the literature, especially for the case of the hydrocarbon intumescent coatings [3]. To optimize the formulation of hydrocarbon intumescent coatings, it is fundamental to understand the effect (or synergic effect) of ingredients on the physical (expansion and strength) and chemical (thermal conductivity and thermal stability) properties of char.

Specific Objectives

This Ph.D. project aims at:

- Validation of equipment for fire tests and characterizations with two typical hydrocarbon intumescent coatings.
- Design a setup with motion system for continuous and reliable fire tests.
- Link varying levels of ingredients with different char characteristics.

Results and Discussion

Two hydrocarbon intumescent coatings (A and B) supplied by Hempel were investigated in terms of fire-resistance performance and variation of complex viscosity with temperature increasing. The formulations of A and B are confidential and not given here. The application of the intumescent coatings starts with mixing the two parts (base and curing agent) according to the specific ratio. Once it is mixed well, about 6 mm of the coating is applied on the surface of a grit blasted steel plate that are squares of 60*60 mm and 3 mm thick. The coatings are cured for 24 h at room temperature before being used.

The fire tests of A and B were carried out with a lab oven (Nabertherm, LHT 01/17D) according to UL 1709. A lab-made insulating model is used to hold the coated plate and a thermocouple is attached to the back of the plate to record the temperature – time (T-t) response. The repeatability of the oven was assessed by testing A thrice and the T-t curves recorded are almost the same. The relative standard deviations of failure time at 400°C and 550°C are less than 1%. It indicates that the results of fire tests from the oven are reliable and reproducible.

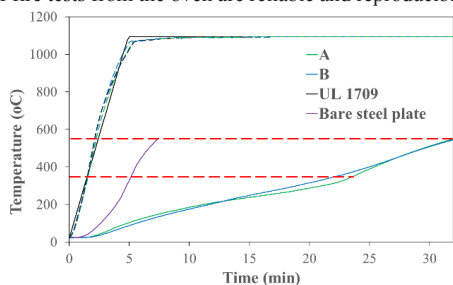


Figure 1: Temperature – time response of A and B tested with UL 1709.

Figure 1 shows the T-t response of A and B under the fire tests of UL 1709. Table 1 lists the corresponding failure time and relative expansion calculated by dividing the coating thickness after the test by the counterpart before the test. The results of bare steel plate are also included for comparison. The dash lines in the figure are the experimental hydrocarbon curves performed with the oven, which show few differences compared with the standard UL 1709 (black solid line).

The bare plate reached its failure temperature (400°C and 550°C) rapidly within 8 minutes due to the lack of protection of intumescent coating. When A and B were applied on the plate, the failure time were greatly extended to around 32 minutes (550°C). The performances of A and B are more or less the same according to the parameter of failure time. However, their T-t curves show an unneglectable difference considering the rather good repeatability of the oven. This difference may reflect the different reactions taking place during the fire tests, which give distinct composition of the incipient char. The XRD and EDS results (not shown here) confirmed that except for amorphous carbon the main components of the final

char are zinc phosphate and boron phosphate (B), and composite of titanium phosphate doped with calcium (A). Their unique composition should result in different thermal conductivities as the unlike relative expansions give similar failure time (Table 1).

Table 1: The failure time and expansion of A and B.

Samples	Temperature (°C)		Relative Expansion
	400	550	
Bare plate	5.5	7.4	-
A	25.45	32.05	9.17
B	25	32.35	4

The diverse expansions are expected in light of the variation of viscosity (see Figure 2). The viscosity measurement was done with the free-film coatings that have diameter of 25 mm and thickness of 3 mm. It was suggested that expansion of intumescent coatings occurs when the viscosity is lowest [4]. The lower minimum complex viscosity of A at around 360°C permits less external stress for the degradation gases released from the blowing agents (or the reactions between other compounds), which thereby leads to substantial expansion.

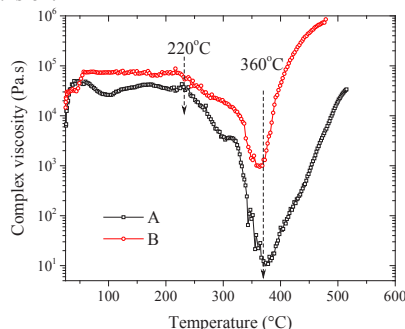


Figure 2: Dynamic viscosity of A and B varied with temperature increasing.

Conclusions

The failure time of steel plate coated with A or B is greatly increased compared with the bare steel plate. The performances of A and B in the fire tests are more or less the same with respect to the failure time. Nevertheless, the differences between both their T-t responses and relative expansions may indicate the divergent reactions occurring during the intumescence. Future work will provide more information about the underlying reactions with the aid of characterizations.

References

1. M. Jimenez, S. Duquesne, S. Bourbigot, Ind. Eng. Chem. Res. 45 (2006) 7475-7481.
2. M. Jimenez, S. Duquesne, S. Bourbigot, Ind. Eng. Chem. Res. 45 (2006) 4500-4508.
3. J. Alongi, Z. Han, S. Bourbigot, Prog. Polym. Sci. 51 (2015) 28-73.
4. M. Jimenez, S. Duquesne, S. Bourbigot, Surf. Coatings Technol. 201 (2006) 979-987.



Yu Zhang
Phone: +45 9186 8186
E-mail: yuzha@kt.dtu.dk

Supervisors: Peter Glarborg
Anker D. Jensen
Jakob M. Christensen

PhD Study
Started: September 2016
To be completed: August 2019

Catalytic oxidation of methane

Abstract

Natural gas is an interesting engine fuel for ships in coastal zones, where high sulfur marine fuels cannot be used. However, unburnt methane poses another severe emission problem. The current study seeks to develop a catalyst for methane emission abatement from natural gas engines. Motivated by the good performance of the commercial Rh-Cr-Al catalysts, Rh supported on zeolites catalysts are tested for methane oxidation in the temperature range of 250-550 °C, in a simulated exhaust gas (2500 ppm CH₄, 5 vol.% H₂O, and 20 ppm SO₂ when present). Compared with Pd catalysts, which exhibit the best activity towards CH₄ oxidation but are very sensitive to SO₂, Rh supported on ZSM-5 catalysts shows comparable activity at the same loading (1 wt.%). The presence of H₂O and SO₂ in the reaction stream are two main factors for the catalysts deactivation, which are the main problem for the practical use.

Introduction

Natural gas provides high fuel efficiency compared with diesel and gasoline. Dual-Fuel engine can switch between diesel mode and natural gas mode flexibly to lower NO_x and PM emissions and meet the strict regulations [1]. However, the unburnt CH₄, which has a greenhouse impact of 25 times larger than that of CO₂, becomes another environmental issue for this Dual-Fuel engine. In order to solve this problem, a CH₄ catalytic oxidation unit, which could fully convert the unburnt CH₄ to CO₂ and H₂O, is necessary in the exhaust gas pipe due to the quite stable structure of CH₄ molecular.

The catalysts studied in the literature for CH₄ oxidation can be divided into two groups, noble metals supported catalysts (Pd, Pt, Rh, Au) and non-noble metal based catalysts, shown in Figure 1. Among the catalysts, Pd based catalyst is the most active one for CH₄ oxidation with a mixed metal and oxidized phase as active site [2]. Zeolites are reported to have a pore structure and acidic sites which could incorporate with the active metals to enhance the activity and avoid sintering at high temperatures.[3] 1 wt.% Pd/H-ZSM-5 could fully convert CH₄ to final products at 320 °C and the activity was stable in the subsequent 3 runs even to a temperature as high as 800 °C.

Rh based catalysts also showed great potential towards total oxidation of CH₄. The performance of Rh based catalysts is influenced by the supports indicated by decreasing activity towards partial oxidation of CH₄ in the order: Rh/TiO₂>>Rh/Al₂O₃>>Rh/MgO. [4]

Specific objectives

The objectives of the PhD project focuses on developing a desired catalyst which can be used in practical engine exhaust conditions: low temperature (lower than 500-550 °C), CH₄ concentration of 2000-2500 ppm, the presence of a large amount of H₂O (~ 10 vol.% H₂O) and low concentrations of SO₂ (~ 1 ppm). The scope of the PhD work includes:

- Test activity, stability and poisoning properties of the commercial Rh-Cr-Al catalyst.
- Prepare and test of Pd and Rh based zeolite supported catalysts in a fixed bed reactor.
- Investigate the thermal, water and sulphur deactivation mechanism of the prepared catalysts at different temperatures (400-550 °C), SO₂ concentrations (1-20 ppm).
- Investigate the influence of the promoters (Ti, Cr, Zr) on SO₂ resistance of the Rh catalysts.
- Characterization of catalysts (fresh and spent).
- Identification of the optimum conditions for the process and evaluation of the implications in the process on four-stroke maritime engines.

Results and discussion

As shown in Figure 1 and 2, lab prepared 1 wt.% Pd/ZSM-5 and 1 wt.% Rh/ZSM-5 catalysts have better activity than the commercial Rh-Cr-Al catalysts in the absence of 5 vol.% H₂O but in the absence of any SO₂.

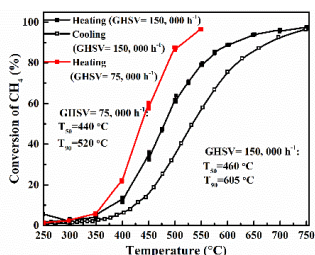


Figure 1: activity of commercial Rh-Cr-Al catalyst (2500 ppm CH₄, 10 vol.% O₂, 5 vol.% H₂O).

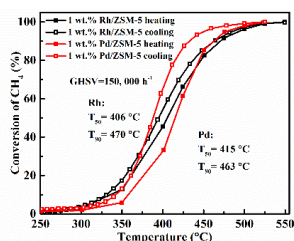


Figure 2: activity of 1wt.% Pd/ZSM-5 and 1 wt.% Rh/ZSM-5 (2500 ppm CH₄, 10 vol.% O₂, 5 vol.% H₂O).

While 1 wt.% Pd/ZSM-5 catalyst lost almost all the activity (50 % CH₄ conversion) immediately upon introduction of 20 ppm SO₂. The activity could be partially restored to 46 % by heating to 550 °C after the first time poisoning. What's worse, the restored CH₄ conversion decreased to 26 % after the second time SO₂ poisoning (Figure.3), which indicates the sensitivity of Pd/ZSM-5 catalyst to SO₂.

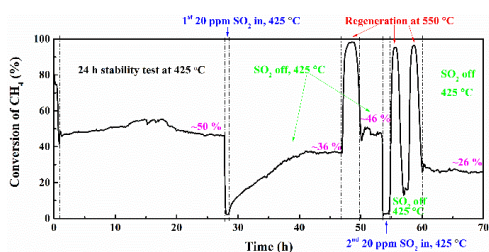


Figure.3 stability of 1 wt.%Pd/ZSM-5 (425 °C, 5vol.% H₂O), SO₂ resistance (20 ppm SO₂).

The activity of Commercial Rh-Cr-Al could maintain at a CH₄ conversion of 22 % after running in the presence 5 vol.% H₂O and 20 ppm SO₂ for 10 days. After removal of SO₂ for 12 h, without any heating, the activity can be mostly self-regenerated to 46 %. (Figure 4)

Lab prepared Rh catalysts showed high and stable low temperature activity in the presence of 5 vol.% H₂O. However, when 20 ppm SO₂ was added into the H₂O containing feed stream, the activity decreased significantly (Figure 5 curve a).

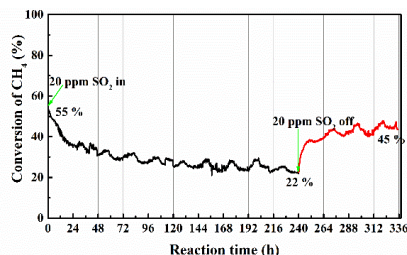


Figure 4: SO₂ resistance of commercial catalyst (450 °C, 5 vol.% H₂O, 20 ppm SO₂)

Compared with the immediate activity loss for a Pd/ZSM-5 catalyst, Rh/ZSM-5 catalysts could maintain the original activity for about 20 min and finally the CH₄ conversion was stable at 5 %. 10wt.% TiO₂ adding in different manners show no apparent improvement on the SO₂ resistance of Rh/ZSM-5 catalysts. (Figure 5)

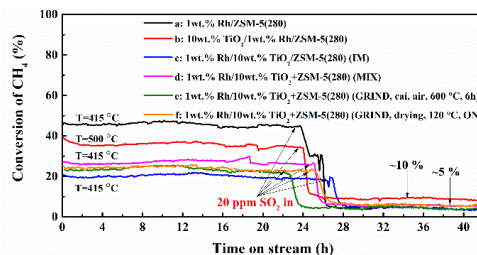


Figure 5: SO₂ resistance of Rh/ZSM-5 with and without TiO₂ promoters (5 vol.% H₂O, 20 ppm SO₂)

Conclusions and Future work

Rh-zeolite catalysts has comparable activity to Pd-zeolite catalysts in the presence of 5 vol.% H₂O. Pd catalyst lost all the activity as soon as 20 ppm SO₂ was introduced into the stream, while Rh catalyst can maintain at the original level for about 20 min and then dropped to 5 %. 10 wt.% TiO₂ shows no enhancement influence on the SO₂ resistance of Rh catalysts. Future work mainly focus on the performance of high loading Rh catalysts, regeneration conditions, and influence of Cr promoters, higher SO₂ resistance testing temperatures and lower SO₂ concentrations (1-5 ppm).

Acknowledgments

This work is funded by the Blue INNOship project and DTU.

References

1. A. Gremminger, P. Lott, M. Merts, Applied Catalysis B: Environmental 218 (2017) 833-843.
2. J.H. Chen, H. Arandiyan, X. Gao, Catal Surv Aisa 19 (2015) 140-171.
3. Y. Lou, J. Ma, W.D. Hu, ACS Catal 6 (2016) 8127-8139.
4. M.P. Cecilia, B. Bernard, A.S. Miguel, Catalysis Today 213 (2013) 155-162.



Zhibo Zhang
Phone: +45 52695821
E-mail: zhiz@kt.dtu.dk

Supervisors: Manuel Pinelo
Suojiang Zhang
Nicolas von Solms

PhD Study
Started: December 2015
To be completed: November 2018

Ionic liquids as bifunctional cosolvents enhanced CO₂ conversion catalysed by NADH-dependent formate dehydrogenase

Abstract

The PhD Project focuses on improving conversion of CO₂ catalyzed by formate dehydrogenase. The main bottleneck of enzymatic reaction is the low solubility of the substrate (CO₂) in the liquid media and the low stability of NADH in the presence of CO₂ (acid gas). In order to overcome these problems, a new novel solvent (Ionic liquids) is evaluated. Enzymatic conversion of CO₂ was improved – as compared to the reaction conducted in buffer- after evaluating different kinds of ionic liquids as co-solvents and the reaction mechanism was studied and proposed.

Introduction

To minimize environmental problems and produce clean energy, efficient utilization of CO₂ and carbon regeneration has been the focus of a tremendous amount of research.¹ Enzymatic conversion of CO₂ to formate, formaldehyde, and methanol has inspired many researchers in the past several years.² However, enzymatic hydrogenation of CO₂ to formic acid (CH₂O₂), formaldehyde (CH₂O) and methanol (CH₃OH) is hampered by the low concentration of CO₂ that is available for the enzyme (formic acid dehydrogenase) in the reaction mixture. Increasing CO₂ concentration could result in an increased conversion, as reported by Liu.³ CO₂ is highly soluble in ionic liquids (ILs), and such high solubility is explained via electrostatic forces, van der Waals forces, hydrogen bonds and other physical effects.⁴ One serious limitation of conducting the reaction in carbon dioxide is to maintain the stability of NADH, as it is easily affected by the solution's pH. The investigations on the interaction between ILs and coenzyme (NADH) could then play a key role in the conversion of CO₂. NADH is used not only as hydrogen donor to catalyze reduction of CO₂ but is also employed to follow the progression of the reaction and thus it can be used to quantify the produced formate. The objective of present work was to investigate the activity of NADH in ILs to improve the efficiency of enzymatic reaction and to increase enzymatic conversion by capturing CO₂ with ionic liquids.

Specific Objective

The objective of this work is to improve the enzymatic conversion of CO₂ in the contained-IL buffer. In order to achieve such a goal, three requirements have to be met: First, ionic liquids must have great ability to absorb CO₂. Second, the coenzyme (NADH) must keep its activity in the presence of the ionic liquids. Last, formate dehydrogenase should be able to keep its activity in the ionic liquid.

Results and Discussion

Table 1. Stability of NADH in aqueous ILs.

Entry	IL	Residue _(NADH) (%) (SD)	pH (SD)
1	IL1	100.0 (± 0.1)	7.8 (± 0.20)
2	IL2	12.8 (± 3.1)	5.3 (± 0.12)
3	IL3	3.1 (± 0.5)	2.8 (± 0.18)
4	IL4	4.7 (± 0.6)	2.6 (± 0.18)
5	IL5	11.1 (± 2.6)	2.3 (± 0.16)
6	IL6	99.7 (± 0.6)	9.3 (± 0.14)

Screen ionic liquids for absorb CO₂.

Six different ILs were selected for enzymatic reaction. These ILs were selected based on the great ability to absorb CO₂ with similar structure in cation and expect to find structure-performance relationship. Besides, these ILs' pH are range from acid to alkali. Therefore, NADH stability will firstly be evaluated in these ILs.

Stability of NADH in ILs

To verify if NADH stability in all kinds of ILs, five ILs were subsequently screened under identical conditions in terms of their respective reactivity with NADH (Table 2, entries 1–5). The results showed that the stability of NADH was found to be highly dependent on the pH value of the system. Under neutral-basic conditions, almost no degradation of NADH was detected (entry 1). In contrast, the concentration of NADH diminished markedly under acidic conditions (entry 2). Notably, under strongly acidic conditions, the absorption at 340 nm assigned to NADH disappeared coincidentally with the appearance of a blue-shifted peak at 332 nm. Finally, when IL6 at known to be a strong basic IL was employed rather than imidazolium-based ILs (entry 6), only traces of degradation of NADH were observed. In the following degradation mechanism investigation, the analysis tools UV, NMR were used for identifying degradation procedure. According to experimental results, there are two possible degradation pathways, which were further confirmed by molecular simulation (DFT calculation).

Activity of Formate dehydrogenase (FDH) in ionic liquids.

Table 2. Enzymatic Conversion of CO₂ to Formate

Entry	Solvent(v/v)	Yield of formate (%) (SD)
1	Phosphate buffer	1.1 (± 0.5)
2	10% IL4	0.2 (± 0.3)
3	20% IL4	2.9 (± 0.4)
4	40% IL4	2.3 (± 0.4)

After evaluating these ILs for NADH stability above, IL4 was used for running enzymatic reaction. In the case of IL4, CO₂ conversion reached the maximum at 20% IL4 (2.9%), which is more than two folds as compared with conversion in phosphate buffer (1.1%). As is known, water with small amounts of salts was considered to be the best media for proteins. Normally, high concentration of ILs (salts) will cause conformational changes of peptide chains and cause enzyme denaturation, due to electrostatic unbalance between peptide chains. Crystallization and aggregation of proteins dramatically occurred upon increasing the concentration of ILs. Furthermore, in pure ILs, enzymes can hardly be dissolved in homogenous phase without causing denaturation.

Conclusion

We demonstrated that degradation of NADH occurs during carbon dioxide hydrogenation at low pH. The mechanism of NADH degradation was investigated by UV, NMR, and DFT. By selecting neutral-basic ionic liquids and adjusting concentration of the ionic liquids in the buffer, 20% IL4 was the one found to be optimal for conducting the reaction. Finally, CO₂ conversion was more than twice as compared with the enzymatic

reaction in the phosphate buffer (traditional buffer). This study is a significant contribution to improve yields formate dehydrogenase catalysed reactions in a novel medium (ionic liquid) and paves the way for improving biocatalysts using ionic liquids.

Acknowledgements

The PhD project has received funding from the Technical University of Denmark (DTU) and institute of process Engineering, Chinese Academy of Science (IPE, CAS).

References

- Xu, B. H.; Wang, J. Q.; Sun, J.; Huang, Y.; Zhang, J. P.; Zhang, X. P.; Zhang, S. J., Fixation of CO₂ into cyclic carbonates catalyzed by ionic liquids: a multi-scale approach. *Green Chem* 2015, 17 (1), 108-122.
- (a) Obert, R.; Dave, B. C., Enzymatic conversion of carbon dioxide to methanol: Enhanced methanol production in silica sol-gel matrices. *J Am Chem Soc* 1999, 121 (51), 12192-12193; (b) Shi, J. F.; Jiang, Y. J.; Jiang, Z. Y.; Wang, X. Y.; Wang, X. L.; Zhang, S. H.; Han, P. P.; Yang, C., Enzymatic conversion of carbon dioxide. *Chem Soc Rev* 2015, 44 (17), 5981-6000.
- Wang, Y. Z.; Li, M. F.; Zhao, Z. P.; Liu, W. F., Effect of carbonic anhydrase on enzymatic conversion of CO₂ to formic acid and optimization of reaction conditions. *J Mol Catal B-Enzym* 2015, 116, 89-94.
- D'Alessandro, D. M.; Smit, B.; Long, J. R., Carbon Dioxide Capture: Prospects for New Materials. *Angew Chem Int Edit* 2010, 49 (35), 6058-6082.

Department of Chemical and Biochemical Engineering
Technical University of Denmark
Building 229
Søltofts Plads 229
DK-2800 Kgs. Lyngby
Denmark

Phone: +45 4525 2800
E-mail: kt@kt.dtu.dk
Web: www.kt.dtu.dk

February 2018
ISBN: 978-87-93054-85-1
Print: STEP

Cover photo: Christian Ove Carlsson